Verification and Implementation of Strut-and-Tie Model in LRFD Bridge Design Specifications

Requested by:

American Association of State Highway
and Transportation Officials (AASHTO)

Highway Subcommittee on Bridge and Structures

Prepared by:

Barney T. Martin, Jr., Ph.D., P.E.
Modjeski and Masters, Inc.
301 Manchester Road, Poughkeepsie, NY 12603
David H. Sanders, Ph.D.
University of Nevada Reno

November, 2007

The information contained in this report was prepared as part of NCHRP Project 20-07, Task 217,
National Cooperative Highway Research Program, Transportation Research Board.

Acknowledgements

This study was requested by the American Association of State Highway and Transportation Officials (AASHTO), and conducted as part of National Cooperative Highway Research Program (NCHRP) Project 20-07. The NCHRP is supported by annual voluntary contributions from the state Departments of Transportation. Project 20-07 is intended to fund quick response studies on behalf of the AASHTO Standing Committee on Highways. The report was prepared by Barney T. Martin Jr., Ph.D., P.E., Wagdy Wassef, Ph.D., P.E. and Thomas A. Cole of Modjeski and Masters, Inc. and David H. Sanders, Ph.D., P.E. and Neil Bahen, Graduate Student, of the University of Nevada Reno. The work was guided by a task group which included Sue Hida, William Nickas, Steve Stroh, Chris White, and Reid Castrodale. The project was managed by David B. Beal, P.E., NCHRP Senior Program Officer.

Disclaimer

CONTENTS

CHAPTER 1 – INTRODUCTION TO STRUT-AND-TIE MODELS

1.1 INTRODUCTION

Strut-and-tie modeling (STM) is an approach used to design discontinuity regions (D-regions) in reinforced and prestressed concrete structures. A STM reduces complex states of stress within a D-region of a reinforced or prestressed concrete member into a truss comprised of simple, uniaxial stress paths. Each uniaxial stress path is considered a member of the STM. Members of the STM subjected to tensile stresses are called ties and represent the location where reinforcement should be placed. STM members subjected to compression are called struts. The intersection points of struts and ties are called nodes. Knowing the forces acting on the boundaries of the STM, the forces in each of the truss members can be determined using basic truss theory.

With the forces in each strut and tie determined from basic statics, the resulting stresses within the elements themselves must be compared with specification permissible values. Since a STM is comprised of elements in uniaxial tension or compression, appropriate reinforcement must be provided. Through the use of this approach, an estimation of strength of a structural element can be made and the element appropriately detailed. Unlike the sectional methods of design, the strut-and–tie method does not lend itself to a cook book approach and therefore requires the application of engineering judgment.

1.2 ELEMENTS OF A STRUT-AND-TIE MODEL

As stated above, a strut-and-tie model is comprised of three primary elements: struts, ties, and nodes. An illustration of the different components using a deep beam example is shown in Figure 1-1.

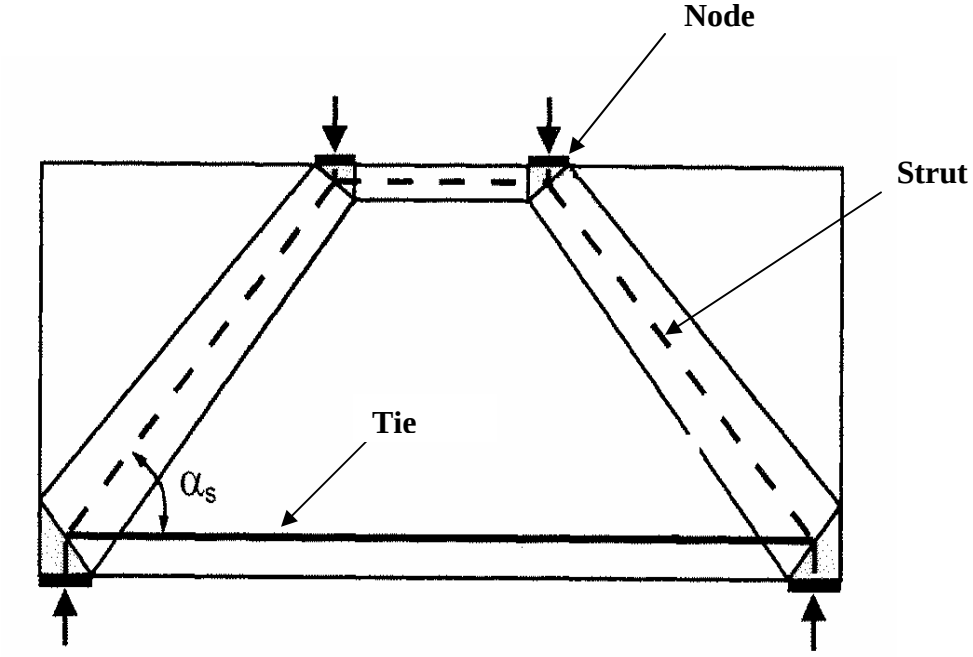

Figure 1-1: Illustration of the different components of a strut-and-tie model using a deep beam.

1.2.1 STRUTS

Most research and design specifications specify the limiting compressive stress of a strut as the product of the concrete compressive strength, f'_c, and a reduction factor. The reduction factor is often a function of the geometric shape (or type) of the strut. The shape of a strut is highly dependent upon the force path from which the strut arises and the reinforcement details of any reinforcement connected to the tie. As discussed by Schlaich and Schäfer, there are three major geometric shape classes for struts: prismatic, bottle-shaped, and compression fan (1991). Fig. 1-2 shows an illustration of the three major geometric shape classes for struts applied to common deep beam STMs.

Prismatic struts are the most basic type of strut. Prismatic struts have uniform cross-sections. Typically, prismatic struts are used to model the compressive stress block of a beam element as shown in Fig. 1-2(a).

Bottle-shaped struts are formed when the geometric conditions at the end of the struts are well-defined, but the rest of the strut is not confined to a specific portion of the structural element. The geometric conditions at the ends of bottle-shaped struts are typically determined by the details of bearing pads and/or the reinforcement details of any adjoined steel. The best way to visualize a bottle-shaped strut is to imagine forces dispersing as they move away from the ends of the strut as shown in Fig. 1-2(b). The bulging stress trajectories cause transverse tensile stresses to form in the strut which can lead to longitudinal cracking of the strut. Appropriate crack control reinforcement should always be placed across bottle-shaped struts to avoid premature failure. For this reason, most design specifications require minimum amounts of crack control reinforcement in regions designed with STMs.

The last major type of strut is the compression fan. Compression fans are formed when stresses flow from a large area to a much smaller area. Compression fans are assumed to have negligible curvature and, therefore, do not develop transverse tensile stresses. The simplest example of a compression fan is a strut that carries a uniformly distributed load to a support reaction in a deep beam as shown in Fig. 1-2(c).

The STM provisions of the *AASHTO LRFD Bridge Design Specifications* do not require the identification of strut type in order to determine the limiting compressive stress for a given strut. Instead, the specification allows the designer to use idealized straight-line struts for all struts and calculate the limiting compressive stress with a given equation. Chapter 4 of this report elaborates on the prescribed limiting strut compressive stress equation given in the AASHTO LRFD specifications.

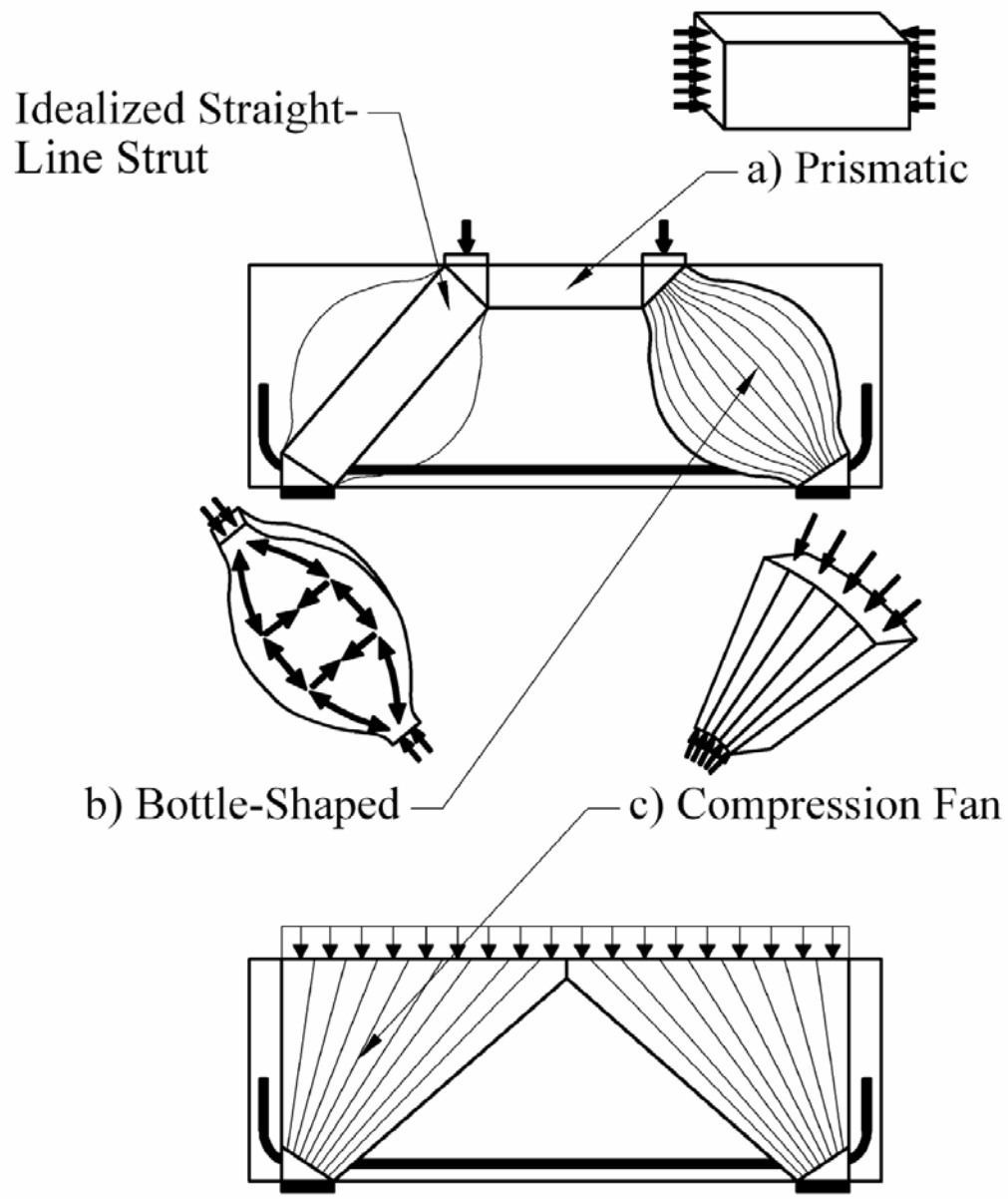

Figure 1-2: Geometric shapes of struts.

1.2.2 TIES

As previously stated, ties are STM members that are subjected to tensile forces. Although, concrete is known to have tensile capacity, its contribution to the tie resistance is normally neglected for strength considerations; therefore, only reinforcing or prestressing steel are used to satisfy the calculated tie requirements. Because only reinforcing or prestressing steel are attributed to the ties resistance, the geometry and the capacity of the tie are much easier to determine. In most of the design specifications, the capacity of a tie composed of reinforcing steel is determined by finding the product of the area of steel, A_{st}, and the yield strength of the steel, f_y. It should be noted that a designer must properly detail the anchorage length of the tie to ensure that the tie develops its yield strength before it reaches any location where the yield force is expected.

1.2.3 NODES

The limiting compressive strength of a node is typically determined by finding the product of the concrete compressive strength and a reduction factor. The reduction factor is determined based on the node type. Most design specifications recognize three major node types: CCC, CCT, and CTT nodes. A CCC node is bound by only struts. A CCT node anchors one tie, and a CTT node anchors two or more ties. Some documents, like Bergmeister et al. (1993), recognize the possibility of TTT nodes; however, most design specifications do not recognize these nodes. The geometry of a node is determined by bearing conditions, the details of anchored reinforcement, and the geometry of struts connected to node. See Fig. 1-3 for illustrations of the different node types taken from Mitchell et al. (2004).

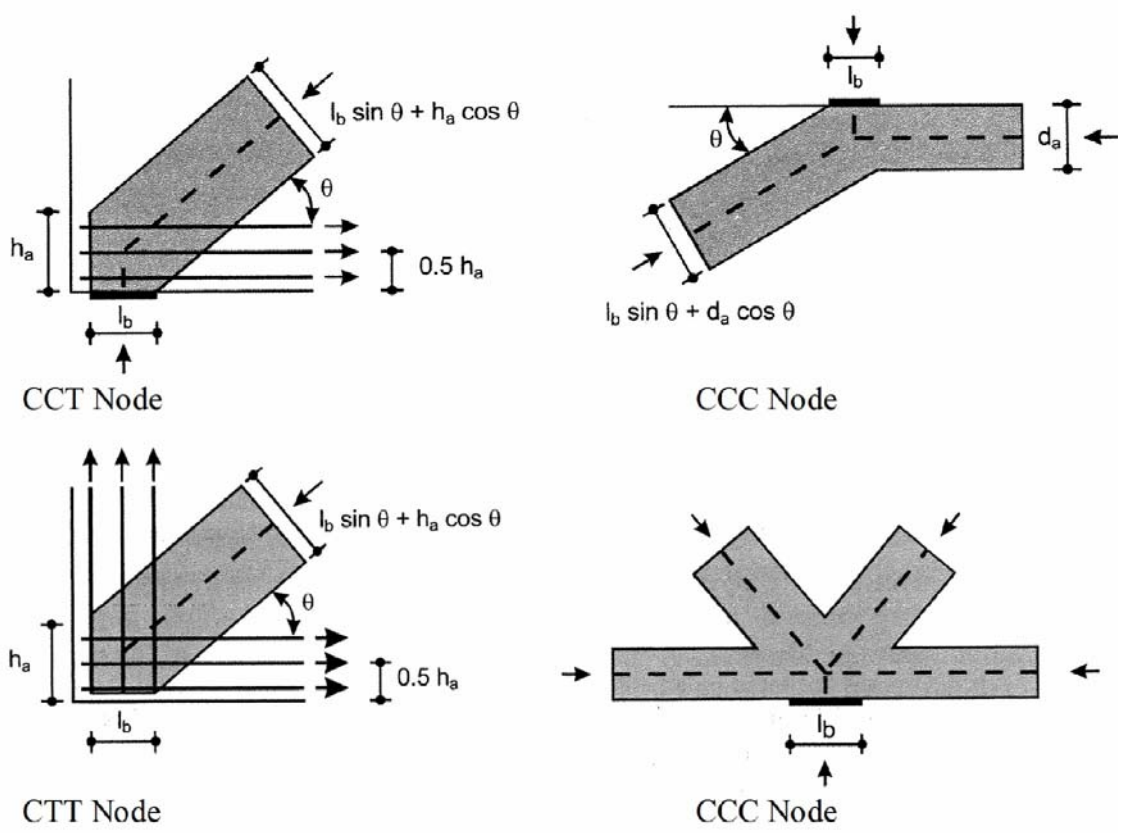

Figure 1-3: Types of strut-and-tie model nodes (Mitchell et al. 2004).

As discussed by Brown et al. (2006) nodes can be detailed to be either hydrostatic or non-hydrostatic in theory. For a hydrostatic node, the stress acting on each face of the node is equivalent and perpendicular to the surface of the node. Because stresses are perpendicular to the faces of hydrostatic nodes, there are no shear stresses acting on the face of a hydrostatic node. However, achieving hydrostatic nodes for most STM geometric configurations is nearly impossible and usually impractical. For this reason, most STMs utilize non-hydrostatic nodes. For non-hydrostatic nodes, Schlaich et al. (1987) suggest that the ratio of maximum stress on a face of a node to the minimum stress on a face of a node should be less than 2. The states of stress in both hydrostatic and non-hydrostatic nodes are shown in Figure 1-4.

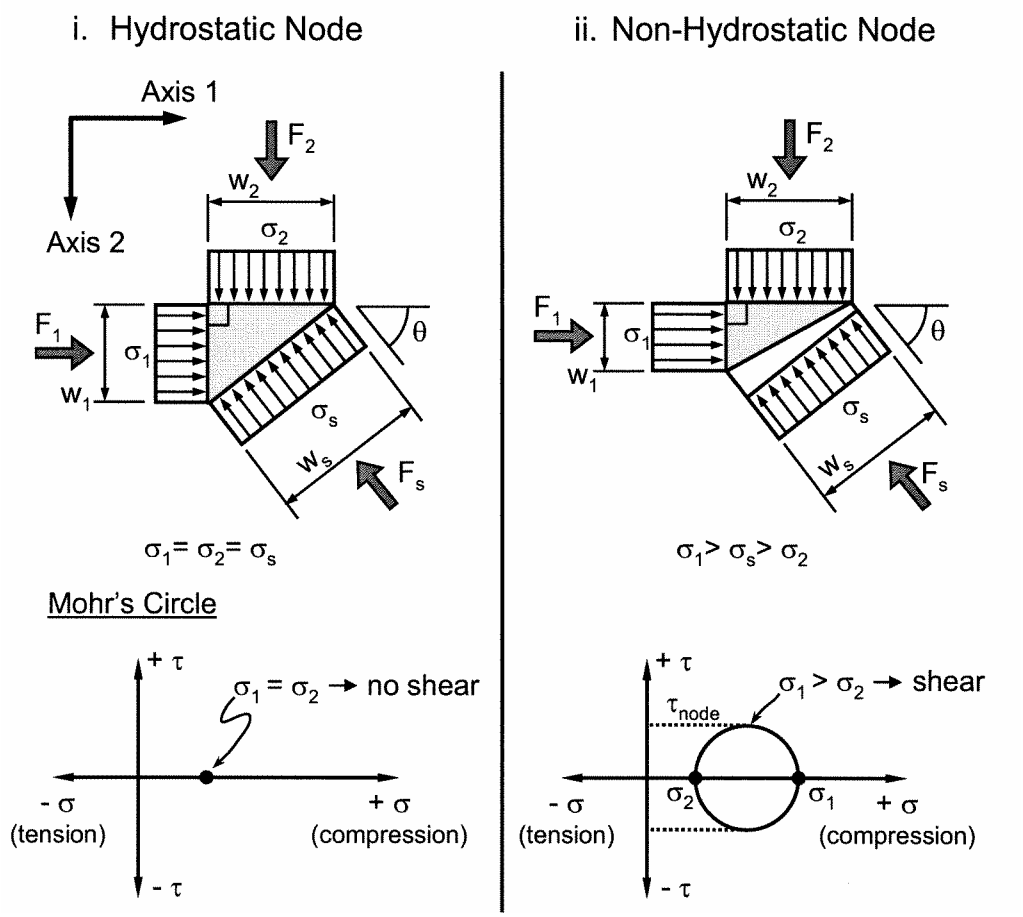

Figure 1-4: States of stress in hydrostatic and non-hydrostatic nodes (Brown et al. 2006).

1.3 HISTORICAL DEVELOPMENT

The idea of using a truss model for design and detailing of concrete structures is not a recent development. The concept was first proposed by Ritter (1899) and Mörsch (1909) in the early 1900's for shear design of flexural members. With the introduction of simple and safe sectional models for shear design, truss modeling fell out of favor in North America. The method began receiving notice again in the early 1970's as a tool for the evaluation of concrete members subjected to a combination of shear and torsion (Lampert and Thurliman 1971). The method began to receive wide-spread acceptance with publications by Collins and Mitchell in 1986 and Schlaich, Schafer, and Jennewein in 1987. The method was considered quite effective in concrete members where load discontinuities or geometric changes occurred and was considered by some to be the first step in the development of a unified design method for structural concrete.

In 1994, the first edition of the AASHTO LRFD Bridge Design Specifications made reference to using the STM for the design and detailing of concrete members under certain circumstances (Highway 1994). This, in conjunction with the mandatory implementation of the LRFD Specification scheduled for projects beginning in October, 2007, has generated a great deal of interest in the method as well as concern by some in the design community regarding the proper

application of STM principles, not only for new designs but in existing structures as well. It is clear that a better understanding of the proper application of STM principles is needed.

1.4 PROJECT OBJECTIVES

The objectives of this project are (1) to critically review and expand, if necessary, existing STM provisions of the AASHTO LRFD Bridge Design Specifications, and (2) to develop design examples to help implement the STM provisions for design of new structures and for evaluation of existing structures.

The project consists of seven tasks. These tasks consist of the following:

- **Task 1** – Conduct a search for analytical and experimental investigations related to STM.
- **Task 2** – Compare predictions of AASHTO LRFD STM provisions with a) data gathered in Task 1, b) designs based on past practices, prior to the adoption of the STM and c) predictions of ACI 318, Canadian, European, and other building and bridge design specifications. Identify gaps and needed guidance to assist designers in the application of STM. The guidelines should include limits of applicability of STM and cases where the application of STM is required.
- **Task 3** – Develop representative basic strut-and-tie models applicable to typical bridge elements. Provide guidance for selection of nodes and nodal zones and nodal spacing, size of struts, critical sections for anchorage or ties, and stiffness values of struts and ties for analysis purposes. Such stiffness expressions are needed to determine forces of statically indeterminate trusses.
- **Task 4** – Propose revisions to AASHTO LRFD specifications for the STM. The STM is intended for design at the strength limit state. Guidance is also needed for service limit state checks.
- **Task 5** – Develop design examples fully illustrating the application of provisions for design and or evaluation. A minimum of 10 examples are expected in addition to those available in PCA's *AASHTO LRFD Strut-and-Tie Model Design Examples*. A format similar to that used in the PCA document is expected.
- **Task 6** – Prepare agenda items for the revised recommended specifications and commentary.
- **Task 7** – Prepare a final report documenting the research effort.

CHAPTER 2- LITERATURE SEARCH (TASK 1)

2.1 INTRODUCTION

A literature search of domestic and international publications has been performed to identify previous analytical and experimental investigations that have been conducted related to strut-and-tie models. A complete list of publications and abstracts arranged by categories related to the project's objective can be found in Appendix B. This is not meant to be an all encompassing listing of articles, but a general listing of those articles that could be considered particularly apropos to this project.

In addition to the publications in Appendix B, the strut-and-tie model provisions of several design specifications were also analyzed. In addition to the AASHTO LRFD Bridge Design Specification, the specifications examined for this research include the ACI 318-05, CSA A23.3 and CSA-S6-06 (Canada), NZS 3101 (New Zealand), DIN 1045-1 (Germany), CEB-FIP Model Code 90, and the 1999 FIP Recommendations. The references for each of these specifications can be found in Appendix C. Comparisons between the AASHTO LRFD and the other specifications are made in Section 4.1 of this report.

The journal articles, research reports, books, and building specifications were collected in order to make a comparison with the strut-and-tie model provisions of the AASHTO LRFD. Some of the collected materials have not been directly used for this report. All research materials directly used or referenced within this document are listed in the Bibliography.

2.2 OVERVIEW OF AVAILABLE LITERATURE

There are a significant number of research articles and other publications dealing with strut-and-tie modeling. Most of the available articles can be categorized as documents that deal with the general principles of strut-and-tie modeling, the process of determining the appropriate strength of struts, ties, and nodes, applying strut-and-tie models to specific structural elements, serviceability requirements, or a combination of these.

By far, information regarding the general principles of strut-and-tie modeling is the most extensively reported. Generally, these types of articles outline the procedure for determining B- and D-regions, determining boundary conditions, developing a truss model, solving for member forces, choosing and detailing reinforcement, and checking the stress conditions of nodes and struts. Work done by Marti (1985), Collins and Mitchell (1986), and Schlaich et al. (1987) are some of the most complete and informative works of this type. In addition to outlining the strut-and-tie model procedure, these documents also give suggestions for strut and node strengths and show some basic models for simple structural elements. These documents were some of the building blocks for in-depth research and reports that more closely examined items such as strut and node strengths, detailing and anchorage requirements for reinforcement, and strut-and-tie models for increasingly complex structural members. A report by Bergmeister et al. (1993) summarizing the results of several research projects is an excellent example of this type of work.

The literature search for articles dealing with the strength of struts and nodes also yielded a large amount of data. Determining the appropriate effective compressive strengths for different types of nodes and struts has been of interest to many researchers. Researchers have tried to determine the strengths for the different types of nodes and struts through both lab testing and analytical research. Some, like Bermeister et al. (1993), made suggestions for node and strut strengths based on data collected in several experiments. Others, like Alshegeir (1992) and Yun and Ramirez (1996), made comparisons to other work or experimental results and performed nonlinear finite element analyses in order to determine the effective compressive strength of nodes and ties. Despite the vast amount of research done in this area, there is no clear consensus among researchers on the strength of struts and nodes. This is also reflected in the different design specifications reviewed for this project.

There are also many references that focus on strut-and-tie models for a particular structural element. The most typical structural elements utilized in these references are deep beams, deep beams with openings, corbels, pile caps and footings, dapped-end beams, and anchorage zones. Usually, these types of documents compare and contrast the performance of a member based on various strut-and-tie model designs to determine if certain models yield more desirable results than others. Maxwell and Breen (2000) performed this type of study on a deep beam with an opening. In addition, some of these papers also explored the effects of changing the reinforcement details for the same strut-and-tie model. Items that are usually adjusted include anchorages, stirrup spacing, longitudinal reinforcement spacing, and crack control reinforcement. Aguilar et al. (2002) performed a similar experiment on a strut-and-tie model for a deep beam. Articles that deal with the development of several different models for a particular structural element can be quite useful in order to give a designer ideas about what types of models work best.

As of now, it does not appear that there is a significant amount of research relating to serviceability requirements when using strut-and-tie modeling for design. The vast differences in the crack control reinforcement from specification to specification indicate that there is absolutely no consensus among researchers and designers as to what the minimum serviceability requirements should be. Research dealing with crack control as it relates to strut-and-tie models is currently limited. Zhu et al. (2003) have done research regarding predicting crack width for dapped-end beams and corbels, but did not comment on the effect of crack control reinforcement. Brown et al. (2006) performed a study about the minimum reinforcement in bottle-shaped struts and were able to comment on what the minimum amount of crack control reinforcement should be, but crack control requirements were beyond the scope of the research. Clearly, more research regarding this topic needs to be done.

CHAPTER 3 – APPLICATION OF THE STRUT-AND-TIE MODEL (TASKS 2 AND 3)

3.1 WHEN IS IT USED?

Concrete structural elements can be divided into two general regions: flexural regions (Bernoulli or B-regions) and regions near discontinuities (Disturbed or D-regions). In the case of the B-regions, it is accurate to assume that planes remain planes after loading, and the plane section assumption of flexural theory can be applied. In the case of B-regions, the load path of applied forces is of little interest. In general, any portion of a structural member outside of a B-region is a D-region.

Strut-and-tie models are used primarily to design regions near discontinuities or D-regions. Global strut-and-tie models (models used to design an entire structural member) can be used; however, it is best to focus on local strut-and-tie models (models used to design D-regions) since B-regions are more easily designed with conventional methods. A discontinuity in the stress distribution occurs at an abrupt change in the geometry of a structural element (geometric discontinuities), at a concentrated load or reaction (loading or statical discontinuities), or a combination of the two (loading and geometric discontinuities). St. Venant's principle indicates that the stress due to axial load and bending approach a linear distribution at a distance approximately equal to the maximum cross-sectional dimension of a member, h, in both directions, away from a discontinuity. Figure 3-1 shows an illustration of St. Venant's principle.

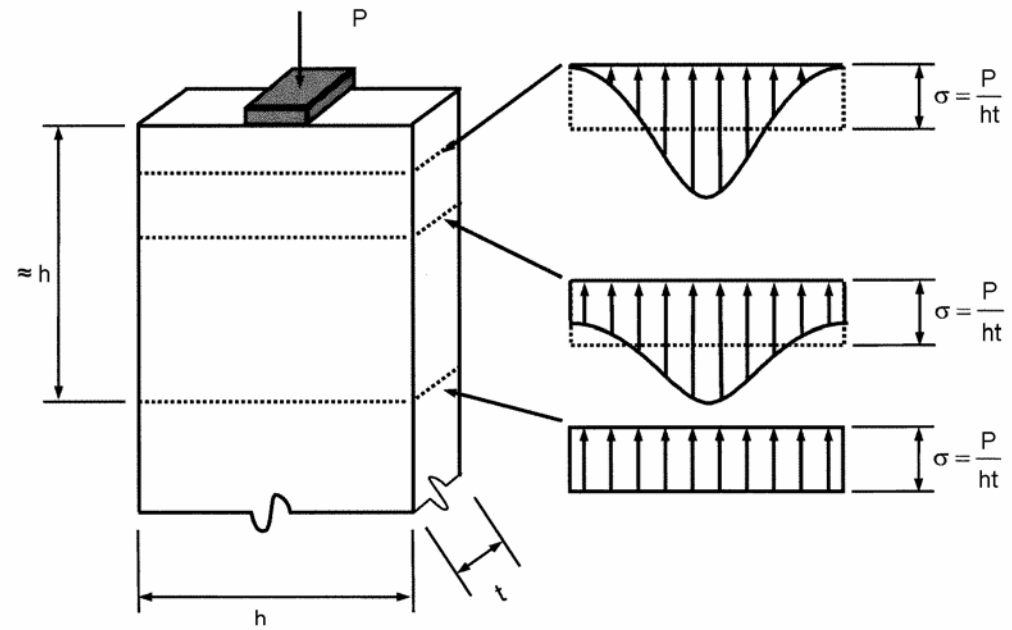

Figure 3-1: St. Venant's principle (Brown et al. 2006).

For this reason discontinuities are assumed to extend a distance h from the section where the load or change in geometry occurs. Figure 3-2 illustrates examples of discontinuities with the resulting D-regions shaded.

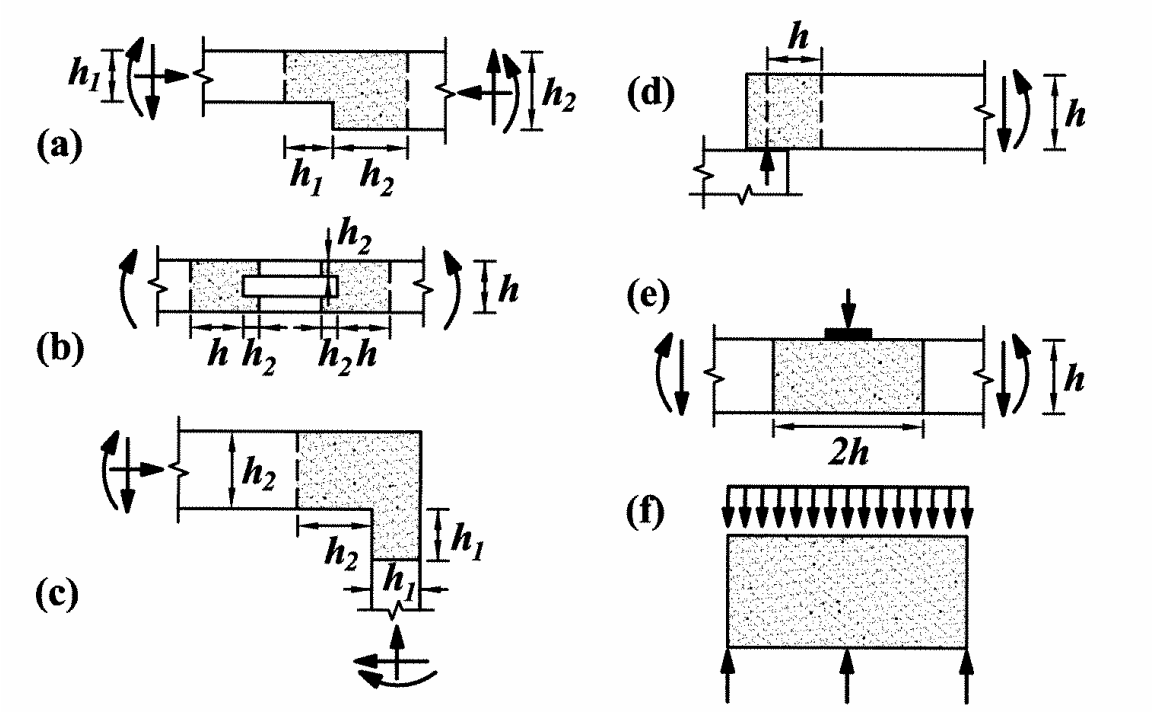

Figure 3-2: Examples of D-regions (ACI 2005).

Consider a simple span beam of depth h with a concentrated load at mid-span (see Figure 3-3). As illustrated this beam has three disturbed regions, one at each end of the beam and one at mid-span. According the St. Venant's principle, the disturbed regions at each end of the beam will have a length equal to h, and the region at mid-span will have a length equal to 2h. If the span of the beam is reduced such that the distance between the applied load and the end reaction is less than 2h, the disturbed regions overlap. Hence the entire beam will be considered a D-region and the behavior of the beam will be strongly influenced by the disturbed flow of stresses. For this case the strut-and-tie model approach would be appropriate for design. Typical girders used in bridge design have span lengths of 20h to 25h. Therefore, with the exception of the ends of the girders, if there are no geometric discontinuities within the span, the presence of disturbed regions due to loading have little effect on the overall behavior of the member and the localized effects can generally be ignored.

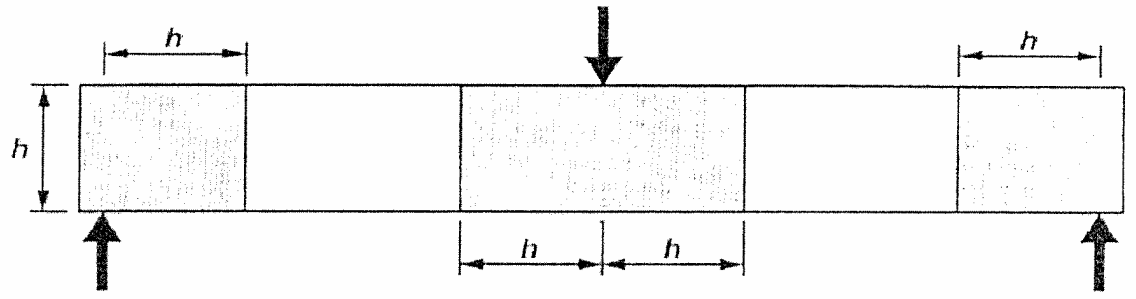

Figure 3-3: Simple span beam used for discussion above.

For B-regions, the AASHTO LRFD Specifications permit the use of either traditional section models or the strut-and-tie model. For regions near significant discontinuities, the use of the strut-and-tie model or some type of inelastic approach should be used. A concentrated load which causes more than 50% of the shear at the face of a support and is closer than 2d from the support face is a situation that requires a strut-and-tie model or some type of inelastic approach.

3.2 PROCEDURE FOR STRUT-AND-TIE MODELING

The process used in the development of a STM model is illustrated in Figure 3-4.

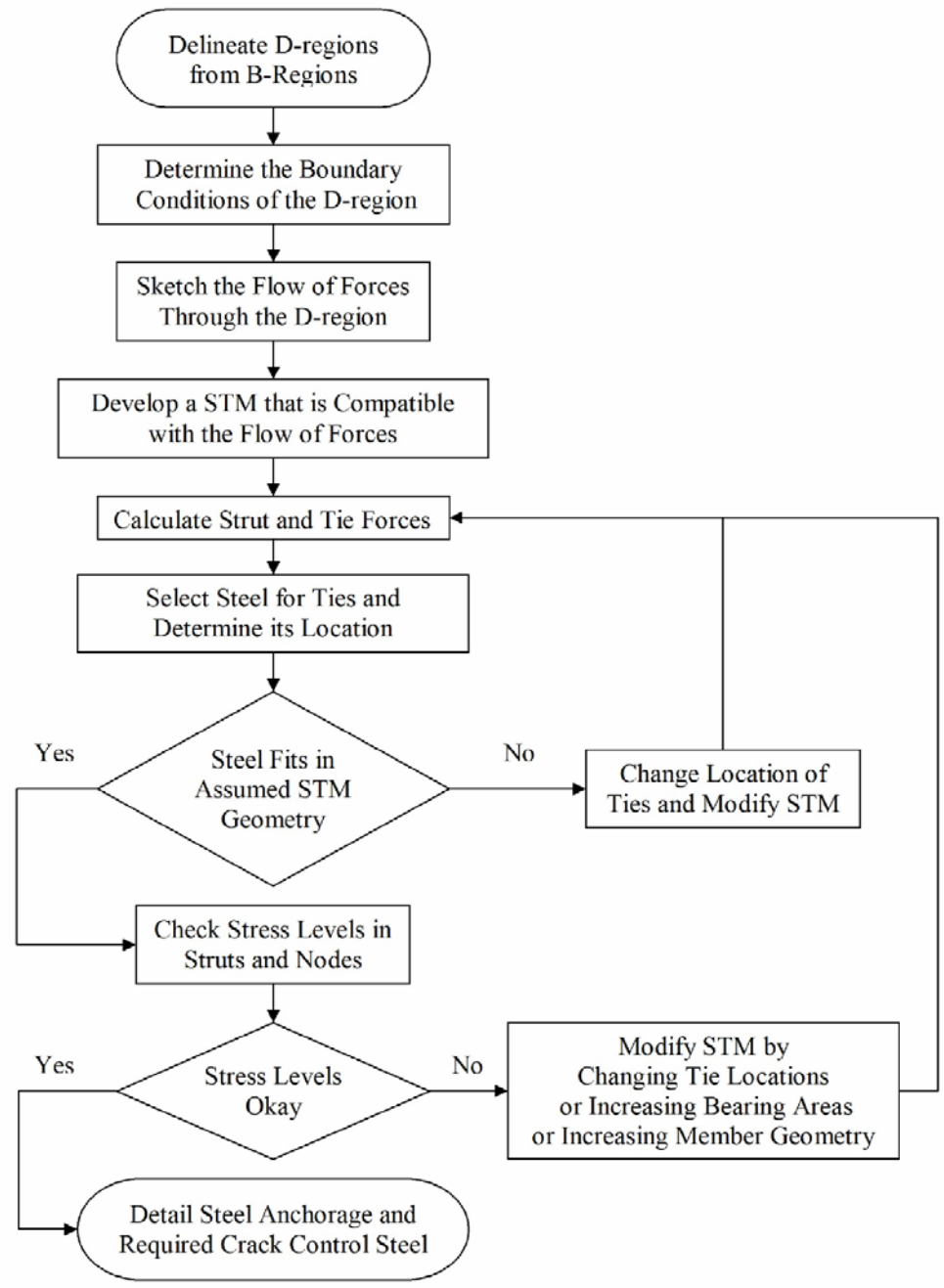

Figure 3-4: Flowchart illustrating STM steps. (Brown et al. 2006)

3.2.1 STEP 1 – DELINEATE THE D-REGIONS

As discussed in the previous section, the extent of a D-region can be determined using St. Venant's principle. Using St. Venant's principle, a D-region is assumed to extend a distance equal to the largest cross-sectional dimension of the member away from a geometrical discontinuity or a large concentrated load. The determined B-region/D-region interface is the assumed location where the stress distribution becomes linear again. Using this basic assumption, the D-regions can be delineated.

3.2.2 STEP 2 – DETERMINE THE BOUNDARY CONDITIONS OF THE D-REGIONS

Once the extent of a D-region has been determined, the bending moments, shear forces, and axial forces must be determined at the B-region/D-region interface from analysis of the B-region. Using B-region analysis, the bending moment, shear force, and axial force are then used to determine the stress distribution at the B-region/D-region interface. The calculated stress distributions at the B-region/D-region interface can then be modeled as equivalent point loads. The location and magnitude of the equivalent point loads is determined from the stress distributions directly. When determining the boundary conditions on the B-region/D-region interface, it is essential that equilibrium be maintained on the boundary between B- and D-regions. If the bulk of the structure falls into a D-region it may be expediate to use a global model of the structure and use the external loads and reactions as the boundary conditions.

3.2.3 STEP 3 – SKETCH THE FLOW OF FORCES

After the stress distributions acting on the B-region/D-region interface have been modeled as equivalent point loads, the flow of forces through the D-region should be determined. For most design cases, the flow of forces can easily be seen and sketched by the designer. When the flow of forces becomes too complex to be approximated with a sketch, a finite element analysis can be used to determine the flow of forces through a reinforced concrete structural member. For most D-regions, such efforts are unwarranted since the stress paths can be estimated easily. Another method used by many to determine the flow of forces is the load path method as proposed by Schlaich et al. (1987). The reader is encouraged to review this approach as well.

3.2.4 STEP 4 – DEVELOP A STM

A STM should be developed to model the flow of forces through the D-region determined in the previous step. When developing a STM, try to develop a model that follows the most direct force path through the D-region. Also, avoid orienting struts at small angles when connected to ties. According to Collins and Mitchell, as the angle between a strut and tie decreases, the capacity of the strut also decreases (1986). For this reason, many design specifications specify a minimum angle between struts and ties. It should be noted that the AASHTO LRFD provisions do not specify a minimum angle between struts and ties; however, the limiting strut compressive stress equation defined in the specification is a function of the angle between the strut and tie and decreases as the angle between the strut and tie decreases. A detailed presentation of different code provisions are givenin Chapter 4.

A D-region may be subjected to more than one type of loading. It is imperative that a STM be developed and analyzed for each different loading case. On a similar note, for a given load case for a D-region, more than one STM can be developed. Schlaich and Schäfer (1991) suggest that models with the least and shortest ties are the best. In addition, Schlaich and Schäfer also

suggest that two simple models can sometimes be superimposed to develop a more sophisticated model that better models the flow of forces through a D-region.

Also, Brown et al, (2006) explain that "it is preferable to have a model that is statically determinant". Statically determinant models require no knowledge of the member stiffnesses which makes it simple to calculate member forces. Conversely, statically indeterminant structures require that member stiffnesses be estimated. Estimating the member stiffnesses of a STM is often difficult because the true geometry of the struts can be difficult to accurately determine.

3.2.5 STEP 5 – CALCULATE THE FORCES IN THE STRUTS AND TIES

The strut and tie forces can be calculated knowing the geometry of the developed STM and the forces acting on the D-region. It is desirable to use a computer program to calculate the forces because, often times, the geometry of the STM may need to be modified during the design process which will require the forces in the struts and ties to be recalculated.

3.2.6 STEP 6 – SELECT STEEL AREA FOR THE TIES

The required amount of reinforcement for each tie can easily be determined by dividing the force in the tie by the product of the yield stress of the steel and resistance factor specified by a design specification. The reinforcement chosen to satisfy the steel requirements must be placed so that the centroid of the reinforcement coincides with the centroid of the tie in the STM. If reinforcement chosen to satisfy the tie requirements can not fit in the assumed location of the tie, the location of the tie in the STM needs to be modified, and the member forces need to be calculated again.

3.2.7 STEP 7 – CHECK STRESS LEVELS IN THE STRUTS AND NODES

The stress levels in all of the struts and nodes must be compared to the allowable stress limits given in design specifications. In order to determine the stress levels in the struts and nodes, the geometry of the struts and nodes must first be estimated. The geometry of the struts and nodes can be determined based on the dimensions of bearing pads and the details of reinforcement connected to the struts and nodes.

Accurately determining the geometry of internal struts and nodes not attached to bearing pads and reinforcement is more difficult than finding the geometry of struts and nodes directly in contact with the boundary of the D-region. In the case of internal nodes and struts, it may not be possible to precisely define the strut and node geometry. Brown et al. (2006) explain that this uncertainty is acceptable because force redistribution can take place for internal struts and nodes.

When stresses in struts and nodes are found to be larger than permissible stresses, bearing areas, the reinforcement details, or the overall member geometry of the member can be modified in an effort to increase the overall geometry of the strut and/or node. When changing any or all of these items, the STM will likely need to be modified. If the STM is modified, the member forces need to be calculated again, the ties may need to be redesigned, and then, the stresses in the struts and nodes can be checked again. The concrete strength can be increased if modifying the geometry of the STM or the member itself is not possible.

3.2.8 STEP 8 – DETAIL REINFORCEMENT

Once all the steel chosen for the ties in the STM has been finalized, the anchorage of the reinforcement must be properly detailed in order for it to reach its yield stress prior to leaving nodal zones. In addition, appropriate crack control should be placed in areas that are expected to be subject to cracking. Most design specifications specify a minimum amount of crack control that must be placed in a D-region that has been designed with a STM.

CHAPTER 4 – COMPARISONS OF AASHTO LRFD STM REQUIREMENTS (TASK 2)

The first objective of this chapter is to compare the predictions of the AASHTO LRFD STM provisions with the requirements of other widely accepted design specifications and designs based on past practice prior to the adoption of STM. The second objective is to identify limits of applicability, of STM, where STM is required, gaps in the specification, and guidance needed to assist designers in the application of STM.

4.1 COMPARISONS TO OTHER DESIGN SPECIFICATIONS

4.1.1 PURPOSE OF DESIGN SPECIFICATION COMPARISON

The strut-and-tie model provisions of several design specifications were analyzed in order to make comparisons to the strut-and-tie model provisions of the AASHTO LRFD Bridge Design Specification. The specifications that were analyzed include ACI 318-05, CSA A23.3 (Canadian concrete specification), CSA-S6-06 (Canadian Highway Bridge Design Code), NZS 3101 (New Zealand Concrete Structures Standard), DIN 1045-1 (German concrete specification), CEB-FIP Model Code 90, and the 1999 FIP Recommendations. In addition, to this comparison, the data collected from each of the specifications, including the AASHTO LRFD Bridge Design Specification, was used to determine the capacity of previously tested specimens. The results from these analyses were used to make further comparisons between the AASHTO LRFD and the other specifications. Ultimately, any significant findings may be used to revise the AASHTO LRFD strut-and-tie provisions.

4.1.2 SYNOPSIS OF DESIGN SPECIFICATION COMPARISON

By performing this comparison, it became clear that, even though strut-and-tie models are considered an appropriate design method for D-regions, there is no consensus regarding model geometry, strut and node compressive strengths, and appropriate crack control reinforcement. The contents of the following discussion are summarized in Tables 4-1 and 4-3 which outline the specified strengths of struts, ties, and nodes for each design specification with the corresponding reference. Tables 4-2 and 4-4 give the definitions of the variables for each of the specifications.

All of the design specifications that were investigated provided very little or no guidance with respect to setting up the geometry of a strut-and-tie model. The ACI 318-05, NZS 3101, and DIN 1045-1 specifications all specify minimum angles between a strut and a tie of 25, 25, and 45 degrees respectively. Similarly, the CEB-FIP Model Code 90 suggests that "struts and ties …should normally meet at angles of about 60^{o} and not less than 45^{o}." Neither the AASHTO LRFD, CSA A23.3, nor the CSA-S6-06 specifies a minimum angle between struts and ties. The AASHTO LRFD, however, has an excellent section on anchorage zones which shows several example models for various anchorage zone configurations. With respect to this, AASHTO LRFD contains more guidance on model geometry, but it is limited to anchorage zones with the exception of some figures in the commentary for various other structures generally associated with strut-and-tie models.

Typically, after the geometry of a strut-and-tie model has been established and the forces in the ties and struts have been determined, most designers will select their tensile reinforcement to fulfill the calculated tie requirements. Designers do this because selecting steel is the most

straight forward part of performing a strut-and-tie analysis, and the arrangement of the steel often determines the widths of struts and nodes. For the most part, all of the specifications specify the capacity of the tie as the product of the yield stress and the area of steel. The product of the stress and the area of the prestressing tendons are also added to tensile force of the tie when appropriate.

The limiting compressive stress of struts varies from specification to specification. The AASHTO LRFD, CSA A23.3, and CSA-S6-06 all specify the strut compressive strengths as a function of the tensile strain in the concrete in the direction of a tie and the angle between the strut and the tie. In addition, both the CSA A23.3 and the AASHTO LRFD limit the maximum compressive stress in a concrete strut to 85 percent of the uniaxial cylinder compressive strength (f'_c). For the CSA-S6-06, this value can drop to 67 percent depending on the concrete strength used. The ACI 318-05, NZS 3101, DIN 1045-1, CEB-FIP Model Code 90, and 1999 FIP Recommendations specify the strut compressive strength as a function of the product of the concrete compressive strength and a reduction factor. Reduction factors take into account strut geometry, the type of concrete (normal weight, light weight, etc.), whether the strut is in a cracked or uncracked region, and whether appropriate crack control reinforcement has been used.

All of the specifications specify node compressive strengths as the product of the concrete compressive strength and a reduction factor. Most of the specifications specify the reduction factor based on the type of nodes. In total, there are three basic types of nodes that are acknowledged by design specifications: nodes bound by compression struts only (CCC), nodes anchoring one tension tie (CCT), and nodes anchoring two or more tension ties (CTT). It should be noted that the 1999 FIP Recommendations and the DIN 1045-1 are the only specifications that specify the use of biaxial or triaxial compression for CCC nodes. This allows the designer to use a strength that is larger than the uniaxial concrete compressive strength. All the other specifications still use a reduction factor for CCC nodes.

In addition, all of the specifications specify a minimum amount of crack control reinforcement. With the exception of the CEB-FIP Model Code 90, each specification is very specific about the amount and arrangement of reinforcement required. The AASHTO LRFD, CSA A23.3, and CSA-S6-06 all require an orthogonal grid of reinforcement near each face. The AASHTO LRFD and CSA-S6-06 require a steel reinforcement area to gross concrete area ratio of 0.003 in each direction, and the CSA A23.3 requires a steel reinforcement area to gross concrete area ratio of 0.002 in each direction. The ACI 318-05 and the NZS 3101 both require the ratio of steel area perpendicular to the strut to concrete area to be 0.003. For each specification, the ratio of steel area perpendicular to the strut to gross concrete area is determined as follows:

$$\sum \frac{A_{si}}{b_s s_i} \sin(\alpha_i) \leq 0.003$$

where:

A_{si} = area of surface reinforcement at spacing s_i.
b_s = width of strut.
α_i = angle at which layer of reinforcement crosses strut.

For most strut inclinations, the crack control provisions of the CSA A23.3 and the ACI 318-05 and NZS 3101 are nearly the same. The DIN 1045-1 specifies minimum crack control reinforcement as a function of both the concrete and steel strengths, and the 1999 FIP Recommendations specify spacing limits.

The strut-and-tie model provisions in the AASHTO LRFD, CSA A23.3, and CSA-S6-06 are very similar. Also, the ACI 318-05 and NZS 3101 have very similar strut-and-tie provisions. Besides the aforementioned similar documents, the provisions for node compressive strengths, strut compressive strengths, and crack control reinforcement are inconsistent from specification to specification. All of the specifications, especially the CEB-FIP Model Code 90, could have more detailed strut-and-tie model provisions, and give more guidance about developing the geometry of strut-and-tie models. By far, the 1999 FIP Recommendations are the most thorough and understandable to follow.

Using experimental data from laboratory tests, the accuracy and conservatism of the strut-and-tie model provisions from each of the design specifications was verified. See Section 4.2 of this report for the analysis and results. The CSA-S6-06 was not included in this analysis because the information was added after the strut-and-tie analyses had been performed. Based on the information provided about the strut-and-tie model provisions of the design specifications in this section and the results of the strut-and-tie model analyses in Section 4.2, recommendations for changes to the AASHTO LRFD Bridge Design Specification may be made. Chapter 5 provides recommendations for changes to the strut-and-tie model provisions of the AASHTO LRFD Bridge Design Specification.

Furthermore, in addition to Tables 4-1 through 4-4, more strut-and-tie model provisions are given from other sources in Tables 4-5 and 4-6. These tables are provided for additional comparison to the strut-and-tie model provisions of the AASHTO LRFD Bridge Design Specification.

Table 4-1: Strut strength and crack control comparison for each design specification.

Specification	Strut Compressive Capacity without Longitudinal Reinforcement	Strut Compressive Capacity w/Longitudinal Reinforcement	Minimum Crack Reinforcement Across Strut (Crack Control)
AASHTO LRFD	$f_{cu}A_{cs}$, where $f_{cu} = \frac{f'_c}{0.8 + 170\varepsilon_1} \le 0.85 f'_c$ $\varepsilon_1 = \varepsilon_s + (\varepsilon_s + .002)\cot^2\alpha_s$ (§ 5.6.3.3.3)	$f_{cu}A_{cs} + f_y A_{ss}$ (§ 5.6.3.3.4)	• Must have orthogonal grid of reinforcing bars near each face • Spacing ≤ 12.0 in. • $\frac{AreaReinf_{eachdirection}}{GrossAreaConc} \ge 0.003$ (§ 5.6.3.6)
ACI 318-05	$0.85\beta_s f'_c A_{cs}$ Prismatic: β_s= 1.0 Bottle-Shaped w/reinf. satisfying crack control: β_s= 0.75 Bottle-Shaped not satisfying crack control: $\beta_s = 0.60\lambda$ λ =1.0 for normal weight concrete λ =0.85 for sand-lightweight concrete λ =0.75 for all lightweight concrete Strut in tension members: β_s= 0.40 All other cases: β_s= 0.60 (§ A.3)	$f_{cu}A_c + f'_s A'_s$ (§ A.5)	For $f'_c \le 6000$ psi $\sum \frac{A_{si}}{b_s s_i}\sin(\alpha_i) \ge 0.003$ (§ A.3.3.1)
CSA A23.3	$f_{cu}A_{cs}$, where $f_{cu} = \frac{f'_c}{0.8 + 170\varepsilon_1} \le 0.85 f'_c$ $\varepsilon_1 = \varepsilon_s + (\varepsilon_s + .002)\cot^2\alpha_s$ (§ 11.4.2.3)	$f_{cu}A_c + f'_s A'_s$ (§ 11.4.2.4)	• Must have orthogonal grid of reinforcing bars near each face • Spacing ≤ 300mm • $\frac{AreaReinf_{eachdirection}}{GrossAreaConc} \ge 0.002$ (§ 11.4.5)
CSA S6-06	$f_{cu}A_{cs}$, where $f_{cu} = \frac{f'_c}{0.8 + 170\varepsilon_1} \le \alpha_1 \cdot f'_c$ $\varepsilon_1 = \varepsilon_s + (\varepsilon_s + .002)\cot^2\theta_s$ $\alpha_1 = 0.85\text{-}0.0015 f'_c$ (§ 8.10.3.3)	$f_{cu}A_{cs} + f_y A_{ss}$ (§ 8.10.3.4)	• Must have orthogonal grid of reinforcing bars near each face • Spacing ≤ 300mm • $\frac{AreaReinf_{eachdirection}}{GrossAreaConc} \ge 0.003$ • Not more than 1500 mm^2/m each face (§ 8.10.5.1)
NZS 3101	$0.85\beta_s f'_c A_{cs}$ Prismatic: β_s= 1.0 Bottle-Shaped w/rein. satisfying crack control: β_s= 0.75 Bottle-Shaped not satisfying crack control: $\beta_s = 0.60\lambda$ λ =1.0 for normal weight concrete λ =0.85 for sand-lightweight concrete λ =0.75 for all lightweight concrete Strut in tension members: β_s= 0.40 All other cases: β_s= 0.60 (§ A5.2)	$f_{cu}A_c + f'_s A'_s$ (§ A5.5)	For $f'_c \le 40$ MPa $\sum \frac{A_{si}}{b_s s_i} f_y \sin(\gamma_i) \ge 1.5 MPa$ (§ A.3.3.1)
DIN1045-1	$1.0\eta_1 f_{cd} A_{cs}$ Uncracked Concrete Compressive Zones $0.75\eta_1 f_{cd} A_{cs}$ Parallel to Cracks η_1 = 1.0 for normal weight concrete η_1 = 0.4 + 0.6(ρ/2200) for lightweight concrete (§ 10.6.2)	No direct mention of subject. "design stress in strut reinforcement shall not exceed f_{yd}" (§ 10.6.2)	$\rho_w = \frac{A_{sw}}{s_w b_w \sin(\alpha)} \ge \rho$ $\rho = 0.16(f_{ctm}/f_{yk})$ (§ 13.2.3)*

Table 4-1 (Continued): Strut strength and crack control comparison for each design specification.

Specification	Strut Compressive Capacity without Longitudinal Reinforcement	Strut Compressive Capacity w/Longitudinal Reinforcement	Minimum Crack Reinforcement Across Strut (Crack Control)
1999 FIP Recommendations	$f_{cd,eff}A_c = \upsilon_1 f_{1cd}A_{cs}$ or $\upsilon_2 f_{1cd}A_c$ $\upsilon_1 = (1 - f_{ck}/250)$ rectangular, uncracked stress block $\upsilon_2 = 1.0$ uniform strain/uncracked $\upsilon_2 = 0.80$ parallel cracks w/bonded reinforcement $\upsilon_2 = 0.60$ compression across small cracks $\upsilon_2 = 0.45$ compression across large cracks (§ 5.3.2)	$A_c f_{cd,eff} + A_{sc}\sigma_{scd}$ (§ 5.3.3)	Must have orthogonal grid of "skin reinforcement" with $s_t \leq 100$ mm $A_{st} = 0.01 s_t b_c$ for stirrups $A_{st} = 0.020 s_t b_c$ for longitudinal rein. (gen.) $A_{st} = 0.015 s_t b_c$ for longitudinal rein. (post-tensioned members) (§ 7.5.5)*
CEB-FIP Model Code 90	$f_{cd1}A_{cs}$ or $f_{cd2}A_{cs}$ Uncracked Concrete Compressive Zones $f_{cd1} = .85\left(1 - \frac{f_{ck}}{250}\right) f_{cd}$ Cracked Concrete Compressive Zones $f_{cd2} = .60\left(1 - \frac{f_{ck}}{250}\right) f_{cd}$ (§ 6.8.1.2 and 6.2.2.2)	No direct mention of subject with respect to strut-and-tie models.	Does not give much guidance. States, "A minimum amount of reinforcement…for crack control." Gives some guidance for pure tension and flexure. (§ 7.4.5)

Table 4-2: Definitions for variables referenced in Table 4-1 for each design specification.

AASHTO LRFD	A_{cs} = area of concrete in the strut (in^2) A_{ss} = area of steel in the strut (in^2) f'_c = concrete compressive strength (ksi) f_{cu} = limiting concrete compressive strength (ksi) ε_s = the tensile strain in the concrete in direction of the tension tie (in/in)	CSA A23.3	A_{cs} = area of concrete in the strut (mm^2) A_{ss} = area of steel in the strut (mm^2) f'_c = concrete compressive strength (MPa) f_{cu} = limiting concrete compressive strength (MPa) ε_s = the tensile strain in the concrete in direction of the tension tie (mm/mm)
ACI 318-05	A'_s = area of compression steel (in^2) A_c = area of concrete in the strut (in^2) A_{cs} = area of concrete in the strut (in^2) A_{si} = total area of surface reinforcement at spacing s_i (in^2) f'_c = concrete compressive strength (ksi) f_{cu} = effective concrete compressive strength (ksi) α_i = the angle between the reinforcement and the axis of the strut (DEG.)	NZS 3101	A'_s = area of compression steel (mm^2) A_c = area of concrete in the strut (mm^2) A_{cs} = area of concrete in the strut (mm^2) A_{si} = total area of surface reinforcement at spacing s_i (mm^2) f'_c = concrete compressive strength (MPa) f'_s = steel compressive strength (MPa) f_{cu} = effective concrete compressive strength (MPa) γ_i = the angle between the reinforcement and the axis of the strut (DEG.)
DIN1045-1	A_{sw} = sectional area of the shear reinforcement (mm^2) b_w = width of the web (mm) f_{cd} = design concrete compressive strength = $\alpha(f_{ck}/\gamma_c)$ (MPa) f_{ck} = characteristic concrete compressive strength (MPa) f_{ctm} = mean axial tensile strength of concrete (MPa) f_{yd} = design yield strength of steel = f_{yk}/γ_s (MPa) f_{yk} = characteristic yield strength of reinforcing steel (MPa) s_w = spacing of the shear reinforcement elements (mm) α = angle of the shear reinforcement to the beam axis (§ 13.2.3) (DEG.) α = reduction factor taking into account long term affect on concrete strength = 0.85 γ_c = concrete partial safety factor = 1.5 γ_s = reinforcement partial safety factor = 1.15 ρ = density of concrete (§ 10.6.2) (kg/m^3) ρ = minimum shear reinforcement ratio (§13.2.3)	CEB-FIP Model Code 90	f_{cd} = design values of concrete compressive strength = f_{ck}/γ_c (MPa) f_{cd1} = uncracked compressive design strength (MPa) f_{cd2} = cracked compressive design strength (MPa) f_{ck} = characteristic concrete compressive strength (MPa) γ_c = concrete partial safety factor = 1.5
		1999 FIP Recommendations	A_c = area concrete compressive strut (mm^2) A_{sc} = area of compression steel (mm^2) A_{st} = area of crack control reinforcement (mm^2) f_{1cd} = uniaxial compressive design strength = $\alpha(f_{ck}/\gamma_c)$ (MPa) $f_{cd,eff}$ = effective compressive strength of strut (MPa) f_{ck} = characteristic concrete compressive strength (MPa) α = coefficient taking account of uniaxial strength in relation to strength control of specimen and duration of loading = 0.85 σ_{scd} = stress in compression steel (MPa)) γ_c = concrete partial safety factor = 1.5 υ_1 and υ_2 = reduction factors
CSA-S6-06	A_{cs} = area of concrete in the strut (mm^2) A_{ss} = area of steel in the strut (mm^2) f'_c = concrete compressive strength (MPa) f_{cu} = limiting concrete compressive strength (MPa) ε_s = the tensile strain in the concrete in direction of the tension tie (mm/mm)		

Table 4-3: Specified tie strengths, node strengths, and α_s[1] for each design specification.

Specification	Min. α_s[1] (deg.)	Tie Nominal Capacity	Node Compressive Stress
AASHTO LRFD	-	$f_y A_{st} + A_{ps}[f_{pe} + f_y]$ (§ 5.6.4.3.1)	CCC: $0.85f'_c$ CCT: $0.75f'_c$ CTT: $0.65f'_c$ (§ 5.6.3.5)
ACI 318-05	$\alpha_s \geq 25$ (§ A.2.5)	$A_{ts}f_y + A_{tp}[f_{se} + \Delta f_p]$ (§ A.4)	$.85\beta_n f'_c$ CCC: $\beta_n = 1.0$ CCT: $\beta_n = 0.8$ CTT: $\beta_n = 0.6$ (§ A.5)
CSA A23.3	-	$f_y A_{st}$ (§ 11.4.3.1)	CCC: $0.85f'_c$ CCT: $0.75f'_c$ CTT: $0.65f'_c$ (§ 11.4.4.1)
CSA-S6-06	-	$f_y A_{st} + f_{py} A_{ps}$ (§ 8.10.4.1)	CCC: $\alpha_1 \psi_c f'_c$ CCT: $0.88\alpha_1 \psi_c f'_c$ CTT: $\alpha_1 f'_c$ (§ 8.10.5.1)
NZS 3101	$\alpha_s \geq 25$ (§ A4.5)	$A_s f_y + A_{tp}[f_{se} + \Delta f_p]$ (§ A6.1)	$.85\beta_n f'_c$ CCC: $\beta_n = 1.0$ CCT: $\beta_n = 0.8$ CTT: $\beta_n = 0.6$ (§ A7.2)
DIN 1045-1*	$\alpha_s \geq 45$ (§ 10.6.3)	f_{yd} Max Stress of Tie $f_{p0.1k}/\gamma_s$ Max Stress in Prestressing Tie (§ 10.6.2)	$1.1\,\eta_1 f_{cd}$ CCC Nodes $0.75\,\eta_1 f_{cd}$ CCT and CTT Nodes with $\theta_s \geq 45$ $\eta_1 = 1.0$ for normal weight concrete $\eta_1 = 0.4 + 0.6(\rho/2200)$ for lightweight concrete (§ 10.6.3)
CEB-FIP Model Code 90*	$\alpha_s \approx 60$ $\alpha_s \geq 45$ (§ 6.8.1)	Max Stress of Tie f_{ytd} Max Stress in Prestressing Tie $f_{pyd,net} = 0.9f_{ptk}/\gamma_s - \sigma_{do} \leq 600$ MPA (§ 6.8.1.1 and 6.2.4)	CCC and CCT or CTT with $\theta_s \geq 55$ $0.85\left(1 - \frac{f_{ck}}{250}\right) f_{cd}$ CCT and CTT $0.60\left(1 - \frac{f_{ck}}{250}\right) f_{cd}$ (§ 6.9.2.1 and 6.2.2.2)
1999 FIP Recommendations	-	$A_s f_{yd} + A_p f_{ptd}$ (§ 5.2)	CCT and CTT $\upsilon_2 f_{1cd}$, where $\upsilon_2 = 0.85$ CCC Biaxial compression $1.20f_{1cd}$ Triaxial compression $3.88f_{1cd}$ (§ 5.6)

*Nominal stress in tie is specified rather than force.

[1] α_s = the angle between the compressive strut and adjoining tension tie (deg.)

Table 4-4: Definitions for variables referenced in Table 4-3 for each design specification.

AASHTO LRFD	A_{ps} = area of prestressing steel (in^2) A_{st} = total area of longitudinal steel reinforcement in the tie (in^2) f'_c = concrete compressive strength (ksi) f_y = yield strength of longitudinal steel reinforcement (ksi) f_{pe} = stress in prestressing steel due to prestress after losses (ksi)	CSA A23.3	A_{st} = total area of longitudinal steel reinforcement in the tie (mm^2) f'_c = concrete compressive strength (MPa) f_y = yield strength of longitudinal steel reinforcement (MPa)
ACI 318-05	A_{ts} = area of nonprestressed reinforcement in a tie (in^2) A_{tp} = area of prestressing steel in a tie (in^2) f'_c = concrete compressive strength (ksi) f_y = specified yield strength of reinforcement (ksi) f_{se} = effective stress in prestressing steel (after allowance for all prestress losses) (ksi) Δf_p = increase in stress in prestressing steel due to factored loads (ksi)	NZS 3101	A_{st} = area of nonprestressed reinforcement in a tie (mm^2) A_{tp} = area of prestressing steel in a tie (mm^2) f'_c = concrete compressive strength (MPa) f_y = specified yield strength of reinforcement (MPa) f_{se} = effective stress in prestressing steel (after allowance for all prestress losses) (MPa) Δf_p = increase in stress in prestressing steel due to factored loads (MPa)
DIN1045-1	f_{cd} = design value of concrete compressive strength = $\alpha(f_{ck}/\gamma_c)$ (MPa) f_{ck} = characteristic concrete compressive strength (MPa) f_{yd} = design yield strength of tie reinforcement = (f_y/γ_s) (MPa) f_y = yield stress of steel (MPa) α = reduction factor taking into account long-term effects on concrete strength = 0.85 γ_c = concrete partial safety factor = 1.5 γ_s = reinforcement partial safety factor = 1.15	CEB-FIP Model Code 90	f_{cd} = design value of concrete compressive strength = f_{ck}/γ_c (MPa) f_{ck} = characteristic concrete compressive strength (MPa) f_{ptk} = characteristic prestressing tie tensile strength (MPa) $f_{pyd,net}$ = design value for prestressing tie tensile strength (MPa) f_{ytd} = design value for tie tensile strength = f_{ytk}/γ_s (MPa) $f_{ytk} = f_y$ = yield stress of steel (MPa) γ_c = partial safety factor for concrete = 1.5 γ_s = partial safety factor for steel = 1.15 σ_{do} = design tendon stress taken into account in the prestress loading system (MPa)
CSA-S6-06	A_{st} = total area of longitudinal steel reinforcement in the tie (mm^2) A_{ps} = cross-sectional area of tendons in tie (mm^2) f'_c = concrete compressive strength (MPa) f_{py} = yield strength of presressing steel (MPa) f_y = yield strength of longitudinal steel reinforcement (MPa) $\alpha_1 = 0.85\text{-}0.0015f'_c$ ψ = ratio of creep strain to elastic strain	1999 FIP Recommendations	A_s = area of nonprestressing reinforcement (mm^2) A_p = area of prestressing steel (mm^2) f_{1cd} = uniaxial design strength of concrete = $\alpha(f_{ck}/\gamma_c)$ (MPa) f_{ck} = characteristic concrete compressive strength (MPa) f_{yd} = design value for tie tensile strength = f_y/γ_s (MPa) f_y = yield stress of steel (MPa) f_{ptd} = design value for prestressing tie tensile strength = f_{pe}/γ_s (MPa) $f_{p0.1k}$ = characteristic 0.1 % Proof Stress of prestressing steel (MPa) α = coefficient taking account of uniaxial strength in relation to strength control of specimen and duration of loading = 0.85 γ_c = concrete partial safety factor = 1.5 γ_s = reinforcement partial safety factor = 1.15

Table 4-5: Strut provisions from additional sources.

Source	Strut Compressive Stress
AASHTO LRFD (§ 5.6.3.3.3)	$\frac{f'_c}{0.8+170\varepsilon_1} \le 0.85f'_c$ $\varepsilon_1 = \varepsilon_s + (\varepsilon_s + .002)\cot^2\alpha_s$
Schlaich et al. (1987)	$0.85f'_c$ "for an undisturbed and uniaxial state of compressive stress" (prismatic) $0.68f'_c$ "if tensile strains in the cross direction or transverse tensile reinforcement may cause cracking parallel to the strut with normal crack width" $0.51f'_c$ "as above for skew cracking or skew reinforcement" $0.34f'_c$ "for skew cracks with extraordinary crack width. Such cracks must be expected, if modeling of the struts departs significantly from the theory of elasticity's flow of internal forces"
Collins et al. (1991)	$\frac{f'_c}{0.8+170\varepsilon_1} \le 0.85f'_c$ and $\varepsilon_1 = \varepsilon_s + (\varepsilon_s + .002)\cot^2\alpha_s$ where, α_s is the smallest angle between the tie and the strut ε_s is the tensile strain in the tension-tie reinforcement (in/in)
MacGregor (1997)	$\upsilon_1\upsilon_2 f'_c$ where $\upsilon_2 = (0.55 + \frac{15}{\sqrt{f'_c}})$ $\upsilon_1 = 1.0$ Uncracked uniaxially stressed struts or fields $\upsilon_1 = 0.80$ Struts cracked longitudinally due to bottle shaped stress fields, containing transverse reinforcement $\upsilon_1 = 0.65$ Struts cracked longitudinally due to bottle shaped stress fields without transverse reinforcement $\upsilon_1 = 0.60$ Struts in cracked zone with transverse tensions from transverse reinforcement
Bergmeister et al. (1993)*	Fan, bottle, or prismatic struts: $\upsilon_e f'_c$ $\upsilon_e = 0.8$ for $f'_c \le 4000$ psi $\upsilon_e = 0.9\text{-}.25f'_c/1000$ for $4000 < f'_c < 10{,}000$ psi $\upsilon_e = 0.65$ for $f'_c \ge 10{,}000$ psi Compression diagonal struts: $0.6\upsilon_e f'_c$ Confined compression fields: $[\upsilon_e f'_c(A/A_b)^{0.5} + \alpha(A_{core}/A_b)f_{lat}(1\text{-}s/d)^2] \le 2.5f'_c$ $\alpha = 4.0$ for spiral confinement $\alpha = 2.0$ for square closed hoop confinement anchored with longitudinal reinforcement $\alpha = 1.0$ for square closed hoop confinement without longitudinal reinforcement anchorage

* See additional notation below

Bergmeister et al.

f_{lat} = lateral pressure = $2f_yA_s/(ds)$ for $f'_c \le 7000$ psi
= $2f_sA_s/(ds)$ for $f'_c \ge 7000$ psi

$f_s = C\mu 2s/(\pi dA_s) \le f_y$

C = Compression load

μ = Poisson's ratio

A = area of the confined concrete concentric with and geometrically similar to the bearing plate.

A_b = Area of the bearing plate

A_{core} = Area of confined strut

$A/A_b \le 4$

$1 \le A_{core}/A_b \le 3$

Table 4-6: Node provisions from additional sources.

Source	Node Compressive Stress
AASHTO LRFD (§ 5.6.3.5)	CCC: $0.85f'_c$ CCT: $0.75f'_c$ CTT: $0.65f'_c$
Schlaich et al. (1987)	CCC: $0.85f'_c$ CCT or CTT: $0.68f'_c$
Collins et al. (1991)	CCC: $0.85f'_c$ CCT: $0.75f'_c$ CTT: $0.60f'_c$ ($\varphi = 0.7$)
MacGregor (1997)	$\upsilon_1\upsilon_2 f'_c$ where $\upsilon_2 = (0.55 + \frac{15}{\sqrt{f'_c}})$ $\upsilon_1 = 1.0$ Joints bound by struts and bearing plates $\upsilon_1 = 0.85$ Joints anchoring one tension tie $\upsilon_1 = 0.75$ Joints anchoring more than one tension tie
Bergmeister et al. (1993)*	Unconfined nodes without bearing plates: $\upsilon_e f'_c$ $\upsilon_e = 0.8$ for $f'_c \leq 4000$ psi $\upsilon_e = 0.9\text{-}.25f'_c/1000$ for $4000 < f'_c < 10{,}000$ psi $\upsilon_e = 0.65$ for $f'_c \geq 10{,}000$ psi Confined nodes: $[\upsilon_e f'_c(A/A_b)^{0.5} + \alpha(A_{core}/A_b)f_{lat}(1\text{-}s/d)^2] \leq 2.5 f'_c$ $\alpha = 4.0$. for spiral confinement $\alpha = 2.0$ for square closed hoop confinement anchored with longitudinal reinforcement $\alpha = 1.0$ for square closed hoop confinement without longitudinal reinforcement anchorage Unconfined nodes with bearing plates: $\upsilon_e f'_c(A/A_b)^{0.5} \leq 2.5 f'_c$ Triaxially confined node: $f_{c3} \leq 2.5 f'_c$

* See additional notation below

Bergmeister et al.

f_{lat} = lateral pressure $= 2f_yA_s/(ds)$ for $f'_c \leq 7000$ psi $= 2f_sA_s/(ds)$ for $f'_c \geq 7000$ psi

$f_s = C\mu 2s/(\pi dA_s) \leq f_y$

C = Compression Load

μ = Poisson's ratio

A = area of the confined concrete concentric with and geometrically similar to the bearing plate.

A_b = Area of the bearing plate

A_{core} = Area of confined strut

$A/A_b \leq 4$

$1 \leq A_{core}/A_b \leq 3$

4.2 COMPARISONS TO LABORATORY TESTS

In order to make some comparisons between the AASHTO LRFD and the CSA A23.3, ACI 318-05, NZS 3101, CEB-FIP Model Code 90, 1999 FIP Recommendations, and DIN 1045-1 specifications, the capacities of three previously tested specimens were determined using the strut-and-tie model provisions for each. The three specimens included a deep beam, a deep beam with an opening, and a pile cap. For each of the specimens, the analyses utilized the actual concrete compressive strengths (f'_c) and yield strength of the reinforcing bars (f_y) recorded by the researchers. The results for each specimen are summarized in the following sections. Each summary includes a discussion of the methods used for analysis, a discussion of the results, tabular results, and corresponding figures. The deep beam summary also includes an example capacity calculation to demonstrate how strut-and-tie model capacities were determined. In addition, a discussion of what might be gained from these examples follows the summaries.

4.2.1 DEEP BEAM TEST COMPARISON

The deep beam used for this example was originally tested by Aquilar et al. (2002). The dimensions of the deep beam are given in Figure 4-1. For this example, several strut-and-tie models were developed and evaluated using the strut-and-tie provisions for each of the specifications in order to predict the load capacity of the deep beam. In total, five models were analyzed. The calculated capacities were then compared to the experimental capacity of 289 kips.

The geometry and dimensions of each of the strut-and-tie models are shown in Figures 4-2 through 4-7. Model 1 (Figure 4-2) is similar to the strut-and-tie model used by Aguilar et al.; however, the width of the tie was shortened to be the distance from the bottom of the beam to the top of the top layer of reinforcement (Aguilar et al. used a tie width of 9 inches), and the width of the top compression strut (C2) was reduced to 6 inches (Aguilar et al. used a top strut width of 7 inches). By choosing a smaller tie width, it is implied that the centroid of the tie is assumed to be lower than its actual location. This was done to determine how using a smaller tie width would affect the results of the calculation. The width of the inclined struts was determined from the geometry of the tie and top strut. Model 2 (Figure 4-3) is the same model that Aguilar et al. used except that the top strut (C2) was increased to 8 inches instead of 7 inches. It is similar to Model 1, but the tie and the top compression strut (C2) widths were increased. Because of this, the angle between the inclined struts and tie is reduced, and the width of the inclined struts increased. For Models 3 through 5, the member labels are given in Figure 4-4. Model 3 (Figure 4-5) is a "split-strut" model based on the provisions of Section 6.5.2.3 from the 1999 FIP Recommendations. The vertical tie (T2) is comprised of two #3 stirrups. Models 4 and 5 (Figures 4-6 and 4-7) are modified versions of Model 3 that include three and four #3 stirrups in the vertical tie respectively.

Except for the AASHTO LRFD and CSA A23.3, the capacity was calculated in the same manner. First, all of the member forces (demands) of each of the strut-and-tie model members were determined based on the maximum possible tie force. Second, the strut capacities were determined and compared to the demand for each of the struts. If one or more of the struts could not meet the demand based on the maximum tie force, the member forces were recalculated based on the limiting strut. Finally, the node capacities were compared to the demand. Once

again, if any of the nodes could not meet the demand, the member forces were recalculated. The calculated deep beam shear capacities were based on these strut-and-tie model member forces. This method of finding the deep beam capacity is referred to as the "straight forward method".

For the AASHTO LRFD and CSA A23.3, the capacity of a strut connected to a tie is a function of the principal tensile strain in the strut which is a function of the tensile strain in the tie connected to the strut and the angle between the strut and the tie. Therefore, if a strut connected to a tie did not have enough capacity, the force in the tie that the strut was connected to was systematically decreased until the strut could meet the demand based on the force in the tie. Once the capacity of each of the struts met the demand, the suitability of the nodes were checked. If the nodal zones were unable to meet the demands, member forces were recalculated according no the limiting nodal capacity. This method of finding the deep beam capacity is referred to as the "iterative method". In order to better demonstrate how these calculations were actually performed, section 4.2.1.1 shows the complete AASHTO LRFD calculation of the shear capacity for Model 2 starting from the strut-and-tie model development to checking the crack control reinforcement.

Once again, the actual shear capacity of the beam was 289 kips. The results for each specification are presented in Tables 4-7 and 4-8. The results in Table 4-7 utilized resistance factors, and the results in Table 4-8 neglected the resistance factors. For each of the specifications, the accuracy of the predictions improved with the more complex models (Models 3 to 5). It should be noted that this summary is not advocating the use of the more elaborate models. The use of the complex models was an academic endeavor to determine whether a more accurate prediction of the shear capacity could be attained. In addition, in all but one case, the AASHTO LRFD gave the most accurate predictions.

Important Information of About Deep Beam Models

- The crack control reinforcement provided for the deep beam satisfies the crack control reinforcement for the ACI 318-05 and NZS 3101 (Sections A.3.3.1 and 11.4.5 respectively); however, this amount of crack control reinforcement does not satisfy the amount that is specified by Section 5.6.3.6 of the AASHTO LRFD.

- All of the strut-and-tie models used to determine the capacity of the deep beam did not conform to the DIN 1045-1 and CEB-FIP Model Code 90 because each of the models included angles of less than 45 degrees between struts and ties (Sections 10.6.3 and 6.8.1 respectively).

Tables

Table 4-7: Summary of results using resistance factors.

Specification	Model 1		Model 2		Model 3		Model 4		Model 5	
	Predicted Load (kips)	Actual/ Predicted	Predicted Load (kips)	Actual/ Predicted	Predicted Load (kips)	Actual/ Predicted	Predicted Load (kips)	Actual/ Predicted	Predicted Load (kips)	Actual/ Predicted
AASHTO LRFD	140.0	2.06	165.2	1.75	187.9	1.54	195.4	1.48	199.4	1.45
CSA A23.3	140.0	2.06	165.2	1.75	187.9	1.54	195.4	1.48	199.4	1.45
ACI 318-05	136.0	2.12	165.7	1.74	166.2	1.74	163.5	1.77	162.5	1.78
NZS 3101	136.0	2.12	165.7	1.74	166.2	1.74	163.5	1.77	162.5	1.78
CEB-FIP MC 90	89.9	3.22	114.8	2.52	127.4	2.27	131.7	2.20	136.0	2.12
1999 FIP Rec.	121.2	2.38	154.9	1.87	171.1	1.69	177.2	1.63	181.9	1.59
DIN 1045-1	107.0	2.70	136.7	2.11	151.5	1.91	156.7	1.84	161.9	1.78

Table 4-8: Summary of results without resistance factors.

Specification	Model 1		Model 2		Model 3		Model 4		Model 5	
	Predicted Load (kips)	Actual/ Predicted	Predicted Load (kips)	Actual/ Predicted	Predicted Load (kips)	Actual/ Predicted	Predicted Load (kips)	Actual/ Predicted	Predicted Load (kips)	Actual/ Predicted
AASHTO LRFD	200.0	1.44	220.7	1.31	221.6	1.30	230.7	1.25	241.0	1.20
CSA A23.3	200.0	1.44	220.7	1.31	221.6	1.30	230.7	1.25	241.0	1.20
ACI 318-05	181.3	1.59	220.9	1.31	221.6	1.30	218.1	1.33	216.7	1.33
NZS 3101	181.3	1.59	220.9	1.31	221.6	1.30	218.1	1.33	216.7	1.33
CEB-FIP MC 90	134.8	2.14	172.2	1.68	190.4	1.52	209.0	1.38	210.5	1.37
1999 FIP Rec.	181.8	1.59	220.9	1.31	221.6	1.30	217.5	1.33	216.7	1.33
DIN 1045-1	160.5	1.80	205.0	1.41	221.6	1.30	215.0	1.34	216.7	1.33

Figures

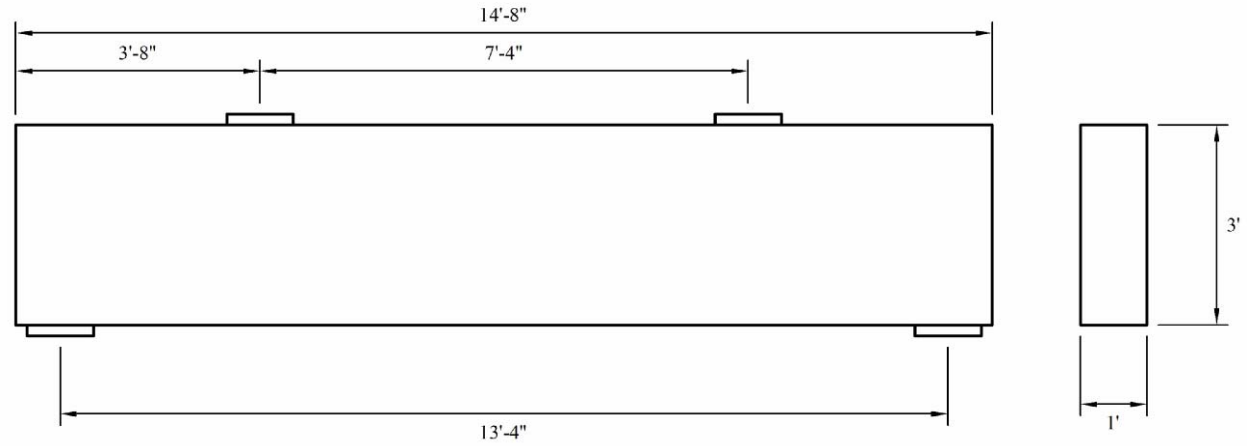

Figure 4-1: Dimensions of deep beam. The bearing plates are 12 in. by 12 in.

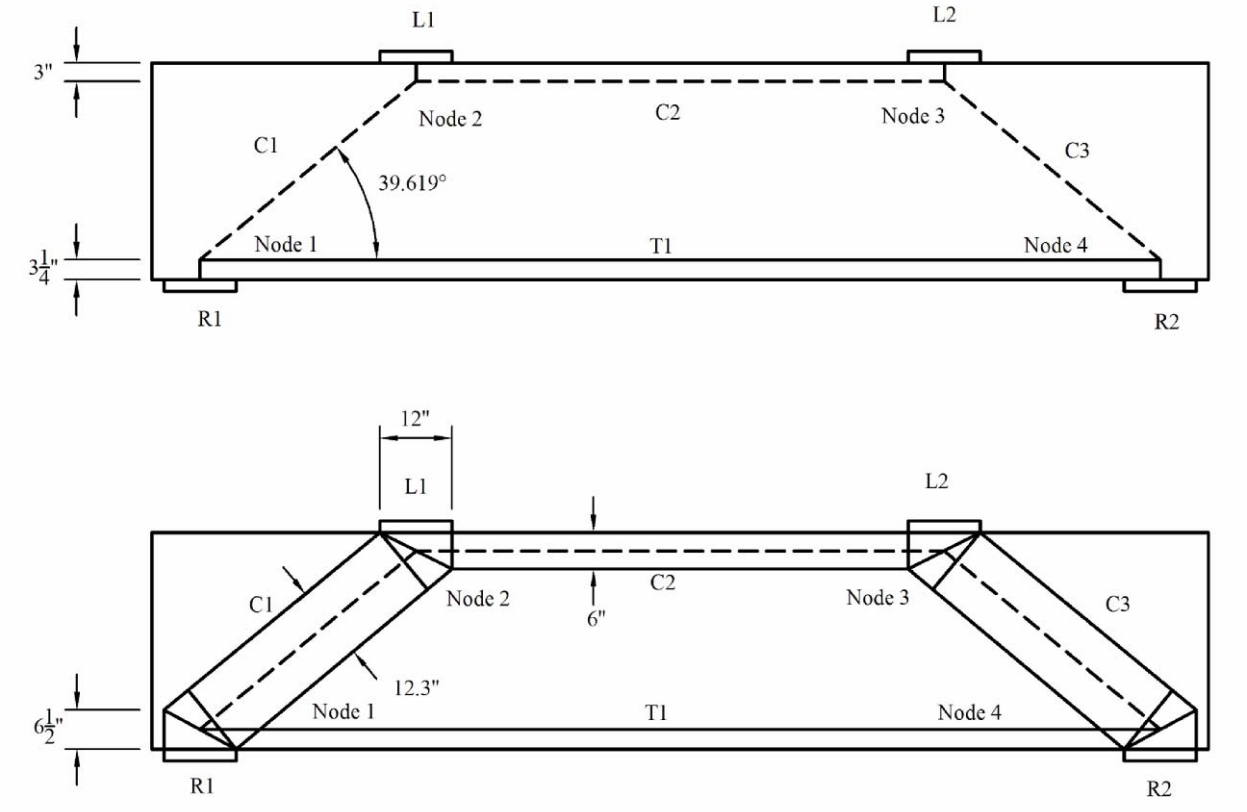

Figure 4-2: Geometry and member identification of STM 1 for deep beam.

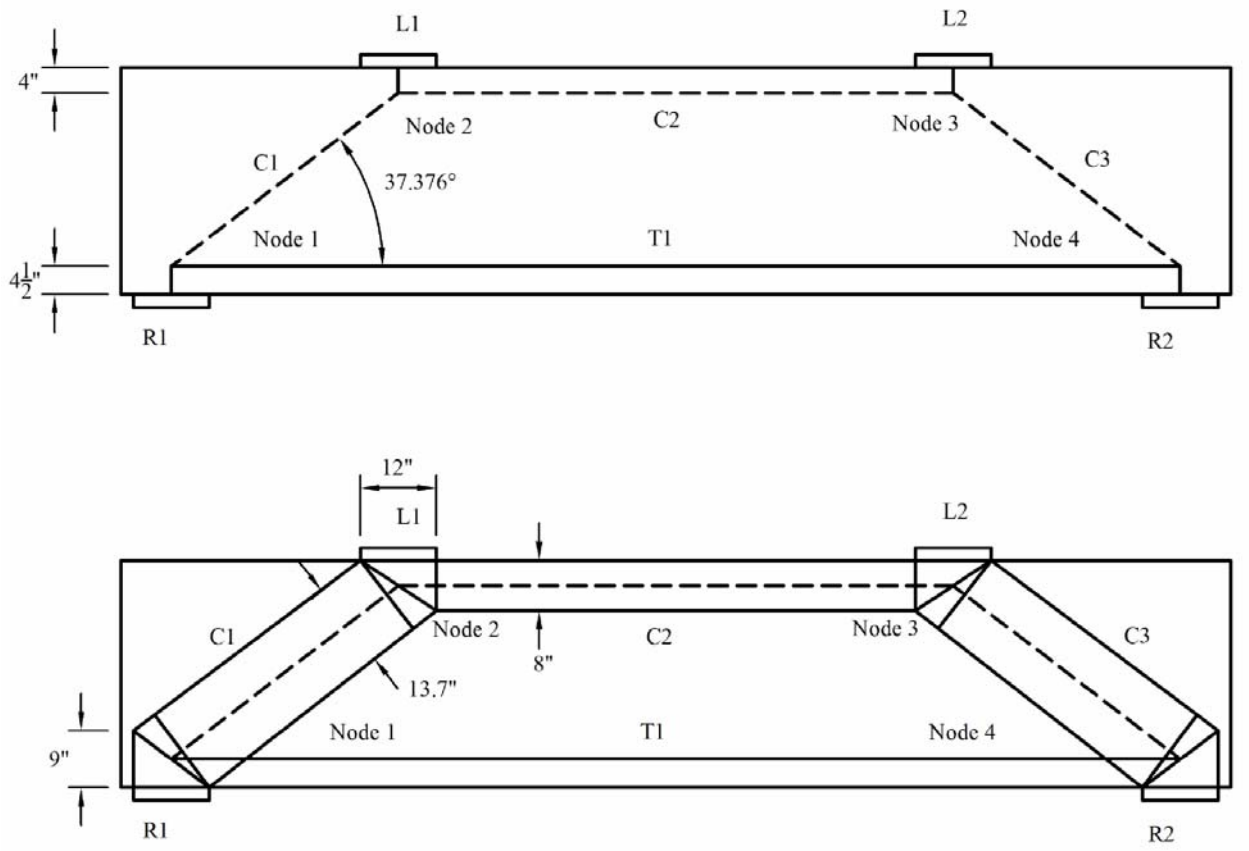

Figure 4-3: Geometry and member identification of STM 2 for deep beam.

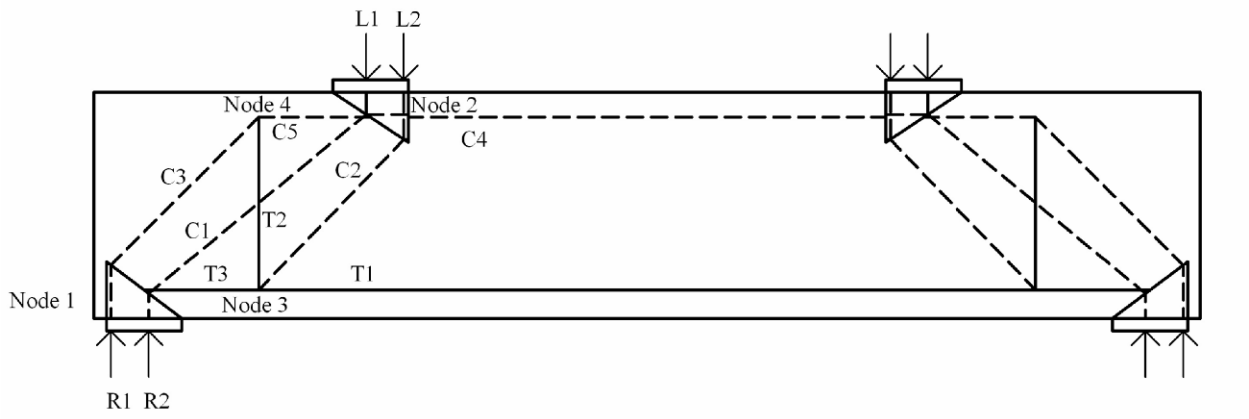

Figure 4-4: Member identification for split-strut models (Figures 4-5 through 4-7).

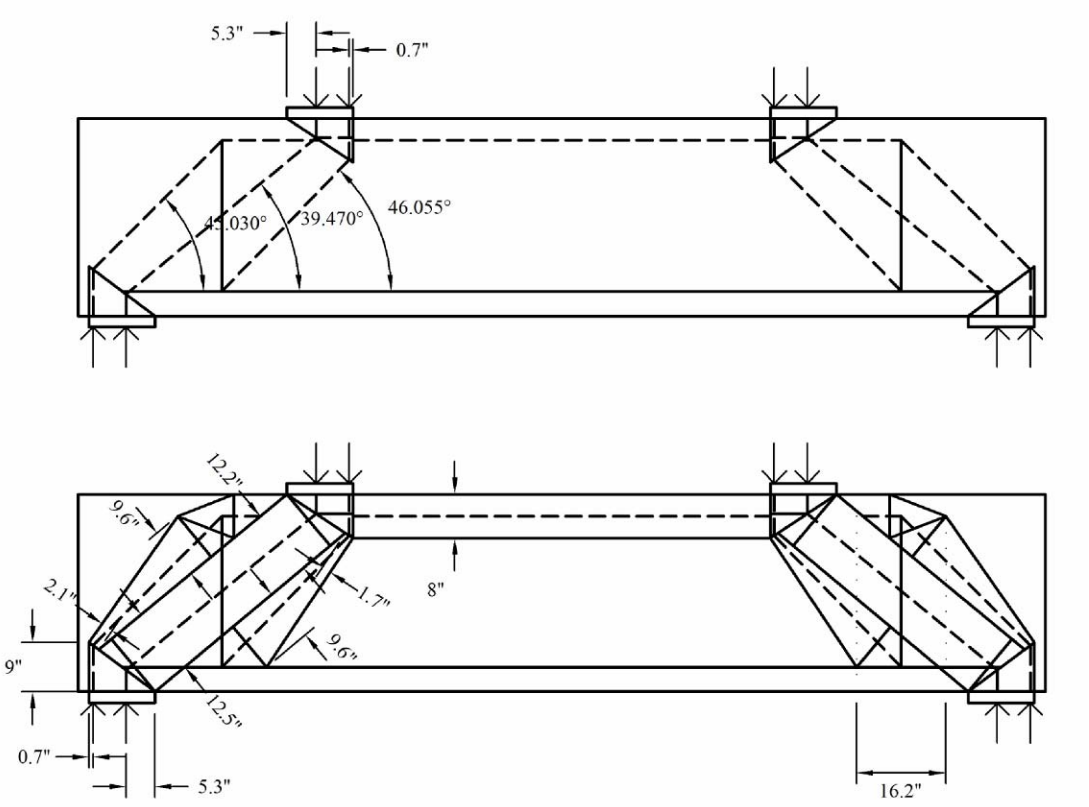

Figure 4-5: Geometry of STM 3 for deep beam.

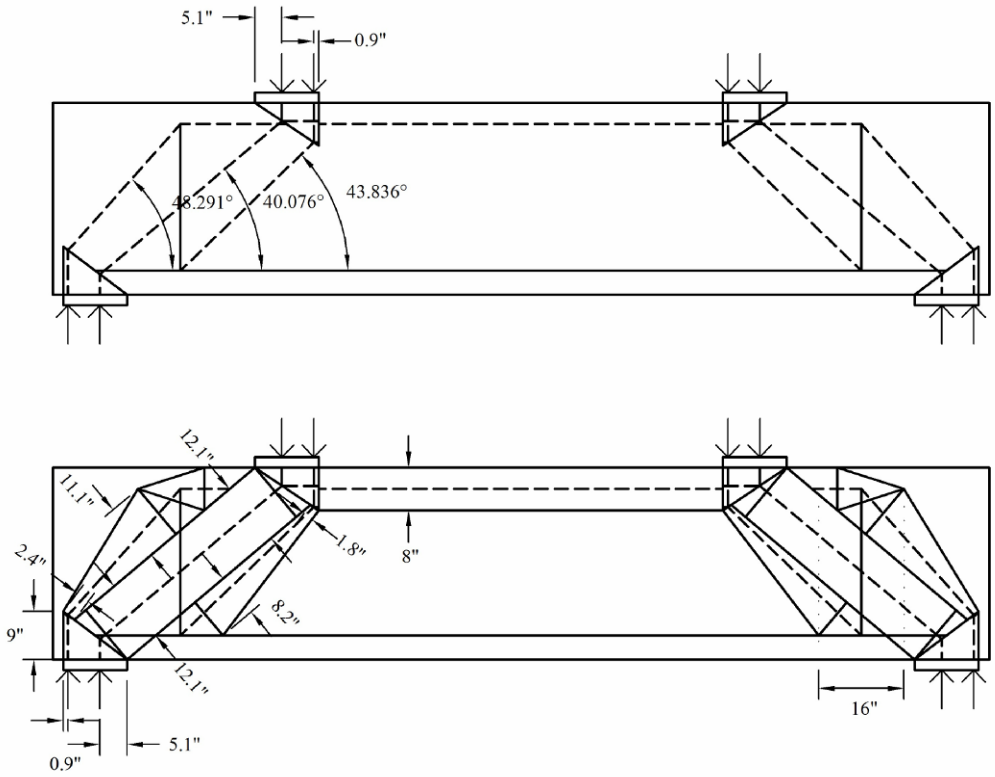

Figure 4-6: Geometry of STM 4 for deep beam.

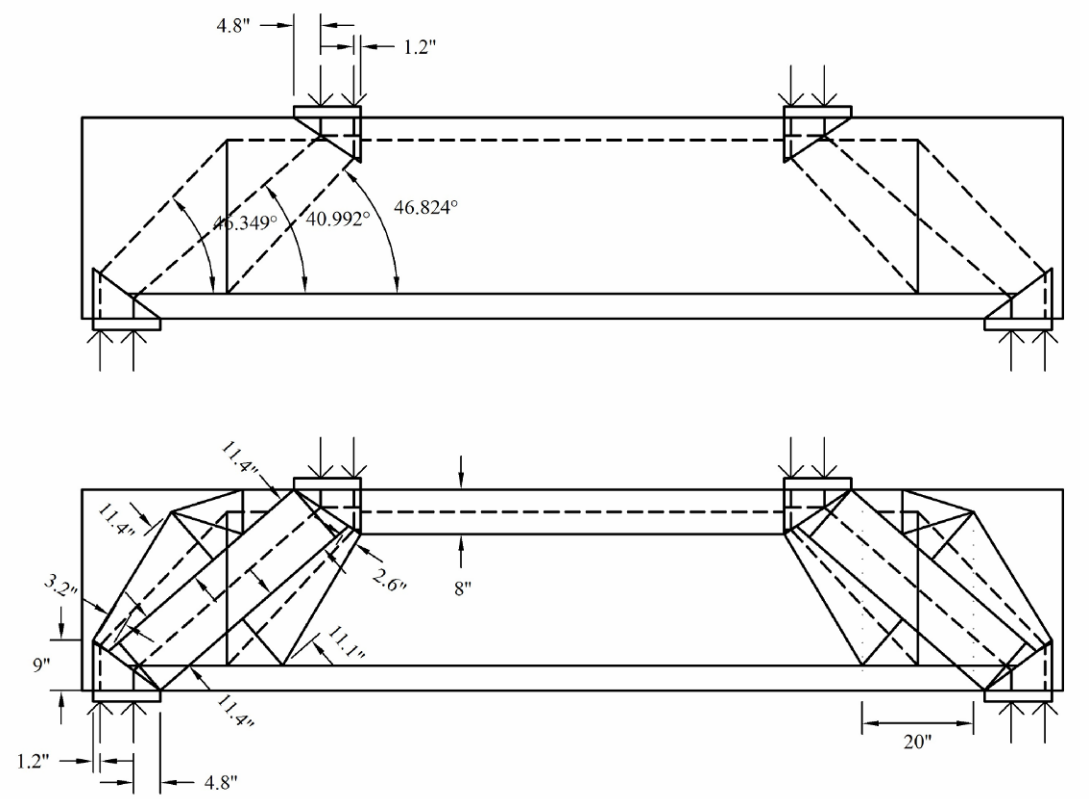

Figure 4-7: Geometry of STM 5 for deep beam.

4.2.1.1 EXAMPLE CALCULATION FOR DEEP BEAM MODEL 2

Problem: Calculate the shear capacity using the AASHTO LRFD Bridge Design Specifications strut-and-tie model provisions for a deep beam with the following dimensions and reinforcement layout (Figures 4-1 and 4-8):

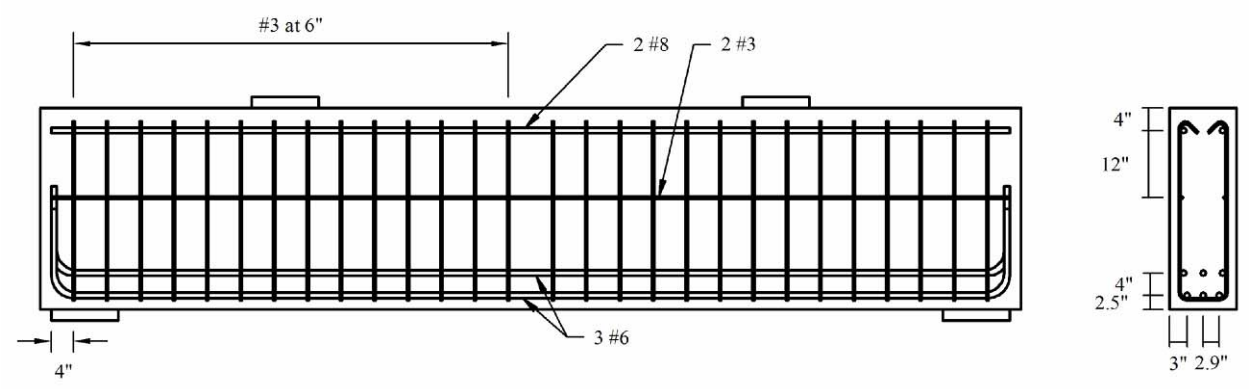

Figure 4-8: Reinforcement layout for deep beam.

Given Values: f'_c = 4.13 ksi, f_y = 61 ksi, E_s = 29000 ksi

Because the strength of the concrete and steel are known, resistance factors will be neglected (ϕ=1). Normally, ϕ_{concrete} is equal to 0.7 and ϕ_{steel} is equal to 0.9.

Because this is not a design problem, the normal procedure for performing a strut-and-tie model analysis was modified.

Solution:

Step 1 – Delineate the D-regions.

Because nearly the entire deep beam is a D-region, only an STM will be used for design.

Step 2 – Determine the boundary conditions of the D-region.

Based on the statements in Step 1, this step is unnecessary

Step 3 – Sketch the flow of forces.

Because of the simple geometry of the deep beam and loading, it was deemed unnecessary to perform this step.

Step 4(a) – Develop a strut-and-tie model that gives a good estimate of the flow of forces.

Figure 4-9 shows a simple strut-and-tie model that is commonly used for deep beams. In Figure 4-9, struts are denoted by dashed lines, and ties are denoted by solid lines. For future reference later in this example, the struts, ties, and nodes have been labeled.

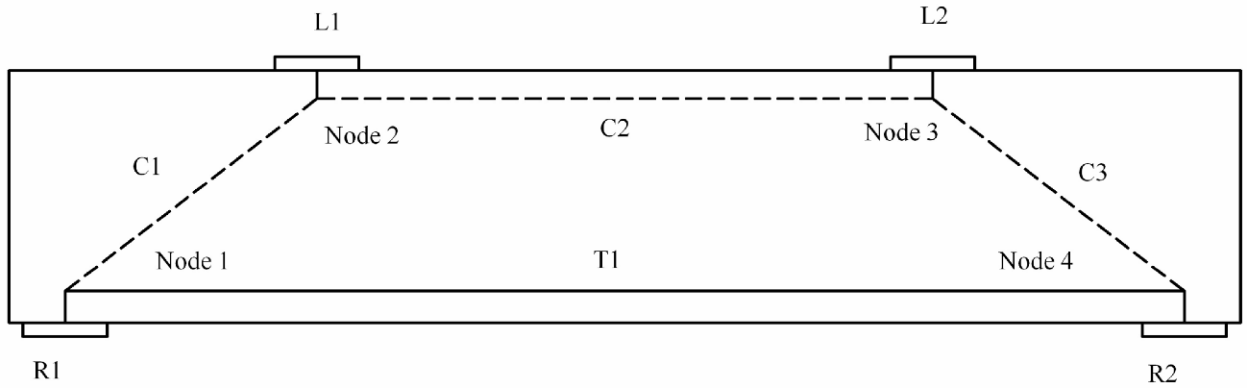

Figure 4-9: Strut-and-tie model to be used.

Step 4(b) – Determine tie widths and constrained strut widths.

According to AASHTO LRFD 5.6.3.3.2, the width of a tie can extend up to six bar diameters from the anchored bar. For tie T1, the bottom layer of number eight bars has a clear spacing of 2 inches. In order to keep the center of the tie equal to the center of the number eight bars, the tie is assumed to extend 2 inches above the top layer of number eight bars which is less than six bar diameters. From this, the tie width is determined to be 9 inches which places the center of the tie 4.5 inches above the bottom of the beam. See Figure 4-10.

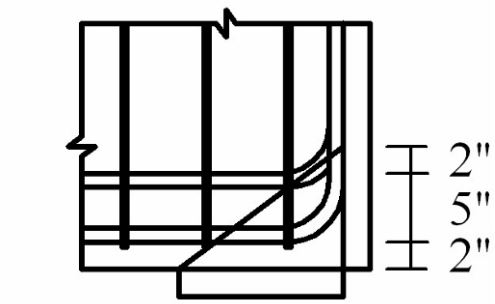

Figure 4-10: Assumed tie width for T1. By determining a tie width, the geometry of nodal zones 1 and 4 can also be determined.

Because strut C2 has reinforcement parallel to the strut (see AASHTO LRFD 5.6.3.3.4), it is possible to analyze strut C2 as a reinforced strut. For this example, the centerline of the strut will be assumed to be concurrent with the centerline of the reinforcement which makes the width of the top compression strut 8 inches. See Figure 4-11.

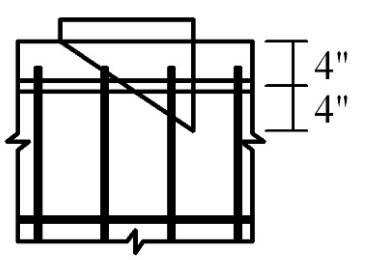

Figure 4-11: Assumed strut width for C2. By determining the strut width of C2, the geometry of nodal zones 2 and 3 can be determined.

Step 4(c) – Determine the remaining geometry of the strut-and-tie model based on the previously determine values.

Given the values for T1 and C2, it is possible to determine the angle between T1 and C1. See Figure 4-12.

Furthermore, given the widths of T1 and C2, it is possible to determine the width of C1 and C3. This can easily be done using a drafting program or using the principles of basic geometry. See Figure 5.6.3.3.2-1 in AASHTO LRFD regarding guidance for calculating strut widths. Figure 4-13 illustrates how the widths of struts C1 and C3 were calculated based on bearing plates and the widths of the tie (T1) and the top strut (C2). Figure 4-14 shows all of the calculated widths that will be used to predict the capacity of the deep beam.

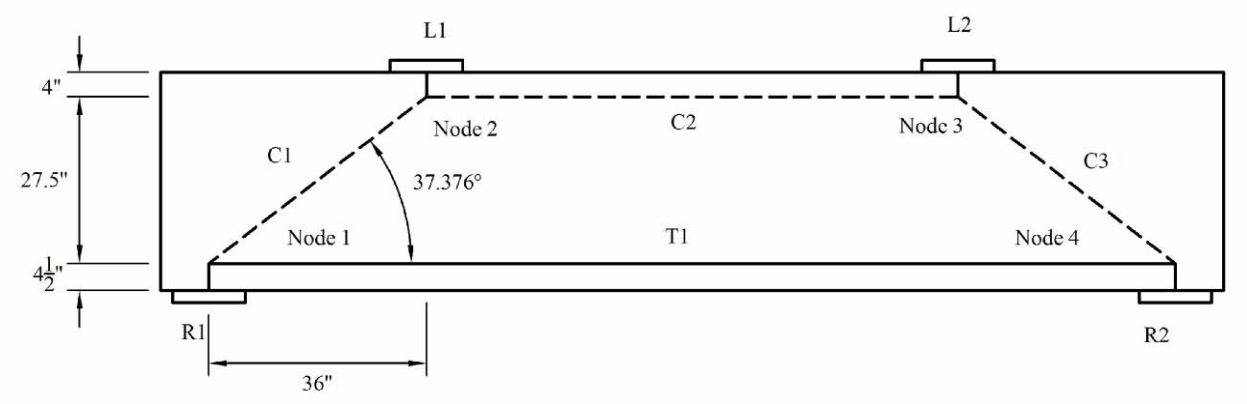

Figure 4-12: Determination of the angle between T1 and C2.

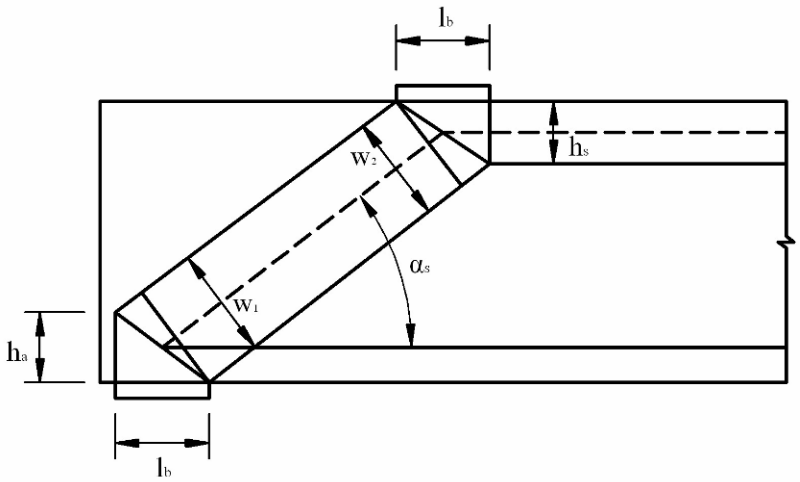

$$w_1 = l_b \sin(\alpha_s) + h_a \cos(\alpha_s)$$

$$w_2 = l_b \sin(\alpha_s) + h_s \cos(\alpha_s)$$

Figure 4-13: Example of how to calculate the width of the inclined strut based on limiting conditions.

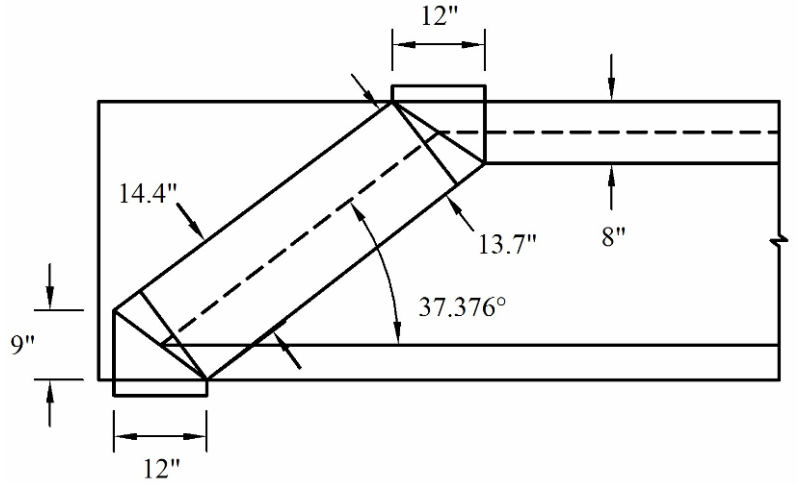

Figure 4-14: Calculated dimensions of strut-and-tie model for deep beam.

Step 6* – Determine the maximum force the tie (T1) can sustain.
*Because the maximum capacity of the beam is being determined, the order of Steps 5 and 6 (explained in Section 3.2) of the strut-and-tie model design process were reversed.

Initially, the tie will be assumed to be the limiting component of the strut-and-tie model. This will have to be verified later on. According to the AASHTO LRFD, the nominal capacity of the tie is:

$$P_n = f_y A_{st} + A_{ps}\left[f_{pe} + f_y\right] \qquad (5.6.3.4.1\text{-}1)$$

Because the section is not prestressed, the second term drops out. All that is left is the product of the yield strength of the steel and the area of the 6 number eight bars. Therefore,

$$P_n = (61ksi)\times\left(6\times 0.79in^2\right) = 289.1kips$$

It should be noted that this step is identical for all of the specifications.

Step 5 – Calculate the demands on the struts based on the maximum force in the tie.

Given the force in T1, it is possible to determine the forces in the struts using basic truss theory. For a more complex strut-and-tie model, it may be desirable to use an analysis program. Table 4-9 shows the calculated member forces based on the maximum possible force in T1.

Table 4-9: Table of calculated member demands based on the maximum possible force in T1.

Given T1 and α_s	
α_s	**37.376**
T1	**289.1**
C1	363.8
C2	289.1
C3	363.8
R1	220.9
R2	220.9
L1	220.9
L2	220.9

This step is identical for all of the specifications.

Step 7(a) – Check the capacity of the struts against the demands.

Struts C1 and C3
The capacities of the inclined struts (C1 and C3) will be checked first. Because the struts are connected to a tie, the principal tensile strain, perpendicular to the direction of the strut, must be determined. First the strain in the direction of the tie, ε_s, must be determined. It should be noted

that the commentary of Section 5.6.3.3.3 of the AASHTO LRFD allows for the strain at the centerline of the strut to be used. To find ε_s, divide the force in the tie at the center of the strut (P_{avg}) by the product of the area of steel (A_{st}) and the modulus of elasticity (E_s). For this example, the force in the tie is assumed to transition from zero at the beginning of the node to its assumed maximum value at the end of the node; therefore, P_{avg} is calculated by dividing the maximum force in the tie by 2. The calculations were performed as follows:

$$\varepsilon_s = \frac{P_{avg}}{A_{st} E_s}$$

$$\varepsilon_s = \frac{(289.1 kips)/2}{(6 \times 0.79 in^2)(29000 ksi)} = 0.00105$$

Next, the principal tensile strain in the strut is determined.

$$\varepsilon_1 = \varepsilon_s + (\varepsilon_s + 0.002)\cot^2(\alpha_s) \qquad \text{(AASHTO LRFD eq. 5.6.3.3.3-2)}$$

$$\varepsilon_1 = 0.00105 + (0.00105 + 0.002)\cot^2(37.376) = 0.0063$$

Because, the principal tensile strain in the strut is calculated is greater than 0.002, the limiting compressive stress can be calculated by the following equation:

$$f_{cu} = \frac{f'_c}{0.8 + 170\varepsilon_1} \qquad \text{(AASHTO LRFD eq. 5.6.3.3.3-1)}$$

In addition, the effective cross-sectional area of the strut (A_{cs}) is taken as the product of the width of the strut (w) and thickness of the bearing plate (t) due to the fact that the thickness of the beam is the same as the thickness of the plate. For the purposes of this example, thickness is referring to the dimension of the beam perpendicular to the elevation view shown in Figure 4-12.

$$A_{cs} = w \cdot t$$

Knowing that the capacity of an unreinforced strut is calculated by:

$$P_n = f_{cu} A_{cs} \qquad \text{(AASHTO LRFD eq. 5.6.3.3.1-1)}$$

The following substitutions can be made.

$$P_n = \frac{f'_c \, wt}{0.8 + 170\varepsilon_1}$$

If the demand on the strut (P_u) is substituted for the nominal capacity of the strut (P_n) and the equation is rearranged, the required width of the strut can be calculated.

$$w_{req.} = \frac{P_u\left(0.8 + 170\varepsilon_1\right)}{f'_c\, t}$$

The required widths of C1 and C3 are then calculated to be

$$w_{req.} = \frac{363.8kips\left(0.8 + 170 \times 0.0063\right)}{\left(4.13ksi\right)\left(12in\right)} = 13.73in > w_{available} = 13.7in$$

The required width, $w_{req.}$, is slightly larger than the smallest available width, $w_{available}$, at the interface of the top node (See Figure 4-14). For all practical purposes, the required width and the actual width could be considered the same; however, for the sake of this example, iterations will be performed by systematically changing the force in the tie until the required width of the strut is less than or equal to the available width of 13.7 inches. See Step 7(b) of this example for a more thorough explanation of the procedure.

Strut C2

Now, the capacity of the top strut (C2) will be checked. Because C2 in not connected to a tie, the limiting compressive stress is:

$$0.85f'_c \qquad \text{(AASHTO LRFD 5.6.3.3.3)}$$

As with the inclined struts, the effective cross-sectional area of the strut (A_{cs}) is taken as the product of the width of the strut (w) and thickness of the beam (t).

$$A_{cs} = wt$$

For a reinforced strut, the nominal capacity is:

$$P_n = f_{cu} A_{cs} + f_y A_{ss} \qquad \text{(AASHTO LRFD eq. 5.6.3.3.4-1)}$$

Substituting in the values for the cross-sectional area of the strut and limiting compressive stress, the equation becomes:

$$P_n = 0.85 f'_c\, wt + f_y A_{ss}$$

As with struts C1 and C3, the demand on the strut (P_u) is substituted for the nominal capacity of the strut (P_n) and the equation is rearranged, the required width of the strut can be calculated.

$$w_{req.} = \frac{P_u - f_y A_{ss}}{0.85 f'_c\, t}$$

The required width of C3 is then calculated to be:

$$w_{req.} = \frac{289.1kips - (61ksi)(2 \times 0.79in^2)}{0.85(4.13ksi)(12in)} = 4.57in < w_{available} = 8in$$

Strut C2 has enough capacity to meet the demand.

Summary
Strut C2 has enough capacity to meet the demand. Struts C1 and C3 do not have enough capacity to meet the demands. Because of this, the deep beam shear capacity predicted by the strut and tie-model will have to be calculated based on the limitations of struts C1 and C3. Table 4-10 summarizes this information.

Table 4-10: Summary of calculations for initial strut capacity check.

Strut	Connected to Tie?	Nodes		Constrained P_u (kips)	Available Width (in.)	ε_s (in./in.)	ε_1 (in./in.)	Required Width (in.)	Limiting Width (in.)	Limiting P_n (kips)
C1	yes	1	2	363.8	13.7	0.00105	0.0063	13.7	13.73	363.5
C2*	no	2	3	289.1	8.0	N/A	N/A	4.6	N/A	N/A
C3	yes	3	4	363.8	13.7	0.00105	0.0063	13.7	13.73	363.5

Besides the CSA A23.3, the other specifications do not require the principal tensile strain in a strut to be calculated. Instead, the specifications specify constant reduction factors for various types of struts/compressive conditions.

Step 7(b) – Calculate deep beam shear capacity based on limiting strut (if necessary).

Because the limiting struts, C1 and C3, are connected to the tie, the deep beam shear capacity can not simply be calculated based on limiting strut capacity calculated in Step 6 due to the fact that the calculated strut capacity is a function of the force in the tie. It would be conservative to keep the principal strain based on the tie yielding; however, to get a more accurate answer, iterations must be performed by changing the value of the force in the tie until the capacity of all the struts just barely exceeds the demands. After a few iterations the maximum force in the tie was found to be 288.9 kips. Table 4-11 shows the corresponding demands placed on the system based on the tie force. Table 4-12 summarizes the strut capacity calculations.

Table 4-11: Modified demands on strut-and-tie system.

Given T1 and α_s	
α_s	**37.376**
T1	**288.9**
C1	363.5
C2	288.9
C3	363.5
R1	220.7
R2	220.7
L1	220.7
L2	220.7

Table 4-12: Summary of calculations for modified strut capacity check.

Strut	Connected to Tie?	Nodes		Constrained P_u (kips)	Available Width (in.)	ε_s (in./in.)	ε_1 (in./in.)	Required Width (in.)	Limiting Width (in.)	Limiting P_n (kips)
C1	yes	1	2	363.5	13.7	0.00105	0.0063	13.7	N/A	N/A
C2*	no	2	3	288.9	8.0	N/A	N/A	4.6	N/A	N/A
C3	yes	3	4	363.5	13.7	0.00105	0.0063	13.7	N/A	N/A

**Note: Except for the AASHTO LRFD and the CSA A23.3, this iterative process is not required for the other specifications. The deep beam shear capacity can be determined using the limiting strut capacities calculated in Step 6 directly.

Step 7(c) – Check the capacity of the nodes based on the demands determined from the strut analysis.

The capacity of a node is calculated by finding the product of the limiting compressive stress in the node region and the cross sectional area of the member at the node interface. The cross sectional area of a member at a node interface can be found by finding the product of the width (w) and thickness (t) of the member at the node interface.

$$P_n = f_{cu} A_{cs} = f_{cu} wt$$

According to the AASHTO LRFD the limiting compressive stress is $0.85f'_c$ for CCC nodes, $0.75f'_c$ for CCT nodes, and $0.65f'_c$ for CTT nodes (5.6.3.5). Table 4-13 summarizes the node capacity calculations. For the calculations in Table 4-13, the thickness for each node is 12 inches because the thickness of the struts and nodes were assumed to be the same as the thickness of the beam.

Table 4-13: Summary of node capacity calculations.

Node	Type	Reduction Factor	Force (kips)		Width (in)	Node Capacity (kips)	okay ?
1	CCT	0.75	R1	220.7	12.0	446.0	yes
		0.75	T	288.9	9.0	334.5	yes
		0.75	C1	363.5	13.7	509.2	yes
2	CCC	0.85	C1	363.5	13.7	577.1	yes
		0.85	C2	288.9	8.0	337.0	yes
		0.85	L1	220.7	12.0	505.5	yes
3	CCC	0.85	C2	288.9	8.0	337.0	yes
		0.85	C3	363.5	13.7	577.1	yes
		0.85	L2	220.7	12.0	505.5	yes
4	CCT	0.75	R2	220.7	12.0	446.0	yes
		0.75	T	288.9	9.0	334.5	yes
		0.75	C3	363.5	13.7	509.2	yes

All of the nodes have enough capacity meet the demands.

It could have been noted that in step 7(b), the limiting compressive stress in strut C1 and C3 was determined to be $0.53f'_c$. Using ε_1 from Table 4-12, this was determined as follows:

$$f_{cu} = \frac{f'_c}{0.8 + 170\varepsilon_1} = \frac{f'_c}{0.8 + 170 \cdot 0.0063} = 0.53 f'_c \quad \text{(AASHTO LRFD eq. 5.6.3.3.3)}$$

Because the limiting compressive stress in the struts is less than the limiting node compressive stresses of $0.75f'_c$ and $0.85f'_c$, the node stresses will not govern, and the node capacity check was not required. However, for the purposes of this example, the node calculations were performed to illustrate how they would be performed if the nodes would govern the design.

Step 7(d) – Calculate the deep beam shear capacity based on limiting node(s) (if necessary).

This step is not necessary for this example.

Calculated Deep Beam Shear Capacity

The calculated capacity of the deep beam, V_r, is 220.7 kips.

Step 8 – Check the reinforcement details

Anchorage of Ties
Because this problem was not a design problem, the anchorage of the ties will be assumed to be sufficient. To check the development length, the provisions of AASHTO LRFD 5.11.2 can be used.

Crack control Reinforcement
According to AASHTO LRFD,

$$\frac{Area\,\mathrm{Re inf}_{eachdirection}}{GrossAreaConc} \geq 0.003 \quad \text{(AASTHO LRFD 5.6.3.6)}$$

For the vertical stirrups, this ratio is:

$$\frac{A_{bar}}{b \times s} = \frac{2 \times 0.11 in^2}{12in \times 6in} = 0.0031 \geq 0.003$$

Therefore, the vertical stirrups satisfy the crack control requirements. The horizontal reinforcement, however, does not satisfy the crack control reinforcement because it exceeds the maximum allowable spacing.

4.2.2 DEEP BEAM WITH OPENING TEST COMPARISONS

The two deep beams with openings analyzed in this section were originally tested by Maxwell and Breen (2000). Maxwell and Breen labeled the beams Specimen 2 and Specimen 4. The dimensions of the deep beams tested by Maxwell and Breen are given in Figure 4-15. In

Maxwell and Breen's research, each beam (there was a total of four) was designed with strut-and-tie models developed by Schlaich et al. (1987). Two of the models were considered to be "simple" models, and the other two models were developed by superimposing the "simple" models on top of each other to make "complex" models. The point that Schlaich was making when he developed these models was the fact that strut-and-tie models can be superimposed to address different types of cracking that might be expected for a given structure and loading.

For this analysis, the capacity of each deep beam with an opening was determined using the strut-and-tie model that Maxwell and Breen designed the beam for. For the AASHTO LRFD and CSA A23.3 specifications, the capacities were determined using the "iterative method". For the rest of the specifications, the "straight forward method" was used. Each of the methods is described in Section 4.2.1. These predicted capacities were then compared to the actual failure load.

The "simple" strut-and-tie model used to determine the capacities of Specimen 2 for each of the specifications is given in Figure 4-16 along with the member labels. The details of each of the members in Specimen 2 are summarized in Table 4-14. Also, Figure 4-17 shows the strut widths superimposed on the strut-and-tie model for Specimen 2. The actual capacity of the beam was 33 kips. The predicted capacities for each of the specifications are given in Tables 4-15 and 4-16. As can be seen in Table 4-15, when resistance factors were used, the AASHTO LRFD and the CSA A23.3 yielded the most accurate prediction. When resistance factors were neglected, all of the specifications, with the exception of the CEB-FIP Model Specification 90, predicted the same capacity due to the fact that the supplied reinforcement was the limiting factor for each specification (Table 4-16).

The strut-and-tie model used to determine the capacities of Specimen 4 for each of the specifications is shown in Figure 4-18 through 4-21. This strut-and-tie model is considered a more "complex" model because it is comprised of two strut-and-tie models superimposed upon each other. The labels for the struts, ties, and nodes are given in Figures 4-18, 4-19, and 4-20, respectively. The details of the members are given in Table 4-17. Figure 4-21 shows the strut widths superimposed on the strut-and-tie model. For this model, the actual capacity was 43 kips. The predicted capacities for each of the specifications are given in Tables 4-18 and 4-19. Similar to the results for Specimen 2, the AASHTO LRFD and CSA A23.3 yielded the most accurate prediction of the capacity of the beam when resistance factors were used (Table 4-18). When resistance factors were neglected, all of the specifications predicted the same capacity because the supplied reinforcement was the limiting component for each specification (Table 4-19).

For each of the specifications, the more "complex" strut-and-tie model (specimen 4) yielded more accurate results. It should be noted that both models are conservative, and that this example does not advocate the use of the more "complex" model; however, "complex" models comprised of "simple" strut-and-tie models superimposed upon each other can be used to address different types of cracking that may occur within a section for a given loading case. For example, the strut-and-tie model used for Specimen 4 shows that reinforcement is necessary below the opening to prevent the section from cracking and breaking away. The strut-and-tie model for Specimen 2 yielded conservative results with respect to the ultimate load, but it did not

indicate that reinforcement should be placed beneath the opening. Because of this, the portion of the member below the opening cracked and broke away.

Notes on Crack Control in Beams

- The beams did not have crack control reinforcement throughout the entire member as specified by AASHTO LRFD 5.6.3.6. For each beam, there was an appropriate amount of crack control across Struts C1 and C2 according to AASHTO LRFD 5.6.3.6. In the areas that did not have the crack control, there was significantly more cracking.
- The beams were very thin (only 3-½ in. thick). Such thin members would not be suitable for bridge application. The member was used solely for the purposes of comparing the STM provisions of the design specifications.

Tables

Table 4-14 Members descriptions for Specimen 2. The angle corresponds to the smallest measured angle from the horizontal.

Member	Length (in.)	Angle (deg.)	Width (in.)
T1	36.88	45.000	1.5
T2	23.95	0.000	3.5
C1	34.99	61.422	3.7
C2	31.11	81.310	2.9
C3	26.05	8.677	3.3
C4	31.10	90.000	3.5

Table 4-15: Summary of calculations with resistance factors for Specimen 2.

Specification	Predicted Load (kips)	Actual/Predicted
AASHTO LRFD	23.0	1.43
CSA A23.3	23.0	1.43
ACI 318-05	18.4	1.79
NZS 3101	18.4	1.79
CEB-FIP MC 90	16.5	2.00
1999 FIP Rec.	22.3	1.48
DIN 1045-1	20.8	1.59

Table 4-16: Summary of calculations without resistance factors for Specimen 2.

Specification	Predicted Shear (kips)	Actual/Predicted
AASHTO LRFD	25.6	1.29
CSA A23.3	25.6	1.29
ACI 318-05	25.6	1.29
NZS 3101	25.6	1.29
CEB-FIP MC 90	24.7	1.34
1999 FIP Rec.	25.6	1.29
DIN 1045-1	25.6	1.29

Table 4-17: Member descriptions for Specimen 4. The angle corresponds to the smallest angle measured from the horizontal.

Member	Length (in.)	Angle (deg.)	Width (in.)
T1	35.13	47.742	3.2
T2	23.95	0.000	3.5
T3	11.71	0.000	3.5
T4	14.34	0.000	3.5
T5	7.17	0.000	3.6
T6	7.17	90.000	3.0
T7	14.34	0.000	3.6
T8	14.34	90.000	3.6
T9	7.17	0.000	3.0
T10	7.17	90.000	3.6
C1	35.00	61.422	4.0
C2	31.10	81.310	2.5
C3	28.9	9.335	3.0
C4	26.17	85.000	1.4
C5	11.60	52.893	2.3
C6	11.60	37.107	2.3
C7	3.17	45.000	2.7
C8	7.51	72.600	2.9
C9	7.51	17.400	2.9
C10	10.41	45.000	3.2
C11	10.14	45.000	3.2
C12	7.17	90.000	2.3
C13	10.14	45.000	3.2
C14	14.34	90.000	3.5
C15	10.14	45.000	2.8
C16	7.17	0.000	2.3
C17	10.14	45.000	3.2

Table 4-18: Summary of calculations with resistance factors for Specimen 4.

Specification	Predicted Load (kips)	Actual/ Predicted
AASHTO LRFD	30.6	1.41
CSA A23.3	30.6	1.41
ACI 318-05	25.5	1.69
NZS 3101	25.5	1.69
CEB-FIP MC 90	25.7	1.67
1999 FIP Rec.	29.5	1.46
DIN 1045-1	29.5	1.46

Table 4-19: Summary of Calculations without resistance factors for Specimen 4.

Specification	Predicted Shear (kips)	Actual/ Predicted
AASHTO LRFD	33.9	1.27
CSA A23.3	33.9	1.27
ACI 318-05	33.9	1.27
NZS 3101	33.9	1.27
CEB-FIP MC 90	33.9	1.27
1999 FIP Rec.	33.9	1.27
DIN 1045-1	33.9	1.27

Figures

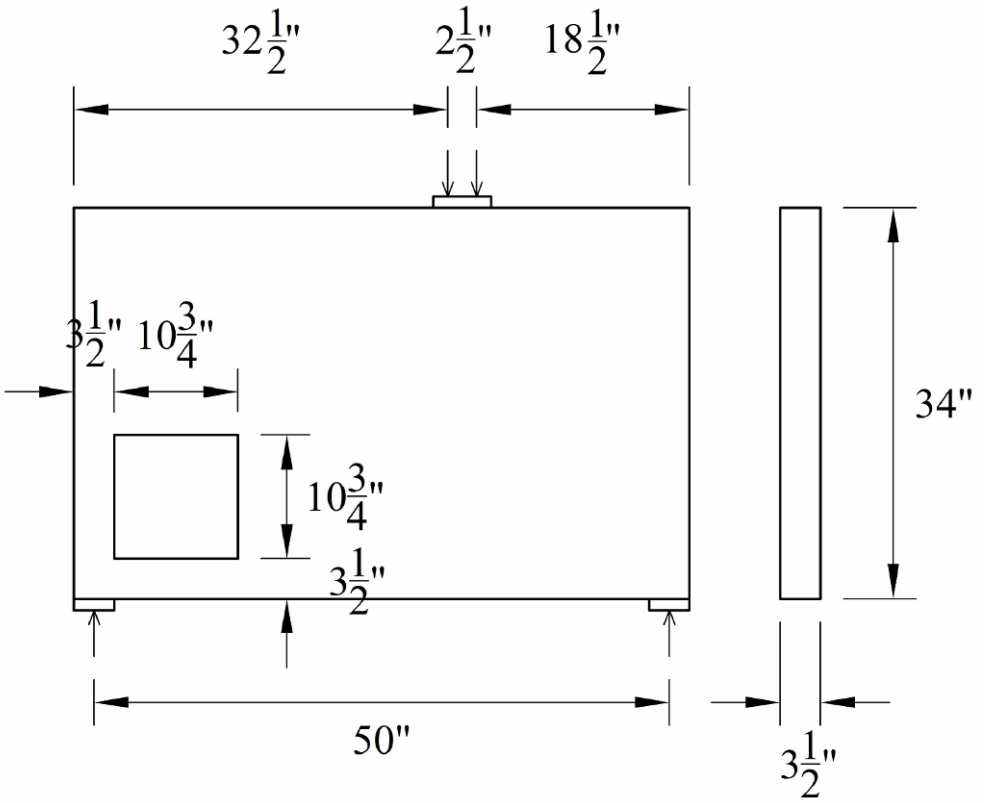

Figure 4-15: Dimensions of deep beam with opening.

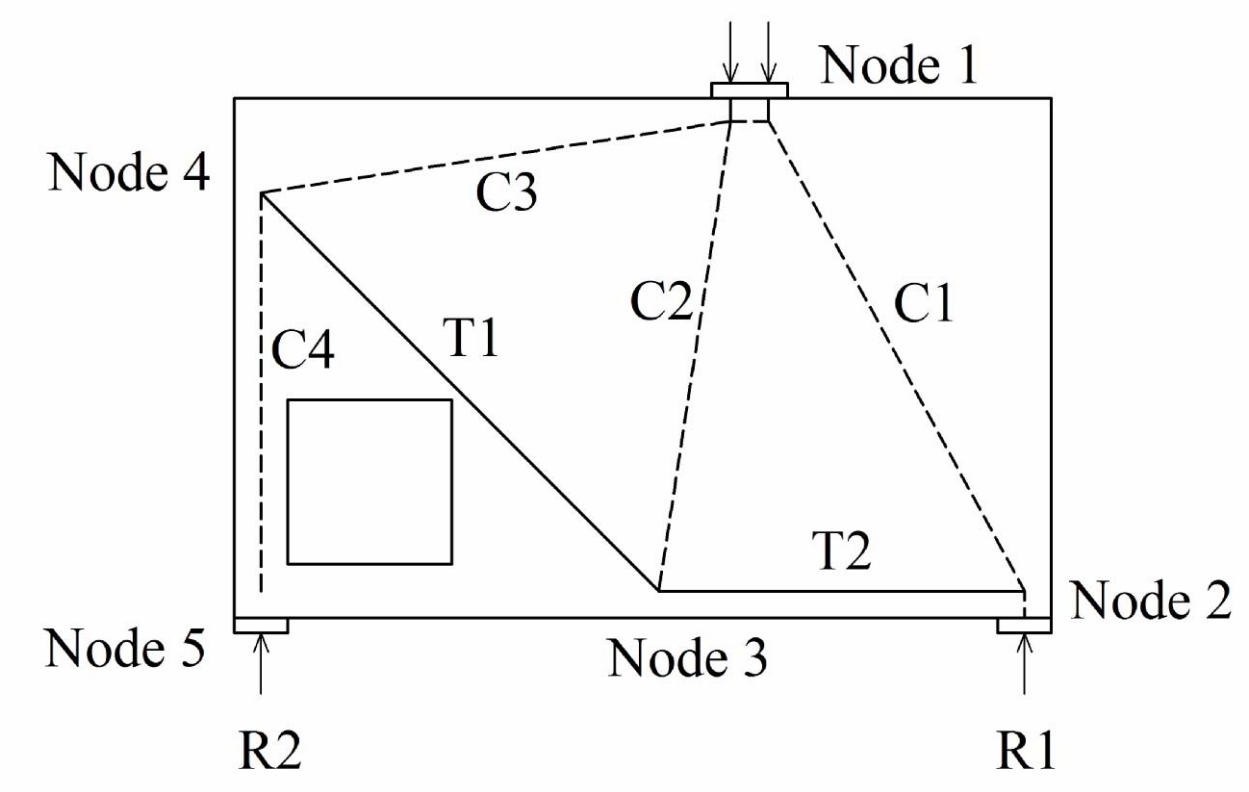

Figure 4-16: Member labels for Specimen 2 strut-and-tie model.

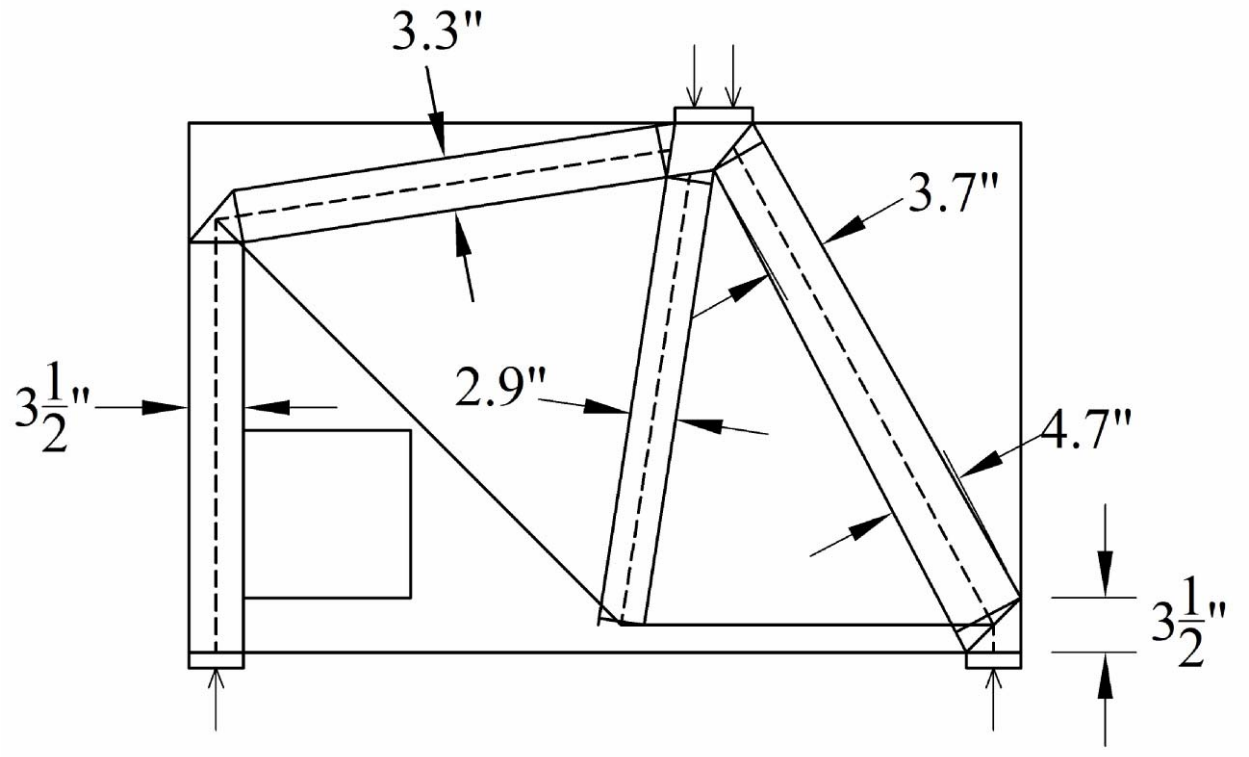

Figure 4-17: Strut widths for Specimen 2.

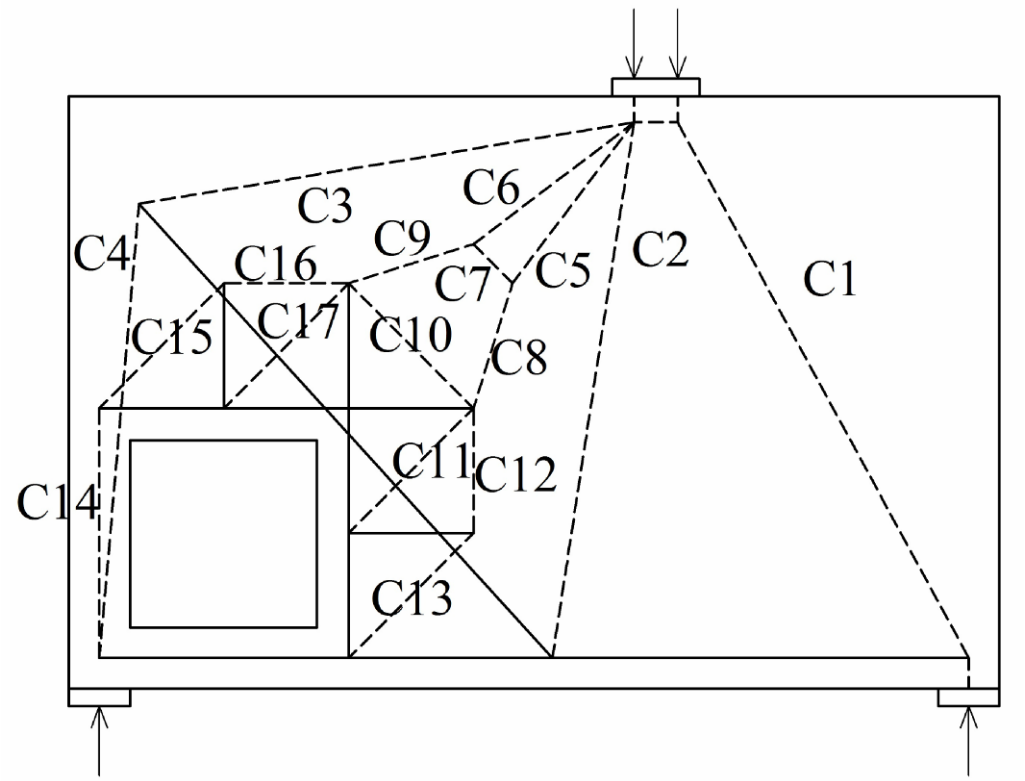

Figure 4-18: Strut labels for Specimen 4.

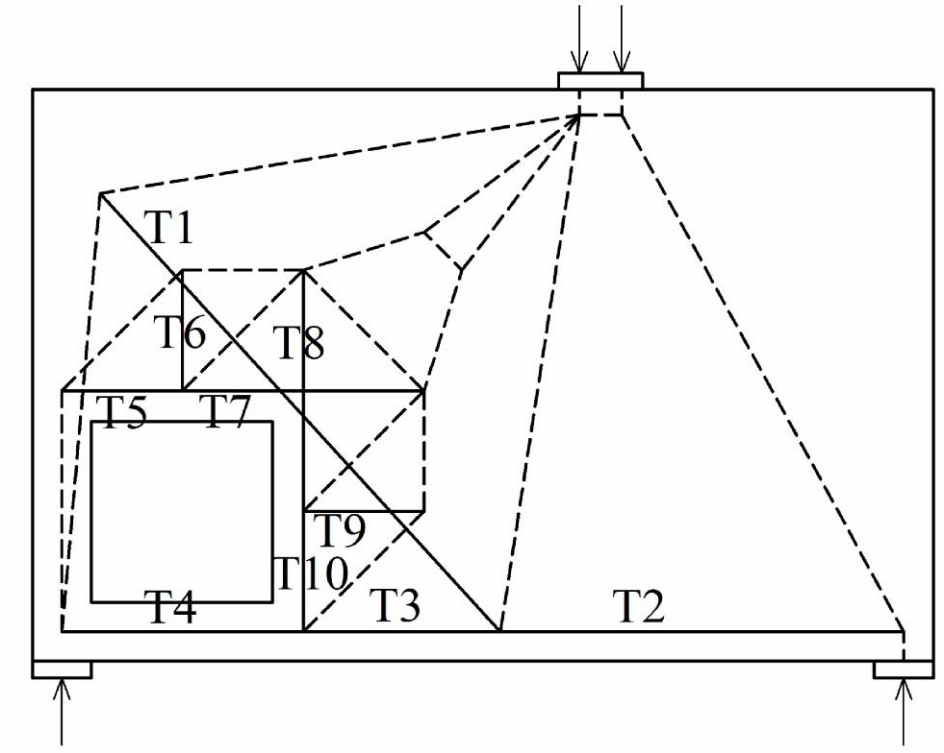

Figure 4-19: Tie labels for Specimen 4.

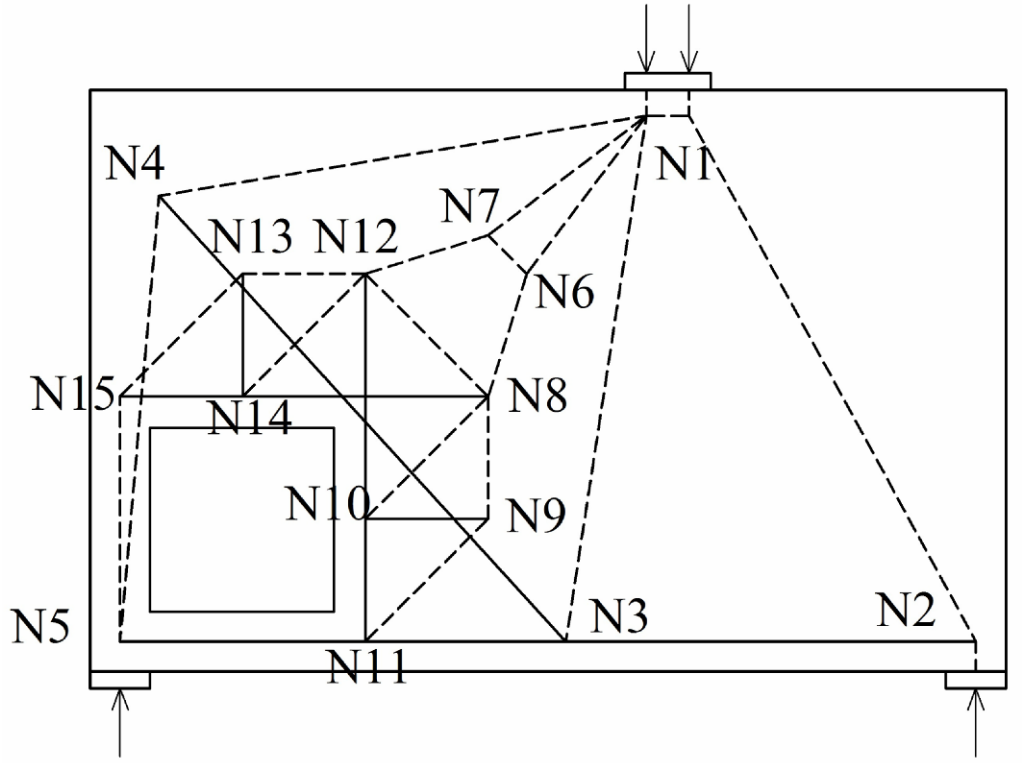

Figure 4-20: Node labels for Specimen 4.

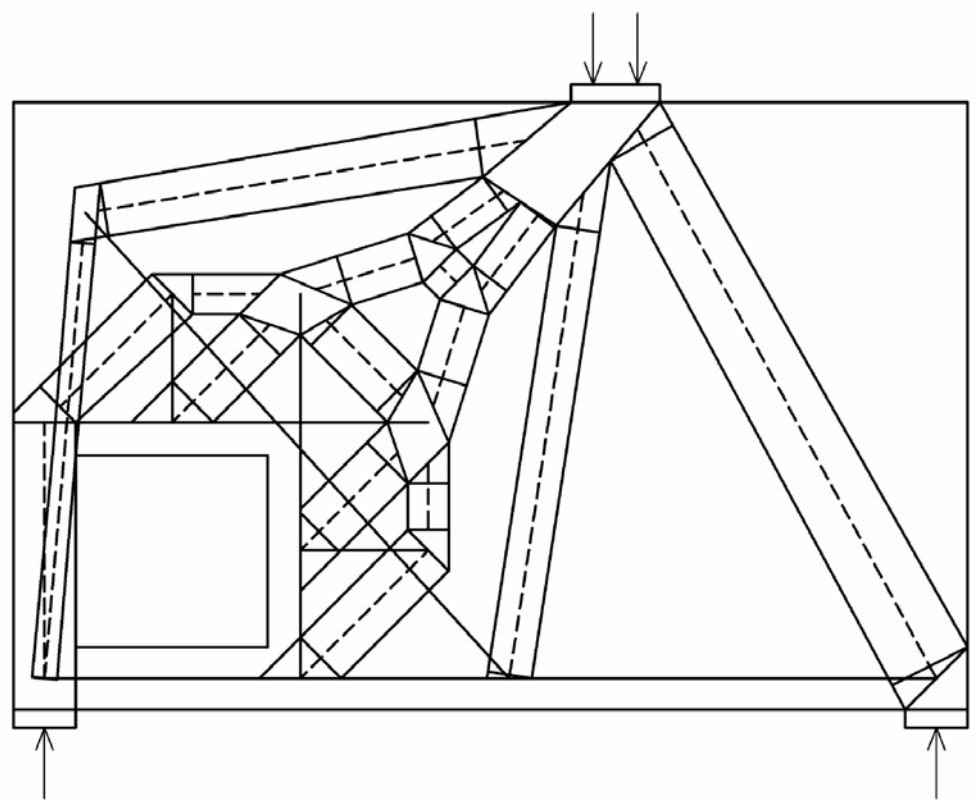

Figure 4-21: Visualization of strut widths for Specimen 4.

4.2.3 PILE CAP TEST COMPARISONS

The capacity of a pile cap (Pile Cap B) tested by Adebar et al. was determined for several different specifications using a strut-and-tie model analysis similar to the previous analyses performed on the deep beam and the deep beam with a hole. The predicted capacities were compared to the experimental failure which was 493kips. According to Adebar, the failure of the pile cap occurred when the stress in the short tie (see Figures 4-22 and 4-23) reached its yield stress due to the fact that the two piles closest to the column were taking a large portion of the total load. At that point, the strain in the short tie increased drastically, the loads in the piles closest to the column decreased, the loads in the piles farthest from the column increased, and large cracks formed which divided the specimen into large pieces. All of the results were also compared the AASHTO LRFD predictions.

The plan view of Pile Cap B is shown in Figure 4-22. The pile cap was designed using the combination of two different strut-and-tie models which were perpendicular to each other. The reason for modeling the pile cap this way was due to the fact that the provided reinforcement was only placed between opposite piles. The dimensions of the strut-and-tie model for Section "1-1" are shown in Figure 4-23. In addition, the node and strut dimensions for Section "1-1" are shown in Figure 4-24. Similarly, for Section "2-2", the dimensions of the strut-and-tie model and dimensions of the nodes and struts are shown in Figures 4-25 and 4-26 respectively.

The predicted capacities for each of the specifications are given in Tables 4-20 and 4-21. The values in Table 4-20 were calculated using resistance factors, and the values in Table 4-21 were calculated neglecting the resistance factors. Both with and without resistance factors, the AASHTO LRFD and the CSA A23.3 gave the most conservative results. For both specifications, this can be attributed to the fact that the strut compressive strength is a function of the strain in the reinforcement and the angle between the strut and the tie. In both sections, the limiting factor is the strut compressive strength which is severely reduced due to the fact that the angles between the struts and ties are small (this is especially true for Section "2-2").

When using the 1984 CSA A23.3, Adebar calculated a much larger predicted capacity. He was able to do this because section 15.5.4 of the 1984 CSA A23.3 allowed for the compressive strength of concrete for piles supported on footings to be increased by a factor of:

$$\sqrt{\frac{A_2}{A_1}} \leq 2$$

where:

A_2 is the maximum cross-sectional area of the portion of concrete that is geometrically similar to and concentric to the stressed area.

A_1 is the stressed area (cross-sectional area of strut).

This factor was also applied to the AASHTO LRFD results. When using resistance factors, the modified calculated capacity was found to be 306 kips. Similarly, when resistance factors were

neglected, the calculated capacity was found to be 370 kips. This data is summarized in Table 4-22. This process yielded better results when compared to the results from the other specifications.

The measured pile load distribution in the experiment is given in Table 4-23. The predicted pile load distributions for each of the specifications using and disregarding resistance factors are given in Tables 4-24 and 4-25 respectively. In terms of percentage of the total load, each of the specifications predicts a more balanced load distribution than what was actually measured. The AASHTO LRFD and CSA A23.3 appear to show a load distribution similar to what was measured, but this is due to the fact that the limiting strut compressive stress in Section "2-2" was severely limited (approximately $0.35f'_c$).

Notes about Pile Cap Design

- The areas of the struts are polygons due to the spreading of forces from the top of the piles to the full width of the ties above the piles, but for the calculations they were approximated to be rectangular areas.

- Footings/pile caps are exempt from the crack control requirements (AASHTO LRFD 5.6.3.6)

Tables

Table 4-20: Calculated capacities using resistance factors. The actual capacity was 493kips.

Specification	Predicted Load (kips)	Actual/Predicted
AASHTO LRFD	218.9	2.25
CSA A23.3	218.9	2.25
ACI 318-05	267.4	1.84
NZS 3101	267.4	1.84
CEB-FIP MC 90	189.0	2.61
1999 FIP Rec.	252.6	1.95
DIN 1045-1	222.9	2.21

Table 4-21: Calculated capacities without resistance factors. The actual capacity was 493 kips.

Specification	Predicted Load (kips)	Actual/Predicted
AASHTO LRFD	293.4	1.68
CSA A23.3	293.4	1.68
ACI 318-05	356.6	1.38
NZS 3101	356.6	1.38
CEB-FIP MC 90	323.9	1.52
1999 FIP Rec.	369.9	1.33
DIN 1045-1	334.3	1.47

Table 4-22: Predicted capacities using 1984 CSA A23.3 concrete strength increasing factor with the AASHTO LRFD provisions.

Calculation	Predicted Load (kips)	Actual/ Predicted
With Resistance Factors	305.7	1.61
Without Resistance Factors	369.7	1.33

Table 4-23: Recorded pile load distribution.

Piles in Section “1-1”		Piles in Section “2-2”	
Load, V (kips)	% of Total	Load, V (kips)	% of Total
354.4	72.0	138.2	28.0

Table 4-24: Calculated pile load distributions using resistance factors.

	Piles in Section "1-1"			Piles in Section "2-2"		
Specification	Predicted Load (kips)	Actual/ Predicted	% of Total	Predicted Load (kips)	Actual/ Predicted	% of Total
AASHTO LRFD	131.7	2.69	60.1	87.3	1.58	39.9
CSA A23.3	131.7	2.69	60.1	87.3	1.58	39.9
ACI 318-05	138.5	2.56	51.8	128.9	1.07	48.2
NZS 3101	138.5	2.56	51.8	128.9	1.07	48.2
CEB-FIP MC 90	97.9	3.62	51.8	91.1	1.52	48.2
1999 FIP Rec.	130.9	2.71	51.8	121.7	1.13	48.2
DIN 1045-1	115.5	3.07	51.8	107.4	1.29	48.2

Table 4-25: Calculated pile load distributions without resistance factors.

	Piles in Section "1-1"			Piles in Section "2-2"		
Specification	Predicted Load (kips)	Actual/ Predicted	% of Total	Predicted Load (kips)	Actual/ Predicted	% of Total
AASHTO LRFD	175.2	2.02	59.7	118.3	1.17	40.3
CSA A23.3	175.2	2.02	59.7	118.3	1.17	40.3
ACI 318-05	184.7	1.92	51.8	171.9	0.80	48.2
NZS 3101	184.7	1.92	51.8	171.9	0.80	48.2
CEB-FIP MC 90	187.3	1.89	57.8	136.6	1.01	42.2
1999 FIP Rec.	187.3	1.89	50.6	182.6	0.76	49.4
DIN 1045-1	173.2	2.05	51.8	161.1	0.86	48.2

Figures

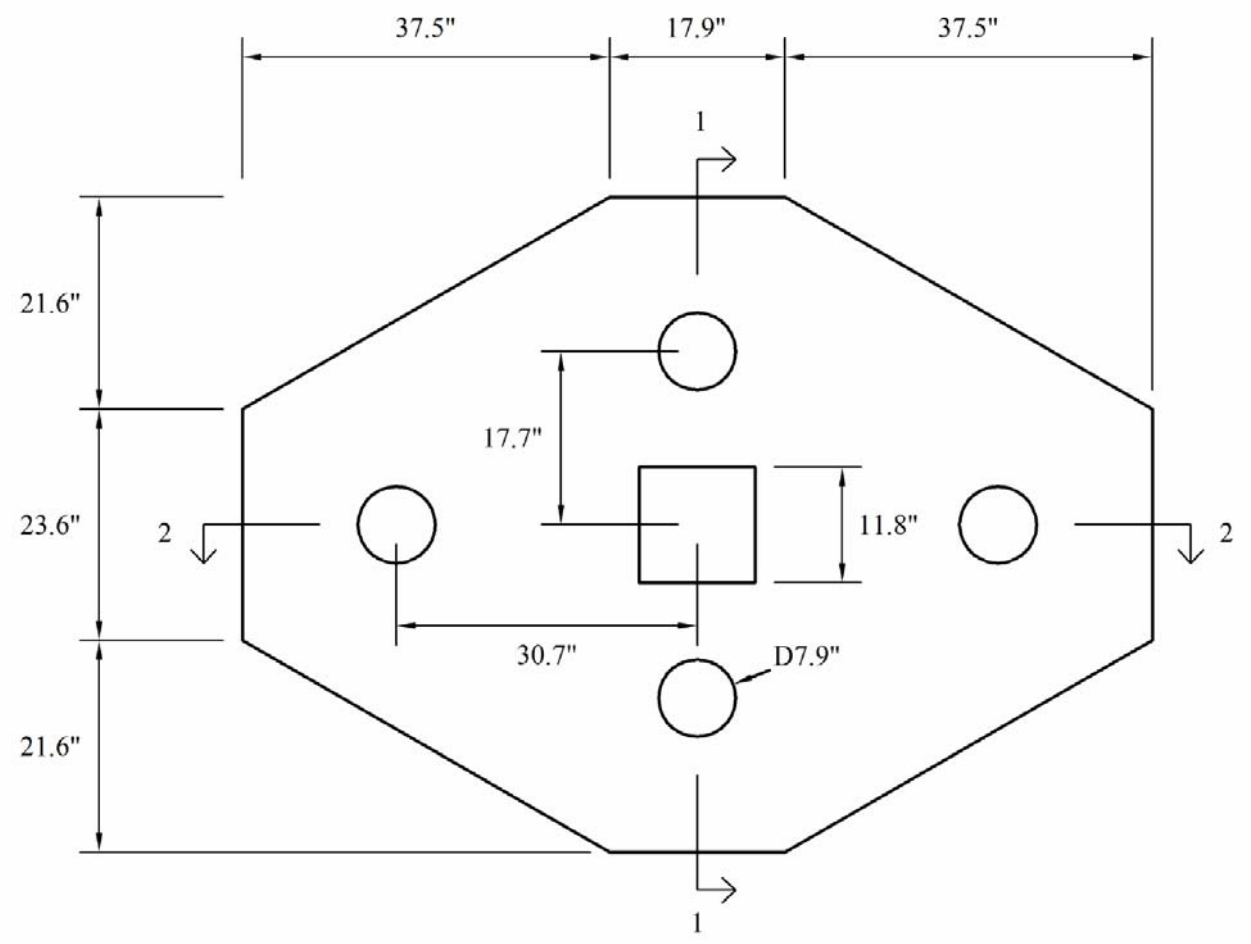

Figure 4-22: Plan view of pile cap.

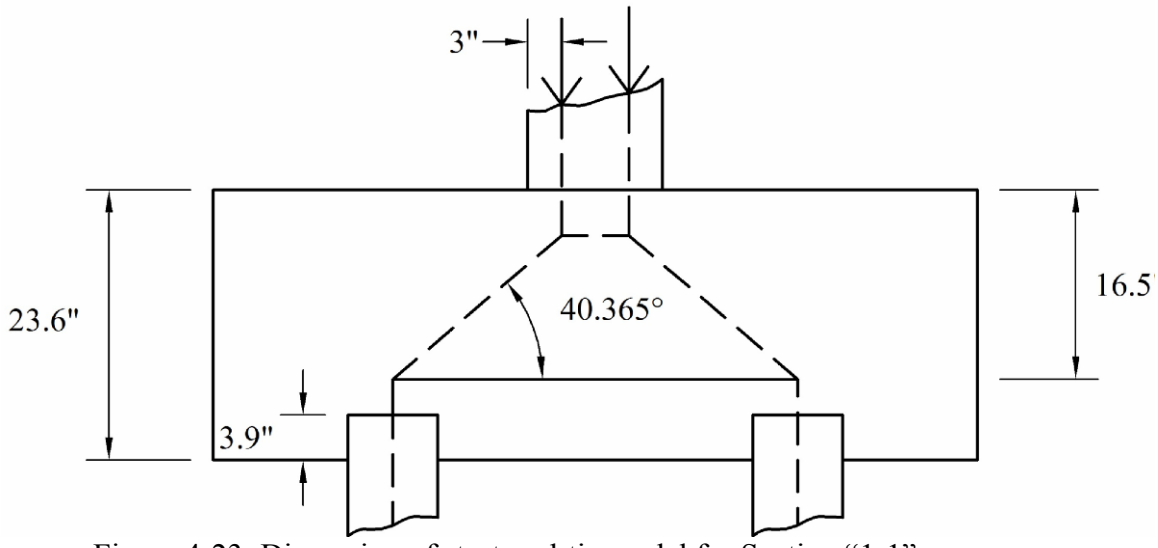

Figure 4-23: Dimension of strut-and-tie model for Section “1-1”.

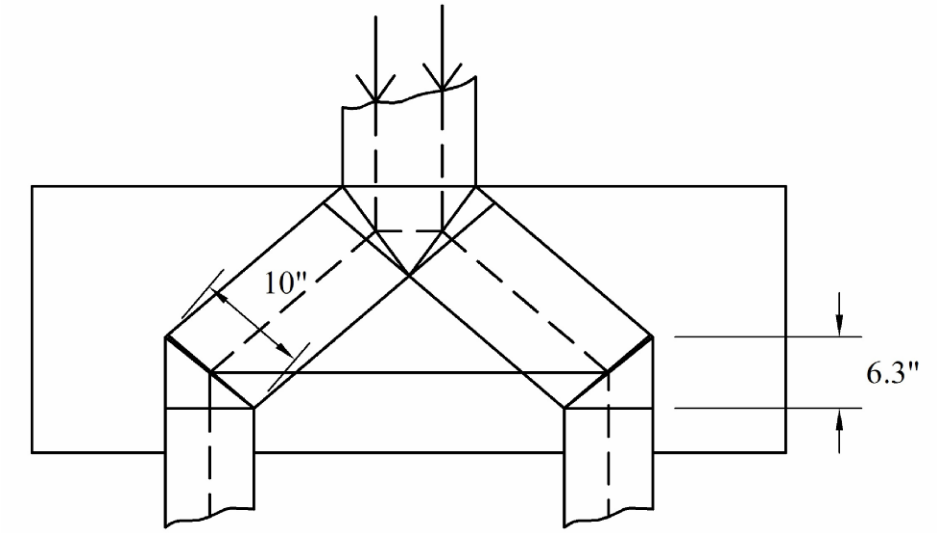

Figure 4-24: Dimensions of struts and nodes for Section “1-1”.

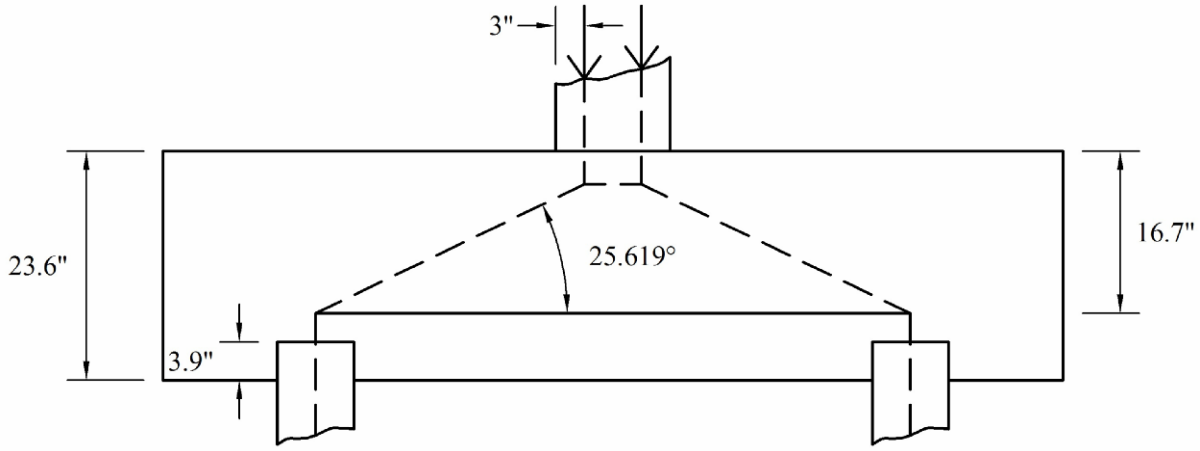

Figure 4-25: Dimension of strut-and-tie model for Section “2-2”.

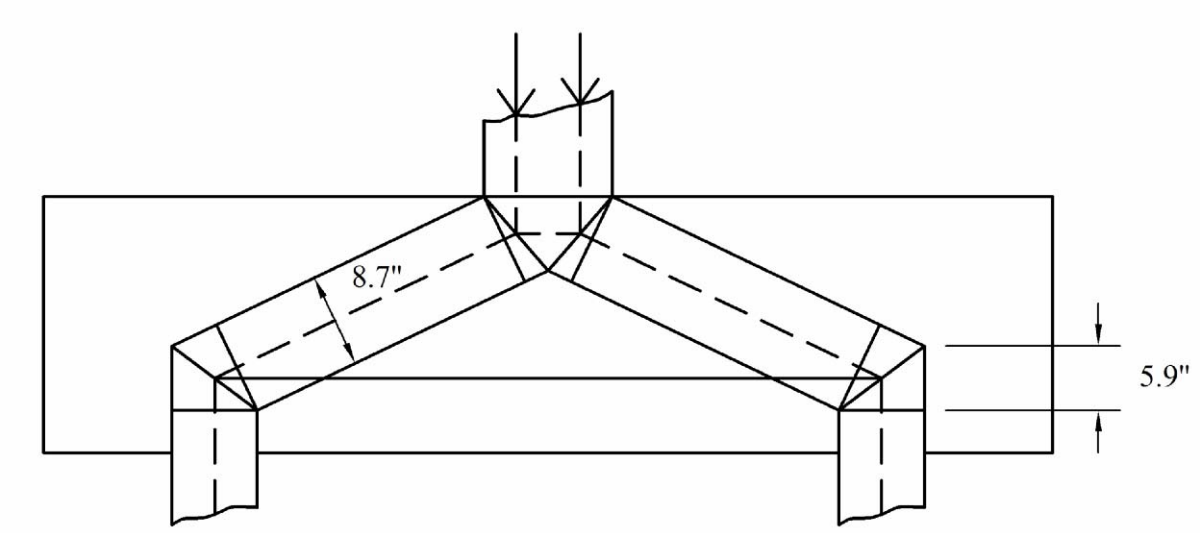

Figure 4-26: Dimensions of struts and nodes for Section “2-2”.

4.2.4 INSIGHT GAINED FROM TEST COMPARISONS

Deep Beam

The deep beam strut-and-tie model examples were performed first. These examples were used to show how variations in the strut-and-tie models affect the predicted capacities of the deep beam. Both the simple and complex models were conservative for design.

Deep Beam with Opening

The areas where the crack control requirements of AASHTO LRFD 5.6.3.6 were satisfied exhibited far less cracking than areas in the beam that did not utilize crack control. This seems to verify the suitability of the orthogonal grid of reinforcing bars; however, not enough information was obtained to comment on the amount of crack control reinforcement specified in each direction. In order to comment on the minimum amount of crack control within in a D-region, research should be performed that compares the crack control provisions of the CSA A23.3, CSA-S6-06, ACI 318-05, and AASHTO LRFD Bridge Design Specification. This type of research would determine if any of the specifications are unconservative or overly conservative.

Pile Cap

In the pile cap, the angle between the inclined struts and the ties was small due to the geometric constraints of the pile cap. With reference to the AASHTO LRFD strut-and-tie model specifications, this small angle greatly reduced the effective compressive strength of the inclined struts which caused the predicted capacity of the pile cap to be significantly less than the true capacity. For these types of structures, it may be desirable to allow for the effective compressive strength to be increased by a factor similar to the one Adebar used (described in the pile cap test comparison), or, maybe, a minimum reduction factor should be implemented.

All Examples

Performing these examples helped identify confusing areas and gaps in the AASHTO LRFD Bridge Design Specification. These issues are addressed in Section 4.5.

4.3 COMPARISONS TO STRUCTURES DESIGNED BASED ON PAST PRACTICES

Most concrete structures in use today were designed prior to the adoption of the STM approach. For this reason, three typical structures designed in the late 1970's were selected for evaluation utilizing the STM approach and a comparison made to the original design. The structures selected were an inverted tee bent cap, a multi-column bent, and a pile-supported footing. The original calculations for each of these examples were reviewed for compliance with the AASHTO Specification in effect at the time of design. Other than some minor designer "conservativeness" they all were designed in conformance with AASHTO criteria. It should be noted, that the inclusion of these examples reflects more on the availability of design calculations for existing structures than on a recommendation to use STM for these specific examples. An effective argument could be built that the application of STM on two of the first two of these structures is needlessly complex and time consuming for use in a design office. No exception is taken to that position. That being said, though somewhat of an academic exercise, the examples do provide a means of explaining the STM process and comparing the results to designs that predate STM provisions.

4.3.1 INVERTED TEE PIER CAP

Illustrated in Figure 4-27 is a three-column intermediate pier bent. The pier cap is an inverted tee section supporting 18 precast beams on each side. The pier was originally designed in 1975 using the AASHTO Specifications for Highway Bridges and Load Factor Design. The concrete strength is 3000 psi and the reinforcement is Grade 60. The bridge has two 52 ft roadways. A cross section of the pier cap is shown in Figure 4-28.

Since the original design for this structure was LFD, the original service level loads that were used in the design were factored in accordance with the LRFD Specifications. Live loads were applied to maximize shear and moment at their controlling locations. It was found that shear due to live loads applied to both adjacent bridge spans controlled over combined shear and torsion resulting from live load being applied to one span only.

For the pier cap evaluation, two strut-and-tie models (STM's) were developed. The first, a local model, was used to evaluate the factored resistance of the beam ledges in transferring the reaction of the precast girders into the stirrups of the pier cap. The second STM, a global model, was then used to evaluate the longitudinal and transverse reinforcement of the pier cap.

Local Model

Step 1 – Delineate the D-regions.

The whole member is a D-region.

Step 2 – Determine the boundary conditions of the D-region.

There is no D- and B-region interface.

Step 3 – Sketch the flow of forces.

This step was deemed unnecessary for this example

Steps 4 and 5 – Draw the STM and solve for the strut and tie forces.

The local STM is shown in Figure 4-29. The girder reactions are transferred to the pier cap stirrups by Struts A-B and A'-B'. Tie A-A' develops to carry the horizontal component of the inclined Strut A-B/A'-B' force. The depth of Strut B-B' is determined based on the greater of following:

- The depth of concrete that is required to provide the minimum required Strut B-B' resistance,
- The development length of the #6 stirrups, calculated in accordance with LRFD Article 5.11.2.6.2,

For this example, the second condition controls. The development length of the stirrup is:

$$l_e = \frac{0.44 d_b f_y}{\sqrt{f'_c}} = \frac{0.44 \times 0.75" \times 60 ksi}{\sqrt{3 ksi}} = 11.4 in.$$

The 2" cover distance is added to this dimension to obtain the 13.4 in. shown.

The resulting STM forces are shown in Figure 4-29.

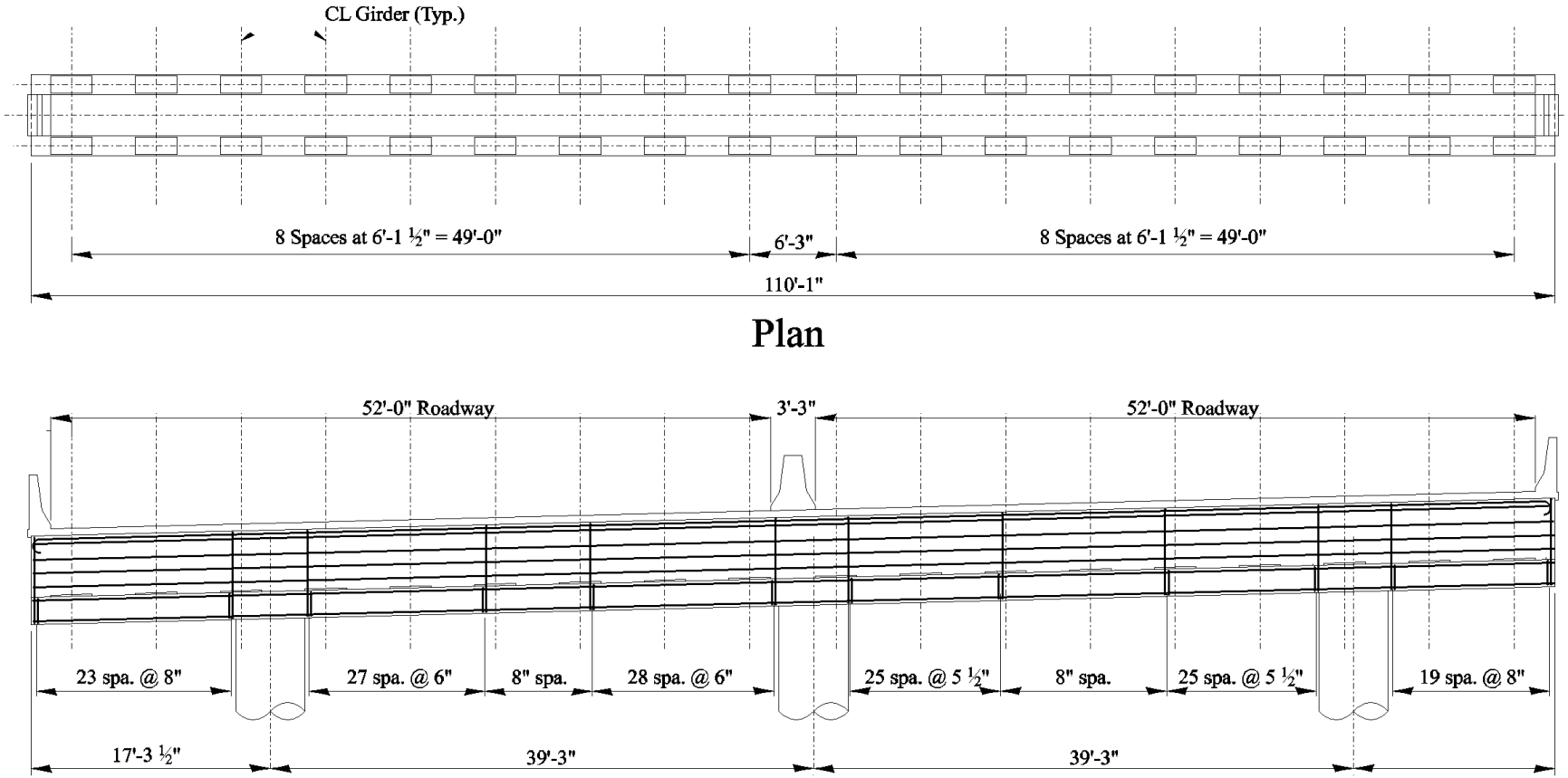

Figure 4-27: Pier cap geometry.

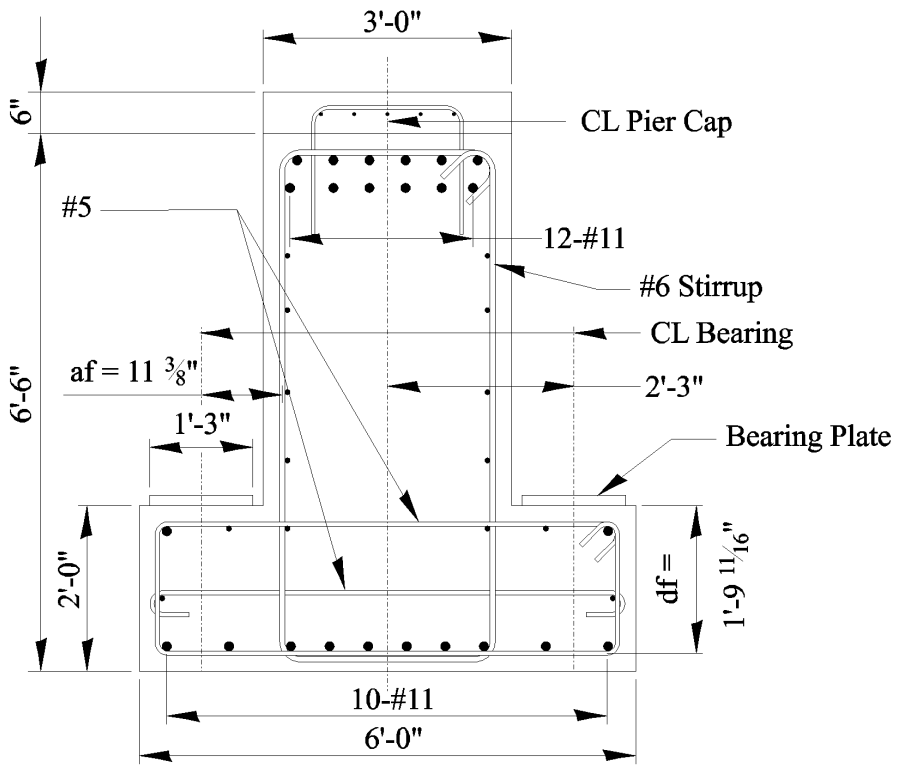

Figure 4-28: Pier cap cross section.

Steps 4 and 5 (continued) – Draw the STM and solve for the strut and tie forces.

Because the edge distance between the edge of the exterior bearing pad and the end of the pier cap is less than the effective depth of the ledge, d_f, of 21.69", per LRFD Article 5.13.2.5.5, the exterior bearing locations control the local STM resistance (all girder reactions are assumed equal).

The dimensions of the strut and the area of steel contributing to the ties are determined in accordance with LRFD 5.13.2.5. The length of cap contributing to the local STM is:

Width of Tie A-A': 51.8" ($W+5a_f$, AASHTO LRFD 5.13.2.5.2)

Width of Strut B-B and Tie C-C': 70.0" (controlled by 2 x edge distance)

See Figure 4-29.

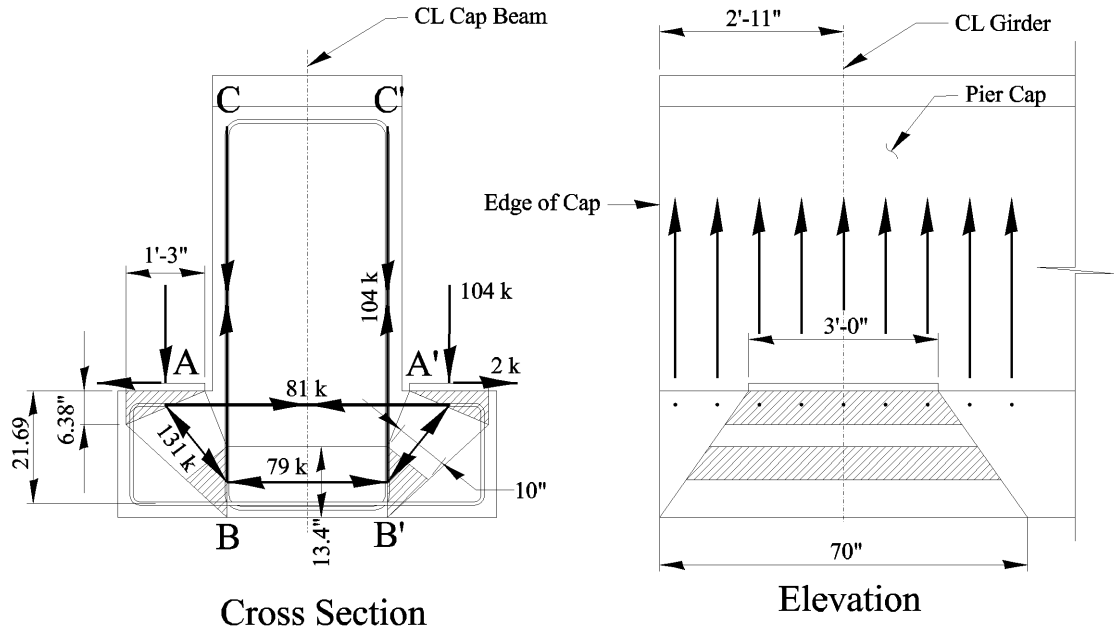

Figure 4-29: Local STM.

Step 6 – Check tie resistance.

Tie A-A' comprises 9-#5 bars with a factored resistance of:

$$P_r = \phi P_n = 0.90 \times 9bars \times 0.31in^2 \times 60ksi = 151kips$$

This is greater than the demand of 81 kips.

Tie B-C comprises 9-#6 bars with a factored resistance of:

$$P_r = \phi P_n = 0.90 \times 9bars \times 0.44in^2 \times 60ksi = 214kips$$

This is greater than the demand of 104 kips.

Step 7(a) – Check strut resistance.

As shown in Figure 4-29, Strut A-B carries a force of 131 kips, while B-B' carries a force of 79 kips. The angle between Strut A-B and Tie A-A' is $52.8°$. Due to its smaller area and larger force, Strut A-B controls over Strut B-B'. Due to its variation in area over its length, and the fact that strut resistance is dependent on STM geometry and tie forces, its resistance at either end will be different. Both ends will therefore be checked.

At node A, using the information developed in Step 4 and the geometry of Figure 4-30, the area of the strut is calculated as:

$$A_s = \left[l_b \sin(\theta_s) + h_s \cos(\theta_s)\right] \cdot Width = \left[15" \sin(52.8°) + 6.38" \cos(52.8°)\right] \cdot 42" = 660in^2$$

The tensile strain in Tie A-A' is:

$$\varepsilon_s = \frac{P_u}{A_{st}E_s} = \frac{81kips}{9bars \times 0.31in^2 \times 29,000ksi} = 0.0010$$

At the centerline of the strut, this strain is reduced to half this value, per LRFD Article C5.6.3.3.3. The angle between Strut A-B and Tie A-A' is 52.8°. The principal tensile strain in the strut is calculated using LRFD Equation 5.6.3.3.3-2:

$$\varepsilon_1 = \varepsilon_s + (\varepsilon_s + 0.002)\cot^2 \alpha_s = 0.0005 + (0.0005 + 0.002)\cot^2 52.8^0 = 0.0019$$

The limiting compressive stress is then calculated using LRFD Equation 5.6.3.3.3-1:

$$f_{cu} = \frac{f'_c}{0.8 + 170\varepsilon_1} = \frac{3ksi}{0.8 + 170 \times 0.0019} = 2.66ksi > 0.85f'_c = 0.85 \times 3ksi = 2.55ksi$$

The limiting stress will be taken as 2.55 ksi.

The factored resistance of Strut A-B at Node A is:

$$P_r = \phi P_n = \phi f_{cu} A_{cs} = 0.70 \times 2.55ksi \times 660in^2 = 1180kips$$

The area of Strut A-B at Node B is:

$$A = \frac{51" + 59.9"}{2} \times 10" = 555in^2$$

The tensile strain in Tie B-C is:

$$\varepsilon_s = \frac{P_u}{A_{st}E_s} = \frac{104kips}{9bars \times 0.44in^2 \times 29,000ksi} = 0.00091$$

Again, at the centerline of the strut, this strain is reduced to half this value. The angle between Strut A-B and Tie B-C is 37.2°. The principal tensile strain in the strut is calculated using LRFD Equation 5.6.3.3.3-2:

$$\varepsilon_1 = \varepsilon_s + (\varepsilon_s + 0.002)\cot^2 \alpha_s = 0.00045 + (0.00045 + 0.002)\cot^2 37.2^0 = 0.0043$$

The limiting compressive stress is then calculated using LRFD Equation 5.6.3.3.3-1.

$$f_{cu} = \frac{f'_c}{0.8 + 170\varepsilon_1} = \frac{3ksi}{0.8 + 170 \times 0.0043} = 1.97ksi \le 0.85f'_c = 0.85 \times 3ksi = 2.55ksi$$

The limiting stress will be taken as 1.97 ksi.

The factored resistance of Strut A-B at Node B is:

$$P_r = \phi P_n = \phi f_{cu} A_{cs} = 0.70 \times 1.97ksi \times 555in^2 = 765kips < 1180kips$$

The controlling Strut A-B resistance is 765 kips, much greater than its demand of 131 kips.

Step 7(b) – Check nodal zone stress limits.

Nodal Zone A has a rectangular top surface, matching the bearing plate shape. As shown in Figure 4-30, the surface adjoining Strut A-B is trapezoidal, with a top width of 36", a bottom width of 45.0", and a depth of 16.3".

The top surface of Nodal Zone A has a stress of:

$$f_c = \frac{104kips}{15" \times 36"} = .193ksi$$

This is much less than the nodal stress limit for a CCT node of:

$$0.75\phi f'_c = 0.75 \times 0.70 \times 3 = 1.58ksi$$

The surface of Nodal Zone A adjoining Strut A-B (shaded in Figure 4-30), has an area of

$$A = \frac{36" + 45"}{2} \times 16.3" = 660in^2$$

and a stress of:

$$f_c = \frac{131kips}{660in^2} = .198ksi$$

This is also less than the stress limit of 1.58 ksi.

Nodal Zone B's surface adjoining Strut A-B (shown in Figure 4-31), is also trapezoidal with a top width of 51.0", a bottom width of 59.9", and a depth of 10.0". The surface area is:

$$A = \frac{51" + 59.9"}{2} \times 10" = 555in^2$$

and a stress of:

$$f_c = \frac{131kips}{555in^2} = .228ksi$$

This is less than the nodal stress limit of 1.58 ksi for a CCT node, as calculated above.

The surface adjoining Strut B-B' has a larger area and a smaller force, and will therefore not control.

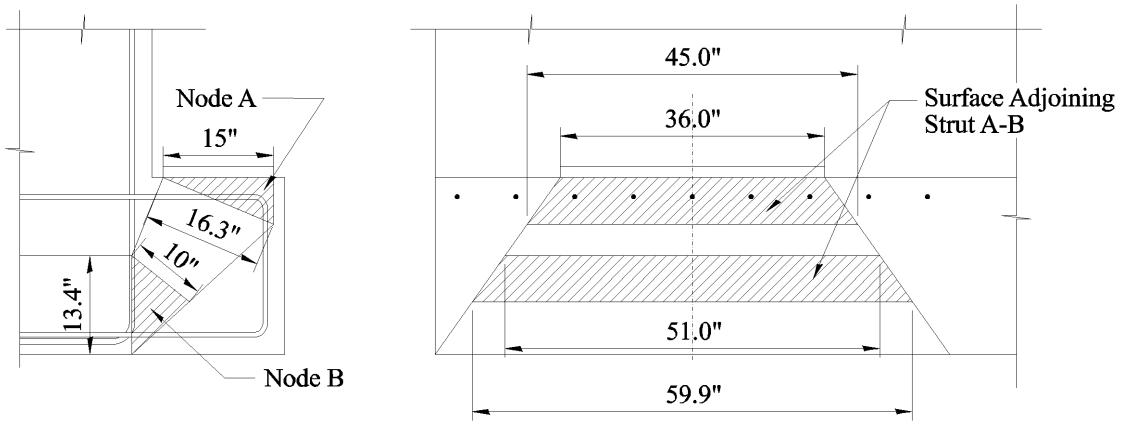

Figure 4-30: Node details.

Step 8 – Check details of reinforcement.

Check development length of Tie A-A'

The required development length is calculated from LRFD Eq. 5.11.2.4.1-1:

$$l_{hb} = \frac{38.0 d_b}{\sqrt{f'_c}} = \frac{38.0 \times 0.625"}{\sqrt{3ksi}} = 13.7in.$$

This is less than the width of Node A and is therefore adequate.

Global Model

Step 1 – Delineate the D-regions.

Due to closely spaced large loads the whole member can be considered a D-region.

Step 2 – Determine the boundary conditions of the D-region.

There is no D- and B-region interface.

Step 3 – Sketch the flow of forces.

The flow of forces has been visualized and results in the STM used in steps 4 and 5.

Step 4 and 5 – Develop the STM and solve for the member forces.

The loading applied to the pier cap is shown in Figure 4-31(a). Live load forces were applied as a uniformly distributed load, in conformance with the original design. Because the flexural reinforcement is uniform over the length of the cap, the loading shown was the only one considered, as it was found to produce the maximum positive moment (mid-span between columns B and C), maximum negative moment (at the outside face of Column A), and maximum shear (on the loaded side of Column B). An analysis was performed to determine the column forces based on this loading.

The loading applied to the STM is shown in Figure 4-31(b). The lane load portion of the live load, which is transferred to the cap through the girder bearings, was applied to the STM at the bottom nodes; the concentrated portion was applied to the top nodes. The self-weight of the cap was applied to the STM equally at the top and bottom nodes.

The locations of the top and bottom chords were determined based on the center of gravity of the longitudinal reinforcement; the exception was the top chord compression members.

Due to the deck slab providing an additional depth of concrete well above the top longitudinal reinforcement, the effective depth of the section is greater for positive moment than for negative moment. The resulting truss model also has a greater depth in the positive moment regions than in the negative moment regions. The depth of the compressive top chord member is determined based on its required resistance.

The resulting STM forces are shown in Figure 4-31(c).

Step 6 – Check tie resistance.

Positive Moment Reinforcement:

From Figure 4-28, there are 10 # 11 bottom reinforcing bars. The tensile factored resistance of the bottom chord therefore is:

$$P_r = \phi P_n = 0.90 \times 10 bars \times 1.56 in^2 \times 60 ksi = 842 kips$$

This is greater than the maximum demand of 521 kips at Panels 12 and 13.

Negative Moment Reinforcement:

From Figure 4-28, there are 12 # 11 top reinforcing bars. The tensile factored resistance of the top chord therefore is:

$$P_r = \phi P_n = 0.90 \times 12 bars \times 1.56 in^2 \times 60 ksi = 1010 kips$$

This is greater than the maximum demand of 828 kips.

For reinforced beams, the requirement that $M_r \geq 1.2 M_{cr}$ will not control and is therefore not checked.

Shear Reinforcement:

Due to the varying spacing of the shear reinforcement, several locations will be checked:

- At Girders 2, 13, and 16, where the stirrup spacing is 8”
- At Girders 12 and 14, where the stirrups are spaced at 5 ½” on one side of the girder and 8” on the other,
- At Girders 11, and 15, where the stirrups are spaced at 5 ½”

8” stirrup spacing:

Number of bars over one panel (6’-1 ½”) = (73.5”/8” spacing +1) x 2 legs = 20-#6 bars

$P_r = \phi P_n = 0.90 \times 20 bars \times .44 in^2 \times 60 ksi = 475 kips$ - This is greater than the maximum demand of 435 kips at Girder 2.

5 1/2” stirrup spacing on one side of girder, 8” spacing on other side:
Number of bars over one panel (6’-1 ½”) = 73.5”/2(1/8” spacing + 1/5 1/2” spacing +1) x 2 legs= 24-#6 bars

$$P_r = \phi P_n = 0.90 \times 24 bars \times .44 in^2 \times 60 ksi = 570 kips$$

This is greater than the maximum demand of 327 kips at Girder 12.

5 1/2” stirrup spacing:
Number of bars over one panel (6’-1 ½”) = (73.5”/5 1/2” spacing +1) x 2 legs= 28-#6 bars

$$P_r = \phi P_n = 0.90 \times 28 bars \times .44 in^2 \times 60 ksi = 665 kips$$

This is greater than the maximum demand of 559 kips at Girder 11.

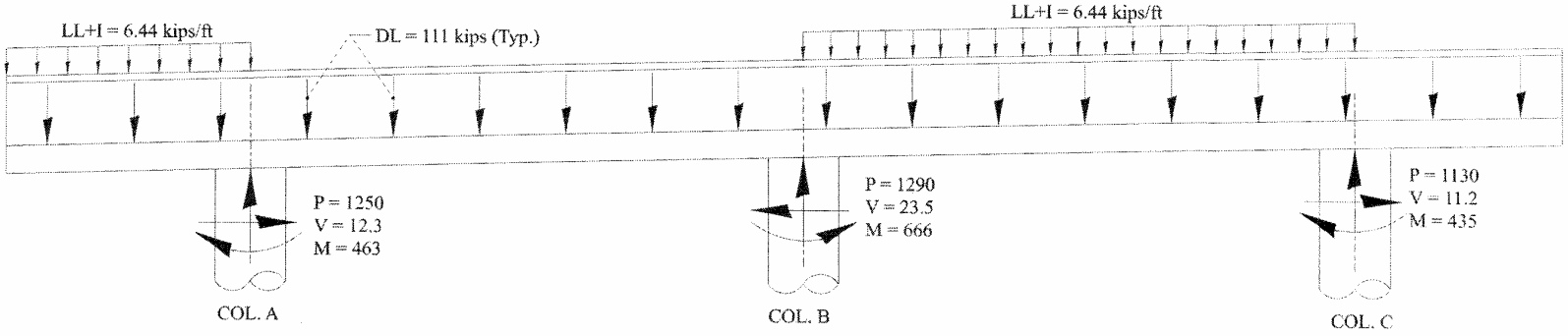

(a) Pier Cap Loading and Column Forces

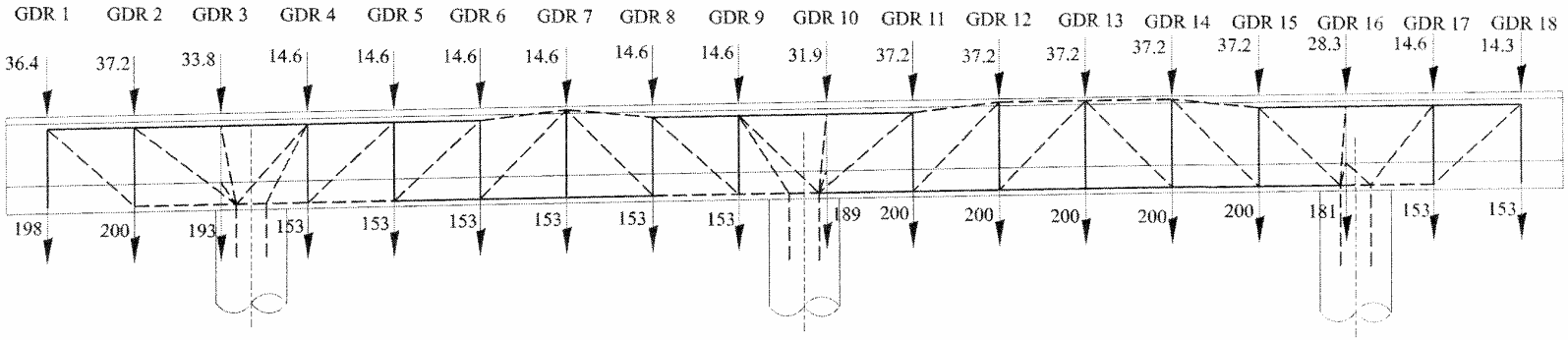

(b) STM Loading

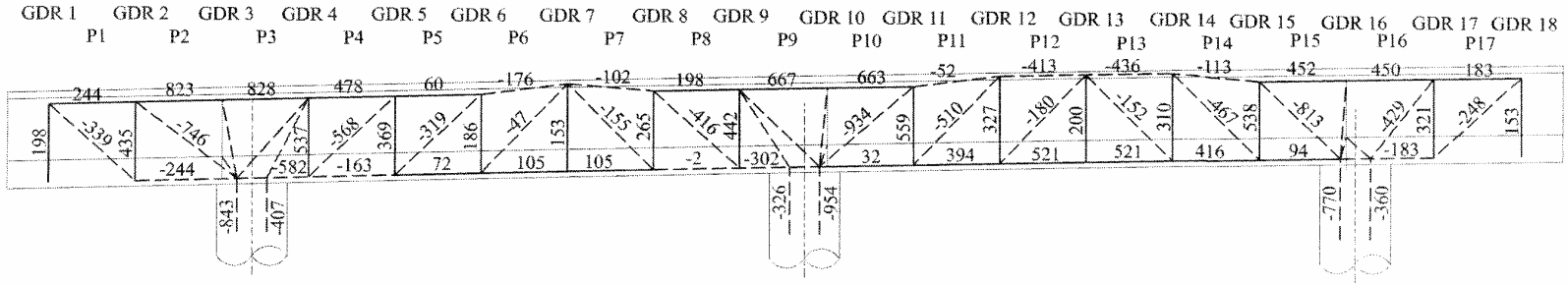

(c) STM Forces

Figure 4-31: Global STM.

Step 7(a) – Check strut resistance.

For all struts, the strain in the stirrup reinforcement shall be conservatively taken as $\varepsilon_s = \varepsilon_y = 0.00207$, and the strut angle taken as $\alpha_s = 45^o$. This results in the following:

From LRFD Eq. 5.6.3.3.3-2:

$$\varepsilon_1 = \varepsilon_s + (\varepsilon_s + 0.002)\cot^2 \alpha_s = 0.00207 + (0.00207 + 0.002)\cot^2 45° = 0.00616$$

From LRFD Eq. 5.6.3.3.3-1:

$$f_{cu} = \frac{f_c^{'}}{0.8 + 170\varepsilon_1} \le 0.85 f_c^{'} = \frac{3ksi}{0.8 + 170 \times 0.00616} = 1.62ksi \le 0.85 \times 3ksi = 2.55ksi$$

Bottom strut:

A strut depth of 0.60'=7.2" was assumed in the development of the STM. Its factored resistance is:

$$P_r = \phi P_n = \phi f_{cu} A_{cs} = 0.70 \times 1.62ksi \times 72in \times 7.2in = 588kips$$

This is greater than the maximum compressive bottom chord force of 582 kips in Panel 3.

Top strut:

A strut depth of 0.90'=10.8" was assumed in the development of the STM. Its factored resistance is:

$$P_r = \phi P_n = \phi f_{cu} A_{cs} = 0.70 \times 1.62ksi \times 36in \times 10.8in = 441kips$$

This is greater than the maximum compressive top chord force of 436 kips in Panel 3.

Diagonal struts:

The depth of a typical diagonal strut is determined from LRFD Figure 5.6.3.3.2-1 (a):

Depth = $\ell_a \sin\theta_s$ = 73.5 in x sin 45^o = 52 in.

Where ℓ_a is equal to the vertical spacing of 73.5".

Length = 2(cover + ½ d_b + 6d_{ba}) = 2(2 in. + ½ x ¾ in. +6x1 3/8 in.) = 21.25 in.

Where d_b is the stirrup diameter and d_{ba} is the diameter of the longitudinal reinforcement.

The strut's factored resistance is:

$$P_r = \phi P_n = \phi f_{cu} A_{cs} = 0.70 \times 1.62ksi \times 52in \times 21.25in = 1250kips$$

This is greater than the maximum compressive top chord force of 934 kips in Panel 10.

Step 7(b) – Check nodal zone stress limits.

Beam elements do not have discrete nodal zones, as the struts and ties are distributed uniformly over the length of the beam. This step is therefore eliminated.

Step 8 – Check details of reinforcement.

The crack control reinforcement satisfies Article 5.6.3.6.

4.3.2 MULTI-COLUMN BENT

Using the AASHTO LRFD Bridge Design Specification strut-and-tie provisions, the adequacy of a three column bent cap was verified for one of the load cases used in the original design. The bent was designed in 1977 using the AASHTO Specifications for Highway Bridges and Load Factor Design. The design was based on a concrete compressive strength of 3.5 ksi and Grade 60 steel. The details of the bent cap and the reinforcement are given in Figures 4-32 through 4-34. The total length of the bent is 81.5 feet, the full depth of the bent is 4.5 feet, and the width of the bent is 4 feet. The cross-section of the columns are 60 inches by 48 inches at the bent-column interface. The elevation of the south (left) end of the bent is two feet lower than the north (right) end of the bent. The horizontal dimensions and stirrup reinforcement details are symmetrical about the center column. Figure 4-32 depicts the horizontal dimensions on the south end of the bent which are identical to the horizontal dimensions of the north end of the bent. Similarly, Figure 4-33 details the stirrup reinforcement layout of the north end of the bent which are identical to reinforcement details for the south end of the bent. Figure 4-34 shows the cross-sections identified in Figure 4-32. The longitudinal reinforcement is labeled in these cross-sections.

Because the original design for this structure was LFD, the original service level loads that were used in the design were factored in accordance with the LRFD Specifications. The factored loads used in this example are given in Table 4-26. It should be noted that the girders are spaced at 10.645 ft, and the loads are applied through 48 inch by 48 inch bearing areas to the bent.

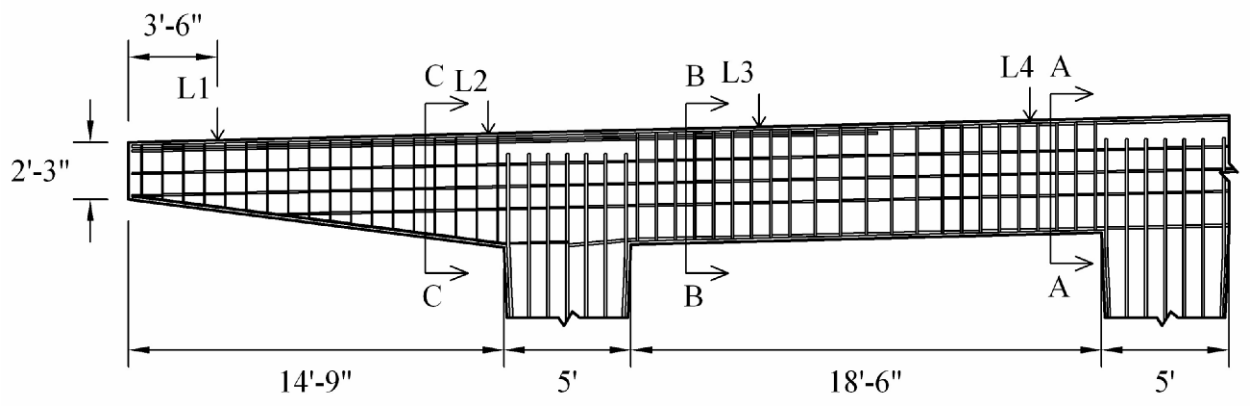

Figure 4-32: South end of bent.

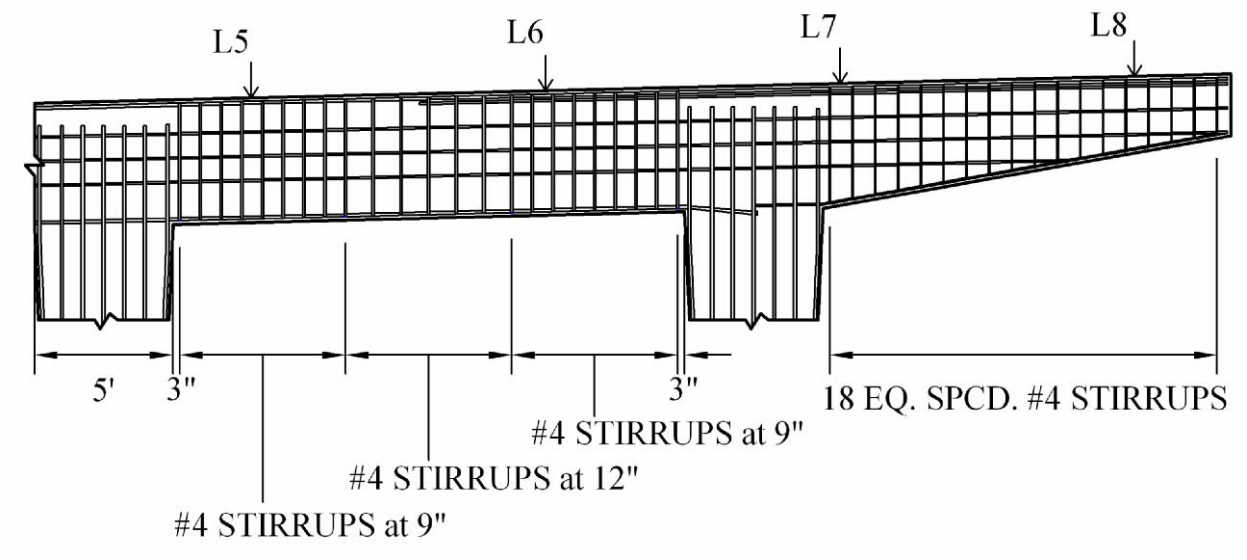

Figure 4-33: North end of bent.

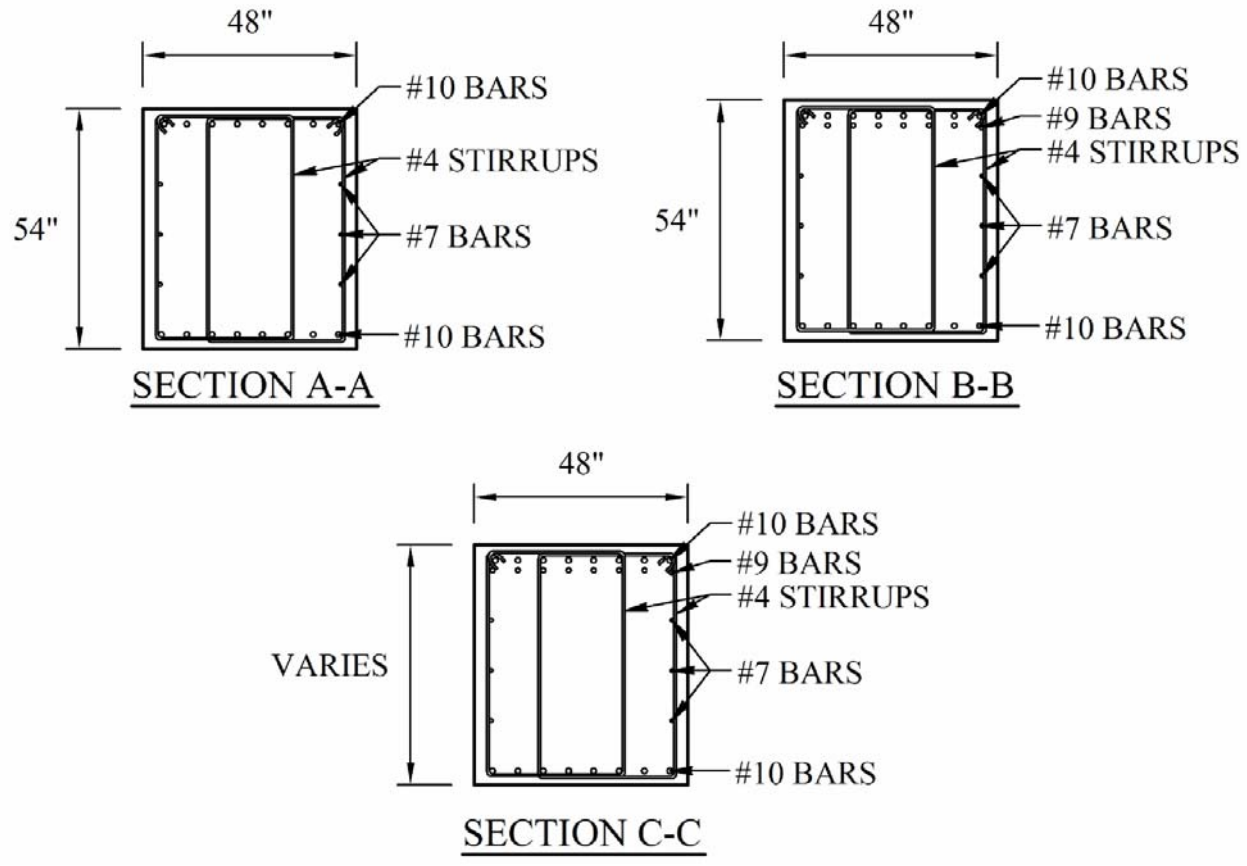

Figure 4-34: Bent cross-sections referenced in Figure 4-32.

Table 4-26: Factored loads used for the bent design. See Figures 4-32 and 4-33 for the location of the loads.

Load	Dead Loads (kips)	Live Loads (kips)	Total (kips)
L1	91.4	52.1	143.5
L2	94.2	69.8	164.0
L3	97.0	65.9	162.9
L4	99.8	66.8	166.6
L5	102.5	66.8	169.3
L6	105.3	65.9	171.2
L7	103.1	69.8	172.9
L8	110.9	52.1	163.0

Step 1 – Delineate the D-regions.

Due to closely spaced girder loads the whole member can be considered a D-region.

Step 2 – Determine the boundary conditions of the D-region.

Based on the assumption in Step 1, there is no D- and B-region interface.

Step 3 – Sketch the flow of forces.

This Step was deemed unnecessary for this example.

Step 4 and 5 – Develop the STM and solve for the member forces.

Based on a loading analysis that showed all of the columns remained in compression, the column reactions were modeled as two point loads placed at quarter-points. The remaining geometry of the strut-and-tie model was developed based on the details of the reinforcement in the bent cap. Figure 4-35 shows the strut-and-tie model for the bent along with the corresponding member labels. Ties 1 through 17 were placed to correspond with the center of gravity of the steel in the top portion of the bent. Similarly, struts 50 through 55 and 61 through 66 and ties 56, 57, 59, and 60 were placed to correspond with the reinforcement at the bottom of the bent. The vertical ties were strategically placed at locations where they would coincide with the center of gravity of a set of stirrups. Details about each of the vertical ties are discussed later in this example. Finally, the inclined struts were connected between vertical ties and loads as needed. In addition to the member labels, Figure 4-36 shows the node labels. It should be noted that struts 52, 58, and 64 were analyzed as part of nodes 21, 26, and 31, respectively.

Once the model was developed the member forces were calculated for the factored loads given in Table 4-26. Table 4-27 summarizes the member force calculations.

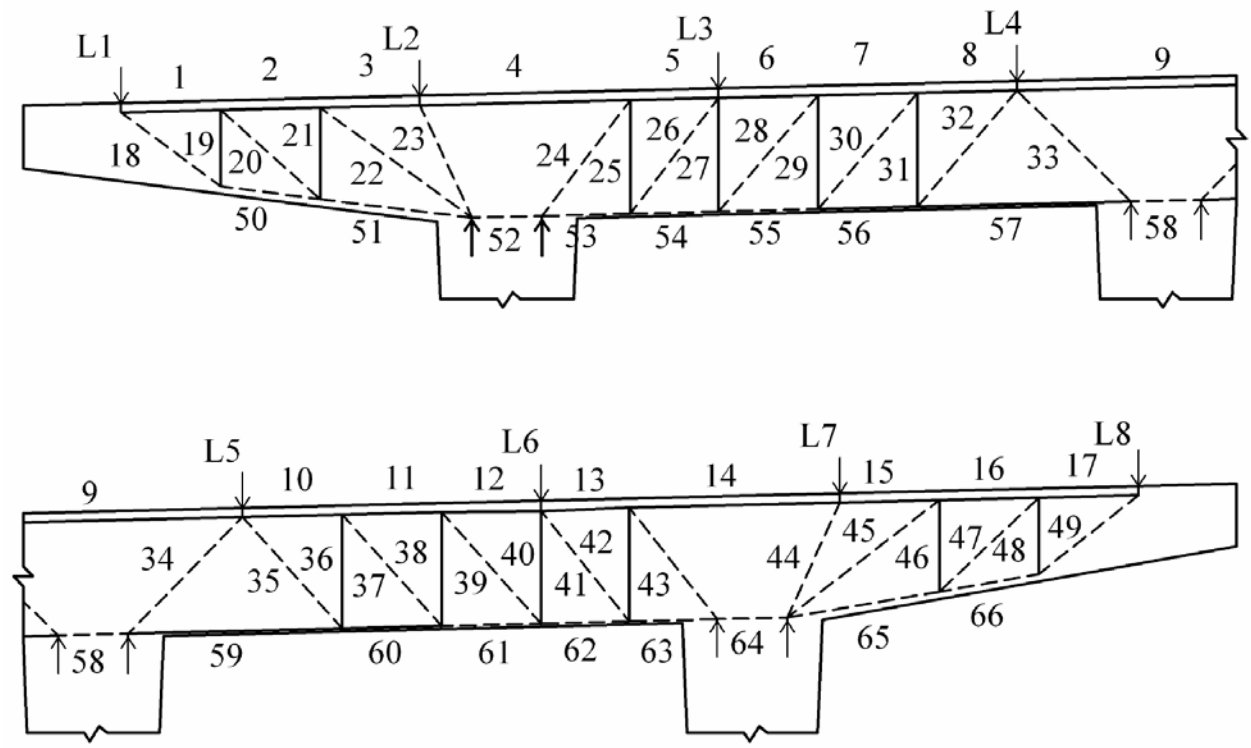

Figure 4-35: Strut-and-tie model for the bent with corresponding member labels.

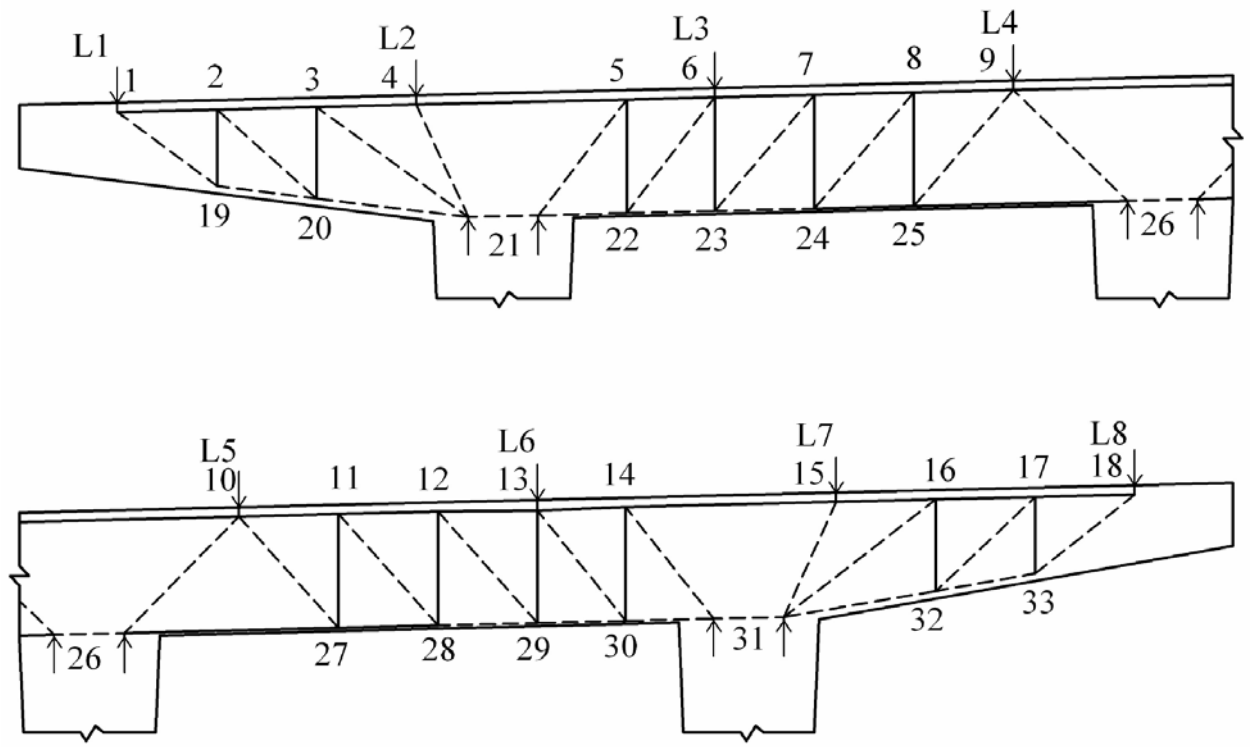

Figure 4-36: Node labels for strut-and-tie model.

Table 4-27: Calculated member forces for the strut-and-tie model.

Model Label	Force	T or C	Model Label	Force	T or C	Model Label	Force	T or C
1	187.0	T	23	-178.8	C	45	-187.8	C
2	312.0	T	24	-277.8	C	46	111.3	T
3	442.7	T	25	217.0	T	47	-195.2	C
4	517.9	T	26	-277.8	C	48	130.6	T
5	349.7	T	27	54.1	T	49	-270.9	C
6	181.6	T	28	-72.8	C	50	-188.4	C
7	134.2	T	29	54.1	T	51	-314.2	C
8	86.9	T	30	-72.8	C	52	0.0	C
9	152.5	T	31	54.1	T	53	-218.5	C
10	103.9	T	32	-72.8	C	54	-50.4	C
11	160.5	T	33	-157.5	C	55	-3.0	C
12	219.6	T	34	-150.2	C	56	44.3	T
13	400.0	T	35	-84.8	C	57	91.7	T
14	582.4	T	36	64.6	T	58	0.0	C
15	502.9	T	37	-84.8	C	59	107.1	T
16	354.4	T	38	64.6	T	60	50.6	T
17	212.4	T	39	-88.7	C	61	-6.0	C
18	-232.9	C	40	67.6	T	62	-65.1	C
19	115.0	T	41	-288.5	C	63	-245.3	C
20	-167.8	C	42	229.8	T	64	0.0	C
21	97.9	T	43	-294.7	C	65	-359.4	C
22	-161.4	C	44	-192.1	C	66	-215.6	C

In order to perform, the strut, tie, and node capacity checks the effective widths of the struts and ties had to be determined. Because the ties were chosen based on the existing reinforcement, the effective widths of the ties were determined based on the spacing of the reinforcement within each tie. The widths of the ties were increased by $6d_b$ on each end of the tie according to AASHTO LRFD 5.6.3.3.2. The widths of the struts were determined based on the effective width of the ties and other geometric constraints such as bearing areas. The widths of the struts on the bottom cord of the bent were simply calculated by doubling the distance from the bottom of the bent to the centerline of the bottom cord. The widths of the inclined struts can be found by using a drafting program or Figure 4-37. Figure 4-38 shows the effective widths of the struts superimposed on the bent cap. The values for the effective widths of the ties, struts, and nodes can be found in the tables summarizing the calculations for ties, struts, and nodes in Steps 6 and 7.

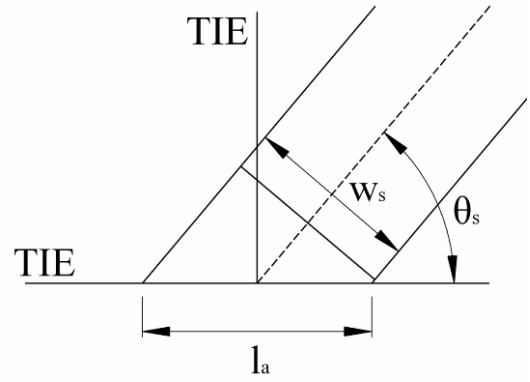

$$w_s = l_a \sin(\theta_s)$$

Figure 4-37: Demonstration of how to calculate the width of the inclined struts at a given node.

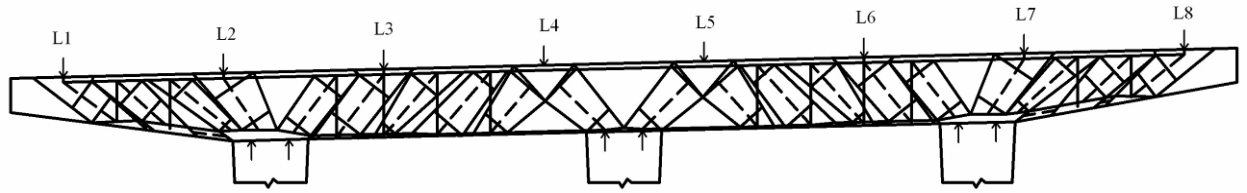

Figure 4-38: Effective width of struts.

*Note: Since the bearing areas of the loads and the columns have the same thickness as the bent (48 inches), the thickness of all the struts and nodes was assumed to be 48 inches.

Step 6 – Check the capacity of the ties.

The calculated demands in the ties were compared to the capacity of the ties. For each of the ties, the demand (P_u) must be less than the capacity (P_n). The capacity is calculated as follows:

$$P_n = \phi f_y A_s$$

Table 4-28 gives information about each tie and summarizes the calculations required to check the ties. All of the ties had sufficient capacity to carry the applied loads.

Table 4-28: Summary of tie check calculations.

Model Label	Force (kips)	Tie Description	A_{st} (in^2)	Effective Width (in)	Available Force (kips)	Available/ Demand	Okay?
1	187.0	8 #10 and 8 #9	18.16	6.40	980.6	5.2	yes
2	312.0	8 #10 and 8 #9	18.16	6.40	980.6	3.1	yes
3	442.7	8 #10 and 8 #9	18.16	6.40	980.6	2.2	yes
4	517.9	9 #10 and 8 #9	18.16	6.40	980.6	1.9	yes
5	349.7	10 #10 and 8 #9	18.16	6.40	980.6	2.8	yes
6	181.6	8 # 10	10.16	4.27	548.6	3.0	yes
7	134.2	8 # 10	10.16	4.27	548.6	4.1	yes
8	86.9	8 # 10	10.16	4.27	548.6	6.3	yes
9	152.5	8 # 10	10.16	4.27	548.6	3.6	yes
10	103.9	8 # 10	10.16	4.27	548.6	5.3	yes

Table 4-28 (cont.): Summary of tie check calculations.

Model Label	Force (kips)	Tie Description	A_{st} (in^2)	Effective Width (in)	Available Force (kips)	Available/ Demand	Okay?
11	160.5	8 # 10	10.16	4.27	548.6	3.4	yes
12	219.6	8 # 10	10.16	4.27	548.6	2.5	yes
13	400.0	8 #10 and 8 #9	18.16	6.40	980.6	2.5	yes
14	582.4	8 #10 and 8 #9	18.16	6.40	980.6	1.7	yes
15	502.9	8 #10 and 8 #9	18.16	6.40	980.6	1.9	yes
16	354.4	9 #10 and 8 #9	18.16	6.40	980.6	2.8	yes
17	212.4	10 #10 and 8 #9	18.16	6.40	980.6	4.6	yes
19	115.0	5-#4 4 leg stirrups	4.00	40.00	216.0	1.9	yes
21	97.9	4-#4 4 leg stirrups	3.20	35.70	172.8	1.8	yes
25	217.0	6-#4 4 leg stirrups	4.80	45.00	259.2	1.2	yes
27	54.1	4-#4 4 leg stirrups	1.60	15.00	86.4	1.6	yes
29	54.1	4-#4 4 leg stirrups	3.20	42.00	172.8	3.2	yes
31	54.1	3-#4 4 leg stirrups	2.40	27.00	129.6	2.4	yes
36	64.6	3-#4 4 leg stirrups	2.40	27.00	129.6	2.0	yes
38	64.6	4-#4 4 leg stirrups	3.20	42.00	172.8	2.7	yes
40	67.6	2-#4 4 leg stirrups	1.60	15.00	86.4	1.3	yes
42	229.8	6-#4 4 leg stirrups	4.80	45.00	259.2	1.1	yes
46	111.3	4-#4 4 leg stirrups	3.20	35.70	172.8	1.6	yes
48	130.6	5-#4 4 leg stirrups	4.00	40.00	216.0	1.7	yes
56	44.3	8 # 10	10.16	4.27	548.6	12.4	yes
57	91.7	9 # 10	10.16	4.27	548.6	6.0	yes
59	107.1	10 # 10	10.16	4.27	548.6	5.1	yes
60	50.6	11 # 10	10.16	4.27	548.6	10.8	yes

Step 7(a) – Check the capacity of the struts.

Similar to the tie analysis, the capacity of the struts were checked to ensure that they could meet the demands. In order to calculate the compressive strength of the strut, the principal tensile strain in the strut must be calculated. The principal tensile strain (ε_1) can be calculated based on the strain in the adjoining tie (ε_s) and the angle between the tie and a strut (α_s) using the following equation:

$$\varepsilon_1 = \varepsilon_s + (\varepsilon_s + 0.002)\cot^2(\alpha_s) \qquad \text{(AASHTO LRFD eq. 5.6.3.3.3-2)}$$

With the calculated principal tensile strains, the compressive strength of each strut can be determined by the following:

$$f_{cu} = \frac{f'_c}{0.8 + 170\varepsilon_1} \le 0.85 f'_c \qquad \text{(AASHTO LRFD eq. 5.6.3.3.3-1)}$$

Many struts were connected to two ties that represent continuous longitudinal reinforcement. For this type of situation, rather then determine the limiting strut strength for each tie, the strut strength was calculated based on the average tensile strain in each of the ties using the following equation:

$$\varepsilon_s = \frac{P_{avg}}{A_{st} E_s}$$

In addition, most of the struts were connected to ties representing longitudinal bars and ties representing stirrups. For struts falling into this category, the limiting strut compressive strength was calculated for each of the ties, and the most critical case was used for the calculations. Table 4-29 summarizes the calculations of the strut capacities and compares them to the demands. For this model, all of the struts were adequate.

Table 4-29: Summary of strut calculations.

Strut Data			Tie Data			Strut Compressive Capacity			Okay?
Model Label	Strut Width (in.)	Force (kips)	Tie	ε_s	α_s (DEG.)	ε_1	Strut Compressive Strength (ksi)	Strut Capacity (kips)	
18	24.9	232.9	1	0.000178	38.024	0.003739	2.44	2039.8	yes
	24.9	232.9	19	0.000496	53.382	0.001874	2.98	-	-
20	22.8	167.8	(2-1)	0.000474	43.256	0.003268	2.58	1978.0	yes
	22.8	167.8	19	0.000496	48.150	0.002498	2.86	-	-
	22.8	167.8	21	0.000528	48.150	0.002556	2.84	-	-
22	13.6	161.4	(3-2)	0.000716	37.354	0.005379	2.04	932.9	yes
	13.6	161.4	21	0.000528	54.052	0.001857	2.98	-	-
23	26.7	178.8	(4-3)	0.000912	66.509	0.001462	2.98	2668.9	yes
24	24.7	277.8	(5-4)	0.000824	51.345	0.002630	2.81	-	-
	24.7	277.8	25	0.000779	37.249	0.005587	2.00	1660.1	yes
26	29.2	277.8	(6-5)	0.000640	51.351	0.002329	2.93	-	-
	29.2	277.8	25	0.000779	37.243	0.005589	2.00	1962.2	yes
	29.2	277.8	27	0.000583	37.243	0.005052	2.11	-	-
28	13.6	72.8	(7-6)	0.000536	48.012	0.002590	2.82	-	-
	13.6	72.8	27	0.000583	40.582	0.004104	2.34	1068.0	yes
	13.6	72.8	29	0.000291	40.582	0.003415	2.54	-	-
30	21.7	72.8	(8-7)	0.000375	48.012	0.002299	2.94	-	-
	21.7	72.8	29	0.000291	40.582	0.003415	2.54	-	-
	21.7	72.8	31	0.000389	40.582	0.003644	2.47	1797.7	yes
	21.7	72.8	56	0.000075	48.012	0.001756	2.98	-	-
32	23.1	72.8	(9-8)	0.000406	48.012	0.002355	2.92	-	-
	23.1	72.8	31	0.000389	40.582	0.003644	2.47	1913.7	yes
	23.1	72.8	(57-56)	0.000231	48.012	0.002038	2.98	-	-
33	25.8	157.5	(9-8)	0.000406	45.581	0.002717	2.77	2404.5	yes
	25.8	157.5	57	0.000156	45.581	0.002225	2.97	-	-
34	25.3	150.2	(10-9)	0.000435	44.161	0.003017	2.67	2266.2	yes
	25.3	150.2	59	0.000182	44.161	0.002495	2.86	-	-
35	23.7	84.8	(10-9)	0.000435	49.604	0.002198	2.99	-	-
	23.7	84.8	36	0.000464	41.802	0.003547	2.50	1986.7	yes
	23.7	84.8	(60-59)	0.000268	49.604	0.001910	2.98	-	-

Table 4-29 (cont.): Summary of strut calculations.

Strut Data			Tie Data			Strut Compressive Capacity			Okay?
Model Label	Strut Width (in.)	Force (kips)	Tie	ε_s	α_s (DEG.)	ε_1	Strut Compressive Strength (ksi)	Strut Capacity (kips)	
37	22.3	84.8	(11-10)	0.000449	49.604	0.002222	2.97	-	-
	22.3	84.8	36	0.000464	41.802	0.003547	2.50	1869.3	yes
	22.3	84.8	38	0.000348	41.802	0.003285	2.58	-	-
	22.3	84.8	(60-59)	0.000268	49.604	0.001910	2.98	-	-
39	13.9	88.7	(12-11)	0.000645	48.837	0.002667	2.79	-	-
	13.9	88.7	38	0.000348	41.802	0.003285	2.58	-	-
	13.9	88.7	40	0.000728	41.802	0.004140	2.33	1086.9	yes
41	28.3	288.5	(13-12)	0.000752	53.638	0.002244	2.96	-	-
	28.3	288.5	40	0.000728	38.633	0.004999	2.12	-	-
	28.3	288.5	42	0.000825	38.633	0.005249	2.07	1966.6	yes
43	24.7	294.7	(14-13)	0.000933	53.129	0.002583	2.83	-	-
	24.7	294.7	42	0.000825	38.277	0.005363	2.05	1697.0	yes
44	26.9	192.1	(15-14)	0.001030	64.152	0.001742	2.98	2688.9	yes
45	12.0	187.8	(16-15)	0.000814	36.328	0.006018	1.92	774.1	yes
	12.0	187.8	46	0.000600	52.266	0.002156	2.98	-	-
47	24.6	195.2	(17-16)	0.000538	41.968	0.003676	2.46	2030.3	yes
	24.6	195.2	46	0.000600	46.626	0.002920	2.70	-	-
	24.6	195.2	48	0.000563	46.626	0.002851	2.73	-	-
49	23.4	270.9	17	0.000202	36.981	0.004084	2.34	1841.5	yes
	23.4	270.9	48	0.000563	51.613	0.002171	2.99	-	-
50	7.9	188.4	19	0.000496	82.707	0.000537	2.98	789.7	yes
	7.9	188.4	21	0.000528	82.707	0.000569	2.98	-	-
51	7.9	314.2	21	0.000528	83.071	0.000565	2.98	789.7	yes
53	4.3	218.5	25	0.000779	88.594	0.000781	2.98	426.8	yes
54	4.3	50.4	25	0.000779	88.594	0.000781	2.98	426.8	yes
	4.3	50.4	27	0.000583	88.594	0.000585	2.98	-	-
55	4.3	3.0	27	0.000583	88.594	0.000585	2.98	426.8	yes
	4.3	3.0	29	0.000291	88.594	0.000293	2.98	-	-
61	4.3	6.0	38	0.000348	88.594	0.000350	2.98	426.8	yes
	4.3	6.0	40	0.000728	88.594	0.000730	2.98	-	-
62	4.3	65.1	40	0.000728	88.594	0.000730	2.98	426.8	yes
	4.3	65.1	42	0.000825	88.594	0.000827	2.98	-	-
63	4.3	245.3	42	0.000825	88.594	0.000827	2.98	426.8	yes
65	7.9	359.4	46	0.000600	79.957	0.000681	2.98	789.7	yes
66	7.9	215.6	46	0.000600	79.957	0.000681	2.98	789.7	yes
	7.9	215.6	48	0.000563	79.957	0.000643	2.98	-	-

Step 7(b) – Check the capacity of the nodes.

As with the ties and struts, the capacity of each node was compared to the demand on each node. The strength of a node can be calculated according to AASHTO LRFD 5.6.3.5 which states that node compressive strengths are $0.85f'_c$, $0.75f'_c$, and $0.65f'_c$ for CCC, CCT, and CTT nodes,

respectively. For this example, all of the nodes were found to be adequate. Table 4-30 summarizes the calculations and results.

Table 4-30: Summary of node calculations.

Node			Force			Available Width (in.)	Available Capacity (kips)	Available/ Demand	Okay?
Label	Type	Reduction Factor	Label	C/T	Load (kips)				
1	CCT	0.75	L1	C	143.5	48.0	4233.6	29.5	yes
		0.75	1	T	187.0	6.4	564.5	3.0	yes
		0.75	18	C	232.9	26.1	2302.0	9.9	yes
2	CTT	0.65	(2-1)	T	125.0	6.4	489.2	3.9	yes
		0.65	19	T	115.0	40.0	3057.6	26.6	yes
		0.65	20	C	167.8	25.6	1956.9	11.7	yes
3	CTT	0.65	(3-2)	T	130.7	6.4	489.2	3.7	yes
		0.65	21	T	97.9	35.7	2728.9	27.9	yes
		0.65	22	C	161.4	21.4	1635.8	10.1	yes
4	CTT	0.65	L2	C	164.0	48.0	3669.1	22.4	yes
		0.65	(4-3)	T	75.3	6.4	489.2	6.5	yes
		0.65	23	C	178.8	37.3	2851.2	15.9	yes
5	CTT	0.65	(5-4)	T	168.2	6.4	489.2	2.9	yes
		0.65	24	C	277.8	27.6	2109.7	7.6	yes
		0.65	25	T	217.0	45.0	3439.8	15.9	yes
6	CTT	0.65	L3	C	162.9	48.0	3669.1	22.5	yes
		0.65	5	T	349.7	6.4	489.2	1.4	yes
		0.65	6	T	181.6	6.4	489.2	2.7	yes
		0.65	26	C	277.8	30.3	2316.1	8.3	yes
		0.65	27	T	54.1	15.0	1146.6	21.2	yes
7	CTT	0.65	6	T	181.6	6.4	489.2	2.7	yes
		0.65	7	T	134.2	4.3	326.4	2.4	yes
		0.65	28	C	72.8	27.5	2102.1	28.9	yes
		0.65	29	T	54.1	42.0	3210.5	59.3	yes
8	CTT	0.65	7	T	134.2	4.3	326.4	2.4	yes
		0.65	8	T	86.9	4.3	326.4	3.8	yes
		0.65	30	C	72.8	21.7	1658.7	22.8	yes
		0.65	31	T	54.1	27.0	2063.9	38.1	yes
9	CTT	0.65	L4	C	166.6	48.0	3669.1	22.0	yes
		0.65	8	T	86.9	4.3	326.4	3.8	yes
		0.65	9	T	152.5	4.3	326.4	2.1	yes
		0.65	32	C	72.8	36.2	2767.1	38.0	yes
		0.65	33	C	157.5	36.3	2774.8	17.6	yes
10	CTT	0.65	L5	C	169.3	48.0	3669.1	21.7	yes
		0.65	9	T	152.5	4.3	326.4	2.1	yes
		0.65	10	T	103.9	4.3	326.4	3.1	yes
		0.65	34	C	150.2	35.7	2728.9	18.2	yes
		0.65	35	C	84.8	36.9	2820.6	33.2	Yes

Table 4-30 (cont.): Summary of node calculations.

Node			Force			Available Width (in.)	Available Capacity (kips)	Available/ Demand	Okay?
Label	Type	Reduction Factor	Label	C/T	Load (kips)				
11	CTT	0.65	10	T	103.9	4.3	326.4	3.1	yes
		0.65	11	T	160.5	4.3	326.4	2.0	yes
		0.65	36	T	64.6	27.0	2063.9	31.9	yes
		0.65	37	C	84.8	22.3	1704.6	20.1	yes
12	CTT	0.65	11	T	160.5	4.3	326.4	2.0	yes
		0.65	12	T	219.6	4.3	326.4	1.5	yes
		0.65	38	T	64.6	42.0	3210.5	49.7	yes
		0.65	39	C	88.7	28.1	2148.0	24.2	yes
13	CTT	0.65	L6	C	171.2	48.0	3669.1	21.4	yes
		0.65	12	T	219.6	4.3	326.4	1.5	yes
		0.65	13	T	400.0	6.4	489.2	1.2	yes
		0.65	40	T	67.6	15.0	1146.6	17.0	yes
		0.65	41	C	288.5	31.5	2407.9	8.3	yes
14	CTT	0.65	(13-14)	T	182.4	6.4	489.2	2.7	yes
		0.65	42	T	229.8	45.0	3439.8	15.0	yes
		0.65	43	C	294.7	28.3	2163.3	7.3	yes
15	CTT	0.65	L7	C	172.9	48.0	3669.1	21.2	yes
		0.65	(15-14)	T	79.5	6.4	489.2	6.2	yes
		0.65	44	C	192.1	37.1	2835.9	14.8	yes
16	CTT	0.65	(16-15)	T	148.6	6.4	489.2	3.3	yes
		0.65	45	C	187.8	21.3	1628.2	8.7	yes
		0.65	46	T	111.3	35.7	2728.9	24.5	yes
17	CTT	0.65	(17-16)	T	142.0	6.4	489.2	3.4	yes
		0.65	47	C	195.2	27.9	2132.7	10.9	yes
		0.65	48	T	130.6	40.0	3057.6	23.4	yes
18	CCT	0.75	L8	C	163.0	48.0	4233.6	26.0	yes
		0.75	17	T	212.4	6.4	564.5	2.7	yes
		0.75	49	C	270.9	25.3	2231.5	8.2	yes
19	CCT	0.75	18	C	232.9	24.9	2196.2	9.4	yes
		0.75	19	T	115.0	40.0	3528.0	30.7	yes
		0.75	50	C	188.4	7.9	696.8	3.7	yes
20	CCT	0.75	20	C	167.8	22.8	2011.0	12.0	yes
		0.75	21	T	97.9	35.7	3148.7	32.1	yes
		0.75	50	C	188.4	7.9	696.8	3.7	yes
		0.75	51	C	314.2	7.9	696.8	2.2	yes
21	CCC	0.85	Col. 1	C	521.3	60.0	5997.6	11.5	yes
		0.85	22	C	161.4	13.6	1359.5	8.4	yes
		0.85	23	C	178.8	26.7	2668.9	14.9	yes
		0.85	24	C	277.8	24.7	2469.0	8.9	yes
		0.85	51	C	314.2	7.9	789.7	2.5	yes
		0.85	53	C	218.5	4.3	426.8	2.0	yes
22	CCT	0.75	25	T	217.0	45.0	3969.0	18.3	yes
		0.75	26	C	277.8	29.2	2575.4	9.3	yes
		0.75	53	C	218.5	4.3	376.6	1.7	yes
		0.75	54	C	50.4	4.3	376.6	7.5	yes

Table 4-30 (cont.): Summary of node calculations.

Node			Force			Available Width (in.)	Available Capacity (kips)	Available/ Demand	Okay?
Label	Type	Reduction Factor	Label	C/T	Load (kips)				
23	CCT	0.75	27	T	54.1	15.0	1323.0	24.5	yes
		0.75	28	C	72.8	13.6	1199.5	16.5	yes
		0.75	54	C	50.4	4.3	376.6	7.5	yes
		0.75	55	C	3.0	4.3	376.6	124.3	yes
24	CCT	0.75	29	T	54.1	42.0	3704.4	68.5	yes
		0.75	30	C	72.8	29.3	2584.3	35.5	yes
		0.75	55	C	3.0	4.3	376.6	124.3	yes
		0.75	56	T	44.3	4.3	376.6	8.5	yes
25	CTT	0.65	31	T	54.1	27.0	2063.9	38.1	yes
		0.65	32	C	72.8	23.1	1765.8	24.3	yes
		0.65	56	T	44.3	4.3	326.4	7.4	yes
		0.65	57	T	91.7	4.3	326.4	3.6	yes
26	CTT	0.75	Col. 2	C	260.6	60.0	5292.0	20.3	yes
		0.75	33	C	157.5	25.8	2275.6	14.5	yes
		0.75	34	C	150.2	25.3	2231.5	14.9	yes
		0.75	57	T	91.7	4.3	376.6	4.1	yes
		0.75	59	T	107.1	4.3	376.6	3.5	yes
27	CTT	0.65	35	C	84.8	23.7	1811.6	21.4	yes
		0.65	36	T	64.6	27.0	2063.9	31.9	yes
		0.65	59	T	107.1	4.3	326.4	3.0	yes
		0.65	60	T	50.6	4.3	326.4	6.5	yes
28	CTT	0.65	37	C	84.8	30.0	2293.2	27.0	yes
		0.65	38	T	64.6	42.0	3210.5	49.7	yes
		0.65	60	T	50.6	4.3	326.4	6.5	yes
		0.65	61	C	6.0	4.3	326.4	54.4	yes
29	CCT	0.75	39	C	88.7	13.9	1226.0	13.8	yes
		0.75	40	T	67.6	15.0	1323.0	19.6	yes
		0.75	61	C	6.0	4.3	376.6	62.8	yes
		0.75	62	C	65.1	4.3	376.6	5.8	yes
30	CCT	0.75	41	C	288.5	28.3	2496.1	8.7	yes
		0.75	42	T	229.8	45.0	3969.0	17.3	yes
		0.75	62	C	65.1	4.3	376.6	5.8	yes
		0.75	63	C	245.3	4.3	376.6	1.5	yes
31	CCC	0.85	Col. 3	C	528.7	60.0	5997.6	11.3	yes
		0.85	43	C	294.7	24.7	2469.0	8.4	yes
		0.85	44	C	192.1	26.9	2688.9	14.0	yes
		0.85	45	C	187.8	12.0	1199.5	6.4	yes
		0.85	63	C	245.3	4.3	426.8	1.7	yes
		0.85	65	C	359.4	7.9	789.7	2.2	yes
32	CCT	0.75	46	T	111.3	35.7	3148.7	28.3	yes
		0.75	47	C	195.2	24.6	2169.7	11.1	yes
		0.75	65	C	359.4	7.9	696.8	1.9	yes
		0.75	66	C	215.6	7.9	696.8	3.2	yes

Table 4-30 (cont.): Summary of node calculations.

Node			Force			Available Width (in.)	Available Capacity (kips)	Available/ Demand	Okay?
Label	Type	Reduction Factor	Label	C/T	Load (kips)				
33	CCT	0.75	48	T	130.6	40.0	3528.0	27.0	yes
		0.75	49	C	270.9	23.4	2063.9	7.6	yes
		0.75	66	C	215.6	7.9	696.8	3.2	yes

Step 8(a) – Check the detailing for the anchorage of the ties.

The exact anchorage of the ties at the ends of the cap is currently unknown; however, it is believed that 90 degree bends equivalent to a standard hook were used. Due to this fact, the anchorage can be assumed to be sufficient. In addition, splices were used in the interior of the bent, so the anchorage of ties in nodes in the interior of the bent will also be assumed to be satisfactory.

Step 8 (b) – Check the detailing of the crack control reinforcement.

When using strut-and-tie models for design, a minimum amount of crack control reinforcement must be used. According to AASHTO LRFD 5.6.3.6, structures or regions of structures that have been designed with strut-and-tie models must have an "orthogonal grid of reinforcing bars near each face." In addition, the ratio of reinforcement to gross area of concrete must be at least 0.003 in each direction with a maximum spacing of 12 inches.

In order to see if the bent satisfied the crack control requirements, the ratio of crack control reinforcement to gross area of concrete was calculated in the cantilevered regions, above the exterior columns, near the face of the exterior columns, at mid-span between the exterior and interior columns, near the face of the interior column, and above the interior column. Table 4-31 summarizes the crack control calculations. The horizontal crack control reinforcement calculations utilized the total area of horizontal reinforcement and total height of the section, and the vertical crack control reinforcement calculations utilized the area of one stirrup and the spacing between the stirrups.

Table 4-31: Summary of crack control calculations.

Location	Reinforcement	A_{st} (in^2)	$A_{concrete}$ (in^2)	$A_{st}/A_{concrete}$	Okay?
Cantilevered Portion	Horizontal	10.68	2592	0.0041	yes
	Vertical	0.8	475.2	0.0017	no
Above Exterior Columns	Horizontal	10.68	2592	0.0041	yes
	Vertical	2.54	432	0.0059	yes
Near Exterior Columns	Horizontal	10.68	2592	0.0041	yes
	Vertical	0.8	432	0.0019	no
Mid-Span	Horizontal	8.68	2592	0.0033	yes
	Vertical	0.8	576	0.0014	no
Near Interior Columns	Horizontal	8.68	2592	0.0033	yes
	Vertical	0.8	432	0.0019	no
Above Interior Columns	Horizontal	8.68	2592	0.0033	yes
	Vertical	2.54	432	0.0059	yes

From Table 4-31, it can be seen that the vertical crack control reinforcement in the cantilevers and between the exterior and interior columns was found to be insufficient based on the provisions of AASHTO LRFD 5.6.3.6.

In conclusion, according to this STM analysis, the design of the bent was conservative. The most critical element is the tie 42 which has a 1.1 capacity to demand ratio.

4.3.3 PILE-SUPPORTED FOOTING

Illustrated in Figure 4-39 is an 11' x 11' x 3' footing supported by 9 piles arranged in a 3 x 3 pattern. The footing was designed in 1977 using the AASHTO Specifications for Highway Bridges and Load Factor Design. The footing was used in a multicolumn bent and Load Group 1 governed the design. The total factored loading, including the pile cap and the soil overburden was 1161 kips with a transverse moment of 384 kip-ft. The concrete used in the original design had an f'_c of 3000 psi and the steel used was Grade 60. The original reinforcement was determined by checking the moment capacity at the face of the column as well as one-way and two-way shear at the critical sections.

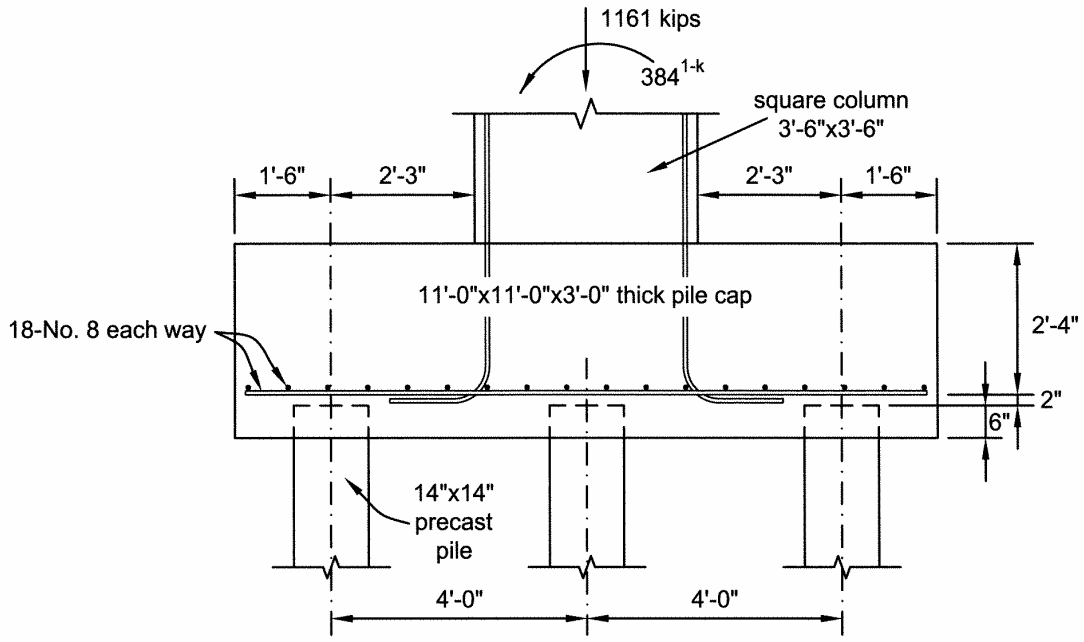

Figure 4-39: Details of the existing footing.

Step 1 – Delineate the D-regions.

The whole member is a D-region.

Step 2 – Determine the boundary conditions of the D-region.

There is no D- and B-region interface.

Step 3 – Sketch the flow of forces.

This step was deemed unnecessary for this example.

Step 4 and 5 – Develop the STM and solve for the member forces.

Figure 4-40 shows the idealized truss model for the pile cap resulting from a visualization of the flow of forces in the pile cap. The load applied to the top of the pile cap includes the factored column load as well as the factored weight of the pile cap and soil overburden. Since this load case has only axial loading, uniform stresses will result at the base of the column. In order to simulate uniform compressive stress at the base of the column, the total factored load at the top of the pile cap has been applied at 9 points in a 3x3 pattern, located at distances equal to the column dimension divided by 6 from the column faces.

For the sake of simplicity, the pile load on the most extreme pile resulting from the transverse moment (the moment divided by the section modulus of the pile group, 384/24 = 16 kips) will conservatively be applied at all 9 locations. It is assumed that these 9 loads will be transferred to the support reaction areas of the 9 piles by the eight inclined compressive struts represented by members AJ, BK, CL, DM, EN, FO, GP, HQ and the one central vertical strut, IR. The loads in the inclined members will result in tension in the ties AC, CE, EG, GA, BF and DH (See Figure 4-40 (b)).

To define the geometry of the truss, the centroid of the tension tie reinforcement will be the 2" above the piles shown on the original plans. Nodes J through R are assumed to be 2" below the top surface of the pile cap to allow for the dimensions of the struts beneath the column. Nodes A through I are located directly above the centers of the piles.

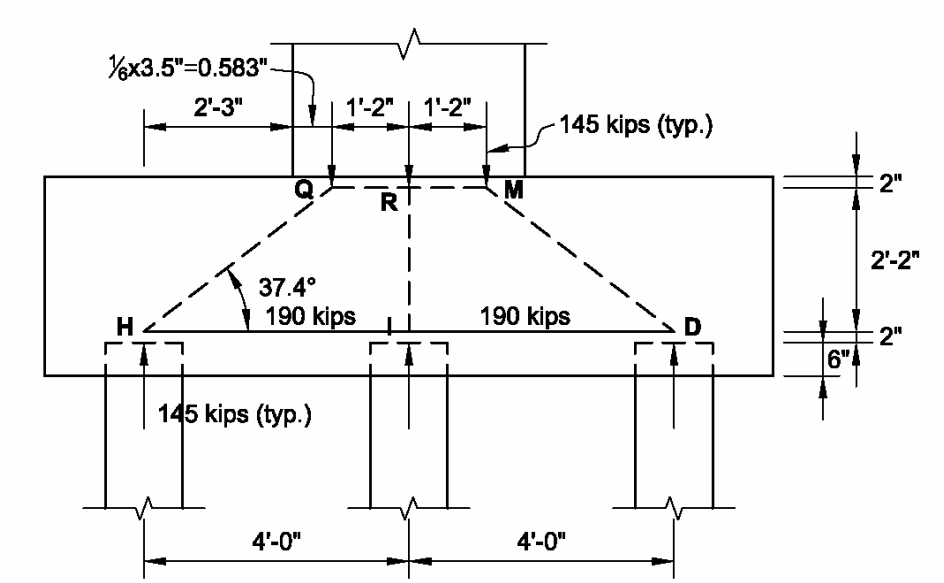

(a) Section through Centerline of Footing

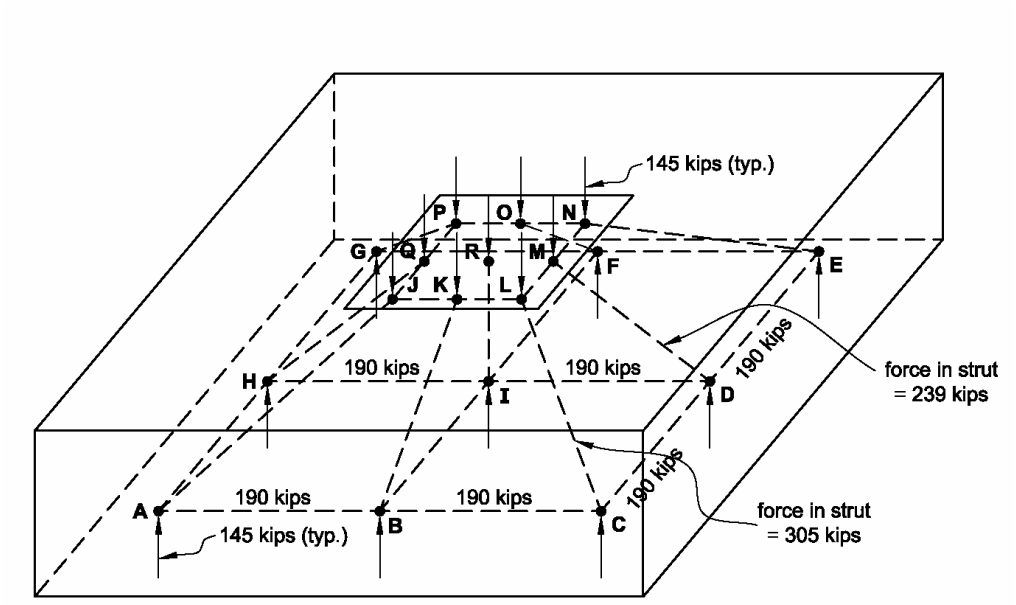

(b) 3-D View of the STM

Figure 4-40: Truss resulting from flow of forces and resulting member forces (In the above, (typ.) means similar elements have the same value).

Step 6 – Check the capacity of the ties.

All of the ties have a factored force of 190 kips. Hence, the required area of reinforcement, A_{st}, is:

$$A_{st} = \frac{P_u}{\phi f_y} = \frac{190}{0.9 \times 60} = 3.52 in^2$$

Check the requirement for 1.2 times the cracking moment. The factored flexural resistance required to resist 1.2 M_{cr} using the modulus of rupture, f_r, of 0.36 root f'_c, is

$$M_r \geq 1.2 \times \frac{bh^2}{6} 0.36\sqrt{f_c'} = 1.2 \times \frac{12 \times 11 \times 36^2}{6} 0.36\sqrt{3} = 21{,}334 kip - in = 1{,}778 kip - ft$$

The minimum area of flexural reinforcement corresponding to 1.2 M_{cr} can be determined by dividing the above factored flexural resistance by the product of the flexural lever arm (2.33') and the factored yield strength of the reinforcement.

$$A_{s,\min} = \frac{1{,}778}{2.33 \times 0.9 \times 60} = 14.13 in^2$$

This area of reinforcement in a typical design would be distributed equally between the parallel ties, e.g. Ties ABC, HID, GFE and AHG, BIF, CDE. Hence, the area of reinforcement required to ensure the factored flexural resistance is at least 1.2 M_{cr} is equal to 14.13/3 = 4.71 in.^{2}

The amount of reinforcement required to resist 1.33 times the factored loads is:

$$A_{st} = 1.33 \times 3.52 = 4.68 in^2$$

The amount of reinforcement required to resist 1.33 times the factored loads is less than the amount required to resist 1.2 M_{cr}; therefore, this smaller amount will be checked against the amount provided by the original design of the footing. There are presently 18 no. 8 bars provided in the lower mat in each direction. This equals 18 x .79 = 14.22 in^2. This results in 14.22/3 = 4.74 in^2 per tie zone. This reinforcement is distributed across the full width of the footing and not the limits of the nodes (See discussion on node dimensions below). Even though the total amount of reinforcement is greater than the 4.68 in^2 required, it is not placed within the region defined by the nodes and therefore does not meet the requirements of STM.

Step 7(a) – Check Capacity of Struts

Struts AJ, CL, EN & GP each carry a compressive force of 305 kips. Struts BK, DM, FO & HQ each carry a compressive force of 239 kips while strut IR carries 145 kips. (See Figure 4-40). In order to determine the nominal resistance of the struts it is necessary to determine the approximate area of each strut near its intersection with the node. Because of the confinement

provided by the mass of concrete around the struts and the fact that the struts will be able to bear directly onto the piles, simplifying assumptions as to the area of the struts will be made.

First of all, it will be assumed that the transfer of loads from the footings to the piles will begin at the top of the pile. The stresses will then be dispersed at a 45^o angle (see Figure 4-41). Since the mid-plane of the reinforcement is 2" above the pile top and the pile cross section is 14" x 14", the effective bearing area will be a square 18" x 18".

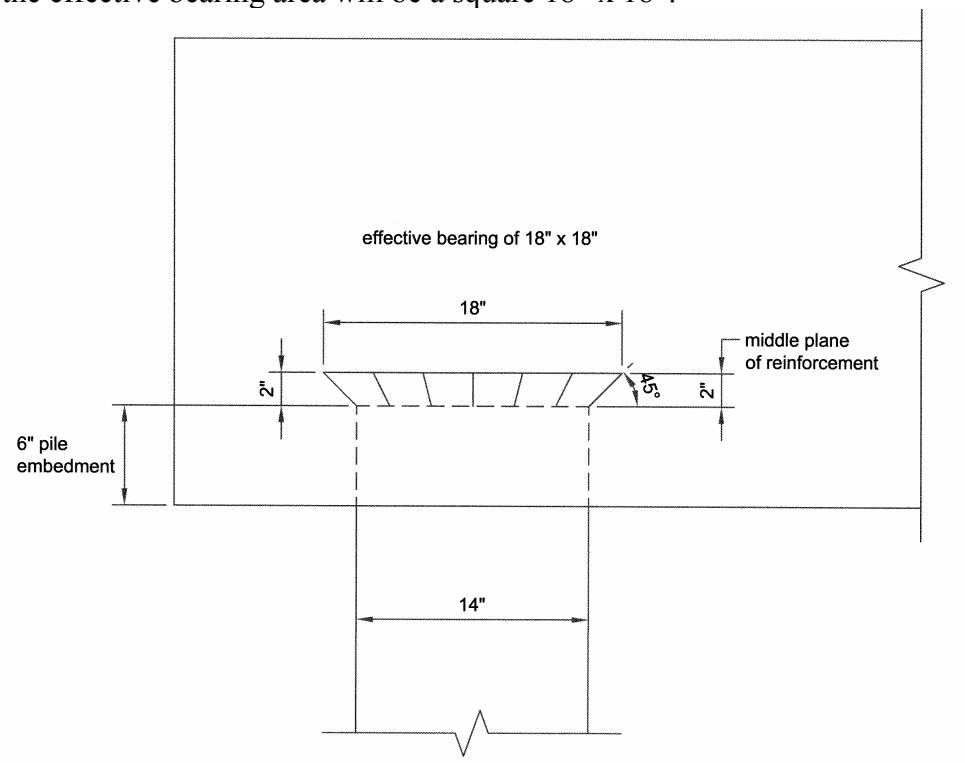

Figure 4-41: Distribution of compression stresses in region above pile.

Struts AJ, CL, EN & GP:

Using node A as representative of all the corner nodes, the vertical rise from A to J is 2'-2", while the horizontal distance from A to a point directly below J is $2.83\sqrt{2} = 4.0\,ft$ (See figure 4-40). Hence, the angle between the centerline of the strut and the horizontal square bearing area is 28.4^o (see Figure 4-42). The cross-sectional area of the strut can be estimated by first looking at a section passing through the vertical plane (Section A-A) shown in Figure 4-42. From geometry the area of the vertical plane can be determined to be 183.70 in^2. The cross section of the strut based on these assumptions is shown in Figure 4-42. The area of the vertical projection of the strut may be calculated as:

$$A_{srut} = \frac{25.45 \times 6.88}{2} + 2 \times 25.45 + \left(\frac{25.45 + 19.8}{2} \right) \times 2 = 87.55 + 50.90 + 45.25 = 183.70 in^2$$

Since the above value is a vertical section of the strut, the cross sectional area perpendicular to the axis of the strut can be calculated by cos(28.4^o) x 183.70= 161.6in^2.

The limiting compressive stress, f_{cu}, in the strut depends on the principal strain, ε_1, in the concrete surrounding the tension ties.

The tensile strain in Tie AB is:

$$\varepsilon_s = \frac{P_u}{A_{st}E_s} = \frac{190}{4.74 \times 29{,}000} = 1.382 \times 10^{-3}\ {}^{in}\!/_{in}$$

The tensile strain in the tie will reduce from $1.382X10^{-3}\ {}^{in}\!/_{in}$ at the inner face of the effective bearing area to a strain of zero at the outer face of the effective bearing area. Hence, in accordance with AASHTO LRFD C5.6.3.3.3, the strain will approximately equal $1.382 \times 10^{-3} / 2 = 0.691 \times 10^{-3}\ {}^{in}\!/_{in}$ at the mid-point of the strut. Using the angle between the plane of the tension ties and the diagonal strut of 28.4°, the principal strain, ε_1, can be determined using the following:

$$\varepsilon_1 = \varepsilon_s + (\varepsilon_s + 0.002)\cot^2 \alpha_s = 0.691 \times 10^{-3} + (0.691 \times 10^{-3} + 0.002)\cot^2 28.4^0 = 9.90 \times 10^{-3}\ {}^{in}\!/_{in}$$

and the limiting compressive stress, f_{cu}, in the strut is then,

$$f_{cu} = \frac{f_c^{'}}{0.8 + 170\varepsilon_1} = \frac{3}{0.8 + 170 \times 9.90 \times 10^{-3}} = 1.21ksi \le 0.85 \times 3 = 2.55ksi$$

Multiplying the limiting compressive stress by the area of the strut, the nominal resistance of the strut is thus:

$$P_n = f_{cu}A_{cs} = 1.21 \times 161.6 = 195.5kips$$

With a capacity resistance factor of 0.7, the factored resistance of the strut is:

$$P_r = \phi P_n = 0.7 \times 195.5 = 137kips$$

Since this is less than the factored load in the strut of 305 kips; the strut capacity is inadequate. To meet the strength requirement of the strut, the depth of the footing would need to be increased by approximately 14". This increase in depth would decrease the load in the strut and increase the area of the strut due to the change in geometry of the STM.

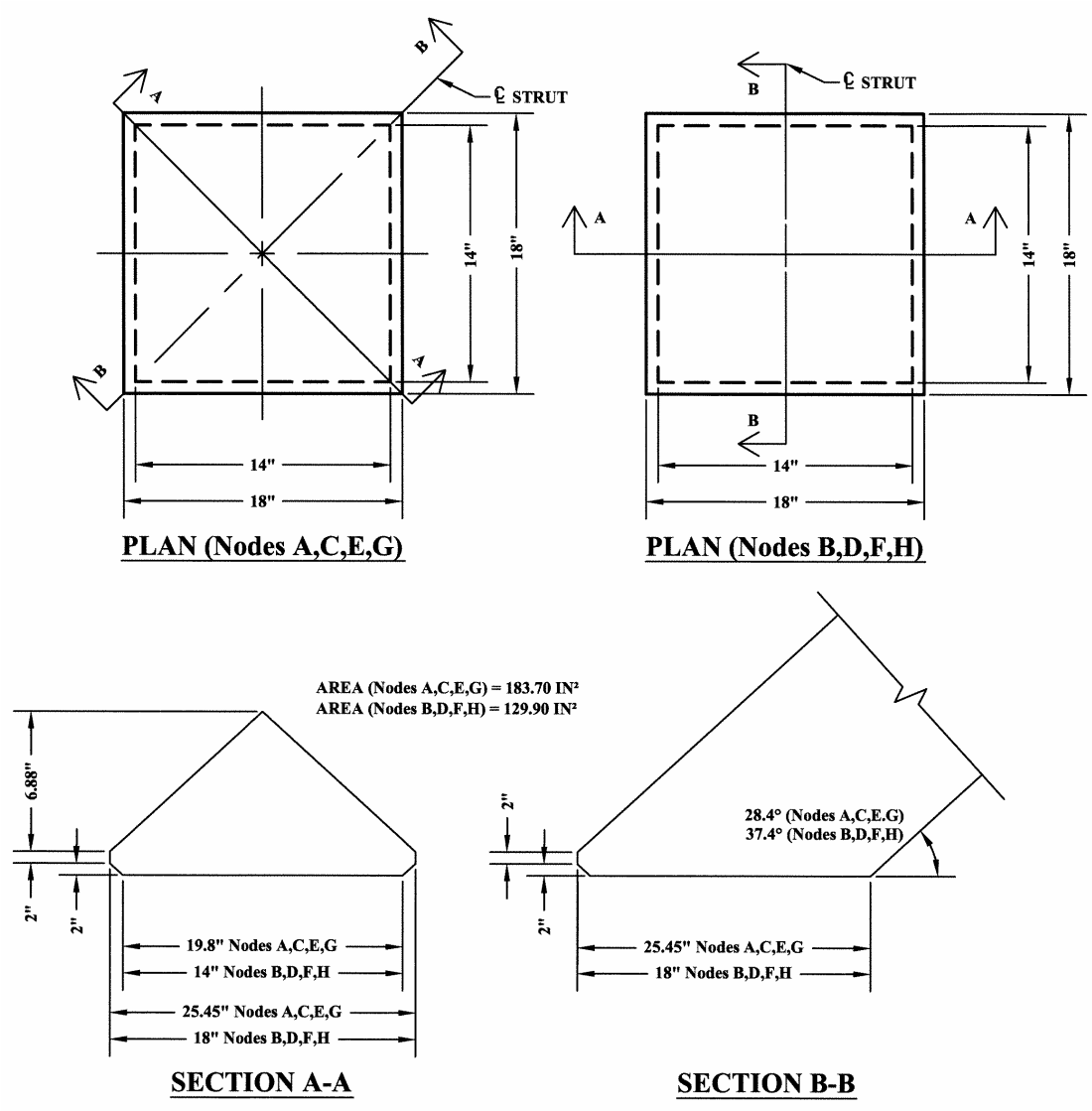

Figure 4-42: Details of strut at nodes.

Struts BK, DM, FO & HQ:

A similar approach will be used for struts BK, DM, FO and HQ. In this case, using node B as representative, the angle between the strut and the tie is 37.4° (see Figure 4-39). This results in a vertical cross-section of the strut as shown in Figure 4-42. The area of the vertical projection is calculated as follows:

$$A_{srut} = \frac{18 \times 6.88}{2} + 2 \times 18 + \left(\frac{18+14}{2} \right) \times 2 = 61.92 + 36 + 32 = 129.9 in^2$$

Since the above value is a vertical projection of the strut, the cross sectional area perpendicular to the axis of the strut can be calculated by cos(37.4°) x 129.9= $103 in^2$.

The limiting compressive stress, f_{cu}, in the strut depends on the principal strain, ε_1, in the concrete surrounding the tension ties.

The tensile strain in Ties CD & DE is:

$$\varepsilon_s = \frac{P_u}{A_{st}E_s} = \frac{190}{4.74 \times 29{,}000} = 1.382 \times 10^{-3}\ in/in$$

These strains will result in an average strain of $1.382X10^{-3}\ in/in$ at the mid-point of the strut. Using the angle between the plane of the tension ties and the diagonal strut of 37.4^o, the principal strain ε_1, can be determined using the following:

$$\varepsilon_1 = \varepsilon_s + (\varepsilon_s + 0.002)\cot^2 \alpha_s = 1.382 \times 10^{-3} + (1.382 \times 10^{-3} + 0.002)\cot^2 37.4^0 = 7.169 \times 10^{-3}\ in/in$$

and the limiting compressive stress, f_{cu}, in the strut is then,

$$f_{cu} = \frac{f_c^{'}}{0.8 + 170\varepsilon_1} \le 0.85 f_c^{'} = \frac{3}{0.8 + 170 \times 7.169 \times 10^{-3}} = 1.486ksi \le 0.85 \times 3 = 2.55ksi$$

Multiplying the limiting compressive stress by the area of the strut, the nominal resistance of the strut is thus:

$$P_n = f_{cu}A_{cs} = 1.486 \times 103 = 153kips$$

With a capacity resistance factor of 0.7, the factored resistance of the strut is:

$$P_r = \phi P_n = 0.7 \times 153 = 107kips$$

Since this is less than the factored load in the strut of 239 kips, the strut capacity is inadequate. As was the case in the struts at the corners, to meet the strength requirements of the strut, the depth of the footing would need to be increased by approximately 14". The resulting change in geometry of the STM would reduce the loads in the strut and increase its area.

Strut IR:

In the case of strut IR, the angle between the strut and the ties is 90^o. Therefore the cross-sectional area of the strut is much simpler to calculate. As can be seen is Figure 4-42, the area of the strut will equal: $A_{srut} = 18X18 = 324in^2$

The limiting compressive stress, f_{cu}, in the strut depends on the principal strain, ε_1, in the concrete surrounding the tension ties.

The tensile strain in Ties BI & IF and HI & ID is:

$$\varepsilon_s = \frac{P_u}{A_{st}E_s} = \frac{190}{4.74 \times 29{,}000} = 1.382 \times 10^{-3}\ {}^{in}\!/_{in}$$

These strains will result in an average strain of $1.382X10^{-3}\ {}^{in}\!/_{in}$ at the mid-point of the strut. Using the angle between the plane of the tension ties and the diagonal strut of 90°, the principal strain, ε_1, will be equal to ε_s, and the limiting compressive stress, f_{cu}, in the strut is then,

$$f_{cu} = \frac{f_c^{'}}{0.8 + 170\varepsilon_1} \le 0.85 f_c^{'} = \frac{3}{0.8 + 170 \times 1.382x10^{-3}} = 2.9ksi$$

Since this value is greater than $0.85 \times 3 = 2.55ksi$ use 2.55 *ksi*.

Multiplying the limiting compressive stress by the area of the strut, the nominal resistance of the strut is thus:

$$P_n = f_{cu}A_{cs} = 2.55 \times 324 = 826.2kips$$

With a capacity resistance factor of 0.7, the factored resistance of the strut is:

$$P_r = \phi P_n = 0.7 \times 826.2 = 578kips$$

Since this exceeds the factored load in the strut of 145 kips, the strut capacity is adequate.

Step 7(b) – Check nodal zone stress limits.

The nodal zone at the column-cap interface has a stress of:

$$f_c = \frac{9 \times 145}{42 \times 42} = 0.74ksi$$

This is below the nodal stress limit for a CCC node of

$$0.85\phi f_c^{'} = 0.85 \times 0.70 \times 3 = 1.78ksi$$

The stress in the nodal zone immediately above the piles is:

$$f_c = \frac{145}{14 \times 14} = 0.74ksi$$

Since the nodal zones immediately above the piles have tension ties in at least two directions the nodal zone stress limit is:

$$0.65\phi f_c^{'} = 0.65 \times 0.70 \times 3 = 1.36ksi > 0.74ksi$$

Step 8(a) – Check the detailing for the anchorage of the ties.

The No. 8 bars are required to develop a force of 190 kips at the inner face of the piles. The inner face of the effective bearing area is at a distance of 18+9 = 27 in. from the outside face of the pile cap. The original plans called for 3 in. of cover leaving 24 in. available for the embedment length. The original plans called for no hooks or any other anchorage device. The stress in the No. 8 bars at the inner faces of the piles is:

$$f_s = \frac{190}{6 \times 0.79} = 40.0ksi$$

In accordance with AASHTO LRFD paragraph 5.11.2.1.1, the basic tension development length of a No. 8 bar, l_d, is 34.2 in. The development length can be reduced as a function of the amount of stress in the bar, hence (40/60) x 34.2 = 23 in. Since there is 24 inches provided, the original anchorage details are acceptable.

Step 8(b) – Check the detailing of the crack control reinforcement.

Since this is a footing type element, it is exempt from the crack control requirements of the specifications and verification of meeting the minimum flexural reinforcement requirements were satisfied earlier.

General Conclusions regarding the Review of the Original Pile Cap Design:

As originally designed and detailed this footing does not meet the requirements of AASHTO LRFD STM. The footing depth would need to be increased by approximately 14". In this example, like the one examined in section 4.2.3 of this report, the angle between the inclined struts and the ties are relatively small due to the geometric constraints of the pile cap. With reference to the AASHTO LRFD, this small angle greatly reduces the effective compressive strength of the inclined struts which caused the predicted capacity of the pile cap to be significantly less than the capacity that has been measured through laboratory testing. For these types of structures, it may be desirable to allow for the effective compressive strength to be increased by a factor similar to the one Adebar used (described in section 4.2.3), or, perhaps, a minimum reduction factor should be implemented.

4.4 COMMENTARY FROM DESIGN FIRMS

Because the ultimate purpose of this project is to improve the strut-and-tie model provisions of the AASHTO LRFD Bridge Design Specifications and provide design examples for bridge designers, several design firms and departments of transportation were informally surveyed about the strut-and-tie model specifications. They were asked to list the types of structural elements that their firms/agencies had designed using the strut-and-tie model specifications and any suggestions or complaints they had about the AASHTO LRFD strut-and-tie model provisions. In total, eleven firms/agencies responded to the survey. The following discussion summarizes their responses which will be taken into account when identifying gaps and needed guidance in the AASHTO LRFD Bridge Design Specification (See Section 4.5).

Table 4-32 lists the firms/agencies that responded to the survey. In Table 4-32, each firm/agency has been labeled with a letter to identify them in Table 4-33. Table 4-33 summarizes the type of structural elements that the firms/agencies have designed using the AASHTO LRFD strut-and-tie model provisions and the number of firm/agencies that have actually performed the design for a given element. As can be seen in Table 4-33, at least half of the firms/agencies have used strut-and-tie models for post-tensioned anchorage zones, pile caps and footings, and around discontinuities and concentrated loads. Similarly, more than a quarter of the firms listed hammer head piers, diaphragms, and dapped-end beams as structural members that had been designed using strut-and-tie models. In addition to these structural members, eleven more were listed as being designed by one or two firms/agencies. The results of this portion of the survey demonstrate the wide range of applicability of strut-and-tie models.

Table 4-32: Firms/agencies responding to informal survey.

Label	Firm/Agency
A	Consulting Firm 1
B	Arkansas DOT
C	Consulting Firm 2
D	Consulting Firm 3
E	Consulting Firm 4
F	Consulting Firm 5
G	Consulting Firm 6
H	Montana DOT
I	Consulting Firm 7
J	Consulting Firm 8
K	Washington DOT

Table 4-33: List of structural elements designed by private design firms and departments of transportation using strut-and-tie models.

Design Use	Firms/Agencies	Total Number of Firms/Agencies	Percentage of Agencies
P-T anchorages (General Zone)	A-F, H, J, K	9	82
Around Discontinuities/Concentrated Loads	A-D, J, K	6	55
Pile Caps	A, C, G, I, J, K	6	55
Footings	B, E, G, I, K	5	45
Hammer Head Piers	B, F, G, H, K	5	45
Diaphragms	A, B, E, J	4	36
Dapped Beams	A, G, J	3	27
Bent Caps	G, I	2	18
Deep Beams	B, K	2	18
Expansion Joint Segments	E, K	2	18
Cap Column/Footing Column Connections	F, G	2	18
Abutments and Piers	I	1	9
Anchor Blocks	E	1	9
Corbels	C	1	9
Hammer Head Footings	I	1	9
Inverted Tees	J	1	9
Outriggers (Cantilever Portions of Multi-Column Bents)	G	1	9
Pier Caps	E	1	9

In addition, both design firms and departments of transportation commented on a variety of issues relating to strut-and-tie models and the AASHTO LRFD strut-and-tie model provisions. Table 4-34 summarizes the comments from each of the contributing design firms. Some of the firms/agencies feel that strut-and-tie models are not widely used due to difficulties generating a proper model and a lack of proven computer software to aid the design process. More specifically, a design engineer warned that it is easy to make a mistake when idealizing a uniform load as a set of point loads. Commentary given by some of the firms/agencies was more specific. For the strength of a tie, a designer believed that the $[f_{pe} + f_y]$ term in equation 5.6.3.4.1-1 should be limited to 0.9GUTS because they expected large crack widths due to the fact that the tie is designed at yield strength, and there are lower load factors for dead loads and prestress. Another designer indicated that there is not enough information about reinforced struts (AASHTO LRFD 5.6.3.3.4). They believed there should be more information on detailing a reinforced strut and providing enough anchorage for reinforcement in compression. Several firms/agencies commented on the AASHTO LRFD crack control provisions (5.6.3.6). Designers typically stated this requirement resulted in a large amount of reinforcement. An engineer pointed out that the crack control provisions give no guidance on predicting crack width. In addition, an engineer said, "C5.6.3.6 indicates that these bars are not just for crack control but also for ductility, but there is no way to actually control that ductility or even evaluate how much ductility is attained."

Table 4-34: Comments from private design firms and departments of transportation.

Design Firm/DOT	Concerns/Suggestions
A	Believes that many firms do not widely use STM provisions because most companies use computer programs to design concrete structures.
B	"Generating proper strut-and-tie model is one of the more difficult issues with the method, but…We feel that the specification language is quite clear and straightforward to use."
C	It is easy to make mistakes when idealizing a uniform load as a set of equivalent point loads.
	Do not believe that it is necessary to locate nodes accurately because STM techniques are approximate.
D	Feel that there is a lack of proven computer programs.
E	In equation 5.6.3.4.1-1, limit the [fpe + fy] term to 0.9GUTS (especially for PT bars): "For load cases with loads that have little uncertainty and lower load factors (DL, PT) I would expect large crack widths since the tension tie is designed at yield stress."
	Specifies crack control, but gives no guidance for determining crack widths at service level.
F	Did not mention any concerns or suggestions.
G	Feel that hesitation to use STM stems from the fact that there is more than one STM solution for a particular problem, and "[o]ne way to encourage the use of STM for specific design situations is to provide bridge design engineers with the exact STM load path for a specific design problem and tell them how to go about designing it."
H	Did not mention any concerns or suggestions.
I	Believe that "designs following AASHTO LRFD STM result in a lot more reinforcement that a traditional design, particularly due to the 0.3% crack control reinforcement which adds a large volume of reinforcement in both directions." In addition, "C5.6.3.6 indicates that these bars are not just for crack control but also for ductility, but there is no way to actually control that ductility or even evaluate how much ductility is attained."
	There is no benefit to the strut capacity due to the crack control reinforcement.
	There is not enough information related to the design of reinforced struts in Section 5.6.3.3.4, "particularly how to detail them to effectively develop reinforcement yield stress in compression (there's no commentary either) or how to provide increased confinement to the concrete within the strut." In addition, reinforce struts will contribute to the overall ductility, and might help reduce the amount of crack control reinforcement.
J	Would like to see "a simple AND widely accepted S & T model for the typical anchorage zone for a prestressed I-Beam or Bulb-Tee girder. For the big bulb-tees, there has been a fair amount of cracking for the projects I've worked on. I've not seen a comprehensive model that accounts for the end reaction, debonding, and transfer length."
K	Did not mention any concerns or suggestions.

4.5 GAPS AND NEEDED GUIDANCE IN THE AASHTO LRFD STM

From the comparisons made between the AASHTO LRFD Bridge Design Specifications and other building specifications, experimental data, old designs from past practices, and commentary made by design firms, confusing areas and gaps were identified in the AASHTO LRFD specification. For clarity, these confusing areas and gaps are summarized in Table 4-35. Based on the information in Table 4-35, revisions to the specification may be proposed; however, not all of the items listed in Table 4-35 will be used as a basis for a proposed change to the specification. Some of the items may be used as a basis to suggest research or may not warrant any action. Suggested research and proposed revisions to the specification can be found in Chapter 5.

Table 4-35: Confusing areas and gaps identified in the AASHTO LRFD specification.

#	Section	Topic	Discussion
1	5.5.4.2.1	Resistance Factors	The resistance factor for ties in a strut-and-tie model is not clearly stated unlike the resistance factor for compression in strut-and-tie models.
2	5.6.3.1	General	The AASHTO LRFD strut-and-tie model provisions do not discuss D-regions or how to determine the size of a D-region in a member that contains both B- and D-regions.
3	5.6.3.1	General	It would be helpful to list typical elements in bridges that should be designed using strut-and-tie models (deep footings and pile caps are already mentioned).
4	5.6.3.1	General	In addition to explaining that strut-and-tie models can be used near support and point loads, also mention that they can be used near geometric discontinuities (holes, dapped-ends, etc.).
5	-	Order of Calculations	A list of the common process of performing a strut-and-tie analysis would be excellent guidance for using the AASHTO provisions.
6	5.6.3.2	Structural Modeling	Reword the definitions for struts, ties, and nodes, so that it is clear ties are members that carry tension, struts are members that carry compression, and nodes are regions of connections between struts and ties. By doing this, the words “compression” and “tension” can be omitted before “struts” and “ties,” respectively.
7	5.6.3.2	Structural Modeling	The specification needs to include a discussion to help designers develop strut-and-tie models that appropriately represent distributed loads.
8	5.6.3.2	Structural Modeling	There should be more information about determining the geometry of struts and nodes based on support conditions and the reinforcement details.

Table 4-35 (cont.): Confusing areas and gaps identified in the AASHTO LRFD specification.

#	Section	Topic	Discussion
9	5.6.3.3.3 And 5.6.3.5	Strength of Struts and Nodes	Both of these sections should discuss allowable stress levels when high strength concrete is used. In order to do this, some research might have to be performed in order to determine allowable limits for high strength concrete struts and nodes.
10	5.6.3.3.2	Effective Cross-Sectional Area of Strut	The specification states, "When a strut is anchored by reinforcement, the effective concrete area may be considered to extend a distance up to six bar diameters from the anchored bar." The specification should state that the extended strut boundaries must be symmetrical about the axis of the strut.
11	5.6.3.3.3	Limiting Compressive Stress in Strut	Give a definition of ε_1, so the designer knows what the value means.
12	5.6.3.3.2	Effective Cross-Sectional Area of Strut	The specification should also address how to model strut spreading and when using a three-dimensional strut-and-tie-model is required.
13	5.6.3.3.3	Limiting Compressive Stress in Strut	In addition to the definition of ε_s, include that ε_s can be calculated by the following: $\varepsilon_s = P_u/(A_{st}E_s)$
14	5.6.3.3.3	Limiting Compressive Stress in Strut	Since ε_s can be taken as the value at the centerline of the strut, the definition for ε_s under equation 5.6.3.3.3-2 should state this fact.
15	5.6.3.3.3	Limiting Compressive Stress in a Strut	The specification needs to clarify how to calculate the compressive strength of a strut when a strut is connected to a node that is anchoring more than one tie (CTT node)
16	5.6.3.3.4	Reinforced Strut	In addition to being parallel to the strut, the specification should state that the reinforcement must be symmetrical about the centerline of the strut.
17	5.6.3.3.4	Reinforced Strut	The specification should address that reinforcement in a strut should provide connectivity between nodes and be properly anchored in the nodal zones.
18	5.6.3.4..2	Anchorage of Tie	The specification should be more specific regarding the limits of the node in which the tie must be anchored. Also, the impact of compression on the anchorage length should be addressed.
19	5.6.3.6	Crack Control Reinforcement	The required amount of crack control in the STM provisions of the AASHTO LRFD is larger than the required amount of crack control in the STM provisions of other specifications.

Table 4-35 (cont.): Confusing areas and gaps identified in the AASHTO LRFD specification.

20	5.13.2.3	Detailing Requirements for Deep Beams	The definition of a deep beam should be given. In other words, clarify a span to depth ratio that can be considered a deep beam.
21	5.13.2.3	Detailing Requirements for Deep Beams	The entire section is confusing. Equation 5.13.2.3-1 and the corresponding definitions are unclear. Also, the specification explaining the equation references Figure C5.13.2.3-1 which is also unclear.
22	5.13.2.3	Detailing Requirements for Deep Beams	In the commentary, Figures C5.13.2.3-1(b) and (d) show strut-and-tie models for a deep beams that utilize fan-shaped struts. If fan-shaped struts are going to be shown in example models, the specification needs to state that fan-shaped struts are analyzed like typical struts.

CHAPTER 5 – PROPOSED RESEARCH AND REVISIONS TO AASHTO LRFD (TASK 4)

5.1 VERIFICATION OF STRUT LIMITING COMPRESSIVE STRESS

Research by Ghoneim (2004) and Brown et al. (2006) has indicated that the strut strength provisions of Section 5.6.3.3.3 of the AASHTO LRFD Bridge Design Manual may be unconservative for high strength concretes. To verify the conservatism of the strut strength provisions of the AASHTO LRFD, several strut-and-tie model analyses were performed on several deep beams from a compiled database of deep beam tests.

5.1.1 INTRODUCTION TO DEEP BEAM DATABASE AND ANALYSIS

Section 5.6.3.3.3 of the AASHTO LRFD Design Specifications states that the limiting compressive stress, f_{cu}, in a strut shall be taken as:

$$f_{cu} = \frac{f'_c}{0.8 + 170\varepsilon_1} \le 0.85 f'_c \qquad \text{(AASHTO LRFD eq. 5.6.3.3.3-1)}$$

in which:

$$\varepsilon_1 = \varepsilon_s + (\varepsilon_s + 0.002)\cot^2(\alpha_s) \qquad \text{(AASHTO LRFD eq. 5.6.3.3.3-2)}$$

where:

ε_1 = the principal tensile strain in the cracked concrete (in./in.).

α_s = the smallest angle between compressive strut and adjoining tie (^{o}).

ε_s = the tensile strain in the concrete in the direction of the tension tie (in./in.).

f'_c = specified concrete compressive strength (ksi).

There are two issues with regards to how equation 5.6.3.3.3-1 is used. In equation 5.6.3.3.3-1, there are no limitations on f'_c; therefore, there is no modification in the equation for high strength concrete. For ε_s, the Commentary for Section 5.6.3.3.3, states that "it is appropriate to use the [strain] value at the centerline of the strut." For struts connected to nodes that anchor one tie, it can be assumed that ε_s is zero at the beginning of the node and fully developed at the end of the node (see Figure 5-1); therefore, in these situations, the average tensile strain in the concrete used in equation 5.6.3.3.3-2 would be calculated to be half the maximum tensile strain in the tie, ε_s.

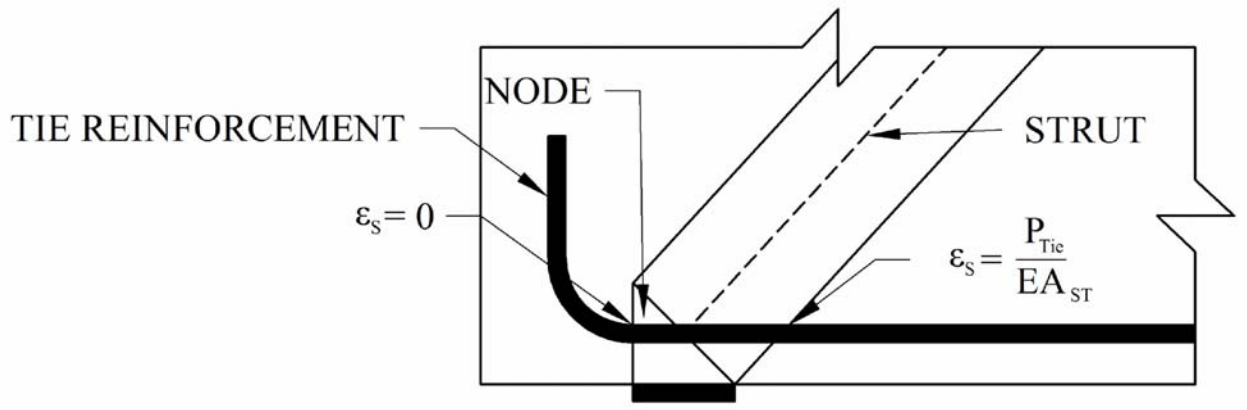

Figure 5-1: Potential assumption for the strain in the tie.

The tensile strain in the concrete in the direction of a tie can be calculated as follows:

$$\varepsilon_s = \frac{P_{tie}}{E_s \cdot A_{ST}}$$

where:

P_{tie} = the maximum force in the tie (kips).

E_s = modulus of elasticity (ksi).

A_{ST} = the area of steel in the tie (in^2).

In order to verify the conservatism of the limiting strut strength provisions of Section 5.6.3.3.3, a database of 282 deep beam tests was compiled and analyzed using a commonly accepted deep beam strut-and-tie model (STM) (See Figure 5-2). Appendix D lists the sources of the deep beam data tests. The geometry, reinforcement details, and concrete strengths of the deep beams varied. All of the deep beams had some type of crack control reinforcement. For each deep beam in the database, the STM was developed based on the width of the loading/bearing conditions (l_b), the depth of reinforcement (d), shear span (a), and the thickness of the beam (t). Figure 5-2 shows how the STMs were developed based on the collected data. Figure 5.6.3.3.2-1 in the AASHTO LRFD also gives details of how to develop the geometry of a STM.

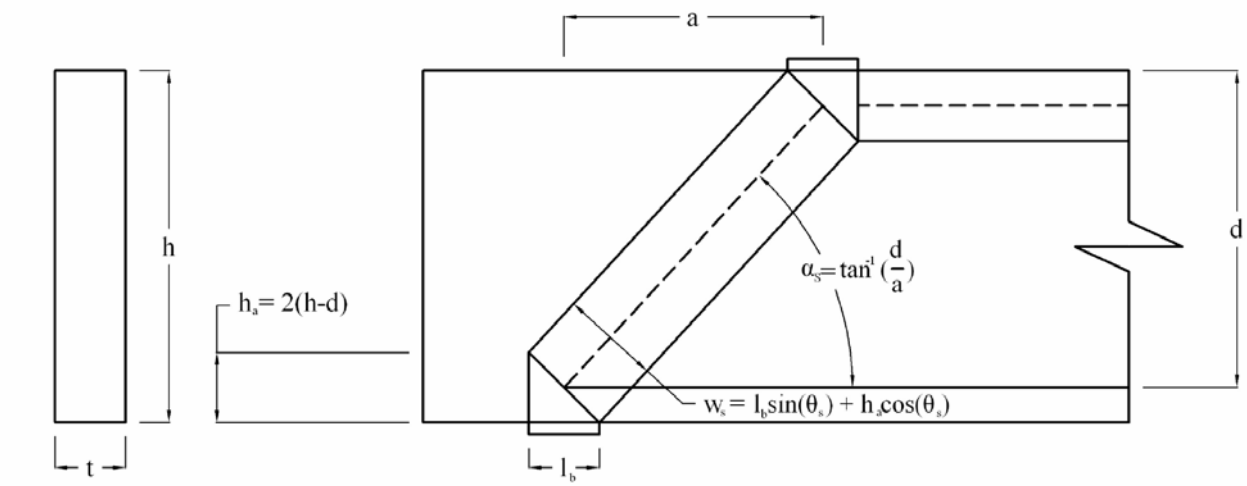

Figure 5-2: STM defined for each deep beam in the database.

Using the determined STM geometry and recorded support reactions at failure for each beam, the final forces in the struts and ties were calculated. Knowing the forces in the struts and ties for each beam, it was then possible to eliminate any beams that failed in the tie. Also, it should be noted that none of the beams failed due to insufficient anchorage. A total of 106 beams were removed from the database due to tension failure. This left 176 beams in the database to be used to investigate the strut strength provisions of Section 5.6.3.3.3. Using the determined geometry of the STM and loading data of the remaining beams, the actual compressive stress in the inclined strut, f_{actual}, was compared to the limiting compressive stress, f_{cu}, calculated using Section 5.6.3.3.3 of the AASHTO LRFD. The actual compressive stress in the inclined strut was determined by dividing the ultimate load in the strut, P_{strut}, by the cross-sectional area of the strut, A_{cs}. The ultimate load in the strut was determined as:

$$P_{strut} = \frac{R_{max}}{\sin(\alpha_s)}$$

where:

R_{max} = maximum support reaction.

The cross-sectional area of the strut, A_{cs}, is the product of the width of the strut, w_s, and the thickness of the strut which is assumed to be equal to the thickness of the beam, t (see Figure 5-2). This assumption is considered valid because, for each of the beams, the reaction plates extended the full thickness of the beams.

$$A_{cs} = w_s t$$

Therefore, the actual compressive stress in the strut was determined as:

$$f_{actual} = \frac{P_{strut}}{A_{cs}} = \frac{R_{\max}}{w_s \cdot t \cdot \sin(\alpha_s)}$$

The limiting compressive stress, f_{cu}, specified in Section 5.6.3.3.3 was calculated twice. For the first calculation, the limiting compressive stress was calculated based on angle between the strut and tie and the strain in the tie, ε_s. The strain in the tie was calculated as follows:

$$\varepsilon_s = \frac{P_{tie}}{E_s \cdot A_{ST}}$$

where:

$$P_{tie} = \frac{R_{\max}}{\cos(\alpha_s)}$$

For the second calculation, the limiting compressive stress was calculated based on the angle between the strut and tie and the average strain in the tie over the bearing plate, $\bar{\varepsilon}_s$. The average strain in the tie was calculated as follows:

$$\bar{\varepsilon}_s = \frac{\varepsilon_s}{2} = \frac{P_{tie}}{2 \cdot E_s \cdot A_{ST}}$$

5.1.2 DEEP BEAM DATABASE ANALYSIS RESULTS

To begin with, the STM analysis described in Section 5.1.1 was performed on each of the deep beams using the calculated strain in the tie, ε_s. Figure 5-3 shows a plot of the ratio of f_{actual}/f_{cu} versus f'_c for all of the beams. In Figure 5-3, data points greater than 1 indicate that the strut equations in Section 5.6.3.3.3 are conservative. Conversely, data points less than 1 indicate that the strut equations in Section 5.6.3.3.3 are unconservative. Figure 5-4 shows the results for all the beams having reinforcement that meet the AASHTO LRFD STM crack control requirements (§5.6.3.6). The figure shows that the limiting strut strength provisions yielded conservative results for the majority of the deep beams; however, all of the results for beams having high strength concrete (HSC), four in total, were found to be unconservative.

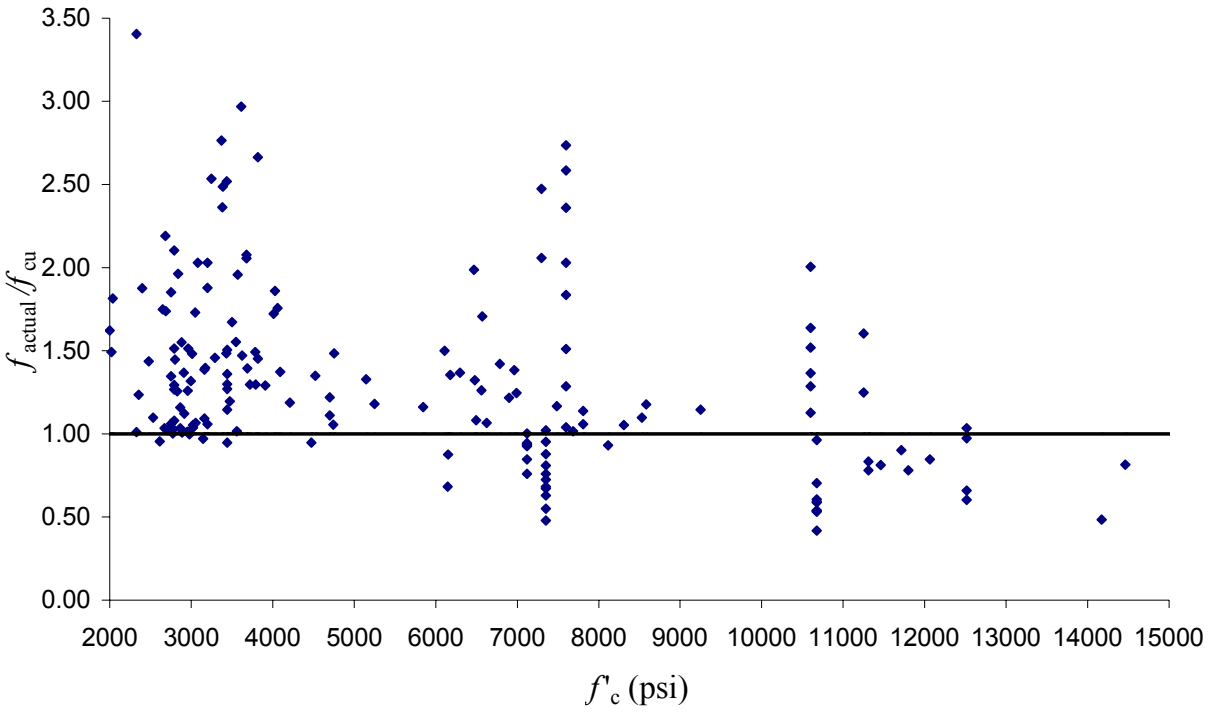

Figure 5-3: Plot of f_{actual}/f_{cu} versus f'_c for all beams using ε_s .

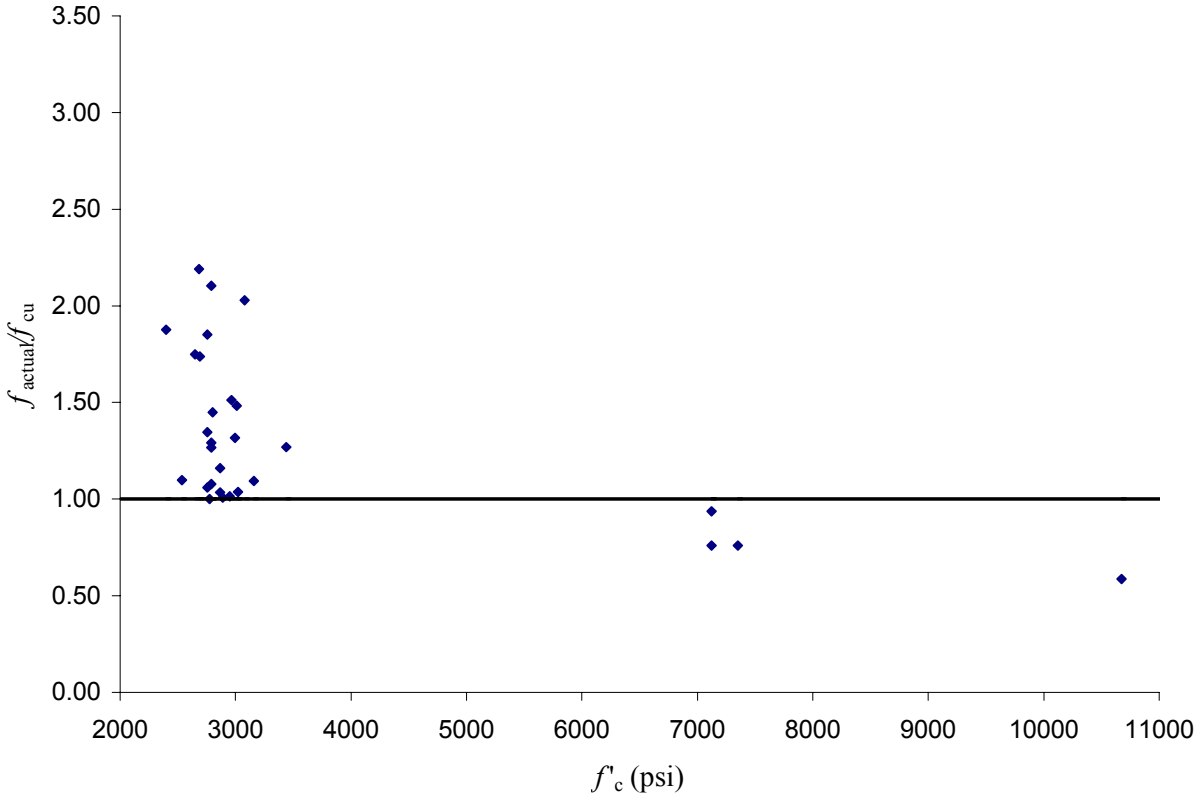

Figure 5-4: Plot of f_{actual}/f_{cu} versus f'_c for all beams with AASHTO LRFD crack control using ε_s .

In addition to Figures 5-3 and 5-4, Table 5-1 numerically summarizes the results. In Table 5-1, the results are divided into three categories (all the beams, beams having an f'_c below 7000 psi, and beams having an f'_c above 7000 psi). Within each of the three categories, data is given for beams having only vertical stirrups, beams having an orthogonal grid of crack control reinforcement, beams with reinforcement meeting the ACI 318-05 STM crack control requirement, beams with reinforcement meeting the CSA A23.3 STM crack control requirement, and beams with reinforcement meeting the AASHTO LRFD STM crack control requirement. The AASHTO LRFD, like the CSA-S6-06, requires a steel reinforcement area to gross concrete area ratio of 0.003 in each direction, and the CSA A23.3 requires a steel reinforcement area to gross concrete area ratio of 0.002 in each direction. The ACI 318-05 crack control requirement is best described as follows:

$$\sum \frac{A_{si}}{b_s s_i} \sin(\alpha_i) \geq 0.003$$

where:

A_{si} = area of surface reinforcement at spacing s_i.
b_s = width of strut.
α_i = angle at which layer of reinforcement crosses strut.

Table 5-1: Summary of STM analysis using ε_s.

f'_c	Category	Total	Conservative	% Conservative
All f'_c	All	176	132	75.0
	Stirrups	70	62	88.6
	Steel Grid	98	67	68.4
	ACI Crack Control	38	13	34.2
	CSA Crack Control	25	17	68.0
	AASHTO Crack Control	29	25	86.2
$f'_c < 7000$ psi	All	110	103	93.6
	Stirrups	41	40	97.6
	Steel Grid	69	63	91.3
	ACI Crack Control	14	13	92.9
	CSA Crack Control	20	17	85.0
	AASHTO Crack Control	25	25	100.0
$f'_c > 7000$ psi	All	66	29	43.9
	Stirrups	29	22	75.9
	Steel Grid	29	4	13.8
	ACI Crack Control	24	6	25.0
	CSA Crack Control	5	0	0.0
	AASHTO Crack Control	4	0	0.0

The same analysis was performed on the beams in the database keeping everything the same except the value $\bar{\varepsilon}_s$ was substituted for ε_s. Figure 5-5 shows the plot of f_{actual}/f_{cu} versus f'_c for all of the beams. Figure 5-6 shows the plot of f_{actual}/f_{cu} versus f'_c for beams having reinforcement that meets the AASHTO LRFD STM crack control requirements (§5.6.3.6). Table 5-2 provides a numerical summary of the STM analysis performed on the database.

Table 5-2: Summary of STM analysis using $\bar{\varepsilon}_s$.

f'_c	Category	Total	Conservative	% Conservative
All f'_c	All	176	98	55.7
	Stirrups	70	54	77.1
	Steel Grid	98	44	44.9
	ACI Crack Control	38	11	28.9
	CSA Crack Control	25	9	36.0
	AASHTO Crack Control	29	16	55.2
$f'_c < 7000$ psi	All	110	79	71.8
	Stirrups	41	37	90.2
	Steel Grid	69	42	60.9
	ACI Crack Control	14	11	78.6
	CSA Crack Control	20	9	45.0
	AASHTO Crack Control	25	16	64.0
$f'_c > 7000$ psi	All	66	19	28.8
	Stirrups	29	17	58.6
	Steel Grid	29	2	6.9
	ACI Crack Control	24	0	0.0
	CSA Crack Control	5	0	0.0
	AASHTO Crack Control	4	0	0.0

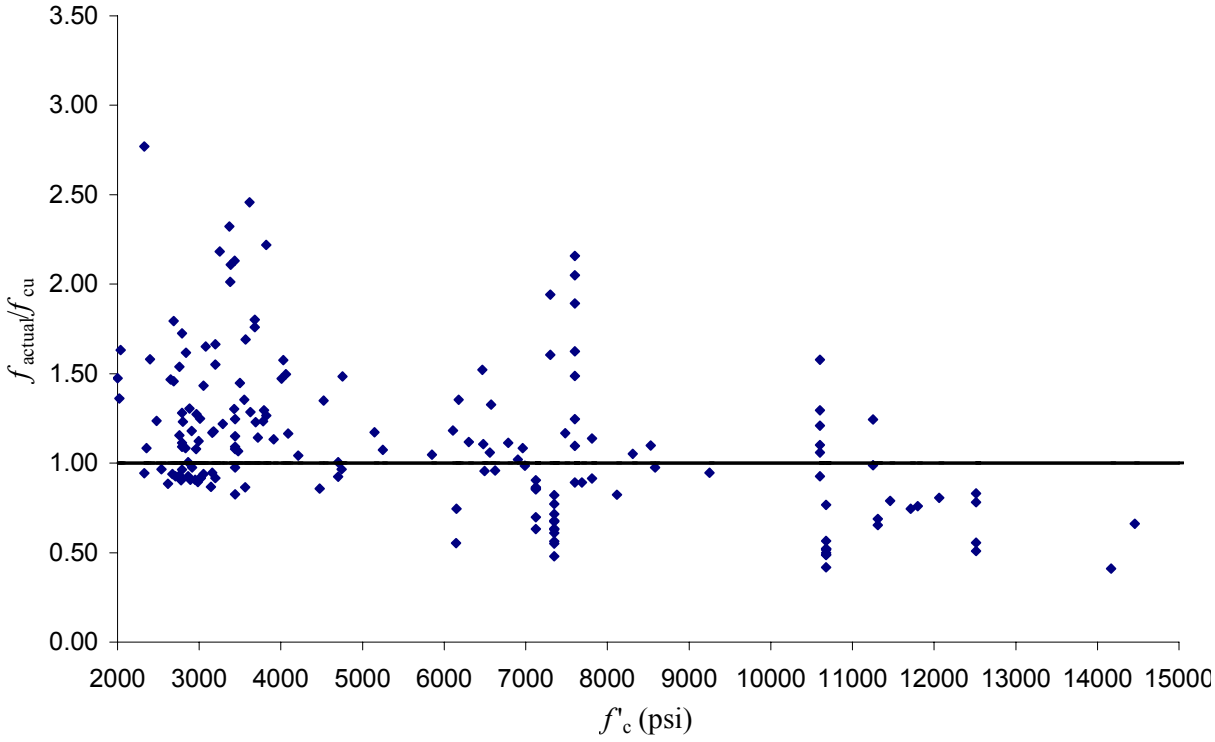

Figure 5-5: Plot of f_{actual}/f_{cu} versus f'_c for all beams using $\bar{\varepsilon}_s$.

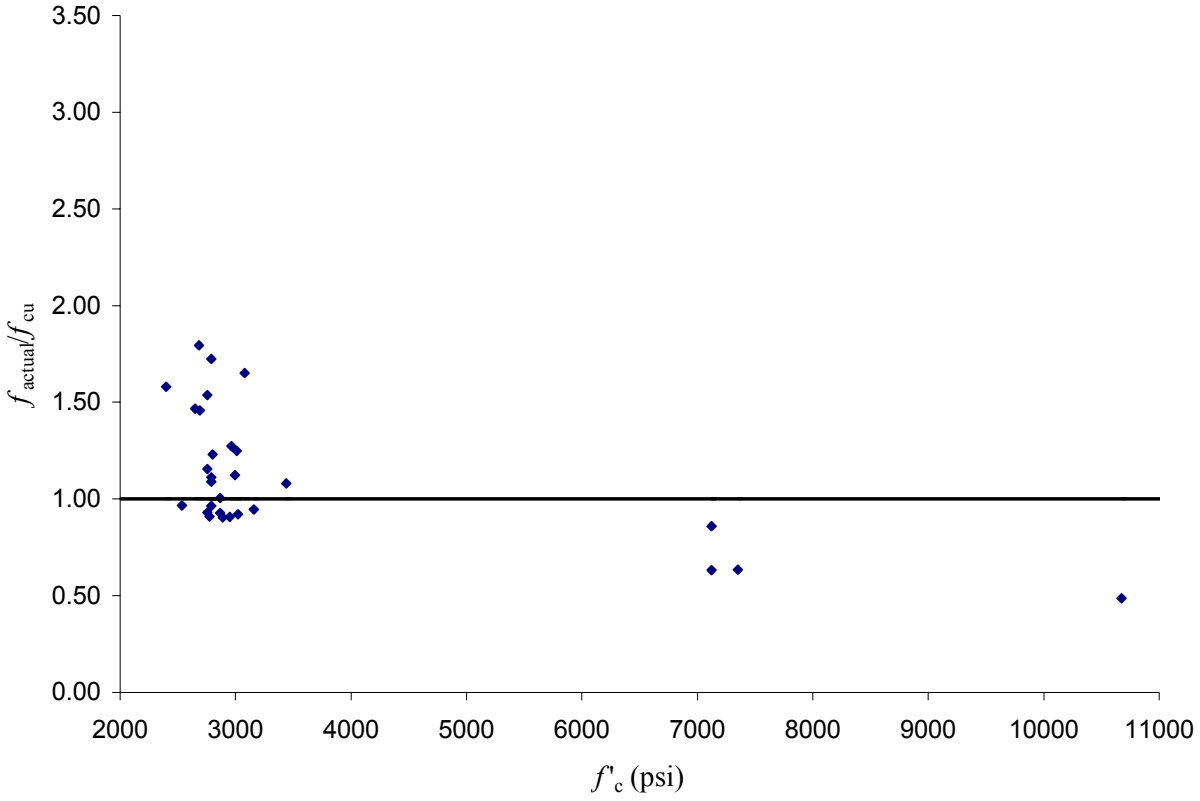

Figure 5-6: Plot of f_{actual}/f_{cu} versus f'_c for all beams with AASHTO crack control using $\bar{\varepsilon}_s$.

5.1.3 DISCUSSION OF DEEP BEAM DATABASE ANALYSIS

The following conclusions can be drawn from the data presented in Section 5.1.2.

When using $\bar{\varepsilon}_s$ instead of ε_s in equation 5.6.3.3.3-2, the percent of conservative results in each category drops significantly (See Tables 5-1 and 5-2). From Table 5-1, it can be seen that nearly 75 percent the results from all the beams are found to be conservative when ε_s is used for calculating f_{cu}; however, when $\bar{\varepsilon}_s$ is used, the percentage of conservative data drops below 56 percent (Table 5-2). More importantly, for beams that satisfy the AASHTO LRFD STM crack control requirements, 86.2 percent of the data is conservative when ε_s is used and 55.2 percent when $\bar{\varepsilon}_s$ is used. It can be concluded that using the ε_s at the centerline of the strut in equation 5.6.3.3.3-2 is unconservative when the assumption that ε_s is zero at the beginning of the node and fully developed at the end of the node for CCT nodes is used (see Figure 5-1).

The calculated limiting compressive stresses of the inclined struts, based on the provisions of Section 5.6.3.3.3, start to be become more unconservative for beams made of higher strength concrete. From Table 5-1, the calculated limiting compressive stress is shown to be conservative for 93.6 percent of the beams that have concrete strengths less than 7000 psi. This value drops to 43.9 percent for beams having concrete strengths greater than 7000 psi (Table 5-2). For beams satisfying the AASHTO LRFD crack control requirements, all of the beams (25 total) having

concrete strengths less than 7000 psi were found to be conservative, and none of the beams (4 total) having concrete strengths greater than 7000 psi were found to be conservative (Table 5-1 and 5-2).

Of all the beams that have an orthogonal grid of crack control reinforcement, the percentage of conservative beams is the highest for beams that satisfy the AASHTO LRFD crack control provisions. Based on this, the limiting compressive stress provisions of Section 5.6.3.3.3 yield more conservative results when used with the crack control specified in Section 5.6.3.6.

5.1.4 RECOMMENDATIONS FROM DEEP BEAM DATABASE ANALYSIS

1. To be conservative, remove wording in the AASHTO LRFD Bridge Design Specification that allows the use of the average strain in the tie at the centerline of the strut in Equation 5.6.3.3.3-2 for CCT nodes.

2. Research should be performed to investigate the validity of equations 5.6.3.3.3-1 and 5.6.3.3.3-2 for high strength concrete. Until research can be performed, the provisions of 5.6.3.3.3 should be modified to account for the effects of concrete having compressive strengths greater than 7000 psi. It is not necessary to modify the equations for concrete having compressive strengths less than 7000 psi because they have been proven to be conservative for concrete having compressive strengths lower than 7000 psi (see Table 5-1).

3. Until further research regarding STMs and crack control reinforcement is performed, maintain the current crack control requirements specified in Section 5.6.3.6.

5.2 MODIFICATION OF STRUT LIMITING COMPRESSIVE STRESS EQUATIONS (SECTION 5.6.3.3.3) FOR HIGH STRENGTH CONCRETE (HSC)

5.2.1 PURPOSE OF INVESTIGATION

In Section 5.1 of this report, STM analysis of the deep beams in the data base containing 176 deep beams showed that the strut limiting compressive stress, f_{cu}, provisions of Section 5.6.3.3.3 of the AASHTO LRFD Design Specifications yield unconservative results for concrete having compressive strengths greater than 7000 psi. Because of this, an investigation was performed to determine whether the provisions of Section 5.6.3.3.3 can be modified to yield conservative results for concrete having compressive strengths greater than 7000 psi. The findings of this investigation may be used to modify the STM specifications until more conclusive research can be performed.

5.2.2 DETERMINATION OF FACTORS AFFECTING CAPACITY

In order to determine how to modify the strut limiting compressive stress provisions for concrete having compressive strengths greater than 7000 psi, the effects of concrete strength (f'_c), angle between strut and adjoining ties (α_s), and crack control reinforcement on the capacity of the inclined struts analyzed in the database were investigated. Because Section 5.6.3.6 requires an

orthogonal grid of crack control reinforcement, only the beams with an orthogonal grid of reinforcement were analyzed. It should be noted that not all of the beams had the required ratio of reinforcement to gross area of concrete of 0.003 in each direction as specified by Section 5.6.3.6. In total, only 98 beams had an orthogonal grid of reinforcement. Of those, 29 beams are made of concrete having compressive strengths greater than 7000 psi. Only 4 of the 29 HSC beams were found to be conservative from the STM analysis.

First, the ratio of f_{actual}/f_{cu} versus f'_c was plotted. Figure 5-7 shows the plot of f_{actual}/f_{cu} versus f'_c for beams made of concrete having compressive strengths less than 7000 psi and having an orthogonal grid of reinforcement. Figure 5-8 shows the plot of f_{actual}/f_{cu} versus f'_c for beams made of concrete having compressive strengths greater than 7000 psi and having an orthogonal grid of reinforcement. From Figures 5-7 and 5-8, no clear relationship between the concrete compressive strength and the ratio of f_{actual}/f_{cu} can be seen other than the fact that the majority of the beams having concrete strengths greater than 7000 psi yielded unconservative results.

Second, the ratio of f_{actual}/f_{cu} versus α_s was plotted. Figure 5-9 shows the plot of f_{actual}/f_{cu} versus α_s for beams made of concrete having compressive strengths less than 7000 psi and having an orthogonal grid of reinforcement. Figure 5-10 shows the plot of f_{actual}/f_{cu} versus α_s for beams made of concrete having compressive strengths greater than 7000 psi and having an orthogonal grid of reinforcement. From Figure 5-10, for HSC concrete, it appears that the provisions of 5.6.3.3.3 overestimate the capacity of struts for increasing values of α_s.

In order to quantify the effects of crack control reinforcement on strut capacity, the ratios of reinforcement to gross concrete area in the vertical direction (ρ_v) and horizontal direction (ρ_h) were converted into an equivalent ratio of reinforcement to gross concrete area perpendicular to the strut, ρ_{eq}. For each inclined strut from each deep beam, $\rho_{eq.}$ was determined as follows:

$$\rho_{eq.} = \rho_v \cdot \sin(\alpha_s) + \rho_h \cdot \cos(\alpha_s)$$

The ratios ρ_v and ρ_h can be calculated as follows:

$$\rho_{v,h} = \frac{A_{s(v,h)}}{b \cdot s_{v,h}}$$

Where:

$A_{s(v,h)}$	=	area of vertical or horizontal crack control reinforcement at s.
b	=	width of deep beam.
$s_{v,h}$	=	spacing of vertical or horizontal crack control reinforcement.

Figure 5-11 shows the f_{actual}/f_{cu} versus ρ_{eq} plot for beams made of concrete having compressive strengths less than 7000 psi and having an orthogonal grid of reinforcement. Figure 5-12 shows the f_{actual}/f_{cu} versus ρ_{eq} plot for beams made of concrete having compressive strengths greater than 7000 psi and having an orthogonal grid of reinforcement. No clear relationship between f_{actual}/f_{cu} and ρ_{eq} can be seen from Figures 5-11 or 5-12.

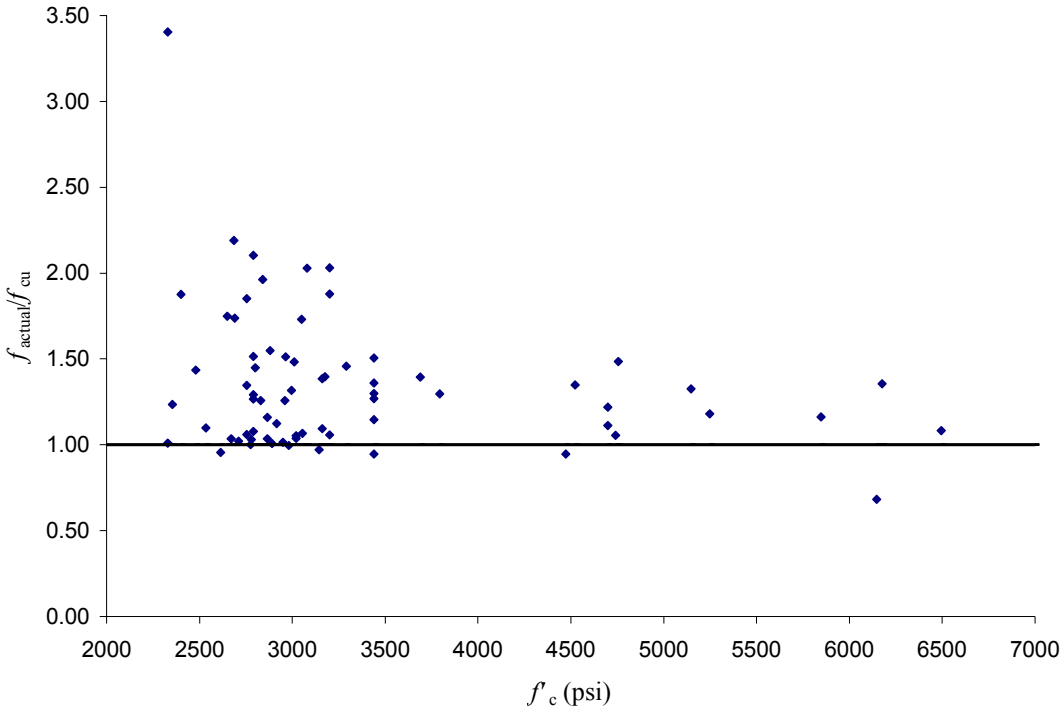

Figure 5-7: Ratio of f_{actual}/f_{cu} versus f'_c for beams having orthogonal grid of crack control reinforcement and concrete compressive strength less than 7000 psi.

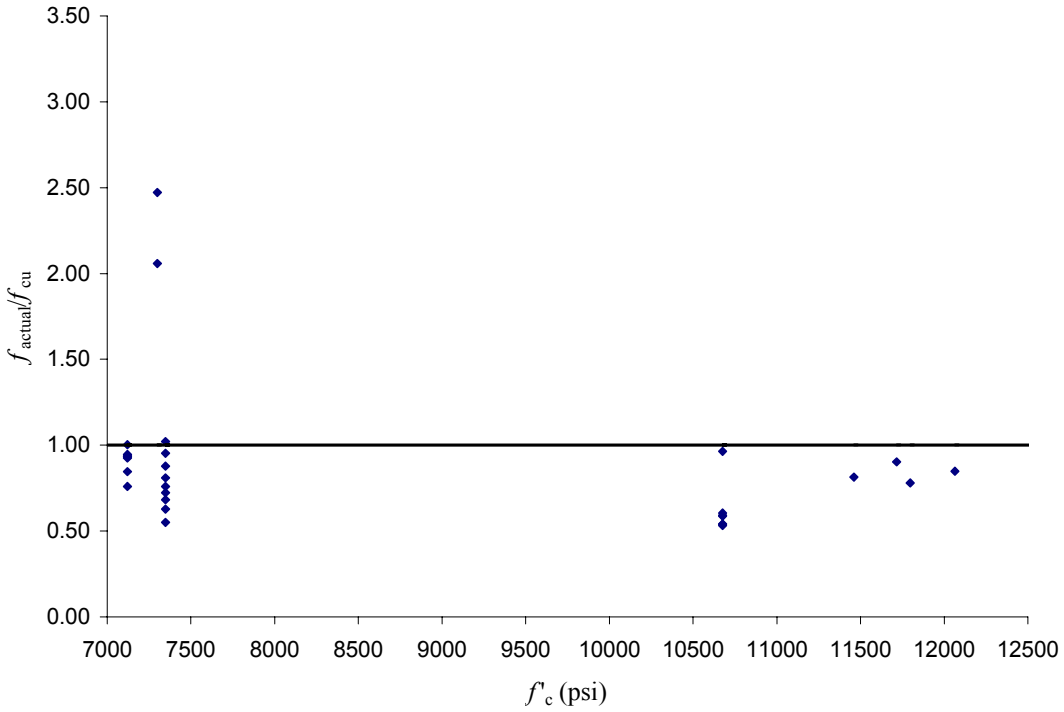

Figure 5-8: Ratio of f_{actual}/f_{cu} versus f'_c for beams having orthogonal grid of crack control reinforcement and concrete compressive strength greater than 7000 psi.

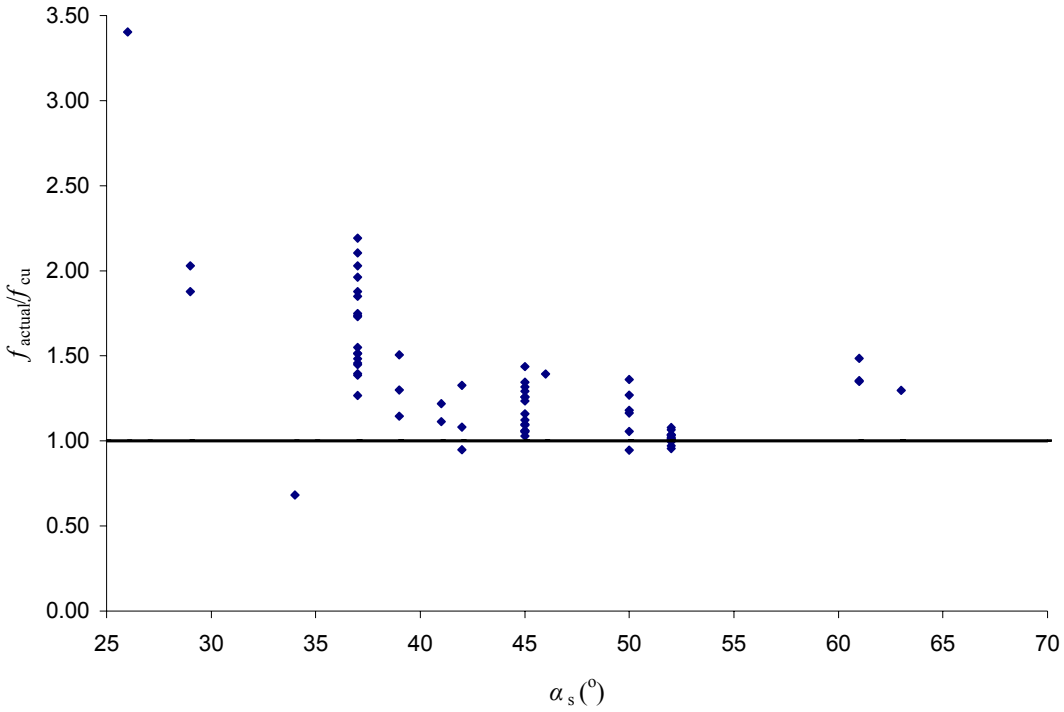

Figure 5-9: Ratio of f_{actual}/f_{cu} versus α_s for beams having orthogonal grid of crack control reinforcement and concrete compressive strength less than 7000 psi.

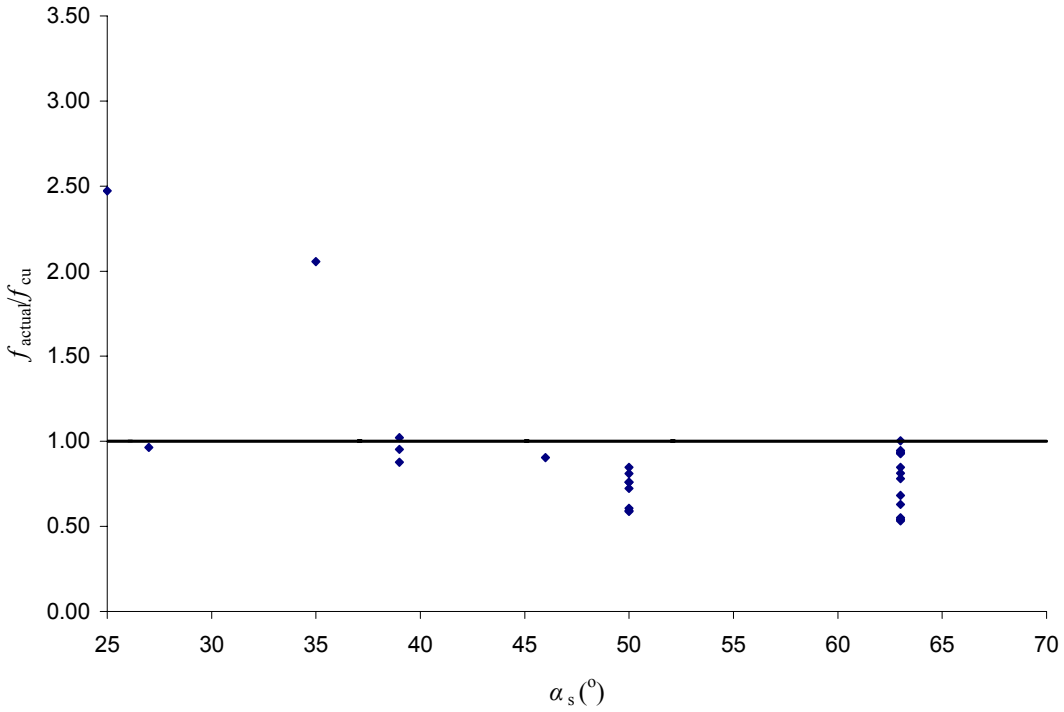

Figure 5-10: Ratio of f_{actual}/f_{cu} versus α_s for beams having orthogonal grid of crack control reinforcement and concrete compressive strength greater than 7000 psi.

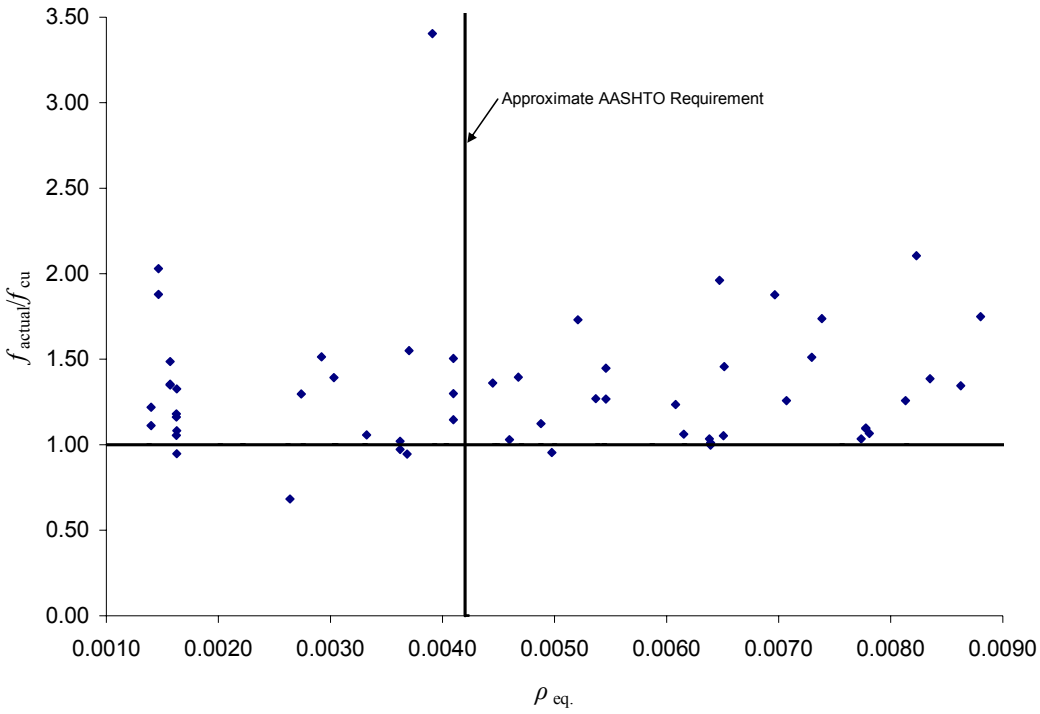

Figure 5-11: Ratio of f_{actual}/f_{cu} versus $\rho_{eq.}$ for beams having orthogonal grid of crack control reinforcement and concrete compressive strength less than 7000 psi.

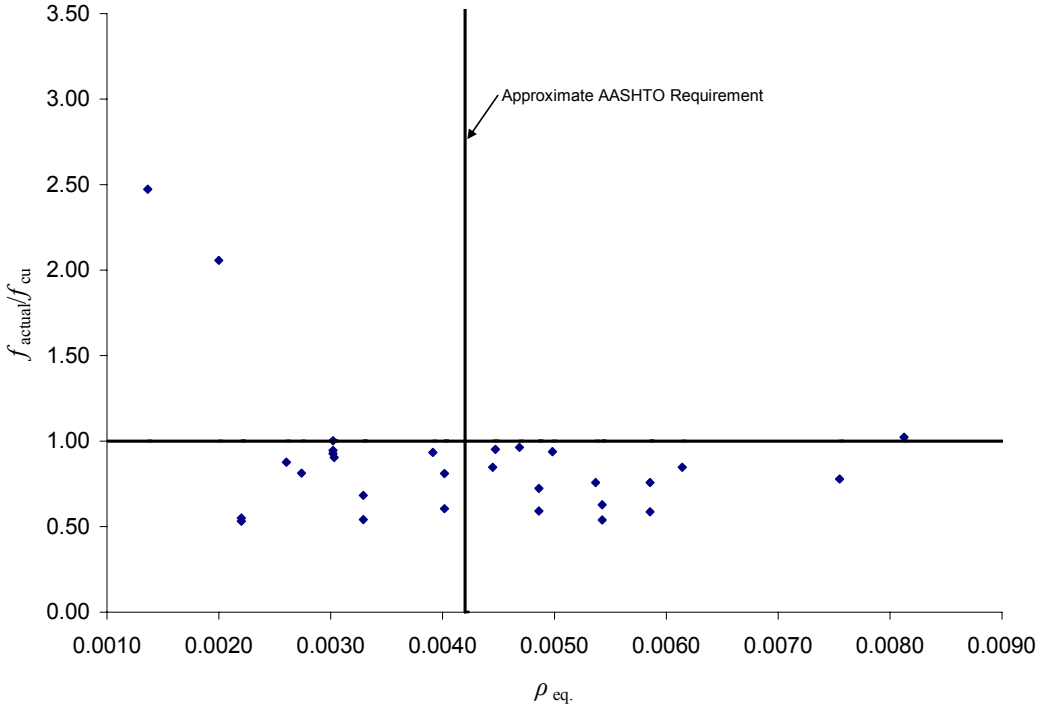

Figure 5-12: Ratio of f_{actual}/f_{cu} versus $\rho_{eq.}$ for beams having orthogonal grid of crack control reinforcement and concrete compressive strength greater than 7000 psi.

5.2.3 TRIAL MODIFICATION EQUATIONS

Based on Section 5.2.2 of this investigation, several modification factors for equation 5.6.3.3.3-1 were developed and tested for conservatism. The modification factors were developed with the knowledge that equation 5.6.3.3.3-1 yielded unconservative results for struts made of HSC, especially for struts with large angles of inclination (α_s). The amount of crack control was not taken into account in the developed modification factors because the AASHTO LRFD requires a minimum amount of crack control, and it was assumed that most designs will be within a reasonable amount of the minimum crack control.

The following modification equations are examples of some of the different types of equations that were tried. In all the equations, f'_c has units of ksi.

Original Equation: $$f_{cu} = \frac{f'_c}{0.8 + 170\varepsilon_1} \le 0.85 f'_c \quad \text{(eq. 5.6.3.3.3-1)}$$

Modified Equation 1: $$f_{cu} = \frac{f'_c \cdot \xi}{0.8 + 170\varepsilon_1} \le 0.85 f'_c$$

where:

$$\xi = 1 \qquad \text{for} \qquad f'_c < 7$$

$$\xi = \left(\frac{7}{f'_c}\right)\cos^{\frac{1}{2}}(\alpha_s) \qquad \text{for} \qquad f'_c \ge 7$$

Modified Equation 2: $$f_{cu} = \frac{f'_c}{0.8 + 170\varepsilon_1 \cdot \xi} \le 0.85 f'_c$$

where:

$$\xi = 1 \qquad \text{for} \qquad f'_c < 7$$

$$\xi = \frac{1}{\cos^2(\alpha_s)} \qquad \text{for} \qquad f'_c \ge 7$$

Modified Equation 3: $$f_{cu} = \frac{f'_c}{0.8 + 170\varepsilon_1 \cdot \xi} \le 0.85 f'_c$$

where:

$$\xi = 1 \qquad \text{for} \qquad f'_c < 7$$

$$\xi = \frac{1}{\cos^2(\alpha_s)} \leq 4 \qquad \text{for} \qquad f'_c \geq 7$$

Modified Equation 4: $$f_{cu} = \frac{f'_c}{0.8 + 170\varepsilon_1 \cdot \xi} \leq 0.85 f'_c$$

where:

$$\xi = 1 \qquad \text{for} \quad f'_c < 7$$

$$\xi = \frac{f'_c}{7} \leq \left(\frac{f'_c}{7}\right)\tan^3(\alpha_s) \leq 4 \qquad \text{for} \quad f'_c \geq 7$$

Modified Equation 5: $$f_{cu} = \frac{f'_c}{0.8 + 170\varepsilon_1 \cdot \xi} \leq 0.85 f'_c$$

where:

$$\xi = 1 \qquad \text{for} \qquad f'_c < 7$$

$$\xi = \frac{f'_c}{7} \qquad \text{for} \qquad f'_c \geq 7$$

Modified Equation 6: $$f_{cu} = \frac{f'_c}{0.8 + 170\varepsilon_1 \cdot \xi} \leq 0.85 f'_c$$

where:

$$\xi = 1 \qquad \text{for} \qquad f'_c < 7$$

$$\xi = \left(\frac{f'_c}{7}\right)^{\frac{1}{2}} \cdot \frac{1}{\cos^2(\alpha_s)} \qquad \text{for} \qquad f'_c \geq 7$$

Each of the above equations was tested on subsets of the database of beams that had orthogonal grids of crack control reinforcement and concrete compressive strengths greater than 7000 psi. The first subset used to determine the conservatism of modification equations included beams that fulfilled the AASHTO LRFD crack control reinforcement with $\rho_{eq.}$ within the range of 1 to 1.5 times the required amount AASHTO LRFD crack control. In order to do this, the crack control provisions of Section 5.6.3.6 were converted into a $\rho_{eq.}$ based on α_s for each beam. The equivalent ratio of reinforcement to gross concrete area perpendicular to the strut required by the AASHTO LRFD, $\rho_{eq.,AASHTO}$, for each beam was determined as follows:

$$\rho_{eq.,AASHTO} = 0.003 \cdot \left[\sin(\alpha_s) + \cos(\alpha_s)\right]$$

The results for the first subset of beams are given in Table 5-3. From Table 5-3, it can be seen that Modification Equations 2, 3, and 6 yield the most conservative results for Subset 1. Modification Equation 3 is better than the other two because the calculated average f_{actual}/f_{cu} ratio and standard deviation are comparable to the f_{actual}/f_{cu} ratio and standard deviation determined for the beams in the subset having concrete strengths less than 7000 psi.

Table 5-3: Results for Subset 1 (Beams having crack control within the range of 1 to 1.5 times what is required by Section 5.6.3.6).

f'_c Range	Modification	Total	Conservative	% Conservative	avg. f_{actual}/f_{cu}	σ
f'_c < 7000 psi	-	11	10	90.9	1.26	0.22
f'_c > 7000 psi	No Mod	11	0	0.0	0.75	0.16
	1	11	7	63.6	1.14	0.19
	2	11	11	100.0	1.33	0.35
	3	11	11	100.0	1.27	0.27
	4	11	9	81.8	1.18	0.29
	5	11	1	9.1	0.83	0.21
	6	11	11	100.0	1.41	0.31

Subset 2 included beams that had crack control between 1.5 and 2 times what is required by Section 5.6.3.6. Table 5-4 summarizes the findings using this subset. Unfortunately, only three beams in the subset had concrete strengths greater than 7000 psi which makes it difficult to make comparisons between the modification equations. All of the beams were found to be conservative when using Modification Equations 1, 2, 3, 4, and 6. Of these, Modification Equation 4 had the smallest f_{actual}/f_{cu} ratio, and Modification Equation 3 had the smallest standard deviation.

Table 5-4: Results for Subset 2 (Beams with crack control between 1.5 and 2 times greater than what is required by Section 5.6.3.6).

f'_c Range	Modification	Total	Conservative	% Conservative	avg. f_{actual}/f_{cu}	σ
f'_c < 7000 psi	-	17	16	94.1	1.35	0.37
f'_c > 7000 psi	No Mod	3	1	33.3	0.88	0.13
	1	3	3	100.0	1.78	0.50
	2	3	3	100.0	1.75	0.28
	3	3	3	100.0	1.59	0.15
	4	3	3	100.0	1.46	0.36
	5	3	2	66.7	1.03	0.06
	6	3	3	100.0	2.03	0.58

Subset 3 included beams that had over 2 times the amount of crack control required by Section 5.6.3.6. There were no beams with concrete compressive strengths greater than 7000 psi, so the Modification Equations could not be analyzed for this subset. Table 5-5 summarizes the results for the beams having concrete strengths below 7000 psi for subset 3.

Table 5-5: Results for Subset 3 (Beams with crack control greater than 2 times the requirement of Section 5.6.3.6). Only beams with f'_c less than 7000 psi.

Total	Conservative	% Conservative	avg. $P_u/P_{calc.}$	σ
17	17	100.0	1.47	0.42

Table 5-6 shows the combined results of the all the beams meeting the AASHTO LRFD crack control provisions. Once again, Modification Equations 2, 3, and 6 yielded the most conservative results. When comparing Modification Equations 2, 3, and 6, Modification Equation 3 has the smallest f_{actual}/f_{cu} ratio and standard deviation.

Table 5-6: Results for all beams with crack control meeting provisions of Section 5.6.3.6.

f'_c Range	Modification	Total	Conservative	% Conservative	avg. f_{actual}/f_{cu}	σ
f'_c < 7000 psi	-	43	41	95.3	1.34	0.34
f'_c > 7000 psi	No Mod.	14	1	7.1	0.78	0.16
	1	14	10	71.4	1.28	0.38
	2	14	14	100.0	1.42	0.37
	3	14	14	100.0	1.34	0.28
	4	14	12	85.7	1.24	0.32
	5	14	3	21.4	0.88	0.20
	6	14	14	100.0	1.55	0.43

In addition to applying the modification equations to the above subsets, the modification factors were also tested using all the beams with an orthogonal grid of reinforcement. Table 5-7 summarizes the results found when analyzing all of the beams with the orthogonal grid of crack control reinforcement. Table 5-7 shows that Modification Equations 2, 3, and 6 give the most conservative results; however, the f_{actual}/f_{cu} ratios and standard deviations computed for each Modification Equation were fairly large when compared to the results of the beams having concrete compressive strengths less than 7000 psi.

Table 5-7: Results for all beams with orthogonal grid of reinforcement.

f'_c Range	Modification	Total	Conservative	% Conservative	avg. f_{actual}/f_{cu}	σ
f'_c < 7000 psi	-	69	63	91.3	1.34	0.41
f'_c > 7000 psi	No Mod.	29	4	13.8	0.88	0.42
	1	29	24	82.8	1.38	0.46
	2	29	29	100.0	1.62	0.55
	3	29	28	96.6	1.51	0.50
	4	29	25	86.2	1.40	0.46
	5	29	7	24.1	0.96	0.43
	6	29	28	96.6	1.51	0.49

5.2.4 REFINEMENT OF TRIAL MODIFICATION EQUATIONS

Modification Equations 2, 3, and 6 presented in Section 5.2.4 of this report provided increased conservatism of the limiting strut strength provisions of Section 5.6.3.3.3 of the AASHTO LRFD; however, none of these equations is suitable to be added to the AASHTO LRFD specifications. Modification Equations 2 and 3 are only a function of the angle between the strut and tie, α_s. It would be more desirable if the equation to be added to the specification was a

function of both the angle between the strut and the tie, α_s, and the concrete compressive strength, f'_c. Modification Equation 6 is a function of both α_s and f'_c, but the calculated f_{actual}/f_{cu} ratios and standard deviations were found to be large for this modification equation.

In order to obtain a more suitable modification factor equation (ξ) for struts made of high strength concrete, a sensitivity analysis was performed using the set of beams meeting the crack control provisions of Section 5.6.3.6 of the AASHTO LRFD (see Table 5-7) and the following set of equations:

$$f_{cu} = \frac{f'_c}{0.8 + 170\varepsilon_1 \cdot \xi} \leq 0.85 f'_c$$

where:

$$\xi = 1 \qquad \text{for} \qquad f'_c < 7$$

$$\xi = \left(\frac{f'_c}{7}\right)^X \cdot \cos^Y(\alpha_s) \leq 4 \qquad \text{for} \qquad f'_c \geq 7$$

The modification factor equation (ξ) was developed based on, Modification Equations 3 and 6 from Section 5.2.4. In the equation, X and Y are values that will be determined based on optimizing the number of conservative test specimens and minimizing the f_{actual}/f_{cu} ratio and standard deviation.

Based on the sensitivity analysis, the value of X was found to be 0.3, and the value of Y was found to be -1.7. Table 5-8 shows the results for the deep beams having the required minimum amount of crack control specified by the AASHTO LRFD using these values in the ξ equation. The values in Table 5-8 can be compared to the values given in Table 5-6. When comparing the two tables, it can be seen that the newly developed modification factor equation (ξ) yields better results than Modification Equations 2, 3, and 6.

Table 5-8: Results for all beams with crack control meeting provisions of Section 5.6.3.6 using the newly developed modification factor equation (ξ).

f'_c Range	Modification	Total	Conservative	% Conservative	avg. f_{actual}/f_{cu}	σ
f'_c < 7000 psi	-	43	41	95.3	1.34	0.34
f'_c > 7000 psi	No Mod.	14	1	7.1	0.78	0.16
	λ	14	13	96.6	1.30	0.28

Table 5-9 shows the results for the deep beams having any type of orthogonal grid of crack control reinforcement using these values in the ξ equation. The values in Table 5-9 can be compared to the values in Table 5-7. From Table 5-9, the f_{actual}/f_{cu} ratio and standard deviation calculated using the newly developed modification factor equation (ξ) are larger than what would be desired; however, the values show improvement when compared to the f_{actual}/f_{cu} ratios and standard deviations for Modification Equations 2, 3, and 6 shown in Table 5-7.

Table 5-9: Results for beams having orthogonal grid of crack control reinforcement using the newly developed modification factor equation (ξ).

f'_c Range	Modification	Total	Conservative	% Conservative	avg. $f_{actual}/f_{cu.}$	σ
f'_c < 7000 psi	-	69	63	91.3	1.34	0.41
f'_c > 7000 psi	No Mod.	29	4	13.8	0.88	0.42
	λ	29	28	96.6	1.47	0.49

5.2.5 RECOMMENDATIONS

Based on the investigation of the modified equations of Section 5.2.3 and the resulting development of a refined modification factor equation (ξ) in Section 5.2.4 of this report, the limiting strut strength equation of Section 5.6.3.3.3 of the AASHTO LRFD can be modified as follows:

$$f_{cu} = \frac{f'_c}{0.8 + 170\varepsilon_1 \cdot \xi} \leq 0.85 f'_c$$

where:

$$\xi = 1 \qquad \text{for} \qquad f'_c < 7$$

$$\xi = \left(\frac{f'_c}{7}\right)^{0.3} \cdot \cos^{-1.7}(\alpha_s) \leq 4 \qquad \text{for} \qquad f'_c \geq 7$$

Figures 5-13, 5-14, and 5-15 show the improved results when applying the modification factor equation (ξ) to the limiting compressive stress equation for deep beams with crack control within 1 to 1.5 times the required amount specified in Section 5.6.3.6, for all deep beams meeting the crack control provisions of Section 5.6.3.6, and for all deep beams having an orthogonal grid of crack control reinforcement. Figure 5-15 can be compared to Figure and 5-8. This modification of the limiting strut strength equation should make the STM provisions conservative for high strength concrete until further research can be performed to develop equations that can give more accurate predictions of the capacity of members designed with STM.

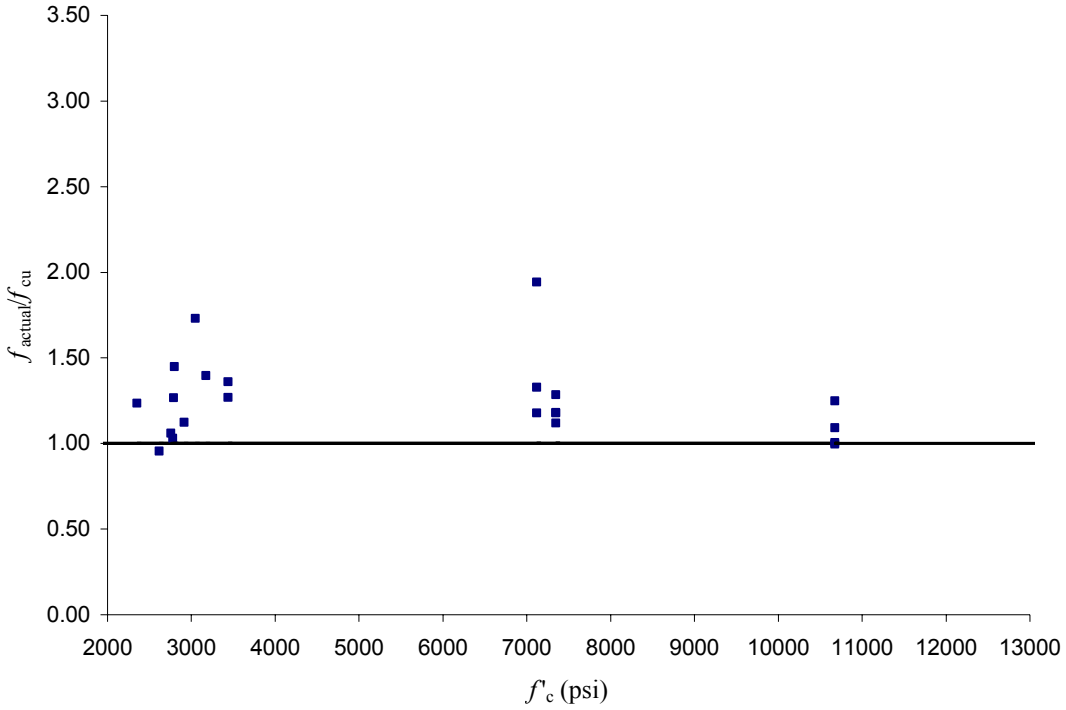

Figure 5-13: Results when applying the modification factor equation (ξ) to all beams with 1 to 1.5 times the required amount crack control specified in Section 5.6.3.6.

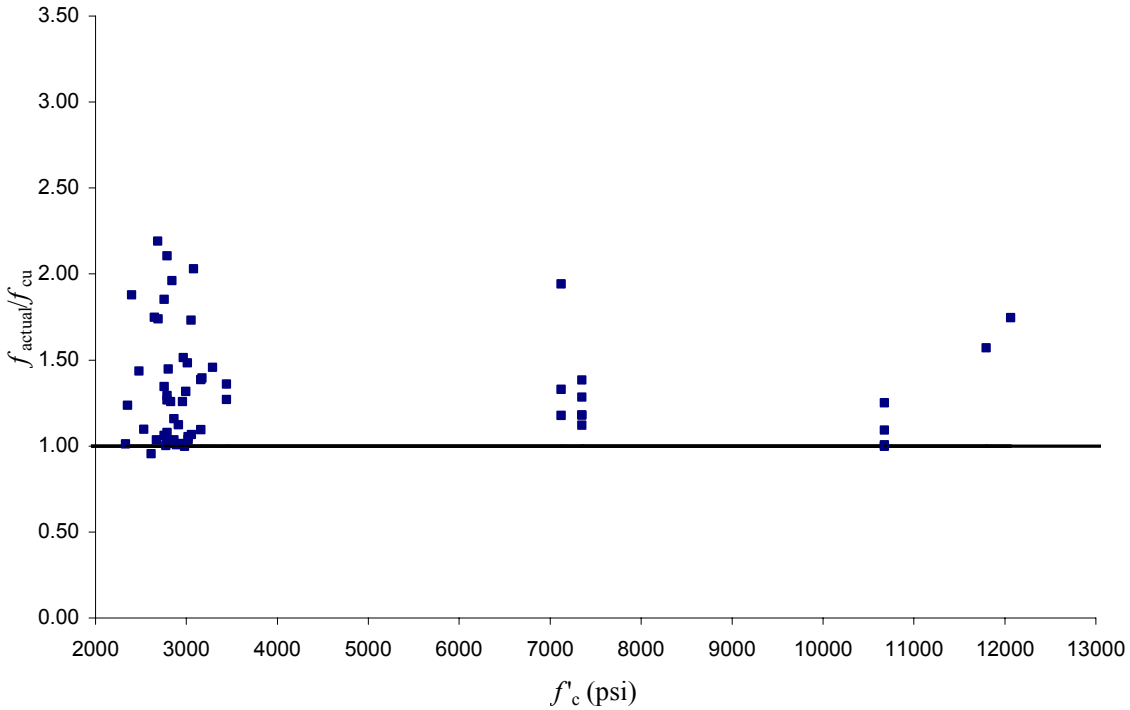

Figure 5-14: Results when applying the modification factor equation (ξ) to all beams meeting the crack control provisions specified in Section 5.6.3.6.

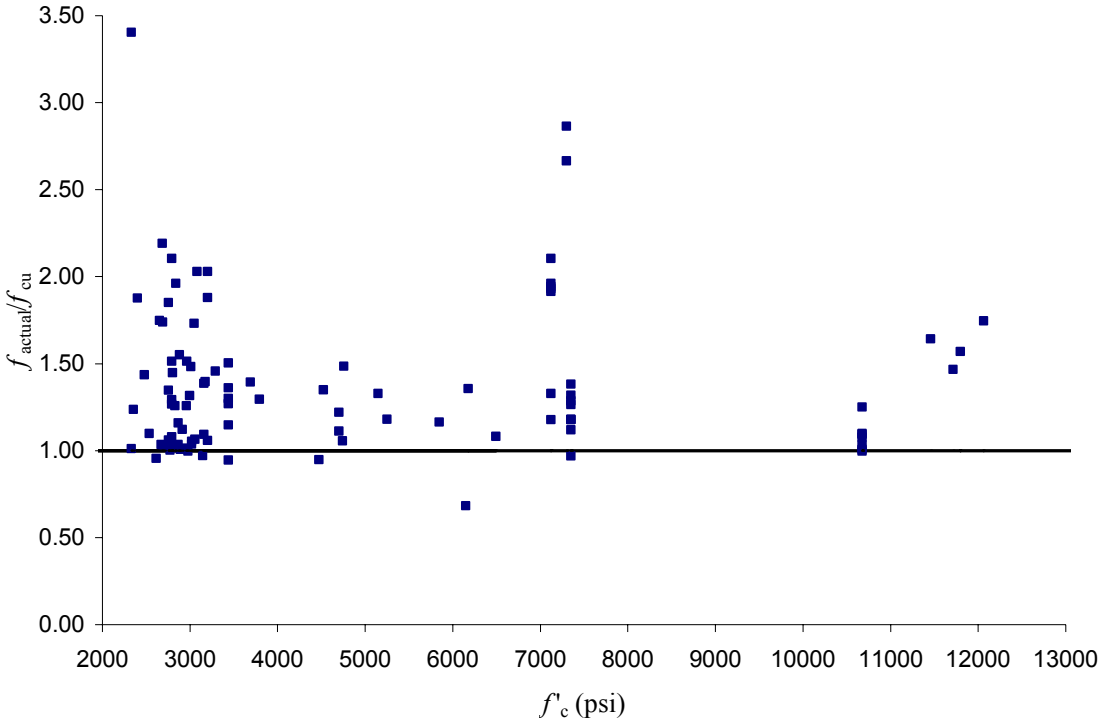

Figure 5-15: Results when applying the modification factor equation (ξ) to all beams with an orthogonal grid of crack control reinforcement.

5.3 PROPOSED RESEARCH

5.3.1 LIMITING COMPRESSIVE STRESS IN STRUT (AASHTO LRFD 5.6.3.3.3)

Because the investigation summarized in Section 5.1 of this report agreed with the research from Ghoneim (2004) and Brown et al. (2006) that found the strut strength provisions of Section 5.6.3.3.3 of the AASHTO LRFD to be unconservative for high strength concrete, an in depth research project should be funded to investigate the validity of the strut strength provisions. The main focus of the research should be on equations 5.6.3.3.3-1 and 5.6.3.3.3-2.

The research could be performed in three parts. The first part of the research should focus on testing the predictions equations 5.6.3.3.3-1 and 5.6.3.3.3-2 for several test specimens. The main variables in this part of the research should be specified concrete compressive strength, f'_c, the tensile strain in the tension reinforcement, ε_s, and the angle between the strut and the tie, α_s. If the research agrees with the research findings of this report, the second part of the research should focus on modifying equations 5.6.3.3.3-1 and 5.6.3.3.3-2 in order to make them conservative for high strength concrete. Finally, if the second part of the research yields undesirable results, the third part of the research should focus on developing new limiting compressive strength equations for struts.

5.3.2 LIMITING COMPRESSIVE STRESS IN STRUTS CONNECTED TO MULTIPLE TIES (AASHTO LRFD 5.6.3.3.3)

Currently the limiting compressive stress in a strut is a function of the angle between the strut and tie, α_s, and the strain in the tie, ε_s (AASHTO LRFD 5.6.3.3.3). For struts connected to one tie, the process of calculating the strut limiting compressive stress is fairly straightforward; however, the specification does not address how to calculate the strength of a strut that is connected to more than one tie. Regardless of whether the limiting strut strength equations remain in a similar format, tests should be performed to determine how to appropriately estimate the limiting strut strength for a strut connected to more than one tie. The tests should utilize specimens that have struts connected to ties in the same plane and specimens that have struts connected to ties in different planes (3-D STMs).

5.3.3 CRACK CONTROL REINFORCEMENT (AASHTO LRFD 5.6.3.6)

Extensive research about the crack control requirement for the AASHTO LRFD STM provisions should be performed (Section 5.6.3.6). As is, the 0.003 ratio of crack control reinforcement to gross concrete area in each direction is likely to be excessive in most members, but it also may not be sufficient in critical locations of some members. The research should focus on developing ways for design engineers to determine the amount of crack control reinforcement required to cross a strut. It would be ideal to develop an equation that has the concrete compressive strength, f'_c, and the angle between the strut and tie, α_s, as variables. By developing this type of equation, it would be possible to reduce the minimum amount of crack control in non-critical areas and ensure that enough crack control is provided in critical areas in members designed using the STM provisions.

5.3.4 ANCHORAGE LENGTH OF TIES (AASHTO LRFD 5.6.3.4.2)

AASHTO LRFD Section 5.6.3.4.2 deals with the anchorage of ties in STMs. The section simply references the AASHTO LRFD reinforcement development provisions (Section 5.11) and gives no specific information regarding the anchorage of ties in a STM. Research should be performed to identify typical anchorage details in STMs that may require more or less development length than what is specified in Section 5.11. An excellent example of a situation that may require less development length than specified in Section 5.11 is shown in Figure 5-16. From Figure 5-16, the development length required for the tie might be able to be reduced due to the fact that it is "pinched" between the strut and the support reaction.

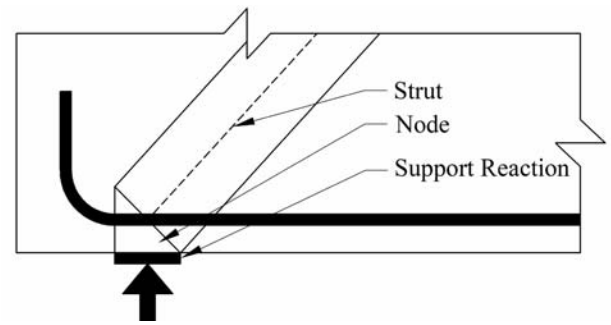

Figure 5-16: Region where anchorage length may be reduced.

5.4 PROPOSED REVISIONS TO AASHTO LRFD SPECIFICATIONS

Based on the work performed as part of this project as discussed in this report, the following changes to the strut-and-tie model provisions of the AASHTO LRFD Bridge Design Specifications can be proposed:

5.4.1 RESISTANCE FACTORS (AASHTO LRFD 5.5.4.2.1)

In article 5.5.4.2.1, add the following notation:

5.5.4.2.1 Conventional Construction

Resistance factor ϕ shall be taken as:

- For tension-controlled reinforced concrete sections as defined in Article 5.7.2.1 ..... 0.90
- For tension-controlled prestressed concrete sections as defined in Article 5.7.2.1 ..... 1.00
- For shear and torsion:
  - normal weight concrete 0.90
  - lightweight concrete 0.70
- For compression-controlled sections with spirals or ties, as defined in Article 5.7.2.1, except as specified in Article 5.10.11.4.1b for Seismic Zones 3 and 4 at the extreme event limit state 0.75
- For bearing on concrete 0.70
- For compression in strut-and-tie models 0.70
- <u>For tension in strut-and-tie models ..... 0.90</u>

5.4.2 GENERAL STM (AASHTO LRFD 5.6.3.1)

Revise Article 5.6.3.1 as follows:

5.6.3.1 General

Strut-and-tie models may be used to determine internal force effects near supports<u>,</u> ~~and~~ the points of application of concentrated loads<u>, and geometric discontinuities</u> at strength and extreme event limit states.

The strut-and-tie model should be considered for the design of deep footings and pile caps<u>, anchorage zones, deep beams, corbels,</u> or other situations in which the distance between the centers of applied load and the supporting reactions is less than about twice the member thickness.

If the strut-and-tie model is selected for structural analysis, Articles 5.6.3.2 through 5.6.3.6 shall apply. <u>For anchorage zones, deep beams and corbels, Articles 5.10.9.4, 5.13.2.3, and 5.13.2.4.1 shall also apply.</u>

5.4.3 GENERAL STM COMMENTARY (AASTHO LRFD C5.6.3.1)

In Article C5.6.3.1, revise as follows:

C5.6.3.1

~~Where~~ The conventional methods of strength of materials are not applicable near supports, concentrated loads, and geometric discontinuities because ~~of nonlinear~~ the strain distributions are nonlinear. ~~, the strut-and-tie modeling may provide a convenient way of approximating load paths and force effects in the structure. In fact, the load paths may be visualized and the geometry of concrete and steel selected to implement the load path.~~ Regions with nonlinear strain distributions are termed discontinuity regions or D-regions and are typically designed using strut-and-tie models.

Strut-and-tie modeling is a process that reduces complex states of stress in a structure into a truss of stress paths represented by simple uniaxial elements. Truss elements representing compressive concrete are called struts, and elements representing tensile reinforcement are called ties. The intersection points of truss elements are called nodes.

To perform a strut-and-tie analysis, a designer must first determine the locations of D-regions, model the flow of forces through the D-region with a strut-and-tie model, and calculate the forces in the struts and ties. Given the calculated forces in the struts and ties, a designer can then proportion the reinforcement required for the ties and check allowable stress levels in struts and nodes.

~~The strut-and-tie model is new to these Specifications.~~ More detailed information about delineating D-regions, developing strut-and-tie model geometry, detailing tie reinforcement, and checking allowable stress levels in struts and nodes ~~on this method~~ is given in ~~by~~ Schlaich et al. (*1987*), ~~and~~ Collins and Mitchell (*1991*)~~.~~, Bermeister et al. (*1993*), ACI SP-208 (*2002*), Mitchell et al. (*2004*), and NCHRP Project 20-07 (*2007*).

~~Traditional section-by-section design is based on the assumption that the reinforcement required at a particular section depends only on the separated values of the factored section force effects V_u, M_u, and T_u and does not consider the mechanical interaction among these force effects as the strut-and-tie model does. The traditional method further assumes that shear distribution remains uniform and that the longitudinal strains will vary linearly over the depth of the beam.~~

~~For members such as the deep beam shown in Figure C5.6.3.2-1, these assumptions are not valid. The shear stresses on a section just to the right of a support will be concentrated near the bottom face. The behavior of a component, such as the deep beam, can be predicted more accurately if the flow of forces through the complete structure is studied. Instead of determining V_u and M_u at different sections along the span, the flow of compressive stresses going from the loads P to the supports and the required tension force to be developed between the supports should be established.~~

~~For additional applications of the strut-and-tie model see Articles 5.10.9.4, 5.13.2.3, and 5.13.2.4.1.~~

5.4.4 EFFECTIVE CROSS-SECTIONAL AREA OF STRUT (AASHTO LRFD 5.6.3.3.2)

Revise Article 5.6.3.3.2 as follows:

5.6.3.3.2 Effective Cross-Sectional Area of Strut

The value of A_{cs} shall be determined by considering both the available concrete area and the anchorage conditions at the ends of the strut, as shown in Figure 1.

When a strut is anchored by reinforcement, the effective concrete area may be considered to extend a distance of up to six bar diameters from the anchored bar, as shown in Figure 1(a).

The boundaries of a strut shall be symmetrical about the axis of the strut.

5.4.5 LIMITING COMPRESSIVE STRESS IN STRUT (AASHTO LRFD 5.6.3.3.3)

In Article 5.6.3.3.3, revise as follows:

5.6.3.3.3 Limiting Compressive Stress in Strut

The limiting compressive stress, f_{cu}, shall be taken as:

$$f_{cu} = \frac{f'_c}{0.8 + 170\varepsilon_1 \cdot \underline{\xi}} \le 0.85 f'_c \qquad (5.6.3.3.3\text{-}1)$$

in which:

$$\varepsilon_1 = \varepsilon_s + (\varepsilon_s + 0.002)\cot^2 \alpha_s \qquad (5.6.3.3.3\text{-}2)$$

$\underline{\xi = 1 \qquad \text{for} \quad f_c' < 7 \qquad (5.6.3.3.3\text{-}3)}$

$$\underline{\xi = \left(\frac{f_c'}{7}\right)^{0.3} \cdot \cos^{-1.7}(\alpha_s) \qquad \text{for} \quad f_c' \ge 7 \qquad (5.6.3.3.3\text{-}4)}$$

where:

α_s = the smallest angle between the compressive strut and adjoining tension ties (°)

ε_s = the tensile strain in the concrete in the direction of the tension tie (in./in.)

$\underline{\xi}$ = $\underline{\text{modification factor for high strength concrete}}$

f'_c = specified compressive strength (ksi)

5.4.6 LIMITING COMPRESSIVE STRESS IN STRUT COMMENTARY (AASHTO LRFD C5.6.3.3.3)

In Article C5.6.3.3.3, revise as follows:

C5.6.3.3.3

If the concrete is not subjected to principal tensile strains greater than about 0.002, it can resist a compressive stress of 0.85 f'_c. This will be the limit for regions of the struts not crossed by or joined to tension ties. The reinforcing bars of a tension tie are bonded to the surrounding concrete. If the reinforcing bars are to yield in tension, there should be significant tensile strains imposed on the concrete. As these tensile strains increase, f_{cu} decreases.

The expression for ε_1 is based on the assumption that the principal compressive strain ε_2 in the direction of the strut equals 0.002 and that the tensile strain in the direction of the tension tie equals ε_s. As the angle between the strut-and-tie decreases, ε_1 increases and hence f_{cu} decreases. In the limit, no compressive stresses would be permitted in a strut that is superimposed on a tension tie, i.e., $\alpha_s = 0$, a situation that violates compatibility.

For a tension tie consisting of reinforcing bars, ε_s can be taken as the tensile strain due to factored loads in the reinforcing bars. For a tension tie consisting of prestressing, ε_s can be taken as 0.0 until the precompression of the concrete is overcome. For higher stresses, ε_s would equal $(f_{ps}-f_{pe})/E_p$.

If the strain ε_s varies over the width of the strut and can be calculated on both sides of the strut, it is appropriate to use the value at the centerline of the strut. When calculating the average strain ε_s, assuming the strain ε_s to be

zero at an edge of a strut was found to result in unconservative estimates of f_{cu} by NCHRP Project 20-07, Task 217 (*2007*).

To calculate f_{cu} for struts connected to multiple ties, a conservative approach is to calculate f_{cu} based on ε_s and α_s for each of the ties and use the smallest calculated f_{cu}.

5.4.7 REINFORCED STRUT (AASTHO LRFD 5.6.3.3.4)

Revise Article 5.6.3.3.4 as follows:

5.6.3.3.4 Reinforced Strut

If the compressive strut contains reinforcement that is parallel to the strut, symmetrical about the axis of the strut, and detailed to develop its yield stress in compression, the nominal resistance of the strut shall be taken as:

$$P_n = f_{cu} A_{cs} + f_y A_{ss} \qquad (5.6.3.3.4\text{-}1)$$

where:

A_{ss} = area of reinforcement in the strut (in.^{2})

Properly detailed compressive strut reinforcement shall provide connectivity between nodes and be properly anchored in the nodes.

5.4.8 ANCHORAGE OF TIE COMMENTARY(AASHTO LRFD C5.6.3.4.2)

Add C5.6.3.4.2-1:

C5.6.3.4.2-1

Figure C1 shows typical tension tie reinforcement anchorage details. In Figure C1, the tension tie reinforcement should be detailed to be fully developed beyond points A, B, and C. The tension tie reinforcement can conservatively be detailed to be fully developed at points D, E, and F.

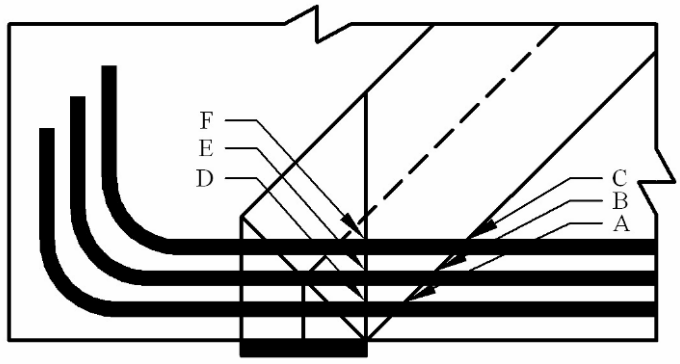

Figure C5.6.3.4.2-1 Anchorage of Tension Tie Reinforcement.

5.4.9 DETAILING REQUIREMENTS FOR DEEP BEAMS(AASHTO LRFD 5.13.2.3)

In Article C5.13.2.3, revise as follows:

5.13.2.3 Detailing Requirements for Deep Beams

The factored tensile resistance, N_R ~~in kips~~, of reinforcement perpendicular to the flexural tension reinforcement ~~transverse pair of reinforcing bars~~ shall satisfy:

$$N_R = \phi f_y A_s \geq 0.12 b_v s \qquad (5.13.2.3\text{-}1)$$

where:

b_v = width of web (in.)

f_y = yield strength of reinforcing steel (ksi)

A_s = area of steel in distance s (in.^{2})

ϕ = resistance factor specified in Article 5.5.4.2

s = spacing of reinforcement (in.)

The spacing of reinforcement perpendicular to the flexural tension ~~transverse~~ reinforcement, s, shall not exceed $d/4$ or 12.0 in.

Bonded reinforcement parallel to the flexural tension reinforcement ~~longitudinal bars~~ shall be well distributed over each face of the vertical elements in pairs. The tensile resistance of a bonded pair of reinforcement bars ~~pair~~ parallel to the flexural tension reinforcement shall not be less than that specified in Eq. 1. The vertical spacing between each pair of reinforcement bars parallel to the flexural tension reinforcement, s, shall not exceed either $d/3$ or 12.0 in. For components whose width is less than 10.0 in., a single reinforcement bar parallel to the flexural tension reinforcement of the required tensile resistance may be used in lieu of a pair reinforcement bars parallel to the flexural tension reinforcement. ~~of longitudinal bars.~~

APPENDIX A

EXAMPLES

LIST OF EXAMPLES

EXAMPLE A.1 ANCHORAGE ZONE AND EXAMPLE A.2 C-BENT JOINT

Problem Statement:

A C-bent that will support a highway superstructure is to be designed using the Strength I Load Case in Table 3.4.1-1 in the AASHTO LRFD. The top of the C-bent needs to be 26.9 ft (322.8 in.) above the grade. The superstructure will transfer its load to the C-bent through four equivalent point loads spaced at 12 ft.-11 in. (154.7 in.). Under critical loading cases the dead load was found to contribute 133 kips to each point load, and the live load was found to contribute 63 kips to each point load. The factored point loads using the Strength I Load Case are calculated to be 276.5 kips. The column and cantilever beam have both been designed to meet the given loading demands (see below). Using strut-and-tie models (STMs) design the post-tensioned anchorage zone in the cantilever beam and the joint of the C-bent.

Beam and Column Design Information:

Both the beam and column have been designed for the loading described above. Figure A-1 shows the details of each member. Figure A-2 shows the cross-sections of the beam and column.

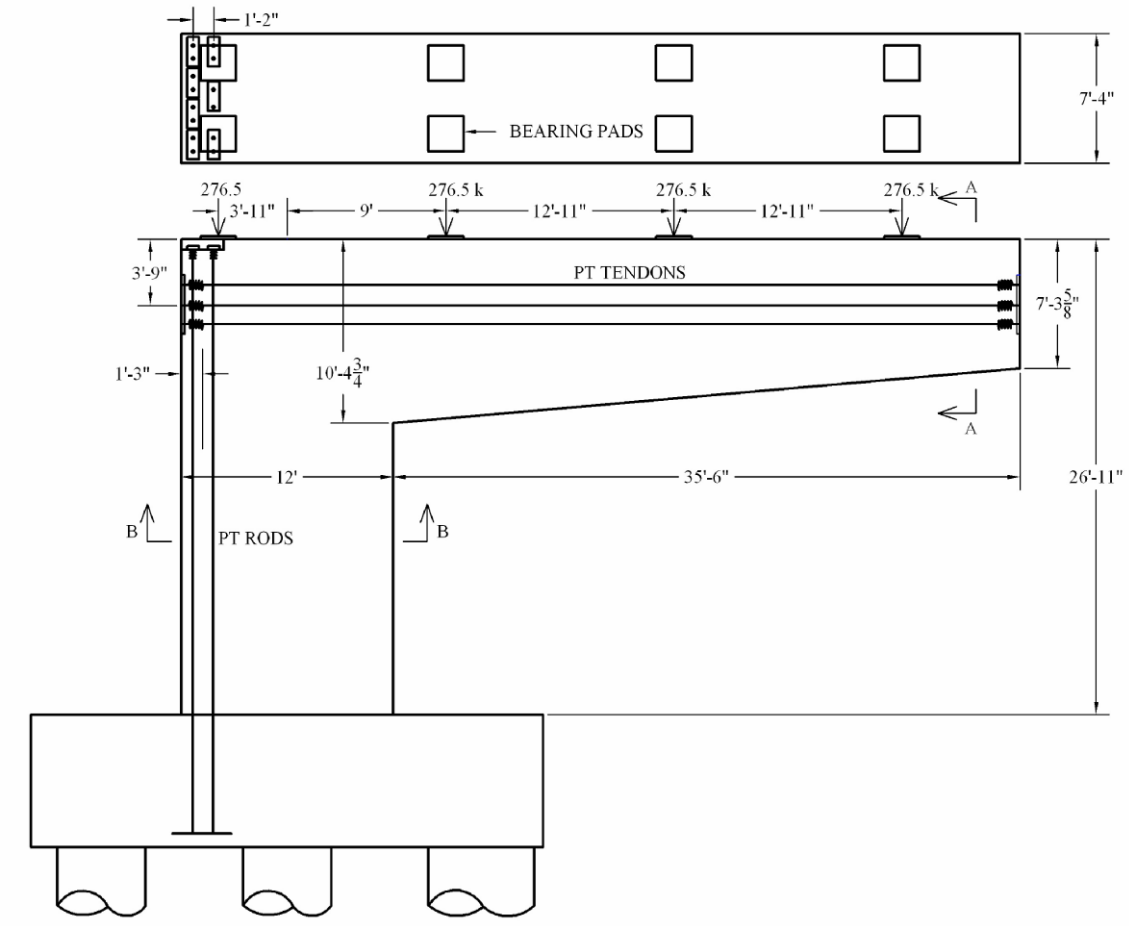

Figure A-1: Dimensions of column and cantilever.

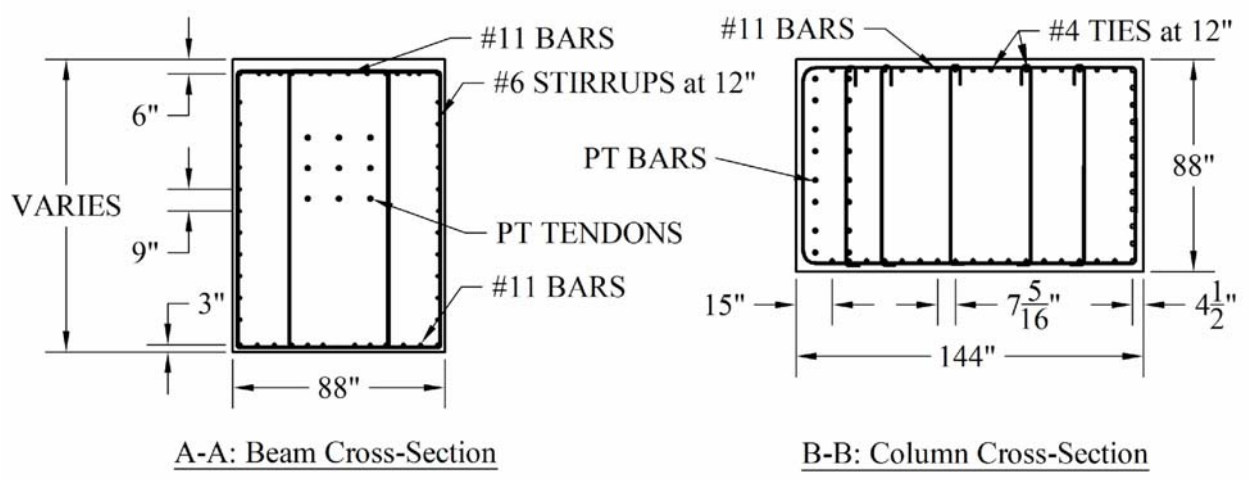

Figure A-2: Cross-section of beam and column referenced in Figure A-1.

Design Values/Assumptions:

- All concrete has f'_c = 5 ksi (assume PT stressing occurs at this value).
- Assumed unit weight of concrete is 150 psf. Using this value, the factored self-weight of the cantilever was approximated with a 12.25 k/ft uniform load across the cantilever. The factored self-weight of the concrete in the joint of the C-bent was calculated to be 164 kips.
- All steel is Grade 60.
- Beam PT tendons comprised of 270 ksi low relaxation strands. Each tendon has an area (A_{ps}) of 1.07 in^2 and is stressed to 189 ksi (203 kips per tendon).
- Column PT bars are 150 ksi high strength bars. Each bar has an area (A_{ps}) of 1.96 in^2 and is stressed to 107 ksi (210 kips per bar).
- For all anchorage zones, the manufacturer specified the confinement length to be 15 in.
- The beam will be post-tensioned first, and the column will be post-tensioned last. For the purposes of this example, it will be assumed that all of the strands/bars in the beam and then the column will be stressed at the same time.
- The cantilever will be supported by falsework during jacking of both the beam and column.
- Bearing pads have dimensions of 24”x 24”x 1”.

Note about the C-Bent Joint Design:

As with many structural members, the joint will be subjected to several different loading cases. For structural members subjected to multiple loading conditions, it is important that a STM be developed for each loading condition. For the C-bent joint example (Example A.2), STMs were developed for three loading cases: for the beam post-tensioning only, for the beam and column post-tensionsing, and for the beam post-tensioning, column post-tensioning, and gravity loads.

Example A.1: Post-Tensioned Anchorage Zone

The post-tensioned anchorage zone in the cantilever beam of the C-bent needs to be designed and detailed according to Section 5.10.9 and 5.6.3 of the AASHTO LRFD Bridge Design Specifications. Nine post-tension cables, each initially jacked to 203 kips, are anchored in the zone. The manufacturer of the anchorage devices designed the local zone to have a length of 15 in. The engineer of record is responsible for designing the general zone (AASHTO LRFD 5.10.9.2.4). The geometry of the anchorage zone can be seen in Figure A.1-1.

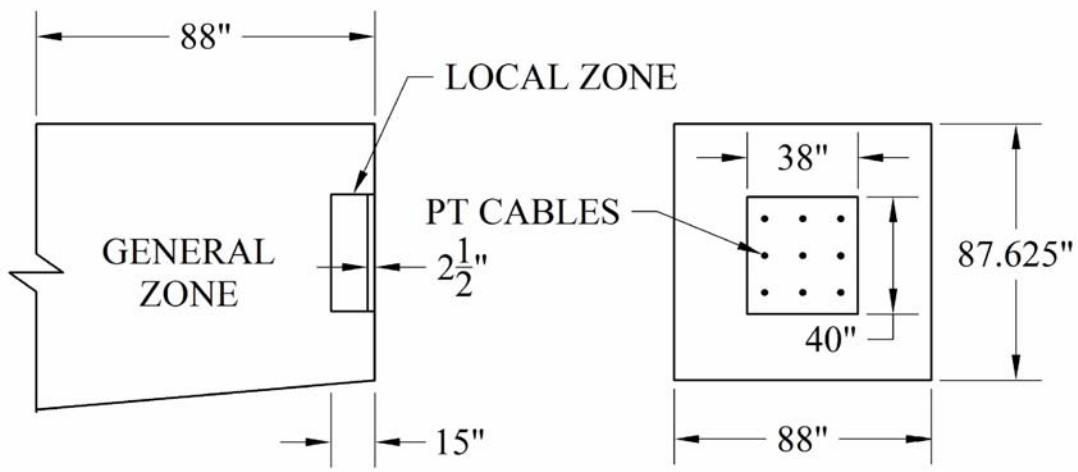

Figure A.1-1: Geometry of P-T Anchorage Zone.

Section 5.10.9.6 of the AASHTO LRFD Bridge Design Specifications allows the use of a simplified approximate analysis and design for anchorage zones meeting certain geometric constraints. The anchorage zone shown in Figure A.1-1 meets the requirements for the simplified analysis and design; however, for the purposes of demonstrating the application of strut-and-tie models to anchorage zones, a general strut-and-tie model approach will be used for this example.

According to AASHTO LRFD 3.4.3.2, the anchorage zone shall be designed for 1.2 times the maximum jacking load. For this anchorage zone:

$$P_u = 1.2 \cdot (9 \cdot 203 kips) = 2192 kips$$

Step 1 – Delineate the D-regions.

The STM to be developed will be designed to transfer the post-tension force from the anchorage to a distance equivalent to the height of the cantilever. The height of the cantilever is approximately 88 in.

Step 2 – Determine the boundary conditions of the D-region.

The stress distribution on the boundary of the D-region will be very close to uniform compression; therefore, it was assumed to be uniform.

Steps 3, 4, and 5 – Sketch the flow of forces, develop a truss model, and solve for member forces.

For the purposes of this design, the steps of sketching the flow of forces and developing a truss model were combined into one step. The STM developed for the anchorage zone can be seen in Figure A.1-2.

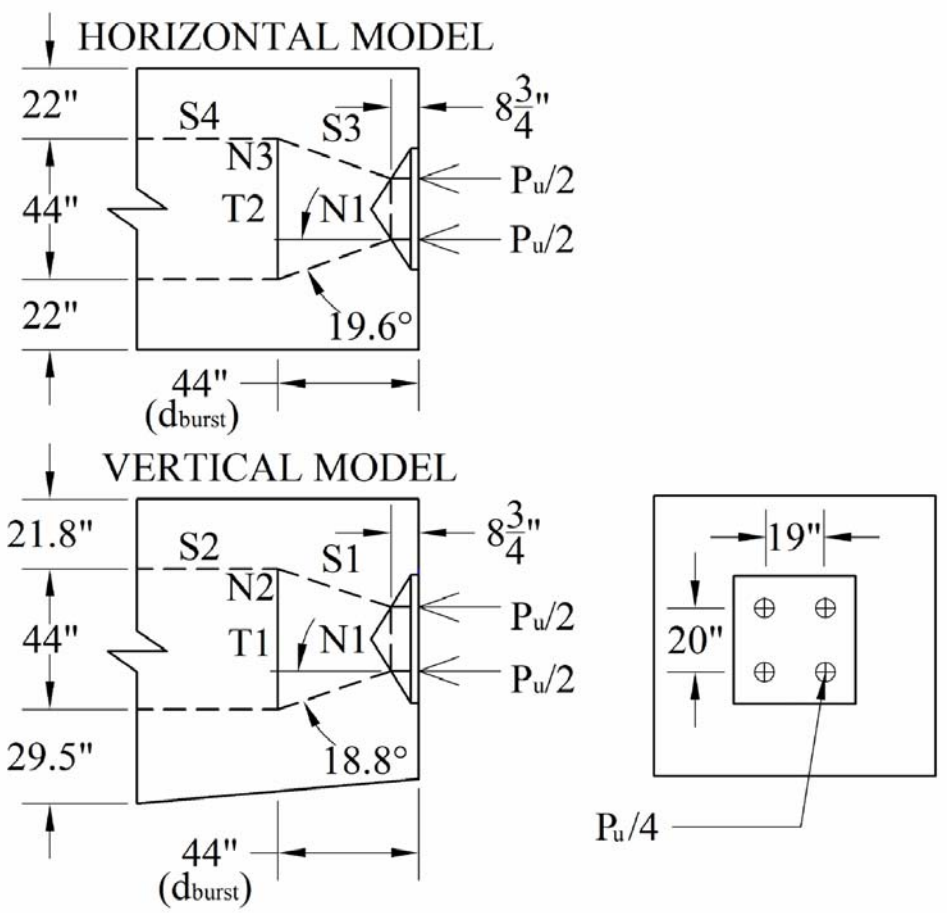

Figure A.1-2: STM developed for anchorage zone.

From Figure A.1-2, in order to model the splitting forces in both the vertical and transverse directions, two STMs were used within the anchorage zone. For each STM, the ties were placed at a distance of approximately half the beam height away from the end face of the cantilever (44”). A designer may choose to locate the ties at a different location; however, the reinforcement chosen to satisfy the tie requirements must be placed within a certain distance of the anchorage (see Step 6 and AASHTO LRFD 5.10.9.3.2). The calculated forces in the struts and ties labeled in Figure A.1-2 are given in Table A.1-1.

Table A.1-1: List of strut and tie forces.

Vertical Model		Horizontal Model	
Member	Force (k)	Member	Force (k)
S1	1158	S3	1164
S2	1096	S4	1096
T1	374	T2	390

Alternatively, a 3-D STM can be used to model the flow of forces through the D-region instead of the two 2-D models used to model the spreading in the horizontal and vertical directions separately.

An example of a 3-D STM that could be used to design the anchorage zone is shown in Figure A.1-3. The geometry of the model is shown in Figure A.1-4 which shows the plan, elevation, and end view of the STM. From the figures, it can be seen that the location of ties T_{1A} and T_{1B} were placed at the same location as tie T1 in the vertical model in Figure A.1-2. Similarly, the location of ties T_{2A} and T_{2B} were placed at the same location as tie T2 in the horizontal model shown in Figure A.1-2.

The calculated member forces for the 3-D STM are shown in Table A.1-2. As can be see when comparing Tables A.1-1 and A.1-2, the sum of the forces in ties T_{1A} and T_{1B} is calculated to be 374 kips which is equal to the force in tie T1 for the vertical model. Similarly, the sum of the forces in ties T_{2A} and T_{2B} is calculated to be 390 kips which is equal to the force in tie T2 in the horizontal model. Based on these observations, in Step 6 of this example, the steel chosen to satisfy the tie requirements of the planar STMs used to model the spreading in both the horizontal and vertical directions (see Figure A.1-2) will be identical to the steel chosen to satisfy the requirements of the 3-D STM.

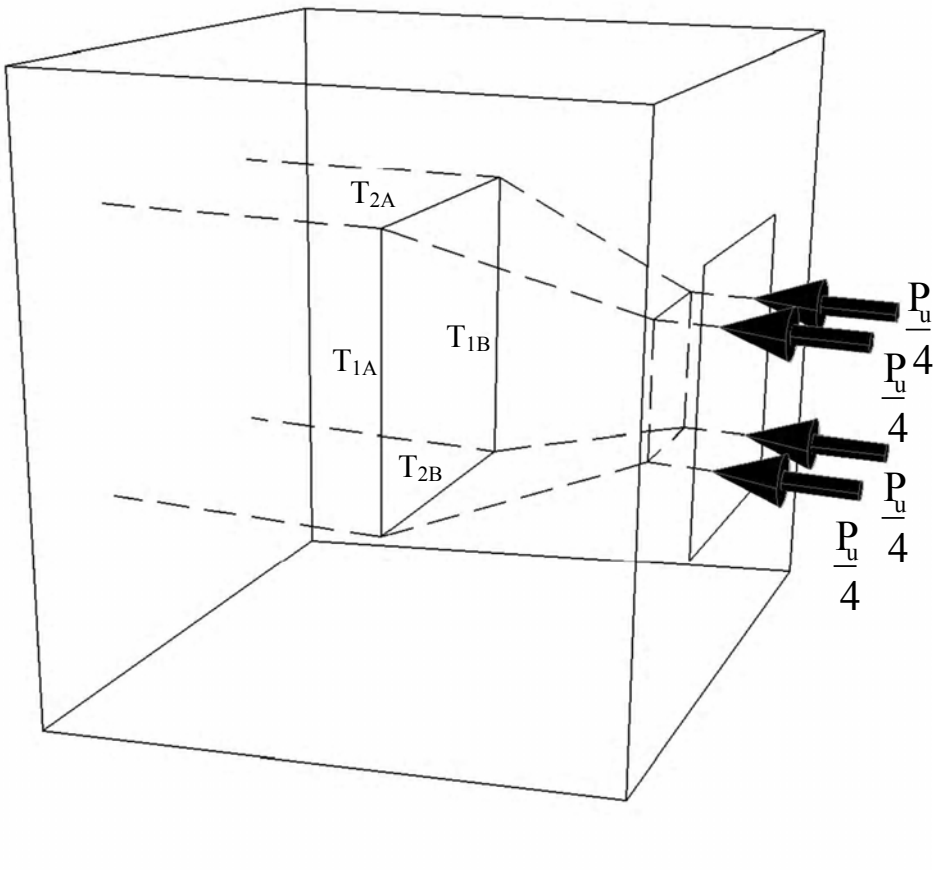

Figure A.1-3: A 3-D STM that could be used to model the anchorage zone.

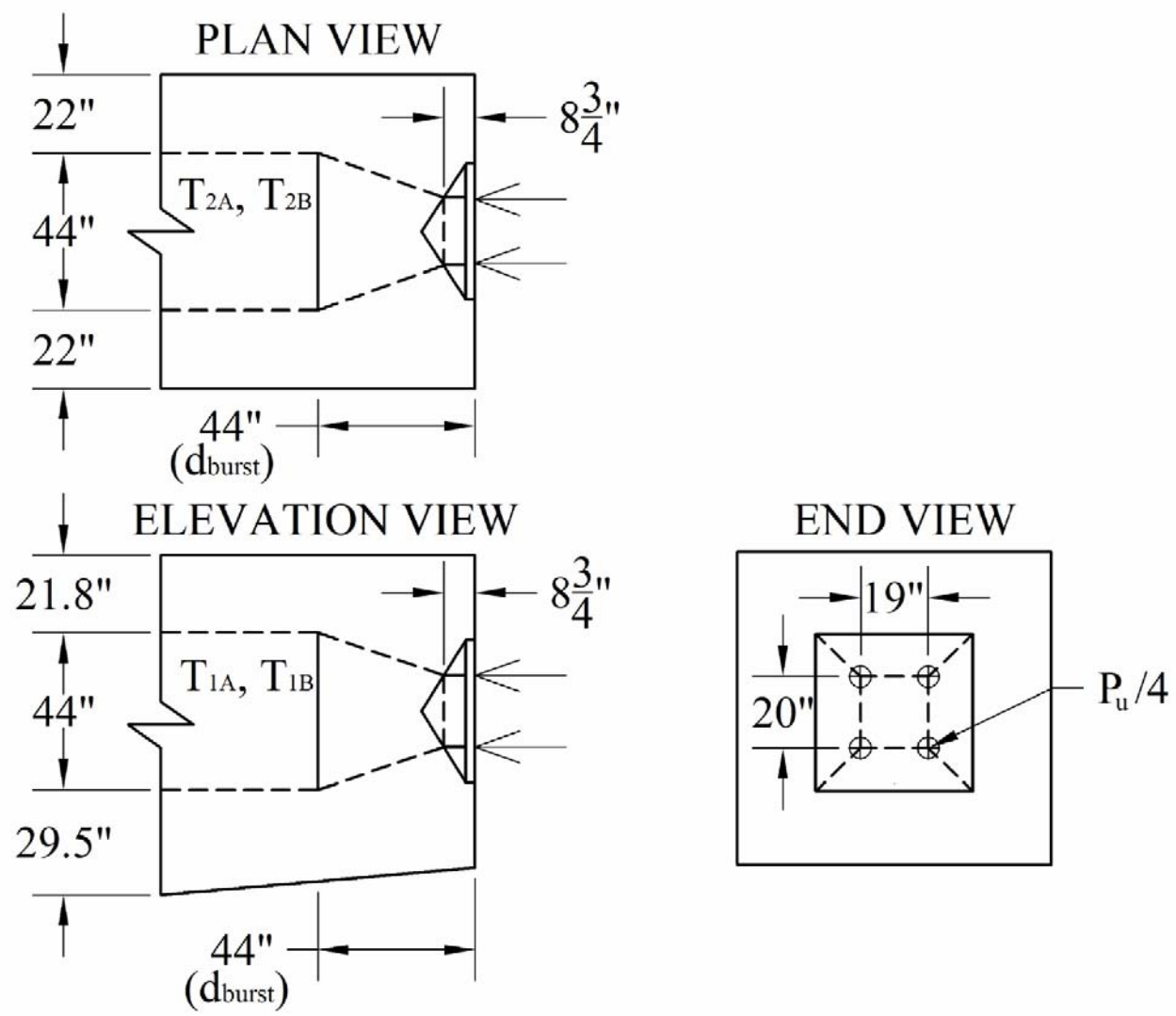

Figure A.1-4: Plan, elevation, and end view of the 3-D STM.

Table A.1-2: Calculated member forces for 3-D STM.

Member	Force (k)
Inclined Struts	611
Horizontal Struts	548
T_{1A}	187
T_{1B}	187
T_{2A}	195
T_{2B}	195

Step 6 – Calculate steel area for the ties.

Based on AASHTO LRFD 5.6.3.4, the area of steel required for each tie can be calculated as follows:

$$A_{stT1} = \frac{T_1}{\phi \cdot f_y} = \frac{374kips}{0.9 \cdot 60ksi} = 6.93in^2$$

$$A_{stT2} = \frac{T_2}{\phi \cdot f_y} = \frac{390kips}{0.9 \cdot 60ksi} = 7.23in^2$$

For each tie, five 4-leg #6 stirrups will satisfy the required area of steel (A_{st} = 8.8in^2). Four-leg stirrups were chosen because the cross-section of the beam is large (88" x 87"). The stirrups must be placed so the centroid of the group of stirrups coincides with the centroid of the tie used in the model. Furthermore, from Section 5.10.9.3.2 of the AASHTO LRFD Bridge Design Specifications, all the stirrups must be placed within the lesser of 2.5d_{burst} and 1.5h (the height of the member). The value d_{burst} is taken to be the distance from the anchorage to the centroid of the tie used in the STM. For this example, 2.5d_{burst} controls; therefore, the stirrups must be placed within 110 in.

In addition, according to AASHTO LRFD 5.10.9.3.2, spalling reinforcement must be placed near the anchorage and must be designed for 2 percent of the total factored tendon force. The required spalling reinforcement is determined as follows:

$$T_{spall} = 0.02 \cdot 2192kips = 44kips$$

$$A_{st,spall} = \frac{T_{spall}}{\phi \cdot f_y} = \frac{44kips}{0.9 \cdot 60ksi} = 0.81in^2$$

The required amount of spalling reinforcement will be accounted for when crack control reinforcement is detailed (See Step 8). The proposed tie reinforcement details are shown in Figure A.1-5.

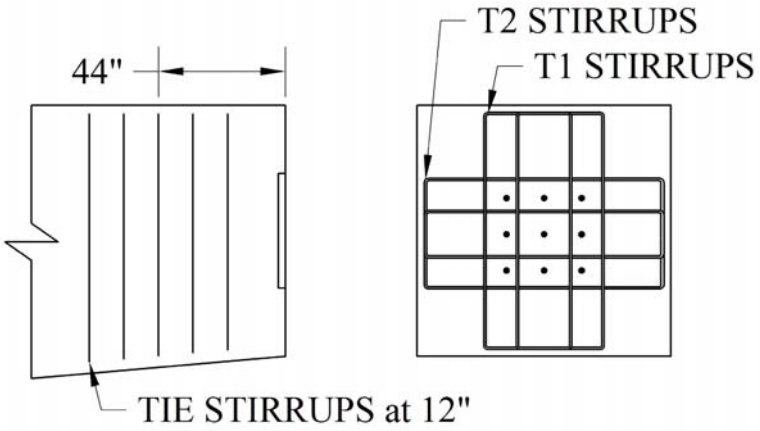

Figure A.1-5: Details of proposed tie reinforcement (#6 stirrups) based on the STM.

Step 7 – Check the capacity of the struts and nodes.

In order to check the capacity of the nodes and struts, the cross-sectional areas at the node/strut interfaces must be estimated. Because of the geometric constraints caused by the four struts extending from rectangular anchorage plate, all of the struts will conservatively be assumed to have triangular cross-sections. In order to estimate the area of the triangular cross-sections, the width and depth of each of the struts must first be determined. The width of the strut is the dimension of the strut in the plane of the STM. The depth of a strut is the dimension of the strut perpendicular to the plane of the STM. See Figure A.1-6 for a visualization of "width" and "depth" of the struts.

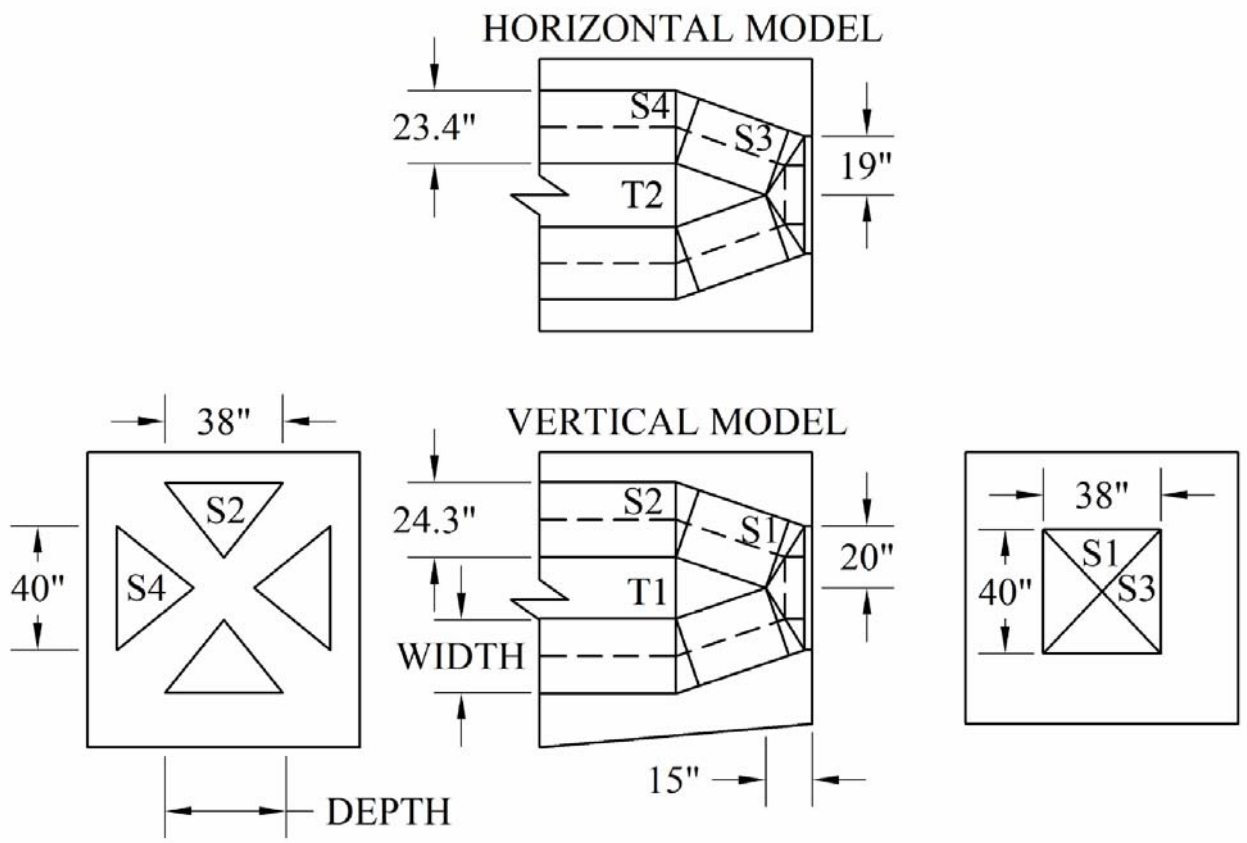

Figure A.1-6: Geometry of struts.

Figure A.1-6 shows how the widths and depths of the struts were determined. First, the center of Node 1 (see Figure A.1-2) was assumed to extend the length of the local zone (15 in.). Next, the strut boundaries were assumed to be parallel to the center of the struts. Finally, using the known and assumed geometries from Figures A.1-2, A.1-5, and A.1-6, the strut widths were calculated. For this example, the strut depths were simply determined from the dimensions of the anchorage plate. Struts in the vertical model were assumed to have depths of 38 in., and struts in the horizontal model were assumed to have depths of 40 in. In other words, the depths of the struts were conservatively assumed not to spread as they travel away from the anchorage. Table A.1-3 states the widths and depths for each of the members.

In Table A.1-3, the listed widths for ties T1 and T2 are based on the total distance between the first and last stirrups plus six times the diameter of the bar away from each end. The values for the ties are given because they are needed for the node capacity check calculations.

Table A.1-3: Strut and tie cross-sectional dimensions.

Vertical Model				Horizontal Model			
Member	Width (in)	Depth (in)	A_{cs} (in^2)	Member	Width (in)	Depth (in)	A_{cs} (in^2)
S1	23.3	38.0	442.7	S3	22.2	40.0	444.0
S2	24.3	38.0	461.7	S4	23.4	40.0	468.0
T1	57.0	38.0	1083.0	T2	57.0	40.0	1140.0

Once the areas of the struts were determined, the capacities of the struts were checked according to Section 5.6.3.3.3 of the AASHTO LRFD. In order to determine the capacity of each strut, four calculations were made. First, the strain in the adjoining tie (ε_s) must be calculated. To estimate the strain in the tie stirrups, use:

$$\varepsilon_s = \frac{P_{u,Tie}}{A_{st} E_s}$$

After the strain in the tie is determined, the principal tensile strain in the concrete (ε_1) can be calculated.

$$\varepsilon_1 = \varepsilon_s + (\varepsilon_s + 0.002)\cot^2(\alpha_s) \qquad \text{(AASHTO LRFD eq. 5.6.3.3.3-2)}$$

The limiting compressive stress (f_{cu}) in the tie can now be calculated.

$$f_{cu} = \frac{f'_c}{0.8 + 170\varepsilon_1} \le 0.85 f'_c \qquad \text{(AASHTO LRFD eq. 5.6.3.3.3-1)}$$

Finally, the capacity of the strut can be calculated by multiplying the limiting compressive stress with the smaller of the strut areas at the nodes.

$$\phi P_n = \phi f_{cu} A_{cs} \qquad \text{(AASHTO LRFD 5.6.3.3.1-1)}$$

For compression in a STM, ϕ is taken as 0.70 (AASHTO LRFD 5.5.4.2.1). Table A.1-4 summarizes the calculations performed for each of the struts. All of the struts were found to have sufficient capacity. It should be noted that, for all of the struts, the maximum value of $0.85f'_c$ governed for all of the calculated strut limiting compressive stresses shown in Table A.1-4.

Table A.1-4: Summary of strut calculations. From Step 6, 8.8 in^2 of steel was provided for each tie.

Strut	P_u (k)	Tie	Tie Force (k)	α_s (degrees)	ε_s	ε_1	f_{cu}	ΦP_n (k)	$\Phi P_n > P_u$?
Strut 1	1158	T1	374	71.2	0.000733	0.001049	4.25	1317	yes
Strut 2	1096	T1	374	90.0	0.000733	0.000733	4.25	1374	yes
Strut 3	1164	T2	390	70.4	0.000764	0.001115	4.25	1321	yes
Strut 4	1096	T2	390	90.0	0.000764	0.000764	4.25	1392	yes

In addition to the strut capacity check calculation, the capacities of the nodes need to be checked for the forces imposed by the anchored ties and at node/strut interfaces where the strut capacity was determined to be larger than the node capacity. Table A.1-5 summarizes the locations where node/strut interfaces need to be checked (where calculated strut capacities are larger than allowable node capacities). According to AASHTO LRFD 5.6.3.5, the limiting compressive stresses are $0.85f'_c$, $0.75f'_c$, and $0.65f'_c$ for CCC, CCT, and CTT nodes, respectively.

Table A.1-5: Summary of determining whether strut capacities exceed node capacities.

Strut	Strut f_{cu} (ksi)	Nodes	Node Type	Node f_{cu} (ksi)	Check Node/Strut Interface?
Strut 1	4.25	Node 1	CCC	4.25	no
	4.25	Node 2	CCT	3.75	yes
Strut 2	4.25	Node 2	CCT	3.75	yes
Strut 3	4.25	Node 1	CCC	4.25	no
	4.25	Node 3	CCT	3.75	yes
Strut 4	4.25	Node 3	CCT	3.75	yes

Based on Table A.1-5, the capacities of Nodes 2 and 3 were checked for forces at critical node/strut interfaces. In addition, the capacities of Nodes 2 and 3 were checked for forces imposed by anchored ties. The capacity of each node was determined by multiplying the limiting compressive stress in the node with the area of the node face to be checked. The concrete areas, A_{cs}, for each node interface were determined in Table A.1-3. Table A.1-6 summarizes the node capacity check calculations. All of the node interfaces in question were found to have sufficient capacity.

Table A.1-6: Summary of node capacity check calculations.

Node	Type	f_{cu} (ksi)	Adjoining Member	A_{cs} (in^2)	P_u (k)	ΦP_n (k)	$\Phi P_n > P_u$?
Node 2	CCT	3.75	Strut 1	442.7	1158	1162	yes
		3.75	Strut 2	461.7	1096	1212	yes
		3.75	Tie 1	1083.0	374	2843	yes
Node 3	CCT	3.75	Strut 3	444.0	1164	1166	yes
		3.75	Strut 4	468.0	1096	1229	yes
		3.75	Tie 2	1140.0	390	2993	yes

An alternative approach to checking capacity of struts and nodes would be to check the general zone/local zone interface.

As stated before, the engineer of record is responsible for the design of the general zone. Typically, the most critical area in the general zone is the location of the load transfer between the local zone and general zone due to the large forces dispersing in a small area of concrete. Therefore, if the capacity of the area of force transfer between the local zone and general zone is found to be sufficient, all the other nodes and struts will be considered to be within acceptable limits. According to AASHTO LRFD 5.10.9.3.1, the factored concrete compressive can be taken as $0.7 \cdot \phi \cdot f'_{ci}$. Figure A.1-7 shows the location of the area to be checked.

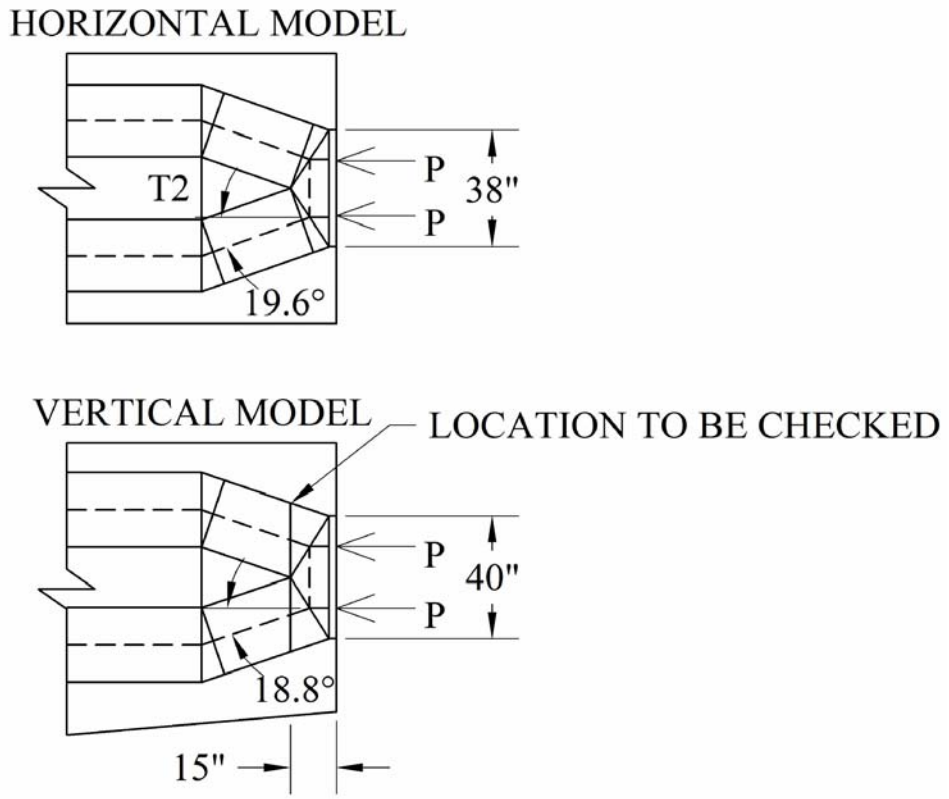

Figure A.1-7: Location of the area to be checked (15 in. from face).

The cross-sectional area of the location will be assumed to be rectangular and must be determined by calculating the effective width, w_{eff} (from the vertical model), and depth, d_{eff} (from the horizontal model), at the location.

$$w_{eff} = 40 + 2 \cdot \left[15 \cdot \tan(18.8^o)\right] = 50.2in$$

$$d_{eff} = 38 + 2 \cdot \left[15 \cdot \tan(19.6^o)\right] = 48.7in$$

$$A_{eff} = (50.2in) \cdot (48.7in) = 2444in^2$$

The capacity of the location can now be calculated as follows:

$$\phi P_n = 0.7 \cdot \phi \cdot f'_c \cdot A_{eff} = 0.7 \cdot 0.7 \cdot 5ksi \cdot 2444in^2 = 5987kips$$

$$\phi P_n \geq P_u = 2192kips$$

The compressive capacity of the area that transfers the load from the local zone to the general zone has been shown to be adequate for the maximum factored load from the anchorage.

Step 8 – Check the detailing for the anchorage of the ties and crack control.

The stirrups chosen for the tie reinforcement have to be detailed to coexist with longitudinal and shear reinforcement determined from the cantilever design (See Figure A-2). The shear reinforcement required from the cantilever beam design will be checked to see if it meets the requirements for crack control per AASHTO LRFD 5.6.3.6. For the vertical crack control, if the spacing of 12 inches is to be maintained for the stirrups, the required area of the crack control reinforcement can be determined as follows:

$$A_{st,crack} = 0.003 \cdot s \cdot b = 0.003 \cdot 12in \cdot 88in = 3.17in^2$$

In order to achieve the required amount of crack control, the vertical stirrups in the post-tensioned anchorage will be changed to 8-leg #6 stirrups. Four-leg stirrups spaced at 6 in. could have been used instead; however, the 8-leg stirrups were deemed desirable due to the fact that the section is over 7 ft. wide.

For the horizontal crack control, if a spacing of nine inches is to be maintained based on the cantilever beam skin reinforcement (see Figure A-2), the required area of crack control is calculated to be:

$$A_{st,crack} = 0.003 \cdot s \cdot b = 0.003 \cdot 9in \cdot 88in = 2.38in^2$$

Based on this, #8 bars can be attached to the outside stirrups and #6 bars can be attached to one of the inner stirrups (See Figure A.1-8).

At the cantilever face that anchors the post-tensioning cables, an orthogonal grid of reinforcement must be designed to meet the larger of the spalling requirement calculated in Step 6 of this example ($A_{st,spall} = 0.40in^2$ in each direction) and the required amount of crack control. The grid will be placed 3 in. from the face (5 in. from the last 8-leg #6 stirrup). If a 12 in. by 12 in. grid is assumed (the maximum spacing allowed by Section 5.6.3.6), the required amount of crack control for both the vertical and horizontal direction at this face is calculated as follows:

$$A_{s,crack} = 0.003 \cdot s \cdot b = 0.003 \cdot 12in \cdot 5in = 0.18in^2$$

A 12 in. grid of # 4 bars will be used to satisfy the crack control ($A_{st} = 0.2\ in^2$). It also satisfies the required spalling reinforcement because the sum of all the #4 bars in the grid in each

direction is greater than the calculated required spalling reinforcement (ΣA_{st} = 1.6 in^2 in each direction).

The anchorage details of the stirrups will be assumed to conform to AASHTO LRFD 5.11.2.6.4; therefore, the anchorage details are considered to be satisfactory.

See Figure A.1-8 for the final design detail of the PT anchorage zone (including all reinforcement from the design of the cantilever beam). It should be noted that the crack control provisions heavily influenced the reinforcement layout in the anchorage zone.

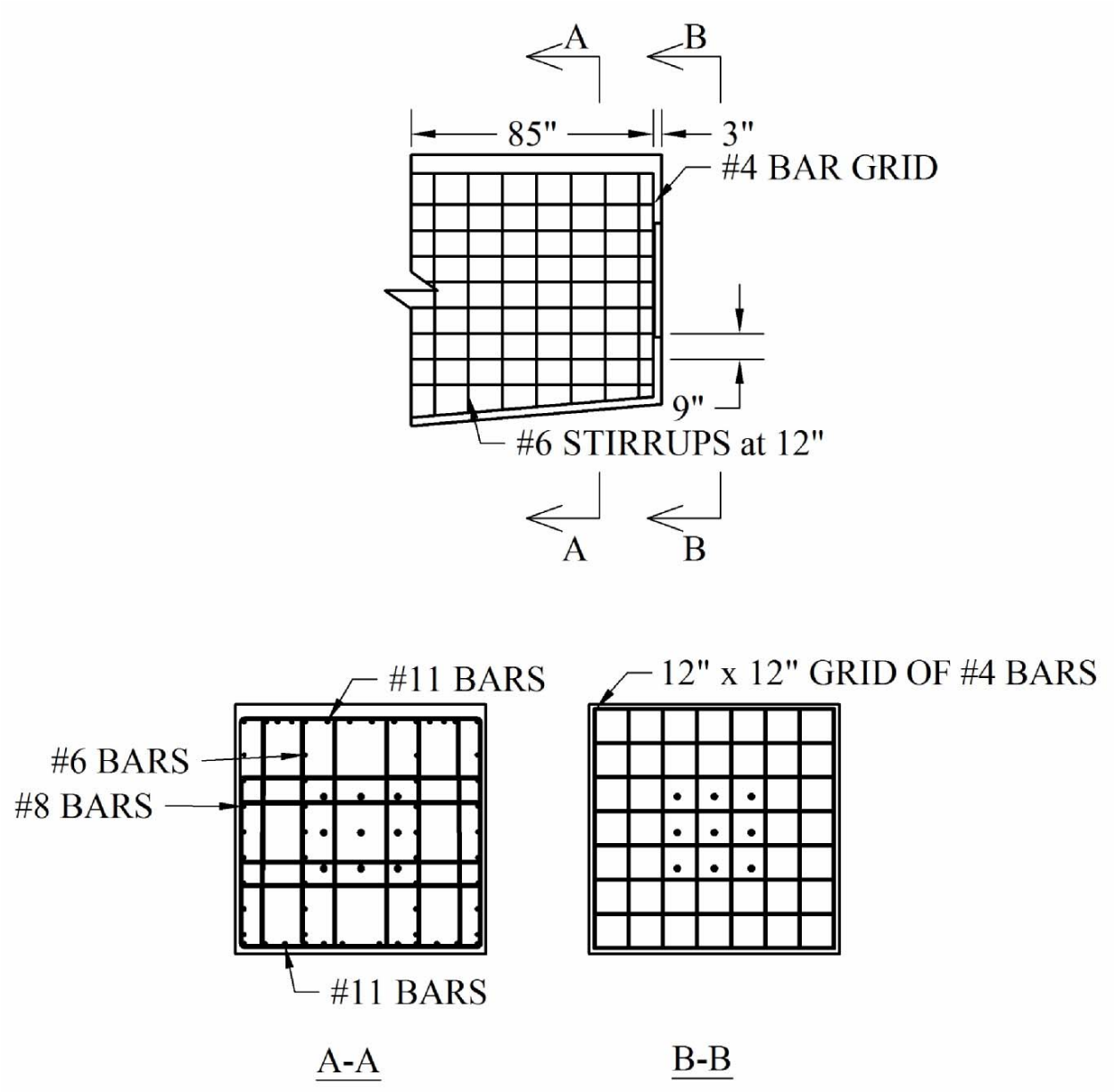

Figure A.1-8: Final details of the post-tensioned anchorage zone.

Example A.2: C-Bent Joint

Because the column and cantilever beam both have post-tensioning passing through the C-bent joint, three STMs must be developed for the C-bent joint to account for the order of the post-tensioning. A STM must be developed for the joint when the beam is first post-tensioned, when the column is post-tensioned after the beam, and when the gravity loading is applied to the bent.

In each of the following examples, the stresses shown on the boundaries of the column and cantilever beam are calculated bending stresses including post-tensioning. For this example, tensile stresses are shown as positive. For all the examples, the bending stresses were calculated as follows:

$$\sigma = \frac{P}{A} + \frac{My}{I}$$

Where: σ = bending stress
P = axial load acting on member
M = moment acting on member
A = cross-sectional area of member
I = gross-area moment of inertia of member
y = distance from center of gravity of member

Example A.2.1: STM for C-Bent Joint for Cantilever Post-Tensioning

The design load for the force in the anchorage at jacking is calculated as follows:

$$P_u = 1.2 \cdot (9 \cdot 203 kips) = 2192 kips \qquad \text{(AASHTO LRFD 3.4.3.2)}$$

Step 1 – Delineate the D-regions.

The post-tensioning anchorage forces cause a D-region that will be considered to extend approximately the height of the joint away from the anchorage face. For simplicity, the STM will be developed to model the transfer of forces from the left face of the column into the beam. The width of the column is 144 in. which is slightly larger than the height of the section. See Figure A.2.1-1 to view the region.

Step 2 – Determine the boundary conditions of the D-region.

The stress distribution on the boundary of the joint and the cantilever due to the post-tensioning force is shown in Figure A.2.1-1. Equivalent point loads based on the stress distribution are also shown in Figure A.2.1-1. The magnitude of each equivalent point load was assumed to be 1096 kips (half of the post-tension design load). The location of the equivalent point loads were then determined based on the assumed magnitudes of the equivalent point loads. This is done by determining which portion of the stress distribution diagram contributes to each of the equivalent point loads, and then, finding the centroid of the contributing portion of the diagram for each equivalent point load. In Figure A.2.1-1, the equivalent point loads are placed at the centroids of the stress distributions between “a” and “c” and “c” and “b”.

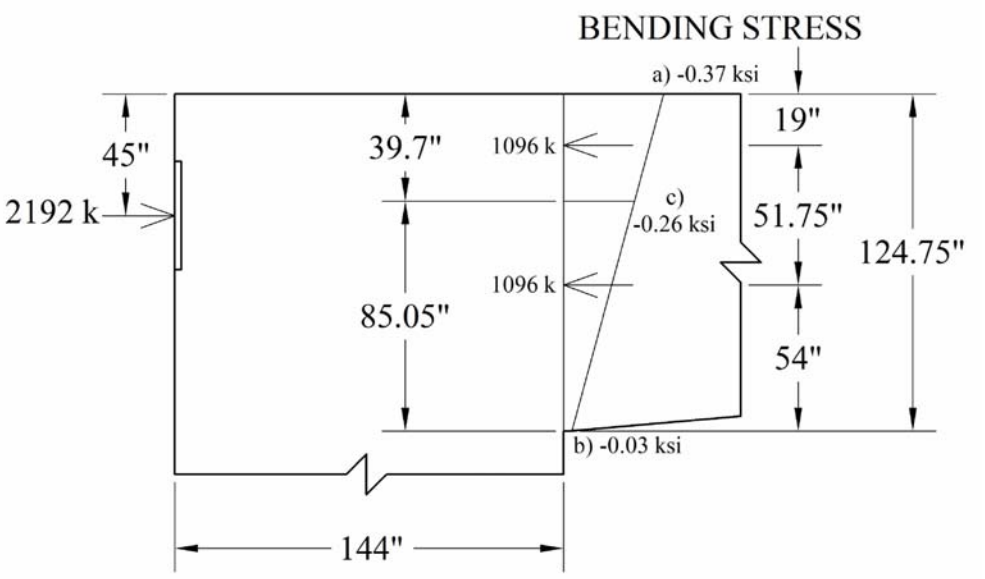

Figure A.2.1-1: Boundary condition of D-region.

Step 3, 4, and 5 – Sketch the flow of forces, develop a truss model, and solve for member forces.

Because the boundary remains in compression, the spreading of the post-tensioning force will be modeled with the same basic STM used for Example A.1. See Example A.1 for a more detailed explanation of calculations. Figure A.2.1-2 shows the STM model to be used.

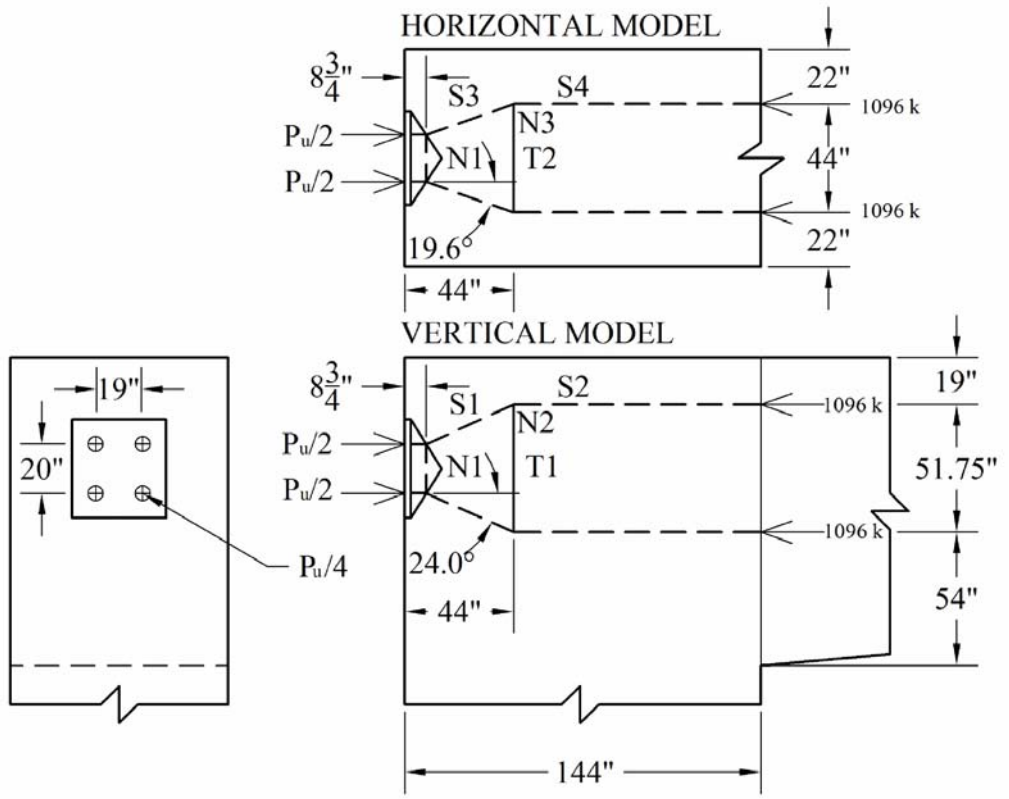

Figure A.2.1-2: STM for post-tensioned anchorage forces.

The calculated member forces are given in Table A.2.1-1 (see Figure A.2.1-2 for the STM member labels).

Table A.2.1-1: Calculated member forces.

Vertical Model		Horizontal Model	
Member	Force (k)	Member	Force (k)
S1	1200	S3	1164
S2	1096	S4	1096
T1	488	T2	390

Step 6 – Select steel area for the ties.

Table A.2.1-2 summarizes the tie calculations and the stirrups chosen to satisfy the steel requirements. See Step 6 in Example A.1 for an explanation of the calculations. See Figure A.2.1-3 to see the placement of the reinforcement. The stirrups chosen to satisfy the tie requirements were placed to match the spacing of the longitudinal bars extending from the column. The columns longitudinal bars are spaced at 7.3 in.

Table A.2.1-2: Summary of tie calculations.

Tie	Tie Force (k)	$A_{st,required}$ (in^2)	Choose	$A_{st,provied}$ (in^2)
T1	488.0	9.04	9 - 4-leg #5 stirrups	11.16
T2	390	7.22	9 - #6 stirrups	7.92

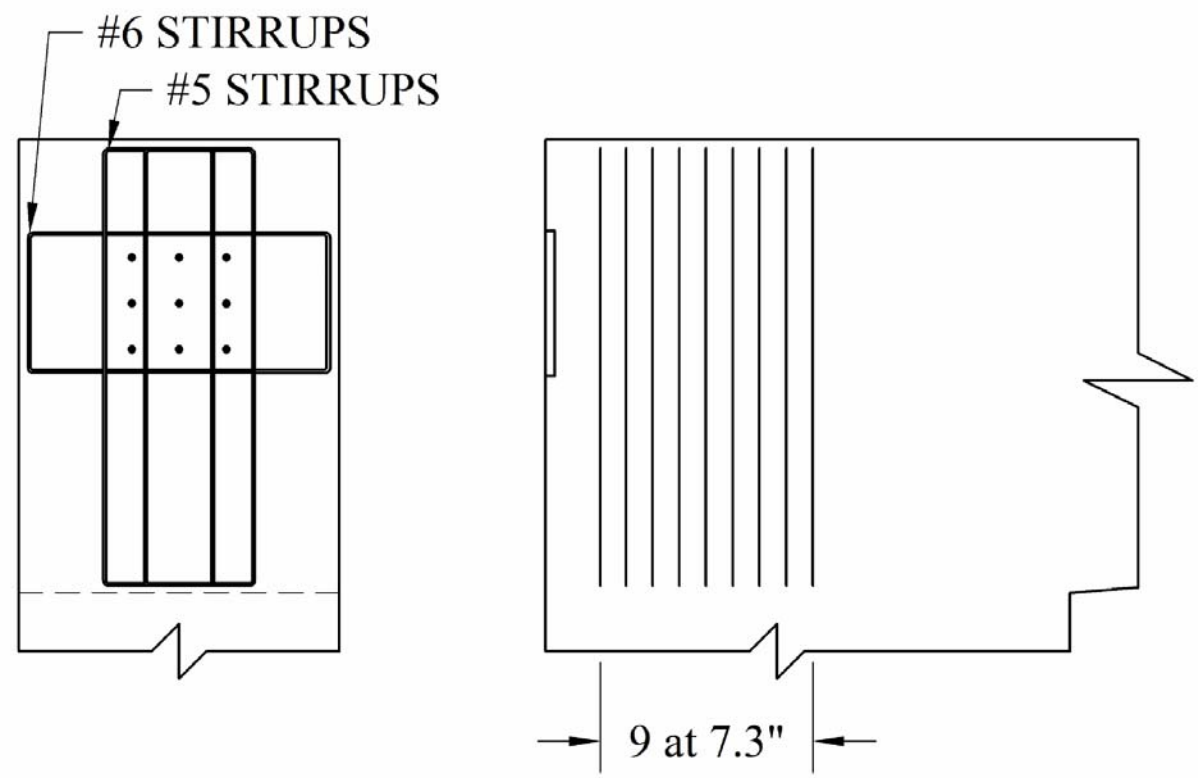

Figure A.2.1-3: Placement of stirrups to match spacing of longitudinal bars.

Also, in addition to the tie reinforcement, at least 0.81 in^2 of spalling reinforcement must be placed at the face that harbors the anchorage (AASHTO LRFD 5.10.9.3.2). This spalling reinforcement requirement will be met when crack control reinforcement is detailed in Example A.2.3.

Step 7 – Check the capacity of the struts and nodes.

To verify the compressive capacity of the concrete in the anchorage zone, the local zone/general zone interface capacity will be checked. Example A.1 outlines this procedure. Figure A.2.1-4 shows the location to be checked.

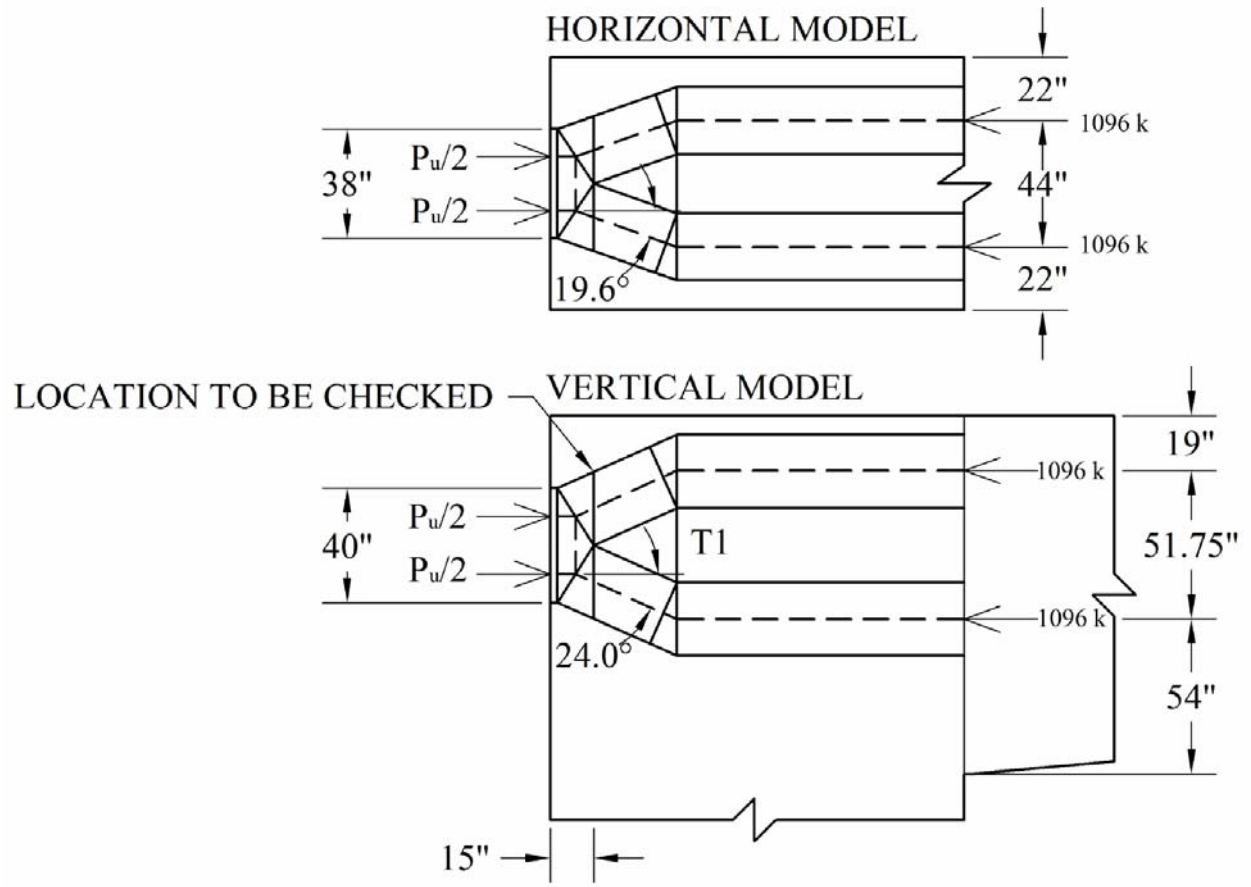

Figure A.2.1-4: Location of the area to be checked (15 in. from face).

The cross-sectional area of the location will be assumed to be rectangular and must be determined by calculating the effective width, w_{eff} (from the vertical model), and depth, d_{eff} (from the horizontal model) at the location given.

$$w_{eff} = 40 + 2 \cdot \left[15 \cdot \tan(24.0^o)\right] = 53.3in$$

$$d_{eff} = 38 + 2 \cdot \left[15 \cdot \tan(19.6^o)\right] = 48.7in$$

$$A_{eff} = (53.3in) \cdot (48.7in) = 2595in^2$$

The capacity of the location can now be calculated as follows:

$$\phi P_n = 0.7 \cdot \phi \cdot f'_c \cdot A_{eff} = 0.7 \cdot 0.7 \cdot 5ksi \cdot 2595in^2 = 6357kips$$

$$\phi P_n \geq P_u = 2192kips$$

The compressive capacity of the area that transfers the load from the local zone to the general zone has been shown to be adequate for the maximum factored load from the anchorage.

Step 8 – Check the detailing for the anchorage of the ties and crack control.

The crack control reinforcement and the anchorage of the ties in the C-bent joint will be detailed in Example A.2.3.

The anchorage details of the stirrups will be assumed to conform to AASHTO LRFD 5.11.2.6.4; therefore, the anchorage details are considered to be satisfactory.

Example A.2.2: STM for C-Bent Joint for Column (and Cantilever) Post-Tensioning

From Example A.1 and A.2.1, the design force from the beam post-tensioning is 2192 kips. The design force for the column post-tensioning is calculated as follows:

$$P_u = 1.2 \cdot (16 \cdot 210 kips) = 4032 kips \qquad \text{(AASHTO LRFD 3.4.3.2)}$$

Step 1 – Delineate the D-regions.

Similar to Example A.2.1, the post-tension anchorage forces cause a D-region that will be considered to extend approximately the height of the joint away from each of the anchorage faces. For simplicity, the STM will be developed to model the transfer of forces from the left face of the column that anchors the beam post-tensioning into the beam (a distance of 144 in.). For consistency, it will also be assumed that the D-region also extends 144 in. away from the column post-tensioning anchorage. See Figure A.2.2-1.

Step 2 – Determine the boundary conditions of the D-region.

Figure A.2.2-1 shows the calculated stress distribution on the boundaries of the C-bent induced by the post-tensioning forces from the column and the beam. Also, in Figure A.2.2-1, the stress distribution has been converted into a set of equivalent point loads on each boundary. As discussed in Example A.2.1-1, the location of each of the point loads was determined by finding the centroid of the portion of the stress distribution that contributes to each of the point loads.

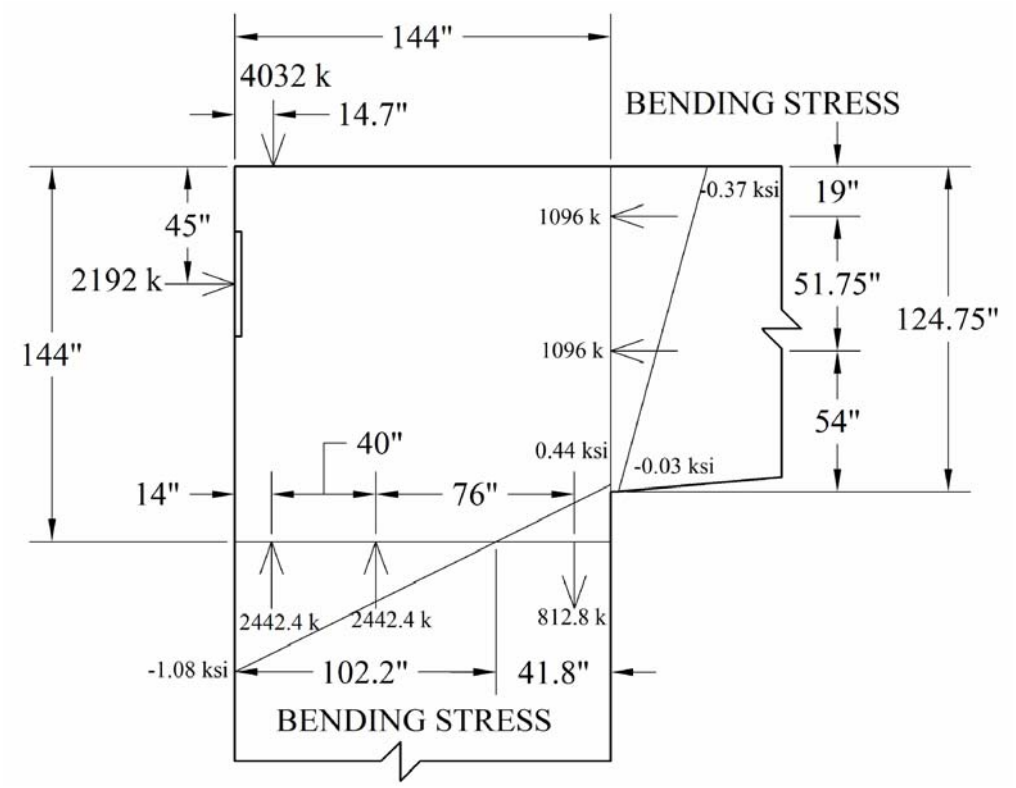

Figure A.2.2-1: Stress distribution and equivalent point loads on D-region boundaries.

Step 3 – Sketch the flow of forces.

In order to help visualize the flow of forces through the C-bent joint, several possible truss models were sketched. Typically, the best model will allow for the most direct transfer of forces across the D-region. Figure A.2.2-2 shows a STM that was deemed suitable to accommodate force transfer in the C-bent joint. In Figure A.2.2-2, the struts extending from both of the post-tensioned anchorage zones cross in front of the post-tensioned anchorage zone of the beam creating four nodes in a very confined area. Typically, placing nodes very close together should be avoided because it becomes difficult to develop strut geometry. For this example, however, the closely spaced nodes in front of the post-tensioned anchorage zone of the beam are shown as "point" nodes that will be incorporated into a larger, more realistic node. The geometry of struts and nodes can be seen in Figure A.2.2-3 in Steps 4 and 5 of this example which discuss the development of the STM based on this step.

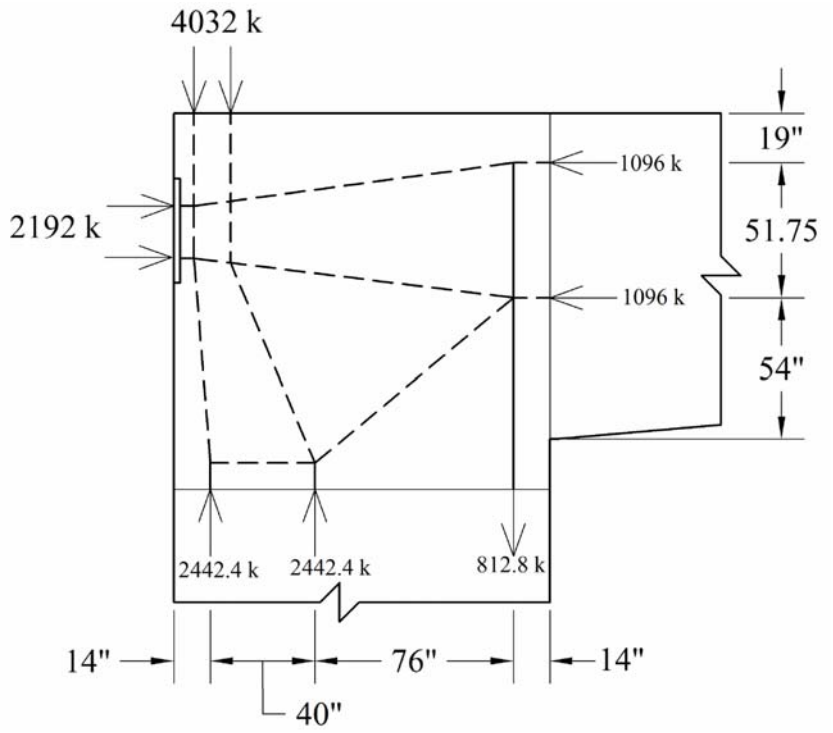

Figure A.2.2-2: Sketch of proposed STM.

Step 4 and 5 – Develop a truss model and solve for member forces.

Based on the proposed STM in Figure A.2.2-2, a detailed STM was developed (see Figure A.2.2-3). All struts, ties, and nodes are labeled in the figure. A description of each of the members in the model can be found in Table A.2.2-1. Table A.2.2-1 includes the inclination of the member (smallest angle from horizontal line), the smallest width of the member, the smallest depth of the member, and the force in the member. The width of a member is the dimension of the strut in the plane of the STM. The depth of a member is the dimension transverse to the plane of the STM.

The widths of the struts in the STM were determined by following some basic rules and assumptions. Because many of the struts in the model are connected to CCC nodes, developing the width of the struts became more complicated because they could not be calculated based on the tie reinforcement configuration. Therefore, many of the strut widths were determined by developing a realistic geometry of the struts as they extend from Node 1. While developing the geometry, three rules were followed: 1.) Struts must be centered with the line of action determined in Figure A.2.2-2; 2.) Struts can not overlap; and 3.) Struts can not extend outside the D-region or beyond $6d_b$ of any adjoined bar (if applicable).

Because the anchorage zone of the beam does not extend the full depth of the D-region, the depth of the struts extending from Node 1 can not be assumed to be constant throughout. On the right side of the D-region, the depth of the struts connected to the ties that will be comprised of longitudinal reinforcement from the column will be equal to the depth of the D-region based on the $6d_b$ rule described in AASHTO LRFD 5.6.3.3.2. To simplify the complex geometry, it has been assumed that the forces spread at a minimum ratio of 2:1 from the beam post-tensioning radially (in other words, in any planar direction). This can be seen in Figure A.2.2-3 for planes in the vertical and horizontal directions. The denoted strut depths in Table A.2.2-1 are the measured depths at the centerline of strut/node interfaces based on the assumed strut spreading. The product of the depth and width of the struts will be used in the strut and node capacity check calculations.

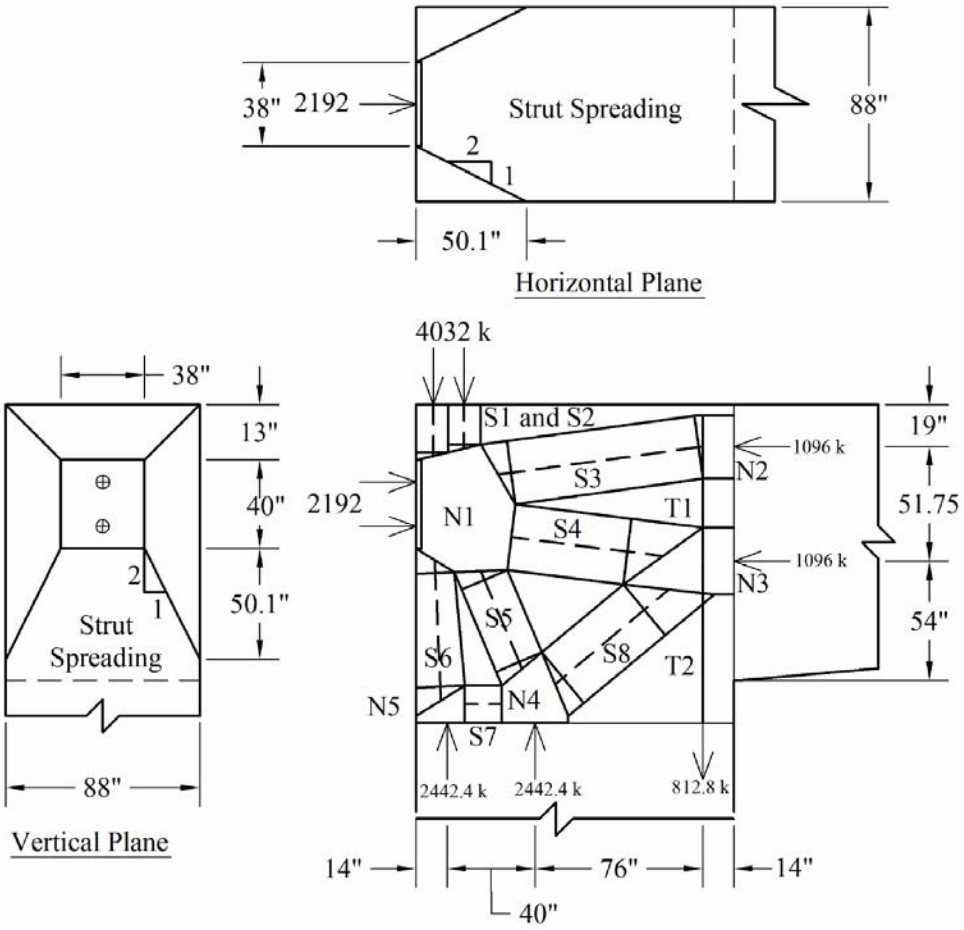

Figure A.2.2-3: Detailed STM developed based on Step 3.

Table A.2.2-1: STM member descriptions.

Member	Angle (degrees)	Width (in)	Depth (in)	Force (k)
Strut 1 + Strut 2	90.0	30.0	53.1	4032
Strut 3	7.7	28.8	72.7	1107
Strut 4	7.0	30.0	78.6	261
Strut 5	67.1	22.4	66.7	1874
Strut 6	87.4	17.4	48.2	2425
Strut 7	0.0	13.8	88.0	110
Strut 8	39.7	29.8	88.0	1090
Tie 1	90.0	to be determined	88.0	149
Tie 2	90.0	to be determined	88.0	813

Step 6 – Select steel areas for the ties.

Section 5.6.3.4 of the AASHTO LRFD Bridge Design Specifications was used to determine the required amount of reinforcement for each tie. The required area of steel in each tie was determined as follows:

$$A_{st,required} = \frac{P_u}{\phi \cdot f_y}$$

For tension in a STM, ϕ is taken as 0.9 (AASHTO LRFD 5.5.4.2.1). Table A.2.2-2 summarizes the tie calculations and the reinforcement chosen to satisfy the required calculated areas. For simplicity, the same reinforcement was chosen for both ties. The reinforcement scheme chosen will utilize longitudinal bars within 28 in. from the face of the column. There are 18 longitudinal bars in this region. Figure A.2.2-4 depicts the placement of the ties. Also, see Figure A-2 to review the details of the longitudinal reinforcement of the column.

Table A.2.2-2: Summary of tie calculations.

Tie	Tie Force (k)	$A_{s,required}$ (in^2)	Choose	$A_{s,provied}$ (in^2)
Tie 1	149	2.8	18-#11 Bars from Column	28.08
Tie 2	813	15.1	18-#11 Bars from Column	28.08

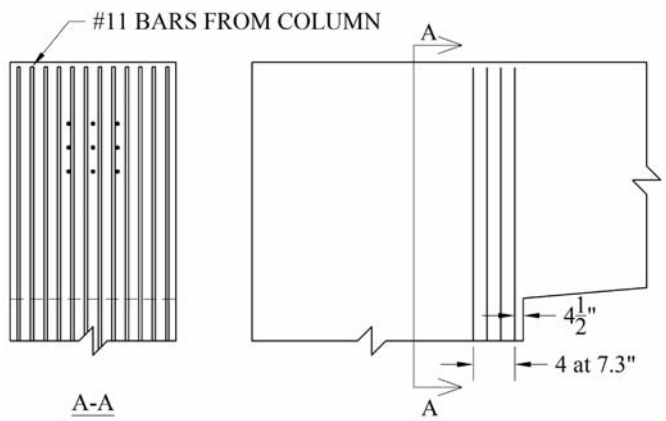

Figure A.2.2-4: Reinforcement provided for Ties 1 and 2.

The required amount of spalling reinforcement near the column post-tensioned anchorage zone will easily be fulfilled by the longitudinal reinforcement that continues from the beam. Spalling reinforcement for the beam anchorage zone has been discussed in Example A.2.1.

Step 7 (a) – Check the capacity of the struts.

The capacities of the struts were checked according to Section 5.6.3.3.3 of the AASHTO LRFD. In order to determine the capacity of each strut, four calculations were made. First, if the strut is adjoined to a CCT Node or a CTT node, the strain in the adjoining ties (ε_s) must be calculated. To estimate the strain in a tie, use:

$$\varepsilon_s = \frac{P_{u,Tie}}{A_{st} E_s}$$

After the strain in the ties is determined, the principal tensile strain in the concrete (ε_1) can be calculated.

$$\varepsilon_1 = \varepsilon_s + (\varepsilon_s + 0.002)\cot^2(\alpha_s) \qquad \text{(AASHTO LRFD eq. 5.6.3.3.3-2)}$$

The limiting compressive stress (f_{cu}) in the tie can now be calculated.

$$f_{cu} = \frac{f'_c}{0.8 + 170\varepsilon_1} \le 0.85 f'_c \qquad \text{(AASHTO LRFD eq. 5.6.3.3.3-1)}$$

Finally, the capacity of the strut can be calculated by multiplying the limiting compressive stress with the smaller of the strut areas at the nodes.

$$\phi P_n = \phi f_{cu} A_{cs} \qquad \text{(AASHTO LRFD 5.6.3.3.1-1)}$$

For compression in a STM, ϕ is taken as 0.70 (AASHTO LRFD 5.5.4.2.1). Table A.2.2-3 summarizes the calculations performed for each of the struts. All of the struts were found to have sufficient capacity.

Table A.2.2-3: Summary of strut calculations.

Strut	A_{cs} (in^2)	P_u (k)	Tie	α_s (degrees)	ε_s	ε_1	f_{cu} (ksi)	ΦP_n (k)	$\Phi P_n > P_u$?
Strut 1 and 2	1593.0	4032	N/A	N/A	N/A	N/A	4.25	4739	yes
Strut 3	2093.8	1107	Tie 1	82.3	0.00032	0.00036	4.25	6229	yes
Strut 4	2358.0	261	Tie 2	83.0	0.00175	0.00181	4.25	7015	yes
Strut 5	1494.1	1874	N/A	N/A	N/A	N/A	4.25	4445	yes
Strut 6	872.4	2425	N/A	N/A	N/A	N/A	4.25	2595	yes
Strut 7	1214.4	110	N/A	N/A	N/A	N/A	4.25	3613	yes
Strut 8	2622.4	1090	Tie2	50.3	0.00175	0.00434	3.25	5969	yes

Step 7(b) – Check the capacity of the nodes.

The capacities of the nodes need to be checked for the forces imposed by the anchored ties, at node/strut interfaces where the strut capacity was determined to be larger than the node capacity, and for bearing caused by applied loads or boundary loads. Table A.2.2-4 summarizes the locations where node/strut interfaces need to be checked due to the fact that the limiting compressive stress in the strut was calculated to be larger than the allowable limiting compressive stress in the node. According to AASHTO LRFD 5.6.3.5, the limiting compressive stresses are $0.85f'_c$, $0.75f'_c$, and $0.65f'_c$ for CCC, CCT, and CTT nodes, respectively.

Table A.2.2-4: Summary of determining whether strut capacities exceed node capacities.

Strut	Strut f_{cu} (ksi)	Nodes	Node Type	Node f_{cu} (ksi)	Check Node/Strut Interface?
Strut 1 and 2	4.25	Node 1	CCC	4.25	no
Strut 3	4.25	Node 1	CCC	4.25	no
	4.25	Node 2	CCT	3.75	yes
Strut 4	4.25	Node 1	CCC	4.25	no
	4.25	Node 3	CCT	3.25	yes
Strut 5	4.25	Node 1	CCC	4.25	no
	4.25	Node 4	CCC	4.25	no
Strut 6	4.25	Node 1	CCC	4.25	no
	4.25	Node 5	CCC	4.25	no
Strut 7	4.25	Node 4	CCC	4.25	no
	4.25	Node 5	CCC	4.25	no
Strut 8	3.26	Node 3	CTT	3.25	yes
	3.26	Node 4	CCC	4.25	no

Based on Table A.2.2-4, the capacities of Nodes 1 through 5 were checked for forces from struts at critical node strut/interfaces and for forces imposed by ties and boundary loads. The capacity of each node was determined by multiplying the limiting compressive stress in the node with the concrete area, A_{cs}, of the node face to be checked. The concrete areas, A_{cs}, of the node faces to be checked were determined by finding the product of the width and depth of the node interface (See Step 4 and Table A.2.2-1). Table A.2.2-5 summarizes the node capacity check calculations. All of the node interfaces in question were found to have adequate capacity.

Table A.2.2-5: Summary of node capacity calculations.

Node	Type	f_{cu} (ksi)	Adjoining Member	A_{cs} (in^2)	P_u (k)	ΦP_n (k)	$\Phi P_n > P_u$?
Node 1	CCC	4.25	Beam PT Load	1516.0	2192	4510	yes
Node 2	CCT	3.75	Strut 3	2093.8	1107	5496	yes
	CCT	3.75	Tie 1	2464.0	149	6468	yes
	CCT	3.75	Boundary Load	2508.0	1096	6584	yes
Node 3	CTT	3.25	Strut 4	813.0	261	1850	yes
	CTT	3.25	Strut 8	2622.4	1090	5966	yes
	CTT	3.25	Tie 2 - Tie 1	2464.0	664	5606	yes
	CTT	3.25	Boundary Load	2675.2	1096	6086	yes
Node 4	CCC	4.25	Boundary Load	2648.8	2423	7880	yes
Node 5	CCC	4.25	Boundary Load	1848.0	2423	5498	yes

Step 8 – Check the detailing for the anchorage of the ties and crack control.

The anchorage length of the #11 longitudinal bars needs to be checked at Node 2. Based on the chosen geometry of the node, the available length is 30.5 in (see Figure A.2.2-5). The basic required development length, ℓ_{db}, is calculated to be:

$$\ell_{db} = \frac{1.25 \cdot A_b \cdot f_y}{\sqrt{f'_c}} = \frac{1.25 \cdot 1.56in^2 \cdot 60ksi}{\sqrt{5ksi}} = 52.4in \quad \text{(AASHTO LRFD 5.11.2.1.1)}$$

For Tie 1, the amount of reinforcement provided surpasses the required amount of reinforcement, so the anchorage length can be reduced by the following factor:

$$\frac{A_{st,required}}{A_{st,provided}} = \frac{2.8in^2}{28.08in^2} = 0.01 \quad \text{(AASHTO LRFD 5.11.2.1.3)}$$

Therefore, the required development length is calculated to be:

$$\ell_d = 52.4 \cdot 0.01 = 0.5" \quad \text{(AASHTO LRFD 5.11.2.1.1)}$$

According to AASHTO LRFD 5.11.2.1.1, the tension development length of a straight bar may not be less than 12 in.; therefore, the required development length is 12 in. See Figure A.2.2-5 for a visual representation of the available anchorage length. From Figure A.2.2-5, it is clear that there is more than enough development length supplied at Node 2.

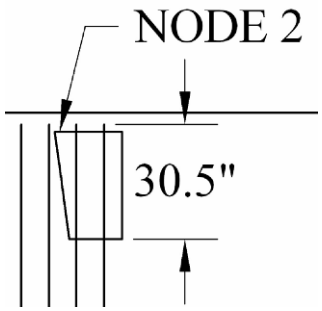

Figure A.2.2-5: Available anchorage length. The required anchorage length is 12 in.

The crack control reinforcement in the C-bent joint will be detailed in Example A.2.3.

Example A.2.3: STM for C-Bent Joint for all Loading

From Examples A.2.1 and A.2.2, the factored design loads for the beam and column post-tensioning are 2192 kips and 4032 kips, respectively. As stated in the initial problem statement, the factored point loads from the superstructure are 276.5 kips each. The self weight of the cantilever and the joint were approximated by assuming the unit weight of the concrete to be 150 lb/ft^3. The factored weight of joint was calculated as follows:

$$W_{joint} = 1.25 \cdot Height \cdot Width \cdot Depth \cdot 150 \frac{lb}{ft^3} = 164 kips$$

The factored distributed dead weight of the cantilever was estimated as follows:

$$w_{cantilever} = 1.25 \cdot \overline{A}_{cross-section} \cdot 150 \frac{lb}{ft^3} = 12.25 \frac{k}{ft}$$

Step 1 – Delineate the D-regions.

See Figure A.2.3-1, to view the C-bent joint region to be designed. The D-region will be assumed to extend a distance equal to the depth of the cantilever beyond the column face. The D-region was not extended into the column because the column has already been designed for the given loading.

Step 2 – Determine the boundary conditions of the D-region.

Figure A.2.3-1 shows the calculated boundary forces on the C-bent joint.

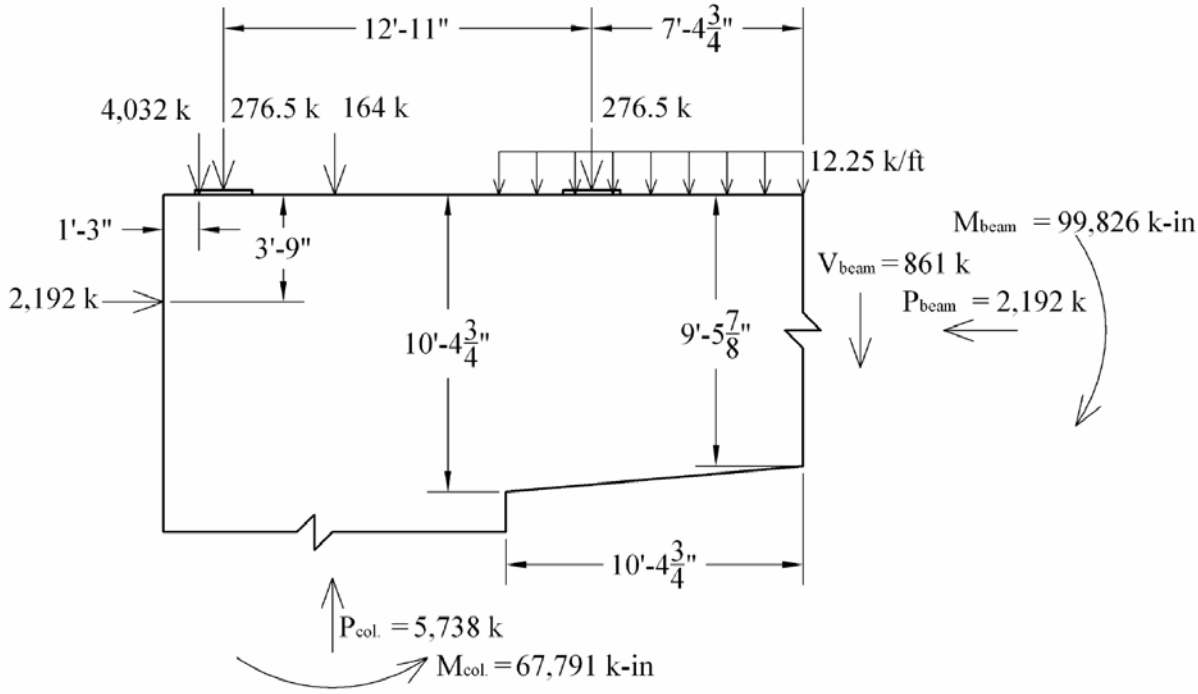

Figure A.2.3-1: Calculated boundary forces.

The calculated boundary forces were converted to stress distributions which can be seen in Figure A.2.3-2. From the bending stress distribution shown in Figure A.2.3-2, it can be noted that the beam is partially prestressed due to the tensile stresses at the top of the beam. Typically, this fact may require a more specialized analysis when designing a beam, but will be ignored for the sake of this example. On the cantilever boundary, the shear force was converted into a shear stress only over the section of the cantilever in compression. The stress distributions were used to calculate equivalent point loads on the boundary. The equivalent shear forces are based on the total shear force contained within the area needed to create each of the 1320 k axial loads. All of

the equivalent point loads can also be seen in Figure A.2.3-2. Also, in Figure A.2.3-2, the additional loads added to the point loads within the D-region represent the self weight of the D-region. The load due to the dead weight of the included portion of the cantilever has been added to the point load in the cantilever (far right point load). The dead weight due to the joint directly above the column has been added to the point load near the column post-tensioning.

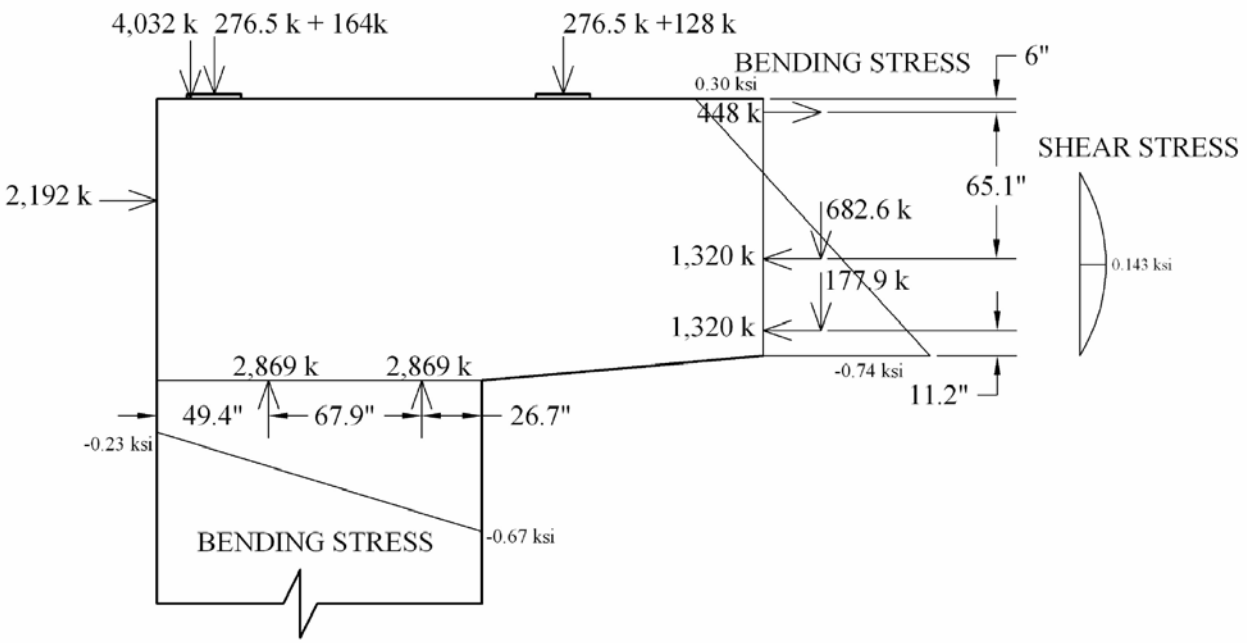

Figure A.2.3-2: Stress distributions and equivalent point loads.

Step 3 – Sketch the flow of forces.

Sketching the flow of forces for this type of region can become complicated. If a designer wishes, he/she can use a finite element computer program that has the capabilities to analyze solid elements to help determine the flow of forces through the C-bent joint. Another alternative is to sketch several STMs that would satisfy static equilibrium within the section. When deciding which model to use, the designer should take into account which model allows for the most direct transfer of forces. Also, any ties in the model should be able to be easily detailed with a realistic reinforcement scheme. Figure A.2.3-3 shows a STM that models the flow of forces through the D-region. In Figure A.2.3-3, the column post-tensioning load and the applied gravity load near the column post-tensioning were combined into one load at the centroid of the column post-tensioning to simplify the model. The equivalent point loads at the right of the model are inclined because of the combination of shear and bending forces.

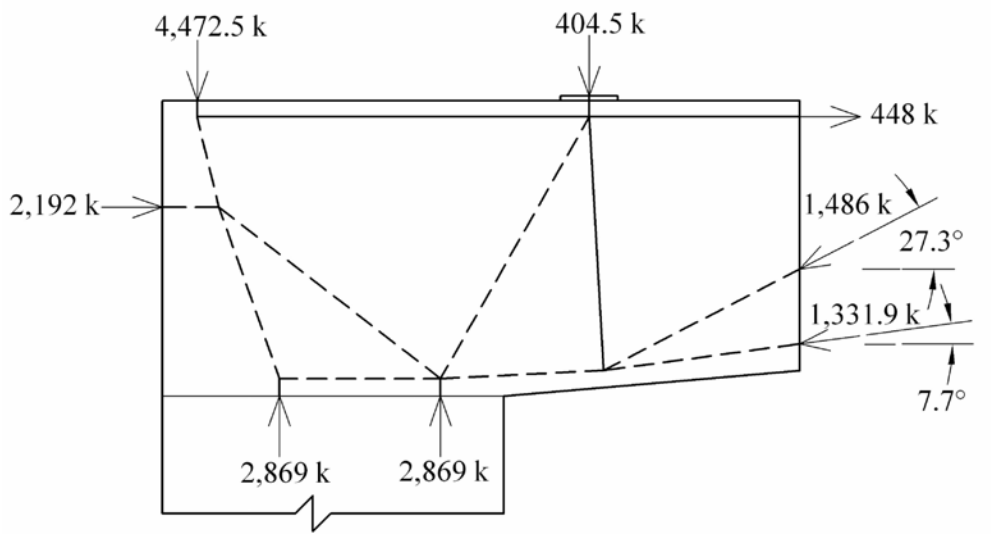

Figure A.2.3-3: STM that models the flow of forces through the C-bent joint.

Steps 4 and 5 – Develop a truss model and solve for the member forces.

Based on Step 3, a STM was developed for the C-bent joint (See Figure A.2.3-4). The struts, ties, and nodes are labeled in the figure. The spreading of the flow of forces was modeled in the same manner as in Example A.2.2.

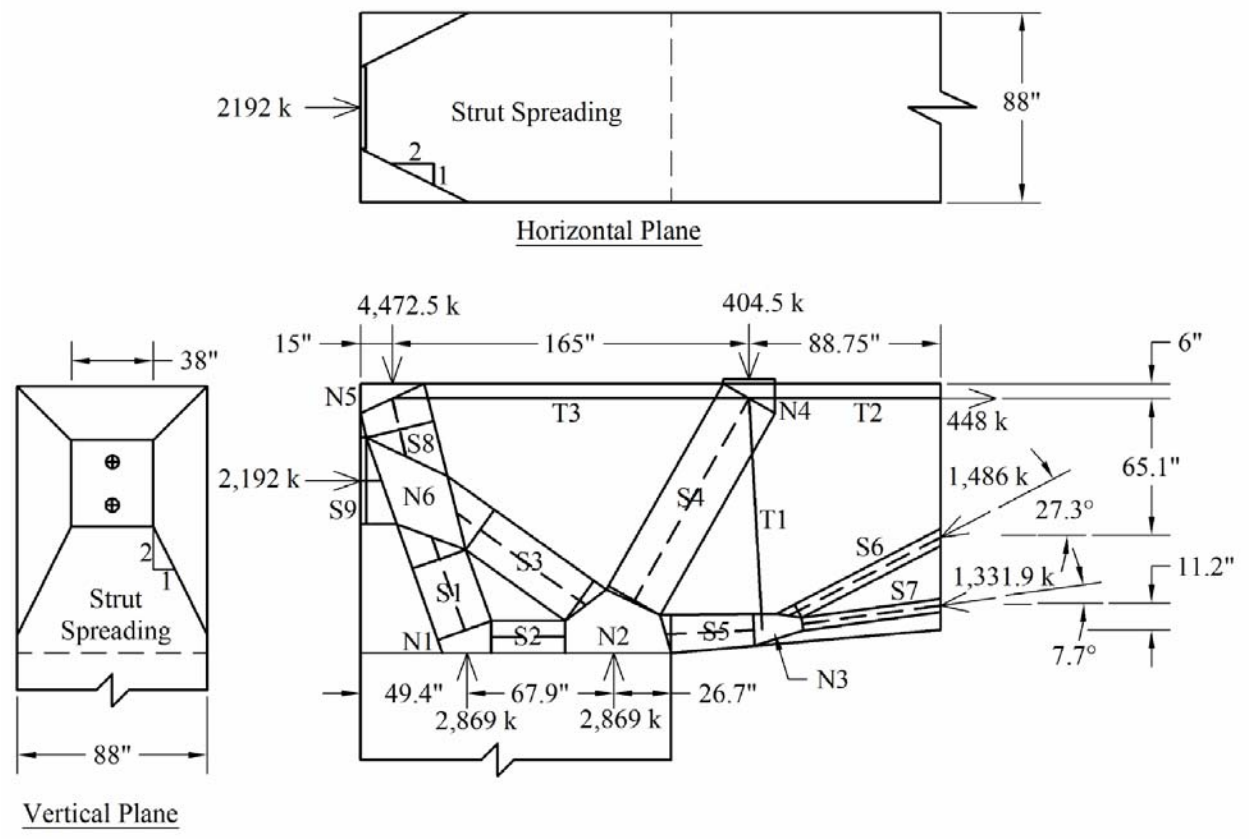

Figure A.2.3-4: STM developed for C-bent joint.

A description of each of the members in the model can be found in Table A.2.3-1. Table A.2.3-1 includes the inclination of the member, the smallest width of the member, the smallest depth of the member, and the force in the member. The width of a member is the dimension of a member in the plane of the STM. The depth of a member is the dimension of a member perpendicular to the plane of the STM. The denoted inclination of the member is the smallest angle from the horizontal. For Ties 2 and 3, the assumed width is based on the assumption that the centroid of the tie coincides with the centroid of the longitudinal tensile reinforcement required for the cantilever beam. The width of Tie 1 can not be determined until the reinforcement for the tie has been designed in Step 6 of this example.

The widths of the struts in the STM were determined by following some basic rules and assumptions outlined in Example A.2.2. Because many of the struts in the model are connected to CCC nodes, developing the width of some of the struts became more complicated because they could not be calculated based on the tie reinforcement configuration. Therefore, many of the strut widths were determined by developing a realistic geometry of the struts as they extend from the Nodes. While developing the geometry, three rules were followed: 1.) Struts must be centered with the line of action determined in Figure A.2.3-3; 2.) Struts can not overlap; and 3.) Struts can not extend outside the D-region or beyond $6d_b$ of any adjoined bar (if applicable).

Because the anchorage zone of the beam does not extend the full depth of the D-region, the depth of the STM can not be assumed to be constant throughout. To simplify the complex geometry, it has been assumed that the forces spread at a minimum ratio of 2:1 from the beam post-tensioning in all directions. This can be seen in Figure A.2.3-4. The denoted strut depths in the Table A.2.3-1 are the smallest measured depths at the centerline of strut/node interfaces based on the assumed strut spreading. The product of the depth and width of the struts will be used in the strut and node capacity check calculations.

It should be noted that the widths and depths of members adjoined to ties will have to be verified after the ties are designed.

Table A.2.3-1: Description of the members in the STM for the C-bent joint.

Member	Angle (degrees)	Width (in)	Depth (in)	Force (k)
Strut 1	70.5	26.0	75.2	3040
Strut 2	0.0	14.9	88.0	1015
Strut 3	35.5	22.9	79.7	2746
Strut 4	60.4	26.9	88.0	233
Strut 5	2.9	16.6	88.0	2573
Strut 6	27.3	7.0	88.0	1486
Strut 7	7.7	6.0	88.0	1332
Strut 8	76.5	32.0	53.7	4808
Strut 9	0.0	40.0	45.1	2192
Tie 1	89.6	to be determined	88.0	672
Tie 2	0.0	12.0	88.0	448
Tie 3	0.0	12.0	88.0	1050

Step 6 – Select steel area for the ties.

Section 5.6.3.4 of the AASHTO LRFD Bridge Design Specifications was used to determine the required amount of reinforcement for each tie (same procedure from Example A.2.2). Table A.2.3-2 summarizes the tie calculations and the reinforcement chosen to satisfy the required calculated areas. For Ties 2 and 3, the longitudinal reinforcement from the cantilever was determined to be suitable. The proposed layout of the tie reinforcement is shown in Figure A.2.3-5.

Table A.2.3-2: Summary of calculations performed to determine reinforcement for ties.

Tie	Tie Force (k)	$A_{st,required}$ (in^2)	Choose	$A_{st,provied}$ (in^2)
Tie 1 (vert)	672	12.4	4-8 legged #6 Stirrups Spaced at 12"	14
Tie 1 (horiz)	4	0.1	Crack Control Reinforcement will Satisfy	-
Tie 2	448	8.3	14-#11 Bars (from cantilever)	21.84
Tie 3	1050	19.4	14-#11 Bars (from cantilever)	21.84

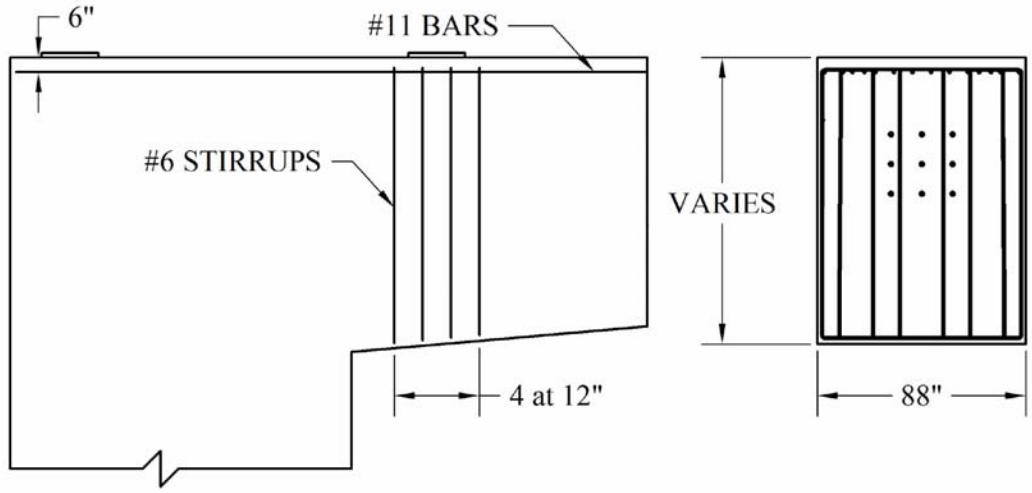

Figure A.2.3-5: Proposed layout of reinforcement to meet the area requirements for Ties 1 through 3.

From Figure A.2.3-5, it is clear that the depths of the struts connected to Tie 1 (Struts 4, 5, 6, and 7) will be the full depth of the member based on the $6d_b$ rule described in AASHTO LRFD 5.6.3.3.2. These depths are consistent with the depths denoted in Table A.2.3-1.

Step 7 (a) – Check the capacity of the struts.

The capacities of the struts were checked according to Section 5.6.3.3.3 of the AASHTO LRFD (same procedure from Example A.2.2). Table A.2.3-3 summarizes the calculations performed for each of the struts. The area was determined from the product of the listed width and depth in Table A.2.3-1. For struts connected to more than one tie, as with Strut 4, the limiting compressive stress in the strut was calculated for the tensile strain in each tie, and the smaller of the two compressive stresses was taken as the limiting compressive stress for the strut. All of the struts were found to have sufficient capacity.

Table A.2.3-3: Summary of strut capacity calculations.

Strut	A_{cs} (in^2)	P_u (k)	Tie	α_s (degrees)	ε_s	ε_1	f_{cu} (ksi)	ΦP_n (k)	$\Phi P_n > P_u$?
Strut 1	1955.2	3059	N/A	N/A	N/A	N/A	4.25	5817	yes
Strut 2	1311.2	1022	N/A	N/A	N/A	N/A	4.25	3901	yes
Strut 3	1825.1	2784	N/A	N/A	N/A	N/A	4.25	5430	yes
Strut 4	2367.2	1301	T3	60.4	0.00166	0.00284	3.90	-	-
	2367.2	1301	T1	29.6	0.00166	0.01300	1.66	2753	yes
Strut 5	1460.8	2648	T1	89.6	0.00166	0.00166	4.25	4346	yes
Strut 6	616.0	1486	T1	62.7	0.00166	0.00263	4.01	1728	yes
Strut 7	528.0	1332	T1	82.3	0.00166	0.00172	4.25	1571	yes
Strut 8	1718.4	4629	T3	76.5	0.00166	0.00187	4.25	5112	yes
Strut 9	1802.8	2205	N/A	N/A	N/A	N/A	4.25	5363	yes

Step 7(b) – Check the capacity of the nodes.

Similar to Example A.2.2, the capacities of the nodes need to be checked for the forces imposed by the anchored ties, at node/strut interfaces where the strut capacity was determined to be larger than the node capacity, and for bearing caused by applied loads or boundary loads. Table A.2.3-4 summarizes the locations where node/strut interfaces need to be checked (where calculated strut limiting compressive stresses exceed allowable node limiting compressive stresses). Once again, according to AASHTO LRFD 5.6.3.5, the limiting compressive stresses are $0.85f'_c$, $0.75f'_c$, and $0.65f'_c$ for CCC, CCT, and CTT nodes, respectively.

Table A.2.3-4: Summary of determining whether strut capacities exceed node capacities.

Strut	Strut f_{cu} (ksi)	Nodes	Node Type	Node f_{cu} (ksi)	Check Node/Strut Interface?
Strut 1	4.25	Node 1	CCC	4.25	no
	4.25	Node 6	CCC	4.25	no
Strut 2	4.25	Node 1	CCC	4.25	no
	4.25	Node 2	CCC	4.25	no
Strut 3	4.25	Node 2	CCC	4.25	no
	4.25	Node 6	CCC	4.25	no
Strut 4	3.90	Node 2	CCC	4.25	no
	3.90	Node 4	CTT	3.25	yes
Strut 5	1.66	Node 2	CCC	4.25	no
	1.66	Node 3	CCT	3.75	no
Strut 6	4.25	Node 3	CCT	3.75	yes
Strut 7	4.01	Node 3	CCT	3.75	yes
Strut 8	4.25	Node 5	CCT	3.75	yes
	4.25	Node 6	CCC	4.25	no
Strut 9	4.25	Node 6	CCC	4.25	no

Based on Table A.2.3-4, the capacities of the nodes were checked for critical node/strut interfaces in addition to forces imposed by anchored ties, applied loads, and boundary loads. As with example A.2.2., the capacity of each node was determined by multiplying the limiting compressive stress in the node with the area of the node face to be checked. The concrete areas, A_{cs}, of the node faces to be checked were determined by finding the product of the width and

depths of the node interface (See Step 4). Table A.2.3-5 summarizes the node capacity check calculations. All of the nodes interfaces were found to have adequate capacity.

Table A.2.3-5: Summary of node capacity calculations.

Node	Type	f_{cu} (ksi)	Adjoining Member	A_{cs} (in^2)	P_u (k)	ΦP_n (k)	$\Phi P_n > P_u$?
Node 1	CCC	4.25	Boundary Load	1997.6	2883	5943	yes
Node 2	CCC	4.25	Boundary Load	4329.6	2883	12881	yes
Node 3	CCT	3.75	Strut 6	616.0	1486	1617	yes
		3.75	Strut 7	528.0	1332	1386	yes
		3.75	Tie 1	3696.0	672	9702	yes
Node 4	CTT	3.25	Strut 4	2367.2	233	5385	yes
		3.25	Tie 1	3696.0	672	8408	yes
		3.25	Tie 3 - Tie 2	1056.0	602	2402	yes
		3.25	Applied Load	2112	403.9	4804.8	yes
Node 5	CCT	3.75	Strut 8	2454.0	4808	6442	yes
		3.75	Tie 3	1056.0	1050	2772	yes
		3.75	Applied Load	2587.2	4500.5	6791.4	yes

Step 8(a) – Check the detailing for the anchorage of the ties.

At Node 5, the reinforcement used to satisfy the requirement of Tie 3 needs to be detailed to meet the anchorage requirements of Section 5.11.2. At Node 5, 90-degree hooks will be used to anchor the #11 bars. According to Section 5.11.2.4.1, the basic development length, ℓ_{hb}, for a #11 bar with a 90-degree hook can be determined as follows:

$$\ell_{hb} = \frac{38.0 \cdot d_b}{\sqrt{f'_c}} = \frac{38 \cdot 1.41in}{\sqrt{5ksi}} = 24.0in \qquad \text{(AASHTO LRFD Eq. 5.11.2.4.1-1)}$$

Because the # 11 bars have been detailed to have a side cover of at least 2.5 in. normal to the plane of the hook and at least 2 in. of cover beyond the extension of the hook in the plane of the hook, the development length, ℓ_d, is calculated to be seventy percent of the basic development length (AASHTO LRFD 5.11.2.4.2). The required development length, ℓ_d, is then calculated to be approximately 16.8 in.

Typically, it is considered to be conservative to ensure that the bar has been developed by the farthest edge of the nodal zone. This is considered to be conservative because the bar has yet to leave the confines of the strut which provides a "clamping" action between the strut and applied load (See Figure A.2.3-6). The available distance in the nodal zone is 27.5 in. as measured from the back of the hook to the edge of the node. Figure A.2.3-6 shows a detail of anchored reinforcement.

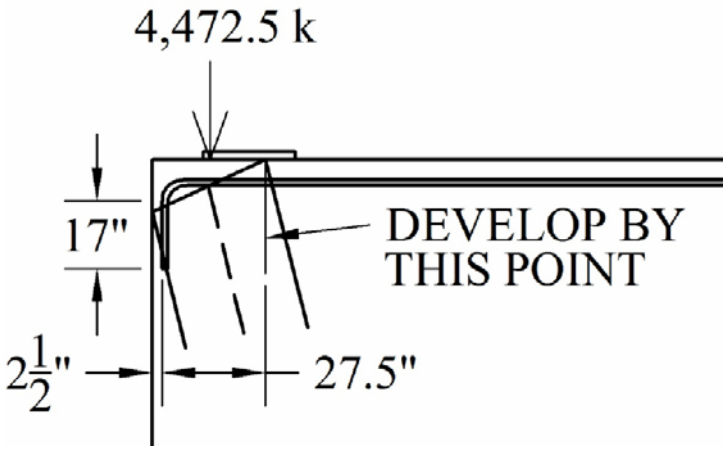

Figure A.2.3-6: Anchorage details in Node 5 of #11 bars used for Tie 3.

The anchorage details of the stirrups used for Tie 1 will be assumed to conform to AASHTO LRFD 5.11.2.6.4; therefore, the anchorage details are considered to be satisfactory.

Step 8(b)- Detail the crack control reinforcement.

The designed reinforcement for each of the STMs in the C-bent joint is shown in Figure A.2.3-7. Figure A.2.3-8 shows the cross-sections referenced in Figure A.2.3-7. Crack control reinforcement details will be determined to conform with the designed reinforcement from the column, beam, and C-bent joint STM analysis.

Crack control for three regions of the C-bent joint needs to be considered: 1.) the joint, 2.) the portion of the cantilever included in the design, and 3.) the face of the joint that anchors the beam post-tensioning.

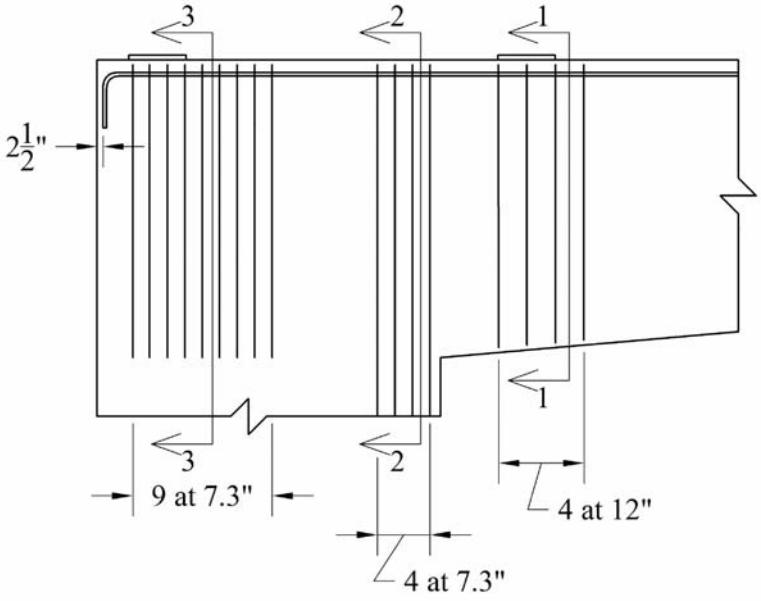

Figure A.2.3-7: Designed reinforcement from Examples A.2.1, A.2.2, and A.2.3. Each line represents a group of stirrups. As previously mentioned, the 7.3 in. dimension was chosen to match the spacing of the column longitudinal reinforcement.

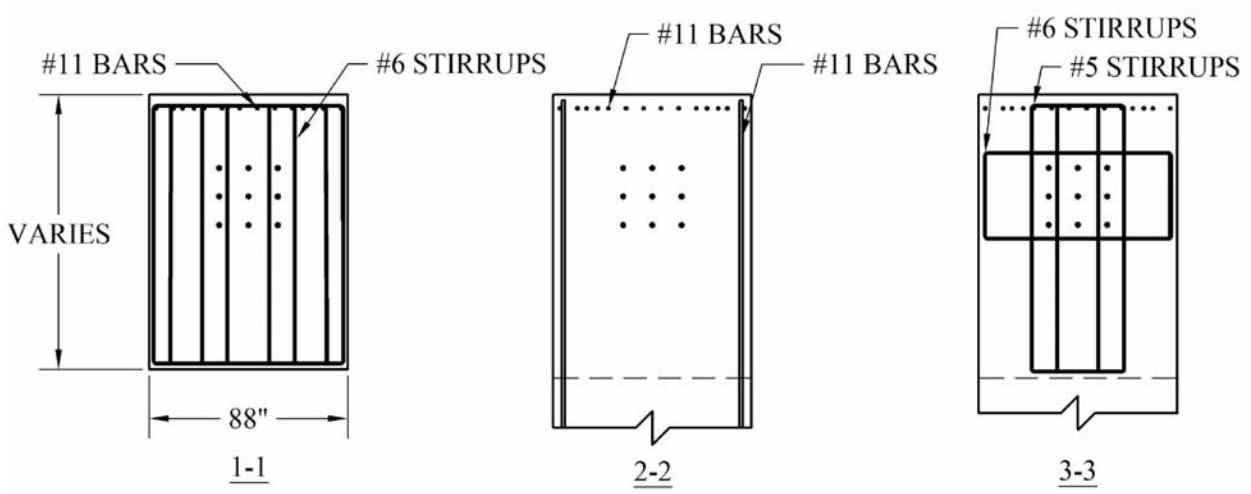

Figure A.2.3-8: Cross-sections referenced in Figure A.2.3.7.

1.) crack control reinforcement in the joint

In order to conform to the AASHTO LRFD crack control specifications (Section 5.6.3.6), the ratio of reinforcement to gross area of concrete must be at least 0.003 in each direction. The vertical crack control reinforcement will be determined first. The vertical reinforcement will be spaced at 7.3 inches to match the spacing of the longitudinal bars extending from the column. Therefore, the required area of steel is calculated to be:

$$A_{st-required} = 0.003 \cdot b \cdot s = 0.003 \cdot 88in \cdot 7.3in = 1.93in^2$$

The #11 longitudinal bars extending from the column satisfy the vertical crack control reinforcement in the joint (A_{st} = 3.12 in^2); however, at locations that have no stirrups provided from the STM analysis of the joint subjected only to the beam post-tensioning, #5 stirrups will still be used in addition to the #11 bars for the purposes of tying horizontal crack control that may need to be placed in the joint (See the final figures). Also, #6 bars will be placed atop each #5 stirrup to provide a grid of crack control reinforcement at the top face of the joint (see section "B-B" and "C-C" in Figure A.2.3-10).

Now, the horizontal crack control will be determined. A spacing of 9 in. will be assumed based on reinforcement that has already been chosen for the cantilever design. The required amount of horizontal crack control reinforcement is calculated to be:

$$A_{st-required} = 0.003 \cdot b \cdot s = 0.003 \cdot 88in \cdot 9in = 2.376in^2$$

To fulfill this requirement, #8 bars will be attached to #11 bars extending from the column, and #6 bars will be attached to the #5 inner stirrups discussed above. See Figure A.2.3-9 and A.2.3-10 to see the placement of the crack control in the joint.

2.) crack control reinforcement in the cantilever

For the cantilever section, if the stirrup spacing is kept at 12 in., the calculated required crack control is determined to be:

$$A_{st-required} = 0.003 \cdot b \cdot s = 0.003 \cdot 88in \cdot 12in = 3.17in^2$$

This requirement can be met with an 8-legged #6 stirrup (A_{st} = 3.52 in^2).

The horizontal crack control reinforcement will be identical to what was determined for the joint.

3.) crack control reinforcement in the face of the joint that anchors the beam post-tensioning

The crack control on this face will be designed based on the fact that the distance from the face to the nearest #11 longitudinal bar extending from the column is 15 in. Also, it will be assumed that a 9" x 9" grid will be used at the face. Based on these two facts, the size of the bar used for the grid can be determined as follows:

$$A_{st} = 0.003 \cdot 15in \cdot 9in = .405in^2$$

Therefore, #6 bars should be used for the 9" x 9" grid. This grid far exceeds the minimum amount of spalling reinforcement discussed in Example A.2.1 (AASHTO LRFD 5.10.9.3.2).

See Figures A.2.3-9 and A.2.3-10 for the final design details of the C-bent joint.

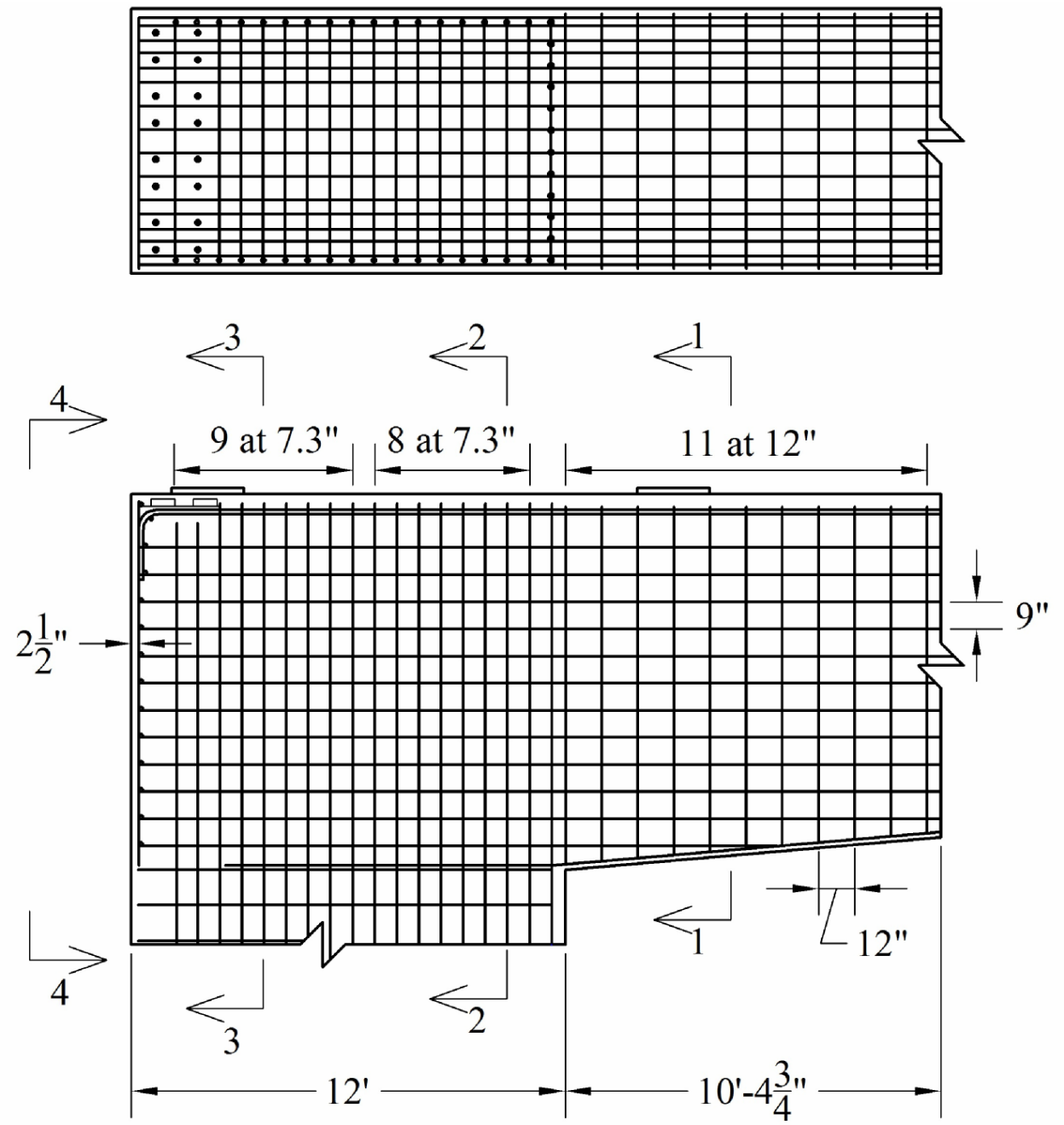

Figure A.2.3-9: Final details of C-bent joint design. See Figure A.2.3-10 for the cross-sections denoted above.

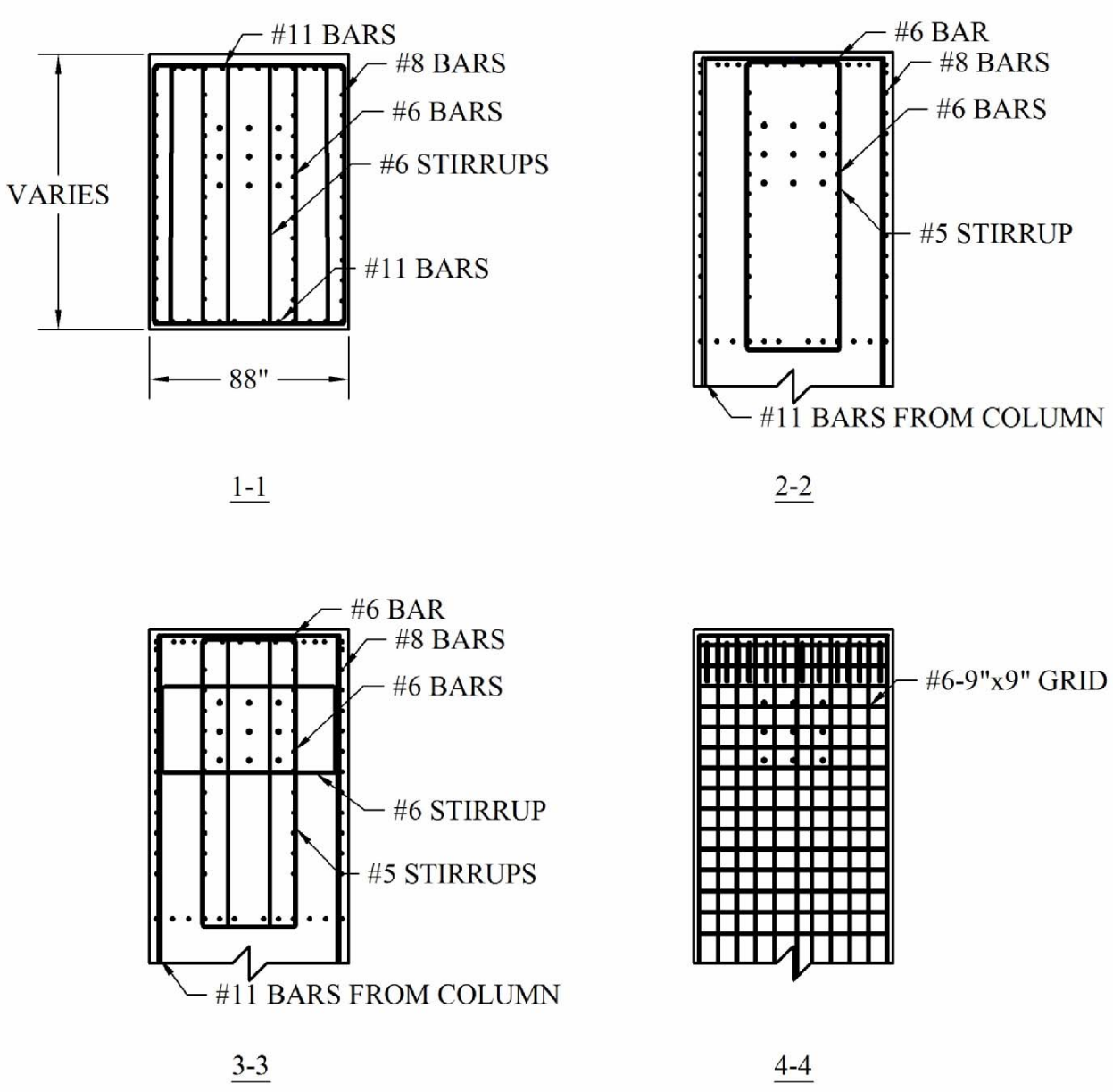

Figure A.2.3-10: Cross-sections referenced in Figure A.2.3-9.

EXAMPLE A.3 – PILE FOOTING

Problem Statement:

The footing of a C-bent similar to the one used in Examples A.1 and A.2 is shown in Figures A.3-1 and A.3-2. It is proposed to support the footing on six, 72" diameter drilled shafts. Post-tensioning added to the bent column is anchored in the bottom of the footing. Design the footing using LRFD STM requirements and HL-93 live loading. The footing concrete has an f_c' of 4 ksi and the mild reinforcing is grade 60.

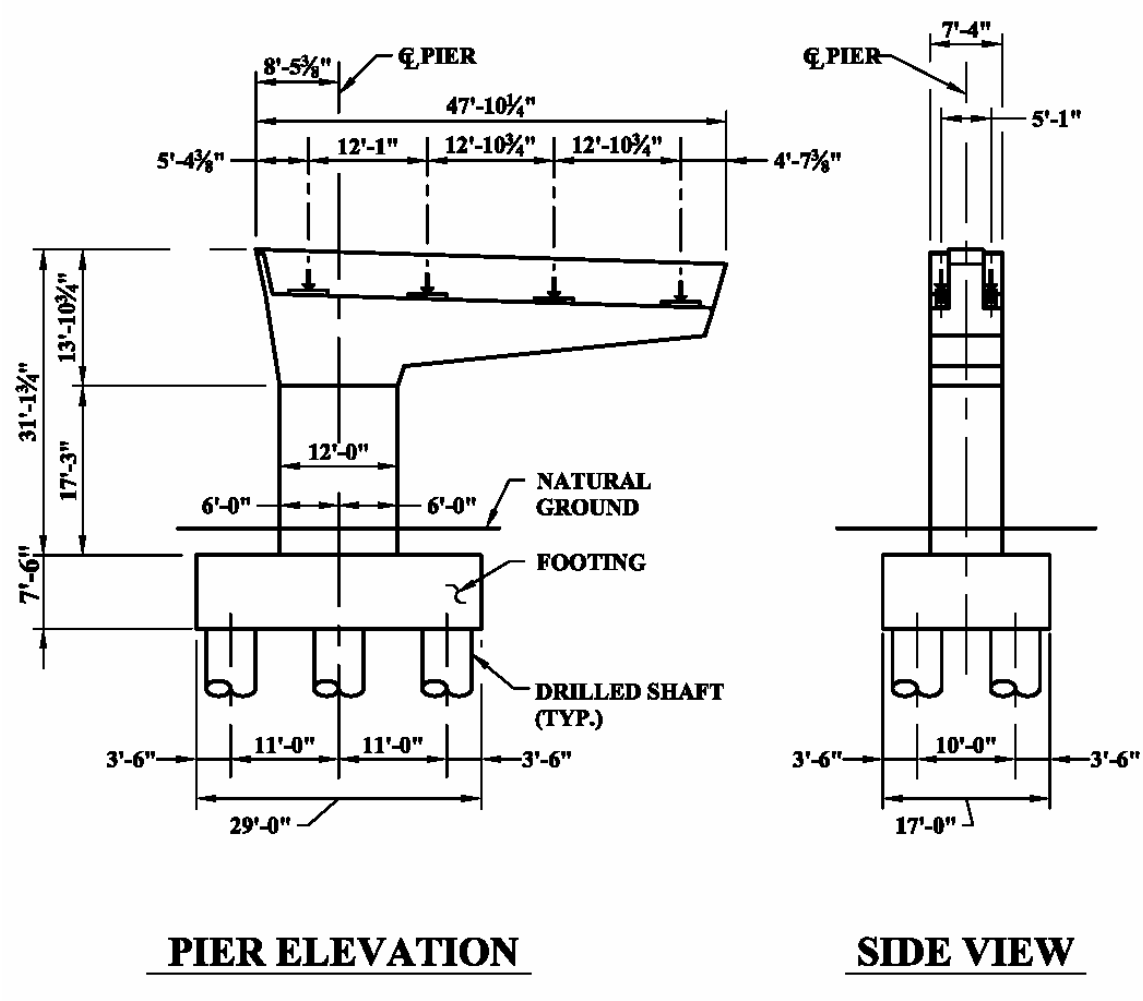

Figure A.3.1 – General Elevation of Pier and Footing

<u>Step 1</u> – Delineate the D-regions.

The entire pile cap is a D-region.

<u>Step 2</u> – Determine the boundary conditions.

As shown in Figure A3-2, the reactions at the base of the column consist of an axial Dead Load from the pier itself and the superstructure of 1130 kips and an axial Live Load of 252 kips. In addition there is an overturning dead load moment of 12,824 foot-kips and a live load moment of 3,892 foot-kips. This results in the following factored loads at the column base:

$$P = 1.25(1130) + 1.75(252) = 1853.5^{k}$$
$$M = 1.25(12{,}824) + 1.75(3892) = 22{,}841^{1-k}$$

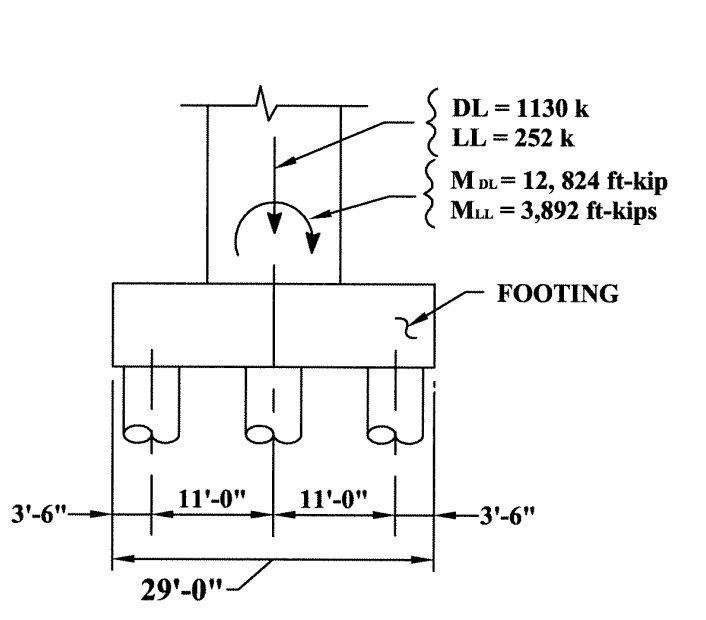

Figure A.3-2 – Loads at the Column Base

Using the dimensions used in Figure A.3-1, the weight of the footing and two feet of soil overburden will be conservatively added to these factored loads at the base of the pier column. The unit weight of the concrete in the footing is assumed to be 0.150 k/ft^3 and the unit weight of the overburden is 0.110 k/ft^3.

$$Footing\ weight = (29)(17)(7.5)(.15) = 555^{k}$$
$$Overburden\ weight = [(29)(17) - (12)(7.33)](2)(.110) = 89^{k}$$

$$Total\ P = 1853.5 + 1.25(555 + 89) = 2658^{k}$$

Using these factored loads at the column base the loads in the drilled shafts and at the top of the footing will be determined.

The drilled shafts are in a 3x2 pattern as shown in Figure A.3-3.

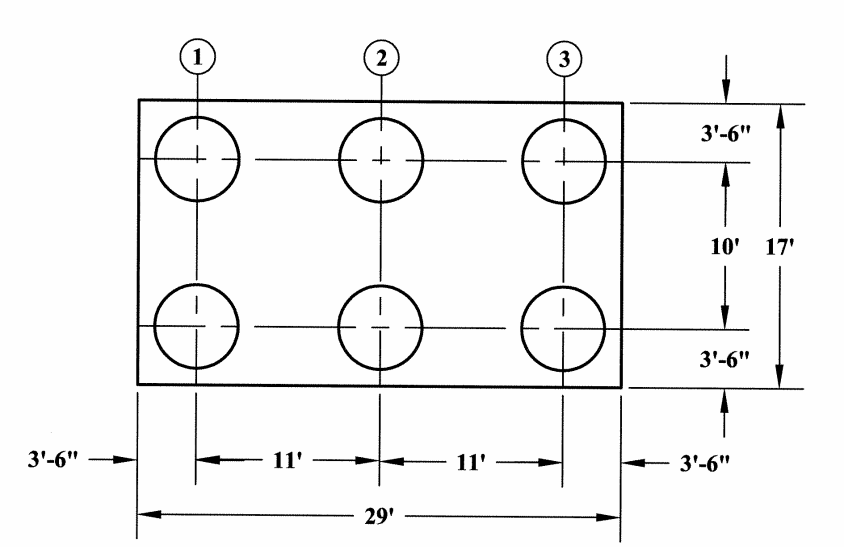

Figure A.3-3 – Plan Indicating Layout of Drilled Shafts

Using the total factored moment and applying simple statics, the total factored load for each drilled shaft is as follows:

$$\text{Each drilled shaft in line 1} = \frac{P}{6} - \left(\frac{M}{4\times 11}\right) = \frac{2658 kips}{6} - \left(\frac{22841 ft-kips}{4\times 11 ft}\right) = -76 kips$$

$$\text{Each drilled haft in line 2} = \frac{P}{6} = \frac{2658 kips}{6} = 443 kips$$

$$\text{Each drilled shaft in line 3} = \frac{P}{6} + \left(\frac{M}{4\times 11}\right) = \frac{2658 kips}{6} + \left(\frac{22841 ft-kips}{4\times 11 ft}\right) = 962 kips$$

The reactions at the bottom of the column will be resolved into six reactions based on the gross properties of the column.

$$A_{col} = (12')(7.33') = 87.96\ ft^2$$

$$S_{col} = \frac{bh^2}{6} = \frac{7.33'(12')^2}{6} = 175.92\ ft^3$$

Stress resulting from the factored axial load

$$\frac{P}{A} = \frac{2658 kips}{87.96 ft^2} = 30.22 ksf$$

Stress at each face due to factored moment

$$\frac{M}{S} = \frac{22{,}841 ft-kips}{175.92 ft^3} = \pm 129.84 psf$$

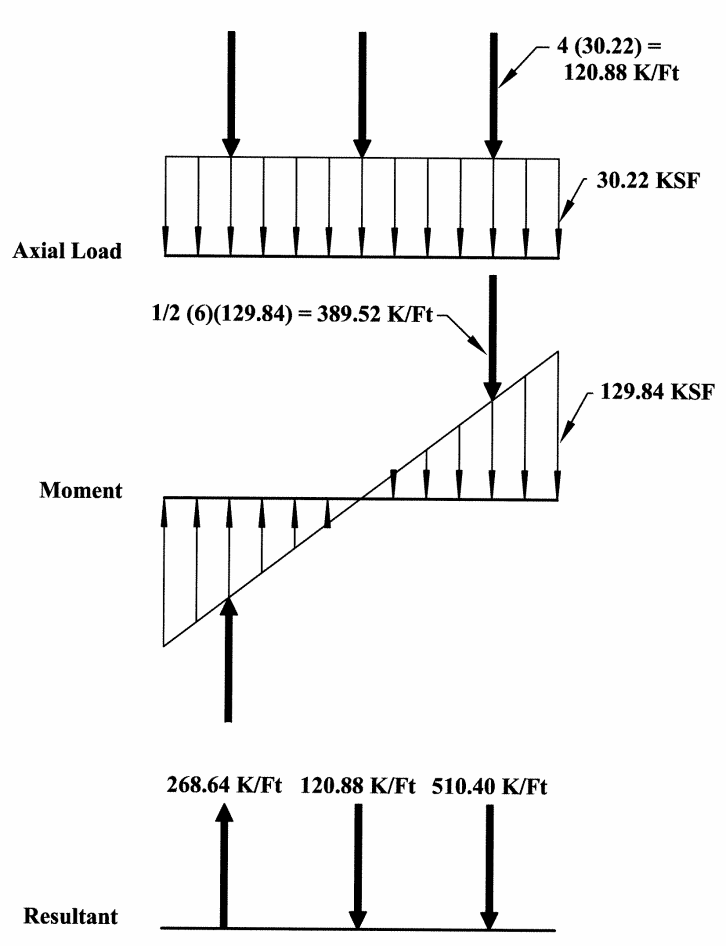

Figure A.3-4 – Resolved loads at the Column Base Due to External Loads

The column is 7.33' wide. Dividing the column into six equal areas, the following forces result:

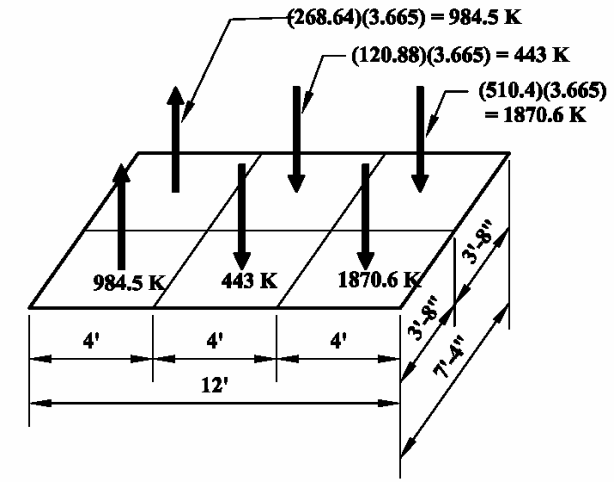

Figure A.3-5 – Loading at Column Base Due to External Loading
Therefore the resulting boundary conditions are

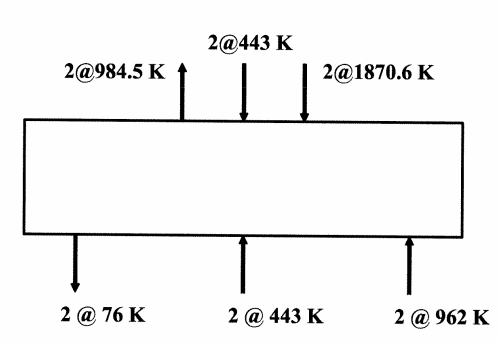

Figure A.3-6 – Boundary Conditions of Footing

<u>Steps 3 & 4</u> – Sketch the flow of forces and Develop the STM.

The STM is illustrated in Figures A.3-7. We will assume the centroid of the top and bottom struts and ties will fall approximately 3" in from the top and bottom of the footing resulting in a STM with a depth of seven feet. Because of the complexity of the model Figure A.3-8 illustrates three views and the dimensions of the model.

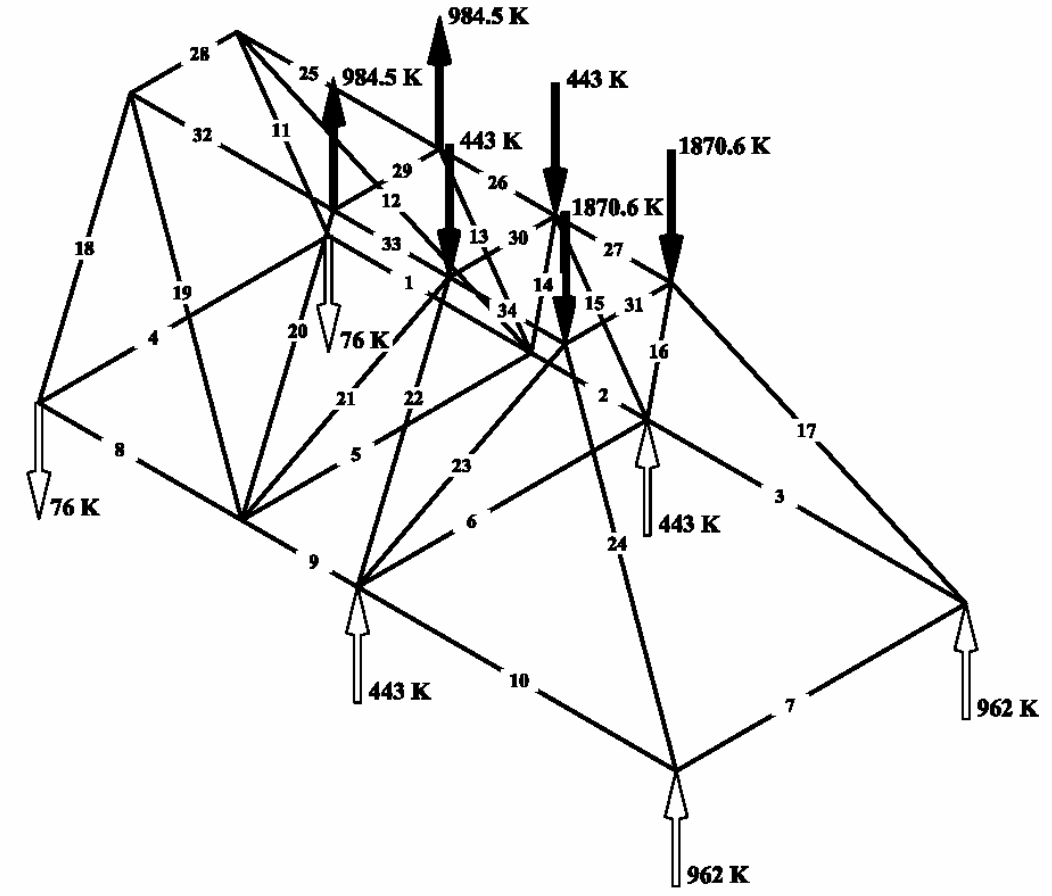

<u>Figure A.3-7 – STM Model (Numbers Shown are Member Numbers)</u>

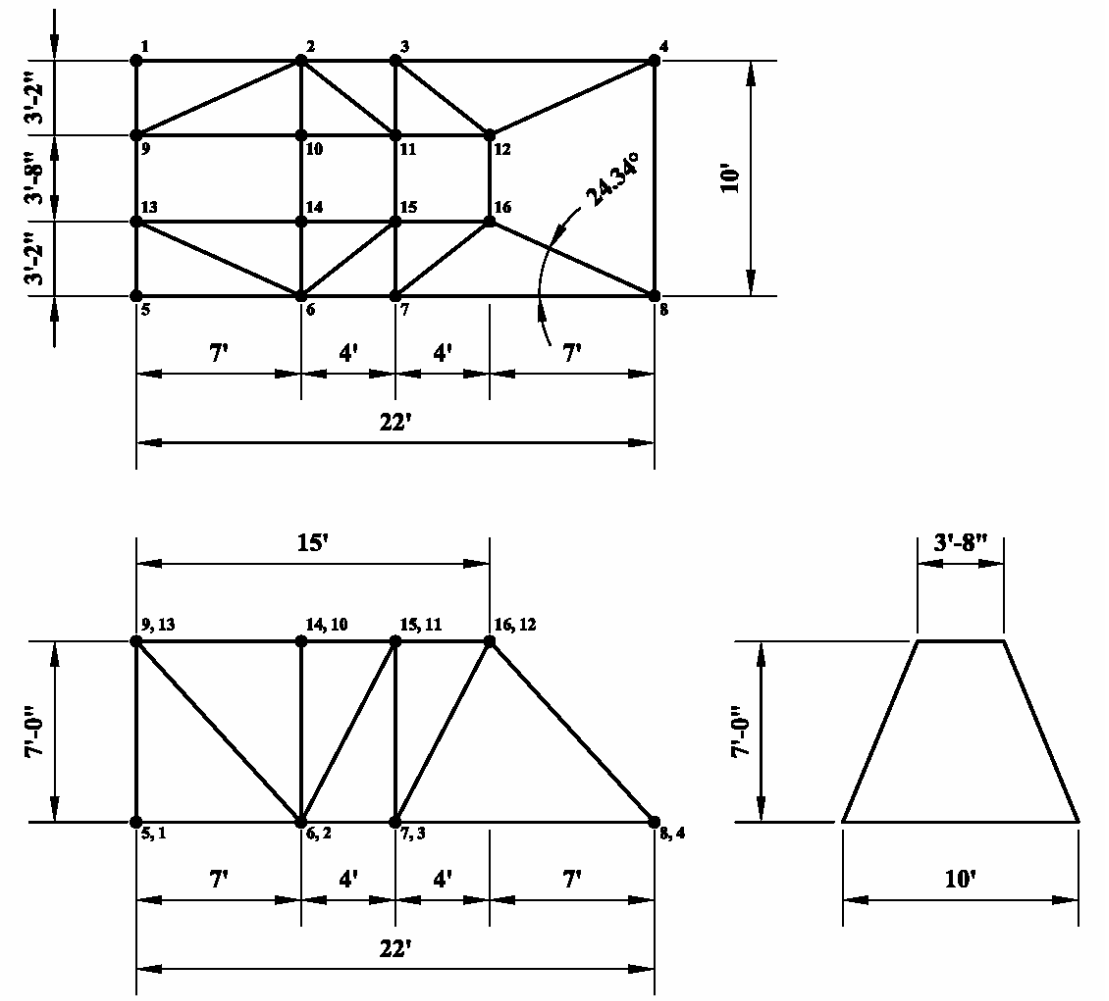

Figure A.3-8 – Plan, Elevation and End View of STM Model (Numbers at Joints are Node Numbers)

The geometry deeloped for the STM is driven primarily by the loading case selected. Due to the large over-turning moment that results from the configuration of the bent, the drilled shafts at nodes 1 and 5 are in tension. A vertical tie is modeled here in order to reflect this tensile force. The inclined strut connecting nodes 4 and 12 and nodes 8 and 16 reflect the large compressive force that results from the compressive loads in the drilled shafts at this end of the structure. There are other load cases, such as dead plus partial live load, that would likely result in a different STM. These other cases, though not likely to govern, would need to be evaluated as well. The load case selected for evaluation in this example was selected because of he magnitude of the resulting loads and its uniqueness.

<u>Step 5</u> – Solve for the Member Forces.

Using the truss model indicated in Figures A.3-7 and A.3-8 the following member forces are determined:

Member	Force (Kips)	T or C	Member	Force (Kips)	T or C
1 and 8	0		4	27.2	C
2 and 9	443	T	5	70.2	T
3 and 10	962.1	T	6	204.5	T
11 and 18	80.6	T	7	433.3	T
12 and 19	113	C	28	7.2	C
13 and 20	1051.6	T	29	375.2	T
14 and 21	1124.1	C	30	204.5	C
15 and 22	509.1	T	31	820.6	C
16 and 23	1124.1	C			
17 and 24	1428.5	C			
25 and 32	76.1	T			
26 and 33	76.1	T			
37 and 34	443	C			

<u>Step 6</u> – Size the Tie Reinforcement.

Looking first at the lower mat, longitudinal direction.

Max tie force $= 962.1 kips$ (Members 3 & 10)

$$A_s = \frac{962.1 kips}{.9(60 ksi)} = 17.81\ in^2$$

Since the footing is subject to flexure, the amount of reinforcement provided must be adequate to develop a factored flexural resistance, M_r at least 1.2 times the cracking moment unless an amount of reinforcement capable of carrying 1.33 times the factored moment is supplied. The factored flexural resistance required to resist $1.2M_r$ using the modulus of rupture F_r of $0.37\sqrt{F_c'}\ ksi$ is:

$$M_r \geq 1.2\frac{bh^3}{6}0.37\sqrt{F_c'} = 1.2\times\frac{12\times17\times90^2}{6}\left(0.37\sqrt{4}\right) = 244{,}555 kip-in = 20{,}380 kip-ft$$

The corresponding minimum area of flexural reinforcement can be determined by dividing this factored flexural resistance by the product of the flexural lever arm (7.0 ft) and the yield strength of the reinforcement giving:

$$A_{s\,\min} = \frac{20{,}380 kip - ft}{7\,ft \times 0.9 \times 60 ksi} = 53.91\ in^2$$

Note that this total area of flexural tension reinforcement A_s will be provided by the reinforcement in the two parallel tension ties, Ties 3 and 10.. Hence the area of tension tie reinforcement required to ensure that the factored flexural resistance is at least $1.2\,M_{cr}$ is equal to $\frac{53.91}{2} = 26.96\ in^2$.

The amount of reinforcement required to resist 1.33 times the factored loads is:

$$A_s = 1.33 \times 17.81 in^2 = 23.69\ in^2$$

Use 15 #11 bars over the dilled shafts. (Area of steel provided = 23.4 in^2. Within 1% of required). For simplicity this area of reinforcement will be used for ties 1, 2, 8 and 9 as well.

Transverse lower mat.

Max tie force = $433.3 kips$ in tie 7.

$$A_s = \frac{433.3 kips}{.9(60 ksi)} = 8.02\ in^2$$

By inspection, we see that the amount of reinforcing required to resist 1.33 times the factored loads will be less than that required to resist the cracking moment. Therefore

$$A_s = (8.02 in^2)(1.33) = 10.67\ in^2$$

Use 11 #9 bars over the most highly loaded 72" drilled shaft. (Area of steel provided = 11in^2.)

Will conservatively use the amount of reinforcing required for tie 6 for tie 4 as well.

$$A_s = \frac{204.5 kips}{.9(60 ksi)} = 3.79\ in^2$$

$$A_s = (1.33)(3.79 in^2) = 5.03\ in^2$$

Use 7 #8's transversely over the other drilled shafts. (Area of steel provided = 5.5 in^2.)

Top mat – transverse.

Tie 29 has a tensile force of $375.2 kips$.

$$A_s = \frac{1.33(375.2 kips)}{0.9(60 ksi)} = 9.2\ in^2$$

Will use 9-#9's at 7½". (Within 3% of area required)

Top mat – longitudinal.

Using Ties 25 and 32

$A_s = \frac{1.33(76.1k)}{0.9(60 ksi)} = 1.87\ in^2$ (Minimum can be used). Since footings are exempt from the crack control requirements of AASHTO §5.6.3.6, will use the same reinforcement between the drilled shafts as required over the drilled shafts.

Ties 13 and 20 have a tensile force of 1051.6 *kips.*

There are 6 P/T bars that pass in the area of this tie. Each bar is a 1¾" diameter, 150 ksi high strength bar. Final effective force = 240 k/bar.

According to AASHTO §5.6.3.4.1 the nominal resistance of a tension tie in kips shall be taken as

$$P_n = f_y A_{st} + A_{pn}\left[f_{pe} + f_y\right] \qquad F_{pe} = 100 ksi$$

$P_n = 6(2.4)[100 + 60] = 2{,}304^k$ This is well above the load of $1051.6^k < 2304(0.9) = 2073.6^k$

Ties 15 and 22 has a tensile force of 509.1 *kips*.

$$A_{st} = \frac{P}{0.9F_y} = \frac{509.1 kips}{.9(60 ksi)} = 9.42\ in^2$$

There are 20, #11 bars extending through this area from each of the drilled shafts as well as the steel extending from the column. These ties are okay by inspection. Ties 11 and 18 also have 20 #11 bars extending through this area and are okay by inspection.

<u>Step 7 –</u> Check the Capacity of the Struts.

Struts 17 and 24 each carry a compression force of $1428.5 kips$. In order to determine the nominal compressive resistance of these struts it is necessary to determine the effective cross-sectional area in the critical region near the intersection of the tension ties and the pile reaction (joints 4 and 8 in Figure A.3-8) and the limiting compressive stress that these struts can carry.

Since the drilled shafts are circular, we will use an equivalent square shape of $0.9(72") = 64.8"$. It will then be assumed that the compressive stresses from the head of the equivalent square disperse into the pile cap at a 45° angle from the bottom of the footing to the middle plane of the reinforcement, a distance of approximately 3.7 inches. This results in the effective bearing area at the middle plane of the tie reinforcement being a square measuring 72.2" on each side.

The vertical rise of the diagonal strut from nodes 4 to node 12 and node 8 to node 16 is 7'. Based on Figure A.3-8, the horizontal distance from node 4 and node 8 to a point directly under node 12 and node 16 is $\frac{7'}{\cos 24.341°} = 7.683'$ the resulting angle between the centerline of the strut and the horizontal bearing area is 42.34°.

The visualization and determination of the configuration of the struts and bearing areas of three-dimensional trusses is extremely difficult. Therefore a simplified approach will be used. The cross-sectional area of the strut can be estimated by first looking at the section passing through the vertical plane (Section A-A) shown in Figure A.3-9.

Using section A-A shown in Figure A.3-9, the area of the strut can be calculated as follows:

$$A = \frac{(36.1" \times 79.24)}{2} + (3.7" X 79.24") + 3.7 * \frac{79.24 + 71.22}{2} = 1430.3 + 293.19 + 278.35 = 2001.8\ in^2$$

Say 2000 in^2

It will be assumed that the cross-sectional area of the strut, which is inclined at 42.34° from the vertical plane, is $(2000) \times \cos 42.34^\circ = 1478\ in^2$.

The tensile strain in ties 3 and 10 is:

$$\varepsilon_s = \frac{P_u}{A_{st} E_s} = \frac{962.1 kips}{(15)(1.56 in^2) 29{,}000 ksi} = .0014 = 1.418 \times 10^{-3}$$

The tensile strain in this tie will reduce from 1.418×10^{-3} at the inner face of the effective bearing area to a strain of about 0 at the outer edge of the effective bearing area. Therefore, near the centerline of the strut, the value of ε_s will be taken as $\frac{1}{2}(1.418 \times 10^{-3}) = 0.709 \times 10^{-3}$. This is the tensile strain in ties 3 and 10. The value of ε_s in tie 7 is

$$\varepsilon_s = \frac{P_u}{A_{st} E_s} = \frac{433.3 kips}{(11 in^2) 29{,}000 ksi} = .00136 = 1.36 \times 10^{-3}$$

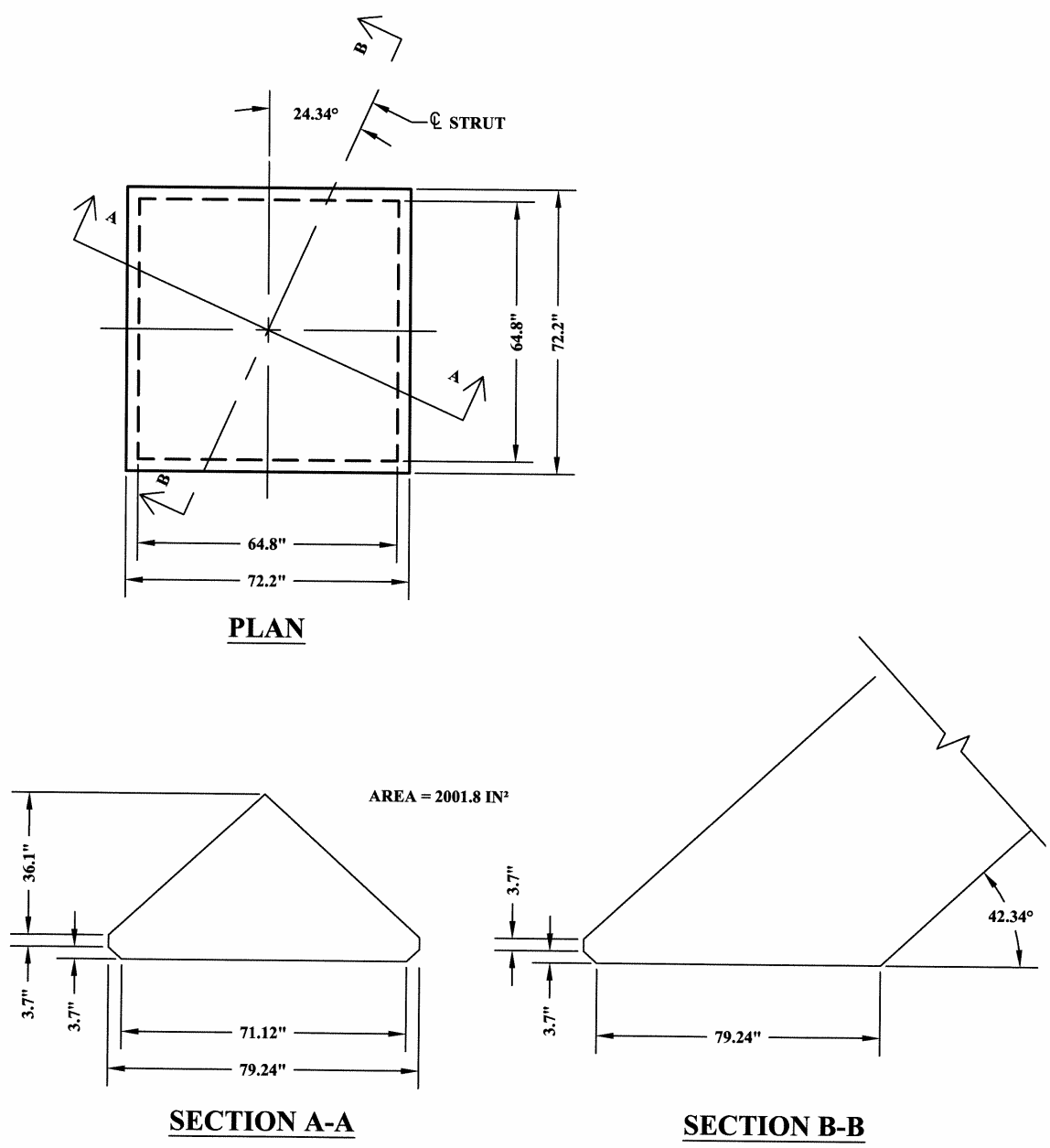

Figure A.3-9 – Cross-Section of Struts 17 & 24

Near the centerline the value will be $\frac{1}{2}\left(1.36\times10^{-3}\right)=0.679\times10^{-3}$

Using the largest of these two strain values and the angle between the plane of the tension ties and the diagonal strut of 42.34°, the principal strain, ε_1, is determined as:

$$\varepsilon_1=\varepsilon_s+\left(\varepsilon_s+0.002\right)\cot^2\alpha_s=0.709\times10^{-3}+\left(0.709\times10^{-3}+.002\right)\cot^2 42.34$$
$$=0.709\times10^{-3}+\left(.002709\right)\cot^2 42.34=0.0039$$

The limiting compressive stress, F_{cu}, in the strut is then:

$$f_{cu} = \frac{f_c}{0.8 + 170\varepsilon_1} \le 0.85F_c' = \frac{4ksi}{0.8 + 170(.0039)} = 2.73ksi \le 0.85(4)$$

Multiplying the limiting compressive stress by the area of the strut, the nominal resistance of the strut is thus:

$$P_n = f_{cu}A_{cs} = (2.73) \times 1478 = 4036kips$$

With a resistance factor of 0.70, the factored resistance of the strut is:

$$P_r = \phi P_n = 0.70 \times 4036kips = 20251kips > 1428.5kips$$

The strut capacity is adequate.

Checking the nodal zone at the drilled shaft – pile cap interface has a load of $984.5kips$

$$f_c = \frac{962kips}{\frac{\pi(72in)^2}{4}} = 0.23ksi$$

The node zones above the drilled shafts have tension ties in two directions passing through the nodal zones (CTT node) and hence have a reduced nodal zone stress limit of

$$0.65\phi f_c = 0.65 \times 0.70 \times 4 = 1.82ksi$$

Therefore we can conservatively say all nodal zones above the piles are okay.

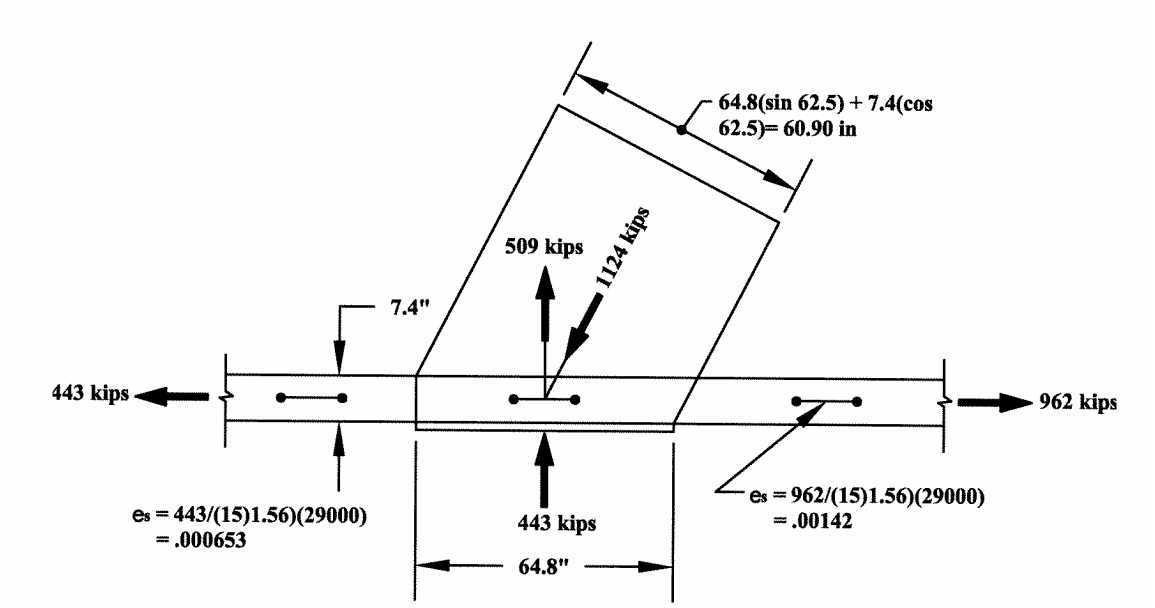

Figure A.3-10 – Strains in Nodes 3 and 7

Evaluating struts 16 and 23.

The strains in ties 9 and 10 due to factored loads are shown in Figure A.3-10. For determining the strut capacity, the larger of these two strains, $\varepsilon_s = 1.42 \times 10^{-3}$ will be used.

The principle strain, ε_1, is determined as

$$\varepsilon_1 = \varepsilon_s + (\varepsilon_s + 0.002)\cot^2 \alpha_s = 1.42 \times 10^{-3} + (1.42 \times 10^{-3} + 0.002)\cot^2 60.26° = 2.536 \times 10^{-3}$$

resulting in a limiting compressive stress, F_{cu}, in the strut of:

$$f_{cu} = \frac{f_c}{0.8 + 170\varepsilon_1} \le .85 f_c' = \frac{4ksi}{0.8 + 170 \times (2.536 \times 10^{-3})} = 3.25ksi < .85 \times 4ksi \text{ use 3.25 ksi.}$$

Conservatively taking the effective thickness of the strut as the width of the equivalent square pile = 64.8" we get an area of the strut:

$$A_{strut} = (60.90")(64.8") = 3{,}946\ in^2$$

$$P_n = f_{cu} A_{cs} = (3.25)(3{,}946 in^2) = 12{,}825 kips$$

The factored resistance of the strut is:

$$P_r = \phi P_n = 0.70 \times 12{,}825 kips = 8{,}977 kips > 1124 kips$$

Step 8 – Detail Reinforcement

8a – Check the Anchorage of the Tension Ties

The No. 11 bars used for the lower longitudinal reinforcement are required to develop a force of 962.1 kips at the inner face of the pile. The inner face of the pile is at a distance of 78 inches from the outside face of the footing. Allowing for a concrete cover of 3 inches a distance of 75 inches is available as the embedment length. The stress in the 15 No. 11 bars at the inner face of the drilled safts is:

$$f_s = 962.1/(15)(1.41) = 45.48 ksi$$

The basic development length of a #11 bar with f_y = 60 ksi and f'_c = 4 ksi is 82 in.

Since the stress in the steel is only 45.82 ksi the development length can be reduce to:
$l_b = (45.48 ksi / 60 ksi)(82) = 62.15"$

The development length, l_b = 62.15 is less than the available length therefore the anchorage is okay.

The anchorages of the remaining ties are acceptable by inspection.

It is also necessary to check if the tension ties are spread out sufficiently in the effective anchorage area. Nodes 4 & 8 are CTT nodes which is 7.4" in depth. (See Figure A.3-9). The nodal zone stress to anchor the tension tie force in ties 3 and 10 of 962.1 kips is:

$$f_c = \frac{962.1 kips}{(7.4)(72)} = 1.81 ksi$$

for this CTT nodal zone, the limiting nodal zone stress is:

$$f_c = 0.65 \phi f'_c = 0.65(0.7)(4) = 1.82 ksi$$

The nodal zone stress limit in the anchorage area is acceptable.

It is noted that footing type elements are exempt from the crack control requirements of §5.6.3.6 and the requirements for minimum flexural reinforcement of §5.7.3.3.2 were satisfied in step 6. However, minimal reinforcing is shown between the tie regions to simplify field layout.

8b – Detail Reinforcement

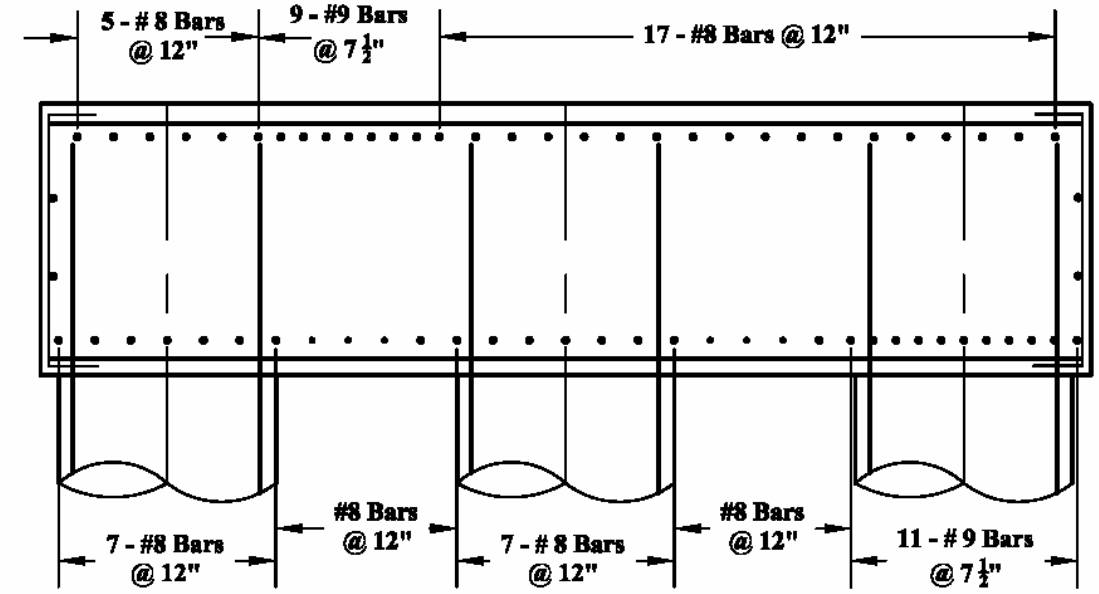

Longitudinal View

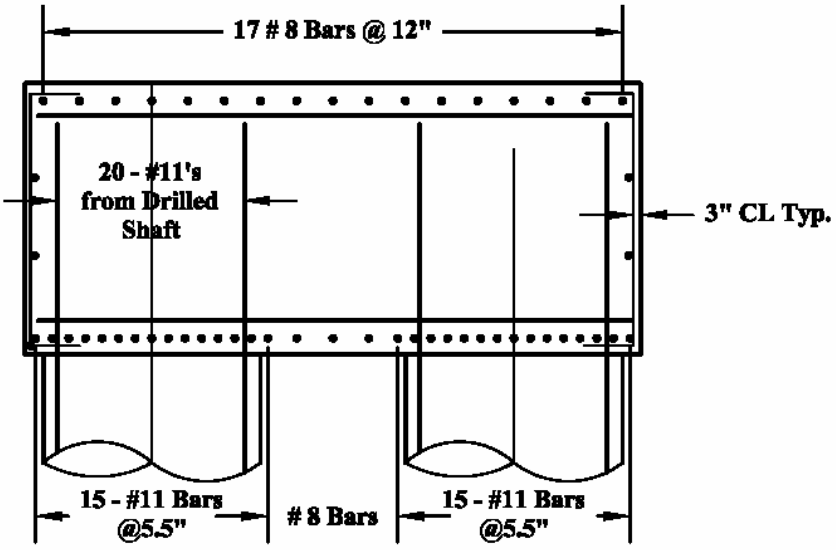

End View

Figure A.3-11: Reinforcing Detailing (Bars from Column and Post-Tensioning omitted for clarity.)

EXAMPLE A.4 –DAPPED END OF A BEAM
AND
EXAMPLE A.5 BEAM WITH A HOLE IN THE WEB

Problem Statement:

A RC beam having a rectangular cross-section and a depth of 30 in. spans a distance of 60 ft. The factored distributed load the beam is subjected to is calculated to be 2 k/ft (including self weight) according to the Strength I Load Case in Table 3.4.1-1 in the AASHTO LRFD. The beam is to have dapped-ends and has a rectangular utility opening 15 ft away from the left support (see Figure A-3 for the geometry of the discontinuities).

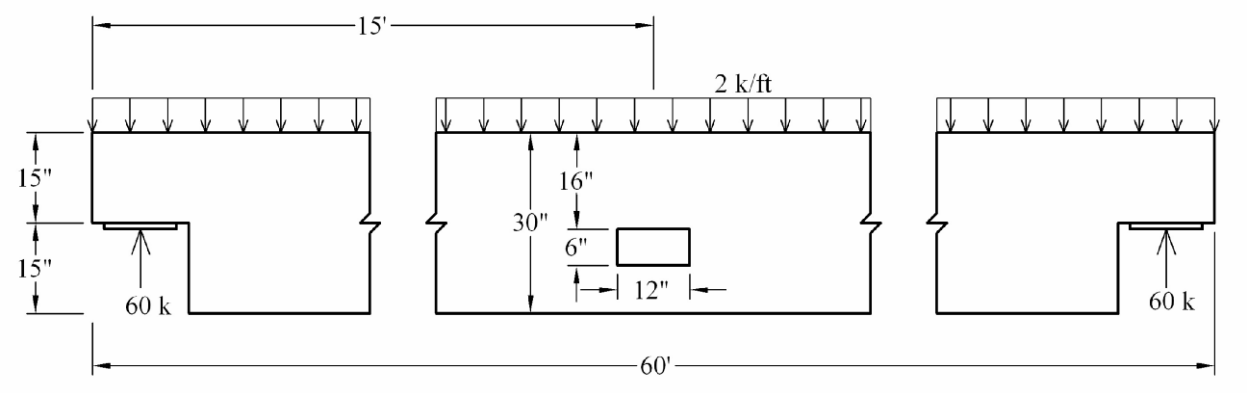

Figure A-3: Geometry of beam and beam discontinuities (inches).

Figure A-4 shows the reinforcement details determined by traditional beam theory.

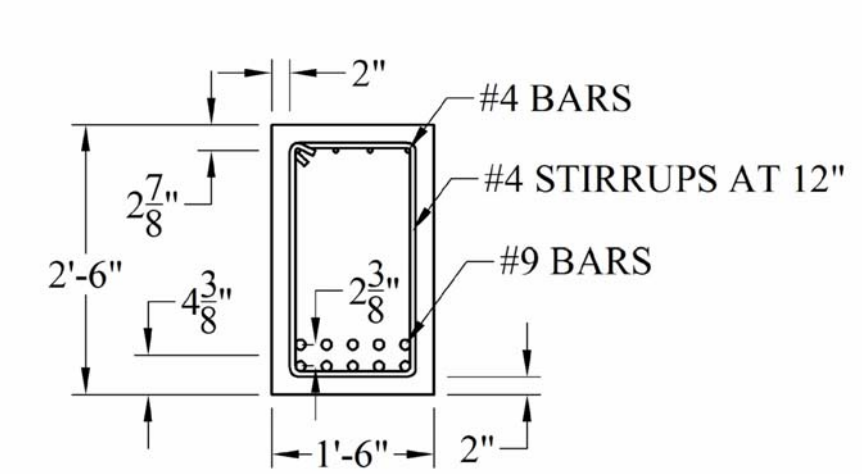

Figure A-4: Beam design for B-regions.

Design the D-regions induced by the dapped-ends and the rectangular utility opening. Use 5 ksi concrete and Grade 60 steel for the design.

Example A.4: Dapped-End of Beam

Step 1 – Delineate the D-regions.

The STM will be developed to model the force transfer up to a distance of 30 in. (the depth of the beam) away from the dapped section of the beam. Figure A.4-1 shows the extent of the D-region.

Step 2 – Determine the boundary conditions of the D-region.

The loading on the boundary is shown in Figure A.4-1. The bending and shears stress distribution at the D-region/B-region interface is also shown in Figure A.4-1. The equivalent point loads on the boundary of the D-region will be determined based on the geometry of the STM developed in Steps 3 through 5 and the loading on the D-region.

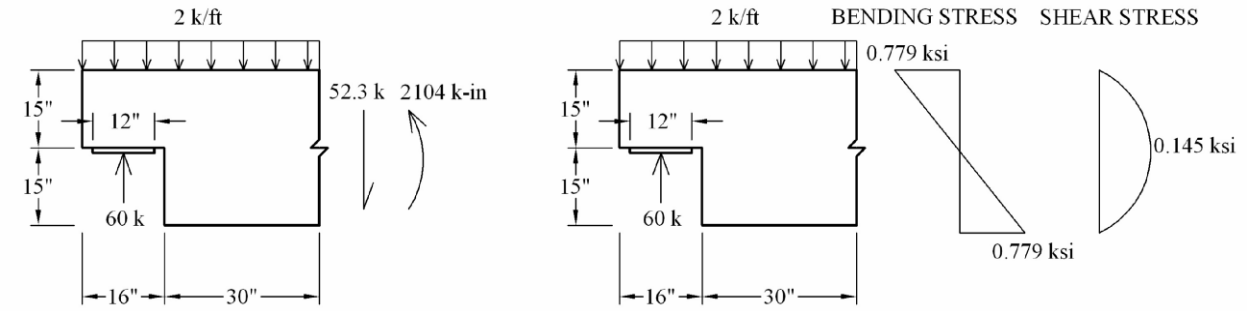

Figure A.4-1: Geometry and boundary conditions of D-region.

Steps 3, 4, and 5 – Sketch flow of forces, develop a truss model, and solve for member forces.

In order to determine the flow of forces through the D-region, a STM that is typically used for dapped-end beams was used. The STM is shown in Figure A.4-2. It should be noted that Strut 5 was placed at the centroid of the horizontal compression steel determined from the beam design (see Figure A-4 to see the details of the reinforcement determined from the B-region design of the beam). Also, Ties 3 and 5 were placed at the centroid of the tension steel determined from the beam design (see Figure A-4 to see the details of the reinforcement determined from the B-region design of the beam). The distributed load on top of the beam has been converted into equivalent point loads based on the truss geometry. Member labels can be seen in the figure. It can be noted that struts S6 and S7 and tie T5 can be considered boundary forces that were determined by solving for the member forces. The calculated member forces are given in Table A.4-1. Table A.4-1 also gives the inclination of each member (smallest angle from the horizontal).

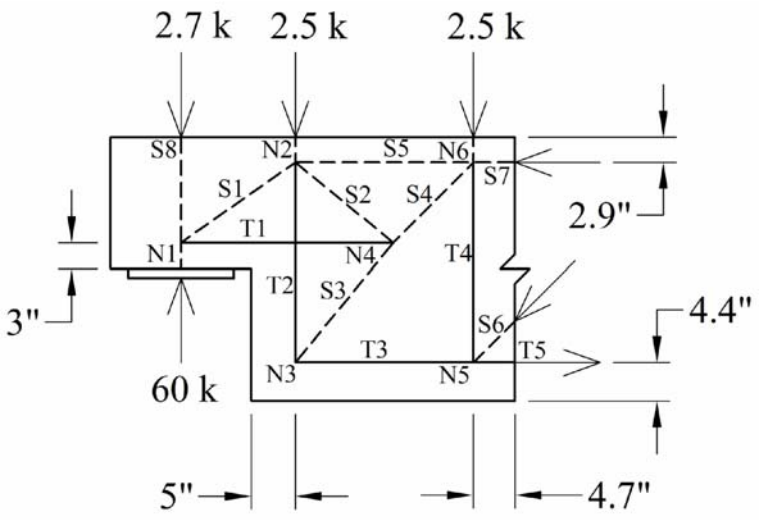

Figure A.4-2: STM developed for dapped-end.

Table A.4-1: Member forces and orientations (smallest angle from horizontal).

Member	Angle (degrees)	Force (k)
S1	35.1	100
S2	39.3	71
S3	50.7	129
S4	45.0	78
S5	0.0	27
S6	45.0	74
S7	0.0	82
S8	90.0	2.7
T1	0.0	82
T2	90.0	100
T3	0.0	82
T4	90.0	53
T5	0.0	134

Step 6 – Select steel area for the ties.

Section 5.6.3.4 of the AASHTO LRFD Specifications was used to determine the required amount of reinforcement for each tie. The required amount of reinforcement for each tie was determined as follows:

$$A_{st,required} = \frac{P_u}{\phi \cdot f_y} \qquad \text{(AASHTO LRFD 5.6.3.4.1)}$$

For tension in a STM, ϕ is taken as 0.9 (AASHTO LRFD 5.5.4.2.1). Table A.4-2 summarizes the tie calculations and the reinforcement chosen to satisfy the required calculated areas. For Ties 3 and 5, the longitudinal bars determined from the beam design will be used to satisfy the reinforcement requirements. Anchorage considerations will be discussed in Step 8. Figure A.4-

3 shows the proposed reinforcement details. In Figure A.4-3, the locations of the centroids of the groups of strirrups are shown (5" and 25.3"). The centroids of the groups of stirrups correspond to the location of the tie that they are modeling.

Table A.4-2: Summary of tie design.

Tie	Tie Force (k)	$A_{st,required}$ (in^2)	Choose	$A_{st,provied}$ (in^2)
T1	82	1.5	5-#5 bars in one layer	1.55
T2	100	1.9	3-#6 stirrups	2.64
T3	82	1.5	10-#9 bars (from beam design longitudinal reinforcement)	10.00
T4	53	1.0	3-# 4 stirrups	1.20
T5	134	2.5	10-#9 bars (from beam design longitudinal reinforcement)	10.00

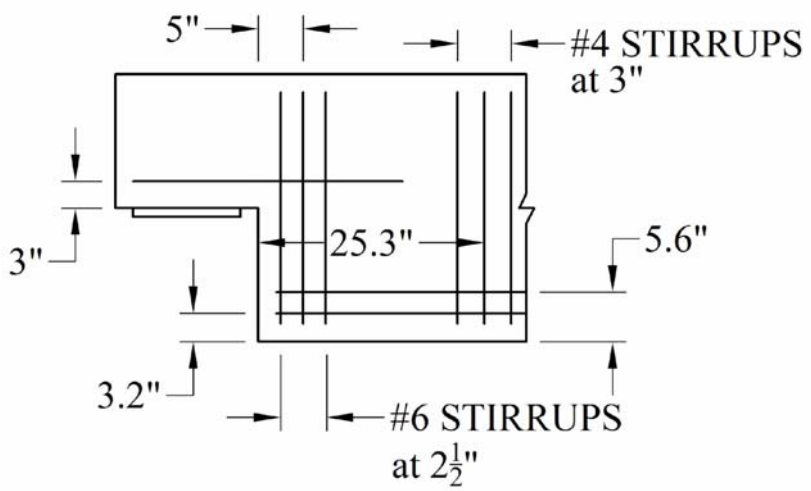

Figure A.4-3: Proposed tie reinforcement details.

Step 7 (a) – Check the capacity of the struts.

In order to check the capacities of the struts, the area of the struts must be determined. The strut areas were calculated by finding the product of the widths and depths of each of the struts. The strut width, w_s, refers to the dimension of the struts in the plane of the STM. AASHTO LRFD Figure 5.6.3.3.2-1 gives guidance of how to determine the width of struts based on the geometry of bearing pads and tie reinforcement details. The widths of Struts 1, 2, 3, 4, and 6 were determined using AASHTO LRFD Figure 5.6.3.3.2-1(a). A portion of AASHTO LRFD Figure 5.6.3.3.2-1(a) has been reproduced in Figure A.4-4. Figure A.4-4 shows that the boundaries of the strut are allowed to extend a distance of up to 6 bar diameters beyond a piece of anchored reinforcement. The only time that this rule does not apply is when extending the boundaries of a strut causes it to overlap with another strut or the boundary of the D-region itself. It should also be noted that Figure A.4-4 displays an equation that can be used to calculate the strut widths. Table A.4-3 summarizes the strut width calculations for Struts 1, 2, 3, 4, and 6.

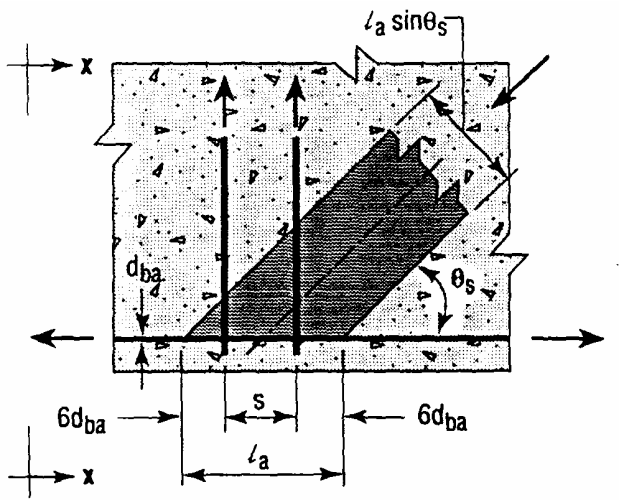

Figure A.4-4: Portion of AASHTO LRFD Figure 5.6.3.3.2-1(a).

Table A.4-3: Calculated strut widths based on Figure A.4-4.

Member	Connecting Tie	θ_s (degrees)	l_a (in)	$w_s = l_a \sin(\theta_s)$ (in)
S1	T2	35.1	10.0	5.7
S2	T2	39.3	10.0	6.3
S3	T2	50.7	10.0	7.7
S4	T4	45.0	9.4	6.6
S6	T4	45.0	9.4	6.6

The widths for struts 5 and 7 were determined by multiplying the distance from the centroid of the tie to the top of the beam by two (the $6d_b$ rule did not govern). The depth of a strut is the dimension transverse to the plane that the STM was developed in. Based on the AASHTO LRFD Figure 5.6.3.3.2-1(a) which shows the $6d_b$ rule, the depth of all the members was determined to be 18 in. (the full depth of the member). Table A.4-4 summarizes the calculated widths and cross-sectional areas of all the members. The values for ties were included in this table because these values are needed for the node capacity check calculations in Step 7(b). Figure A.4-5 shows the strut widths superimposed on the STM.

Table A.4-4: Member effective widths and cross-sectional areas.

Member	Width (in)	at Node	A_{cs} (in^2)
S1	5.7	2	103.4
S2	6.3	2 and 4	114.1
S3	7.7	3 and 4	139.4
S4	6.6	4 and 6	119.6
S5	5.8	2 and 6	104.4
S6	6.6	5	119.6
S7	5.8	6	104.4
T1	6.0	1 and 4	108.0
T2	10.0	2 and 3	180.0
T3	8.8	3	158.4
T4	9.4	5 and 6	171.0
T5	8.8	5	158.4

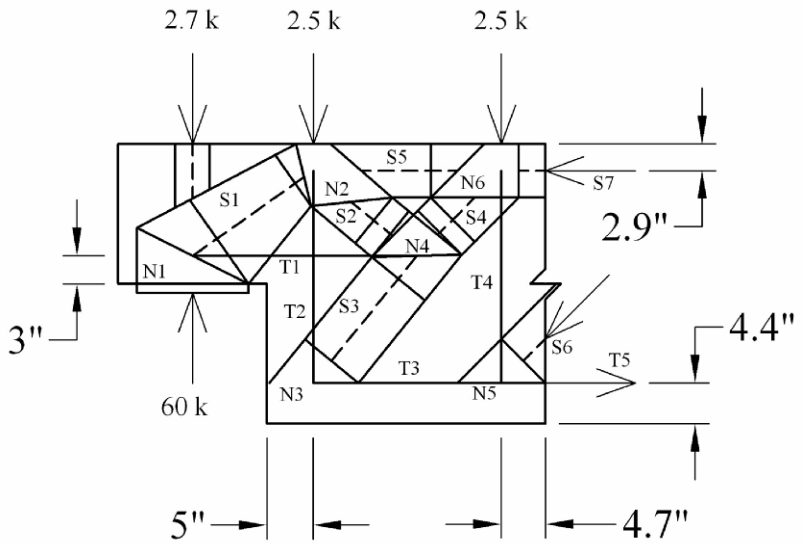

Figure A.4-5: Visualization of strut widths.

Once the areas of the struts were determined, the capacities of the struts were checked according to Section 5.6.3.3.3 of the AASHTO LRFD. For each strut, the strain in the adjoining tie, ε_s, was estimated, in order to determine the principal tensile strain, ε_1, in the strut. The strain in a tie can be estimated to be:

$$\varepsilon_s = \frac{P_{u,Tie}}{A_{st} E_s}$$

After the strain in the tie is determined, the principal tensile strain in the concrete is calculated according to AASHTO LRFD eq. 5.6.3.3.3-2 as:

$$\varepsilon_1 = \varepsilon_s + (\varepsilon_s + 0.002)\cot^2(\alpha_s) \qquad \text{(AASHTO LRFD eq. 5.6.3.3.3-2)}$$

The limiting compressive stress (f_{cu}) in the tie can now be calculated:

$$f_{cu} = \frac{f'_c}{0.8 + 170\varepsilon_1} \le 0.85 f'_c \qquad \text{(AASHTO LRFD eq. 5.6.3.3.3-1)}$$

For members connected to more than one tie, the limiting compressive stress in the strut was calculated based on each of the ties separately, and the smaller of the two compressive stresses was taken as the limiting compressive stress for the strut. Finally, the capacity of the strut can be calculated by multiplying the limiting compressive stress with the smallest calculated area of the strut at either end of the strut.

$$\phi P_n = \phi f_{cu} A_{cs} \qquad \text{(AASHTO LRFD eq. 5.6.3.3.1-1)}$$

For compression in a STM, ϕ is taken as 0.70 (AASHTO LRFD 5.5.4.2.1). Table A.4-5 summarizes the calculations performed for each of the struts. All of the struts were found to have adequate capacity.

It should be noted that Strut 8 was not checked because it will easily be able to support the very small load (2.7 kips) applied to it.

Table A.4-5: Summary of strut calculations.

Strut	P_u (k)	Tie Force (k)	A_{st} (in^2)	α_s (degrees)	ε_s	ε_1	f_{cu}	ΦP_n (k)	$\Phi P_n > P_u$?
S1	100	82	1.55	35.1	0.001824	0.009586	2.06	149	yes
S2	71	82	1.55	39.3	0.001824	0.00752	2.41	192	yes
	71	100	2.64	50.7	0.001306	0.003526	3.57	-	-
S3	129	100	2.64	39.3	0.001306	0.006253	2.68	262	yes
	129	82	10.00	50.7	0.000283	0.001808	4.25	-	-
S4	78	82	1.55	45.0	0.001824	0.005648	2.84	238	yes
	78	53	1.20	45.0	0.001523	0.005046	3.02	-	-
S5	27	100	1.55	90.0	0.002225	0.002225	4.24	310	yes
	27	53	1.20	90.0	0.001523	0.001523	4.25	-	-
S6	74	53	1.20	45.0	0.001523	0.005046	3.02	253	yes
	74	108	10.00	45.0	0.000372	0.002745	3.95	-	-
S7	82	53	1.20	90.0	0.001523	0.001523	4.25	311	yes

Step 7(b) – Check the capacity of the nodes.

The capacities of the nodes need to be checked for the forces imposed by the anchored ties, at node/strut interfaces where the strut capacity was determined to be larger than the allowable node capacity, and for bearing caused by applied loads or boundary loads. Table A.4-6 summarizes the locations where node/strut interfaces need to be checked due to the fact the calculated strut limiting compressive stress is larger than the allowable node limiting compressive stress. According to AASHTO LRFD 5.6.3.5, the limiting compressive stresses are $0.85f'_c$, $0.75f'_c$, and $0.65f'_c$ for CCC, CCT, and CTT nodes, respectively.

Table A.4-6: Summary of determining whether strut capacities exceed node capacities.

Strut	Strut f_{cu} (ksi)	Nodes	Node Type	Node f_{cu} (ksi)	Check Node/Strut Interface?
S1	2.06	Node 1	CCT	3.75	no
	2.06	Node 2	CCT	3.75	no
S2	2.41	Node 2	CCT	3.75	no
	2.41	Node 4	CCT	3.75	no
S3	2.68	Node 3	CTT	3.25	no
	2.68	Node 4	CCT	3.75	no
S4	2.84	Node 4	CCT	3.75	no
	2.84	Node 6	CCT	3.75	no
S5	4.24	Node 2	CCT	3.75	yes
	4.24	Node 6	CCT	3.75	yes
S6	3.02	Node 5	CTT	3.25	no
S7	4.25	Node 6	CCT	3.75	yes

Based on Table A.4-6, the capacities of the nodes were checked at the critical node/strut interfaces in addition to node capacity checks for forces imposed by anchored ties, applied loads, and equivalent loads. The capacity of each node was determined by multiplying the limiting compressive stress of the node with the area of the node face to be checked. The concrete areas, A_{cs}, used to determine the node capacity were determined in Step 7(a). The values are shown in Table A.4-4. Table A.4-7 summarizes the node capacity check calculations. All of the nodes interfaces were found to have adequate capacity.

Table A.4-7: Summary of node capacity calculations.

Node	Type	f_{cu} (ksi)	Adjoining Member	A_{cs} (in^2)	P_u (k)	ΦP_n (k)	$\Phi P_n > P_u$?
Node 1	CCT	3.75	Bearing Pad	216	50	567	yes
	CCT	3.75	T1	108	82	284	yes
Node 2	CCT	3.75	S5	104	27	274	yes
	CCT	3.75	Equivalent Load	67	3	175	yes
	CCT	3.75	T2	180	100	473	yes
Node 3	CTT	3.25	T2	180	100	410	yes
	CTT	3.25	T3	158	82	360	yes
Node 4	CCT	3.75	T1	108	82	284	yes
Node 5	CTT	3.75	T5-T3	158	52	416	yes
	CTT	3.75	T4	171	53	449	yes
Node 6	CCT	3.75	S5	104	27	274	yes
	CCT	3.75	S6	120	74	314	yes
	CCT	3.75	T4	171	53	449	yes

Step 8(a) – Check the detailing for the anchorage of the ties.

At Node 1, the #5 bars chosen for Tie 1 must be properly anchored with a 180-degree or 90-degree hook. Due to the limited height in the dapped section of the beam, a 180-degree hook will be used. According to Section 5.11.2.4.1, the development length, ℓ_{dh}, for a #5 bar with a hook can be determined as follows:

$$\ell_{dh} = \frac{38.0 \cdot d_b}{\sqrt{f'_c}} = \frac{38 \cdot .625in}{\sqrt{5ksi}} = 10.7in \qquad \text{(AASHTO LRFD Eq. 5.11.2.4.1-1)}$$

Typically, for a tie being "pinched" between a bearing pad and an inclined strut, it is considered conservative to ensure the bar is anchored before passing the edge of the bearing plate. Based on this, the available anchorage is 12 in. which is satisfactory. See Figure A.4-6.

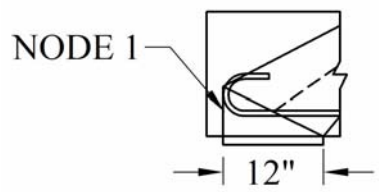

Figure A.4-6: Anchorage details for Tie 1 at Node 1.

At Node 4, #5 bars for Tie 1 will not have hooks. The required development length is calculated to be:

$$\ell_{db} = \frac{1.25 \cdot A_b \cdot f_y}{\sqrt{f'_c}} = \frac{1.25 \cdot 0.31in \cdot 60ksi}{\sqrt{5ksi}} = 10.4in \qquad \text{(AASHTO LRFD 5.11.2.1)}$$

Because more than 12 in. of concrete is cast below the bars, the development length must be increased by a factor of 1.4. Therefore, the bars must be extended at least 15 inches beyond Node 4. To be conservative, the #5 bars will be extended 15 in. beyond Tie 4.

A mechanical anchorage plate will be used to anchor the #9 bars in Tie 3 at Node 3. This detail will be shown in Figure A.4-7 at the end of the example. The capacity of Node 3 has already been verified for the force caused by the plate anchoring Tie 3 in Table A.4-7.

It will be assumed that the details of the stirrups chosen for Ties 2 and 4 will conform to AASHTO LRFD 5.11.2.6.4, and, therefore, the stirrups will be considered properly anchored.

Step 8(b)- Detail the crack control reinforcement.

Appropriate crack control must be detailed in order for the design to conform to Section 5.6.3.6 of the AASHTO LRFD.

In the dapped section of the beam, it will be assumed that 5 stirrups spaced at 3.5 inches are used. Based on this spacing, the required stirrup area is calculated to be:

$$A_{st-required} = 0.003 \cdot b \cdot s = 0.003 \cdot 18in \cdot 3.5in = 0.189in^2$$

Therefore, #3 stirrups will satisfy this requirement (A_{st} = 0.22 in^2).

Between ties T2 and T4, if two stirrups are used spaced at approximately 5 inches, the required stirrup area is calculated to be:

$$A_{st-required} = 0.003 \cdot b \cdot s = 0.003 \cdot 18in \cdot 5in = 0.27in^2$$

Therefore, # 4 stirrups will satisfy this requirement (A_{st} = 0.4 in^2).

If the maximum spacing of horizontal crack control is taken to be 6 in., the required area of steel is calculated to be:

$$A_{st-required} = 0.003 \cdot b \cdot s = 0.003 \cdot 18in \cdot 6in = 0.324in^2$$

Therefore, 2 #4 bars spaced at 6 in. or less will satisfy this requirement (A_{st} = 0.4 in^2).

See Figure A.4-7 for the final details of the dapped-end of the beam.

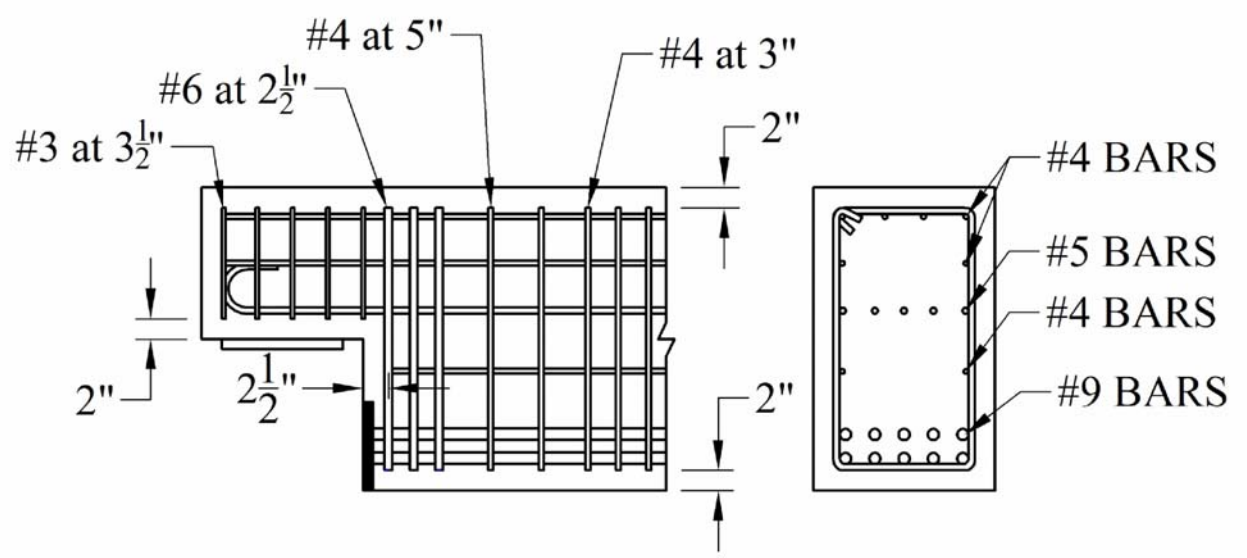

Figure A.4-7: Final detail of the dapped-end of the beam. The maximum spacing between the horizontal #4 bars for crack control should be 6 in. or less.

Example A.5: Beam with Hole in the Web

The problem statement is given as part of the Example A.4 problem statement.

Step 1 – Delineate the D-regions.

The D-region is assumed to extend a distance of 30 in. (the height of the member) in each direction away from the hole in the web. See Figure A.5-1 to see the extent of the D-region.

Step 2 – Determine the boundary conditions of the D-region.

The boundary conditions on the D-region are shown in Figure A.5-1.

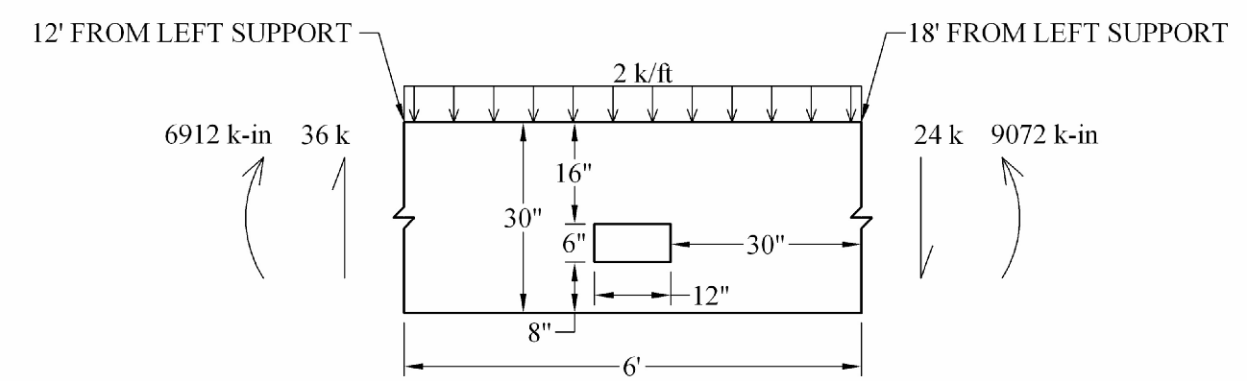

Figure A.5-1: Geometry and boundary conditions of D-region.

Steps 3, 4, and 5 – Sketch flow of forces, develop a truss model, and solve for member forces.

In order to determine the flow of forces through the D-region, a STM was sketched to approximate the flow of forces. The sketch of the STM can be seen in Figure A.5-2. Only the nodes are numbered in the figure. The strut and tie labels can be seen in Figure A.5-3. Struts 1, 3, 6, 8, and 12 are located at the centroid of the calculated compressive stress block determined from the beam design. Ties 2, 3, 8, and 10 are located at the centroid of the tensile reinforcement determined from the beam design. Ties 1, 5, 7, and 9 are intended to represent bands of vertical stirrups, and were spaced at equal distances. Struts 2, 4, 5, 7, 9, 10, 11, and 13 are inclined struts used to carry loads between the ties representing bands of stirrups. The locations of Ties 4 and 6 were determined based on ensuring static equilibrium at Nodes 3, 5, and 7.

Based on the geometry of the developed STM, the distributed load on the top of the beam was converted into three equivalent point loads applied at Nodes 1, 4, and 9. Similarly, the equivalent loads on the boundary of the D-region shown in Figures A.5-2 and A.5-3 were determined based on the geometry of the STM and the known boundary conditions shown in Figure A.5-1. The process of determining equivalent boundary loads based on the geometry of the STM and known boundary conditions is shown in Figure A.5-4.

The calculated member forces are given in Table A.5-1. Table A.5-1 also gives the inclination of each member (smallest angle from the horizontal).

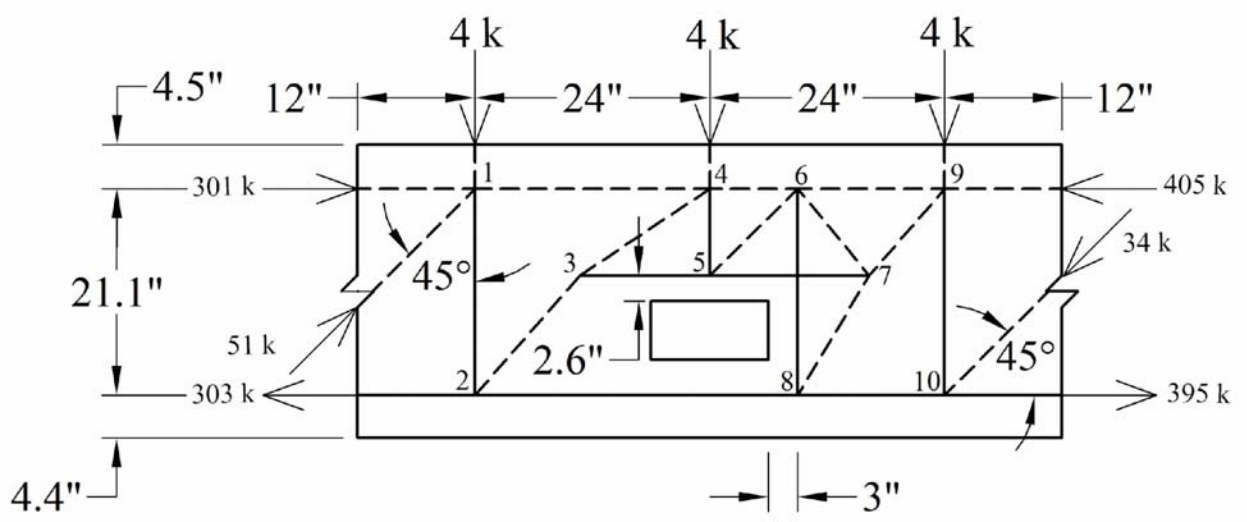

Figure A.5-2: STM developed to model the flow of forces. The nodes are labeled.

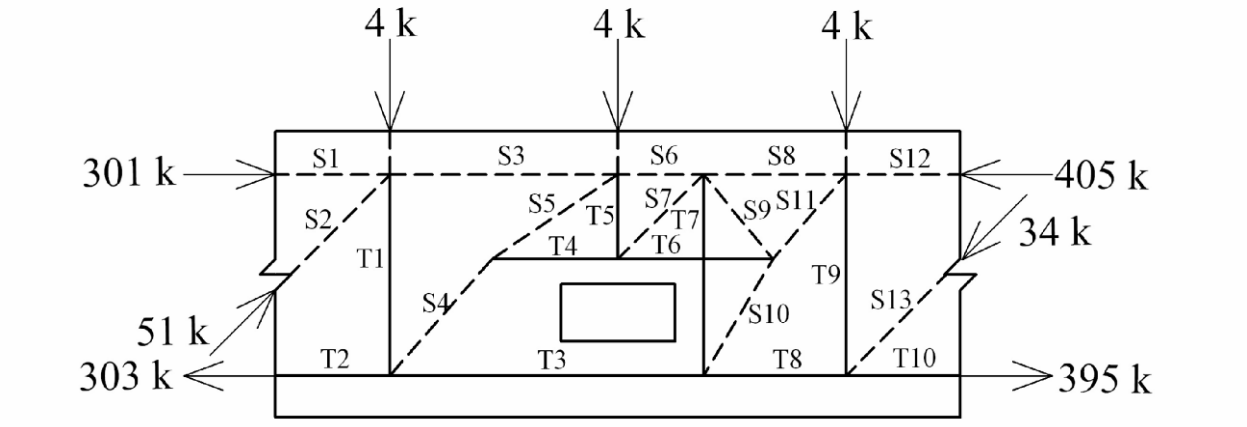

Figure A.5-3: Strut and tie labels.

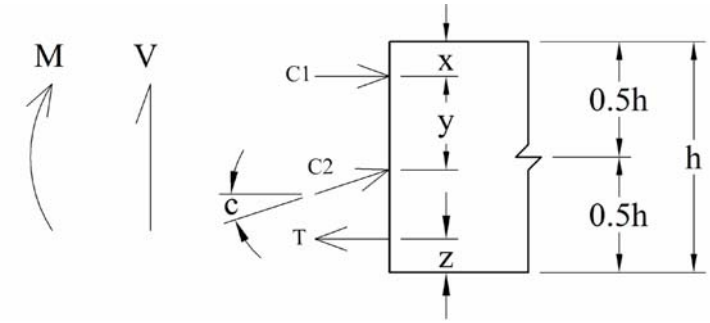

Solve system of equations to determine equivalent boundary loads:

$$\sum F_y: \quad V = C2 \cdot \sin(c)$$

$$\sum F_x: \quad 0 = C2 \cdot \cos(c) + C1 - T$$

$$\sum M: \quad M = C1 \cdot (0.5h - x) - (C2 \cdot \cos(c)) \cdot (x + y - 0.5h) + T(0.5h - z)$$

Figure A.5-4: Illustration of how to determine equivalent boundary loads based on STM geometry and boundary conditions of D-region

Table A.5-1: Member forces and inclinations (smallest angle from horizontal).

Member	Angle (degrees)	Force (k)
S1	0.0	301
S2	45.0	51
S3	0.0	337
S4	48.8	43
S5	33.8	58
S6	0.0	385
S7	44.6	40
S8	0.0	381
S9	50.6	52
S10	59.3	79
S11	49.0	38
S12	0.0	405
S13	45.0	34
T1	90.0	32
T2	0.0	303
T3	0.0	331
T4	0.0	20
T5	90.0	28
T6	0.0	49
T7	90.0	68
T8	0.0	371
T9	90.0	24
T10	0.0	395

Step 6 – Select steel area for the ties.

As with Example A-4, Section 5.6.3.4 of the AASHTO LRFD Specifications was used to determine the required amount of reinforcement for each tie. Table A.5-2 summarizes the tie calculations and the reinforcement chosen to satisfy the required calculated areas. Figure A.5-5 illustrates the proposed tie placement. In Figure A.5-5, it should be noted that the stirrup chosen for Tie 7 was duplicated on the other side of the opening to ensure that the hole is "framed".

Table A.5-2: Summary of tie design.

Tie	Tie Force (k)	$A_{st,required}$ (in^2)	Choose	$A_{st,provided}$ (in^2)
T1	32	0.6	2-#4 Stirrups	0.80
T2	304	5.6	10-#9 Bars (from beam design longitudinal reinforcement)	10.00
T3	332	6.1	10-#9 Bars (from beam design longitudinal reinforcement)	10.00
T4	30	0.6	5-#9 Bars	5.00
T5	28	0.5	2-#4 Stirrups	0.80
T6	87	1.6	5-#9 Bars	5.00
T7	72	1.3	1-#6 4-Legged Stirrup	1.76
T8	367	6.8	10-#9 Bars (from beam design longitudinal reinforcement)	10.00
T9	24	0.4	2-#4 Stirrups	0.80
T10	393	7.3	10-#9 Bars (from beam design longitudinal reinforcement)	10.00

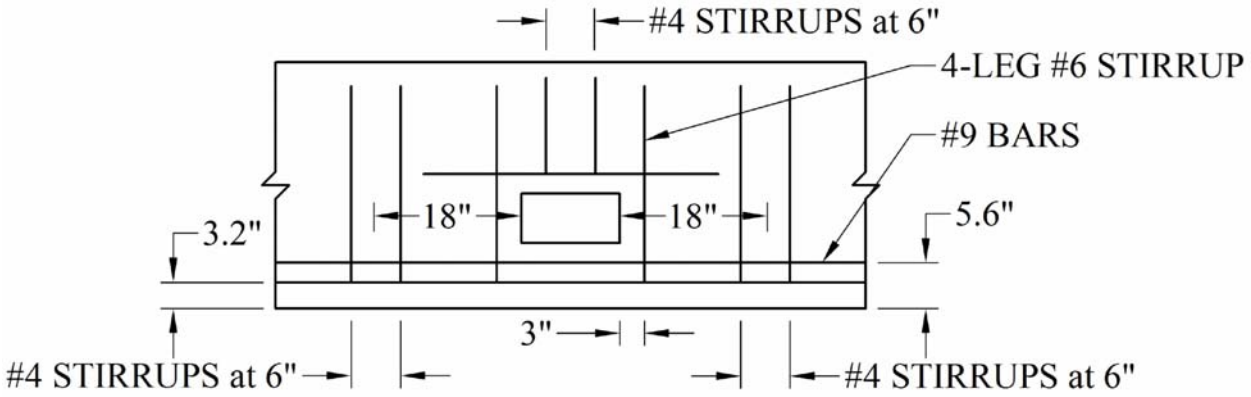

Figure A.5-5: Proposed tie reinforcement placement.

Step 7 (a) – Check the capacity of the struts.

In order to check the capacities of the struts, the area of the struts must be determined. The areas were calculated by finding the product of the widths and depths of each of the struts. The strut width, w_s, refers to the dimension of the strut in the plane of the STM. Struts 1, 3, 6, 8, and 12 can be considered prismatic struts because they are in the compressive stress block region of the beam. The widths of these struts can be determined doubling the distance from the centroid of the strut to the top of the beam; therefore, the widths of Struts 1, 3, 6, 8, and 12 are all calculated to be 9 in.

The widths of inclined Struts 2, 4, 5, 7, 9, 10, 11, and 13 were determined using AASHTO LRFD Figure 5.6.3.3.2-1(a). A portion of the figure has been reproduced in Figure A.5-6.

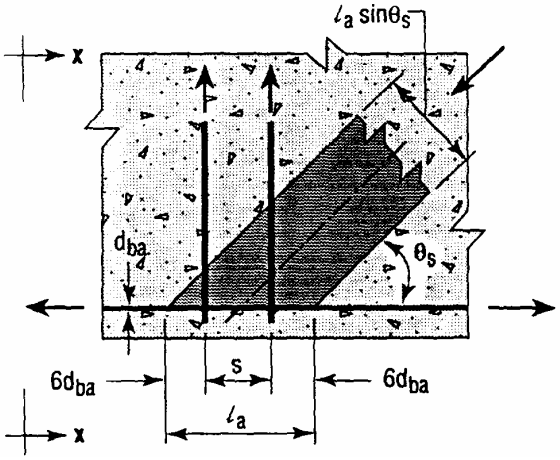

Figure A.5-6: Portion of AASHTO LRFD Figure 5.6.3.3.2-1(a).

Figure A.5-6 shows that the boundaries of a strut are allowed to extend a distance of up to 6 bar diameters beyond a piece of anchored reinforcement. The boundaries of a strut may extend a distance less than 6 bar diameters beyond a piece of anchored reinforcement in order to prevent the strut boundaries from overlapping with other strut boundaries or prevent the strut boundaries from extending beyond the boundaries of the D-region. Also, it should be noted that Figure A.5-6 illustrates how to calculate the strut widths given the inclination of the strut and effective width of the tie. Table A.5-3 summarizes the strut calculations for Struts 2, 4, 5, 7, 9, 10, 11, and 13.

Table A.5-3: Calculated strut widths based on Figure A.5-6.

Member	Connecting Tie	θ_s (degrees)	l_a (in)	$w_s = l_a \sin(\theta_s)$ (in)
S2	T1	45.0	12	8.5
S4	T1	48.8	12	9.0
S5	T5	33.8	12	6.7
S7	T7	44.6	6	4.2
S9	T7	50.6	6	4.6
S10	T7	59.3	6	5.2
S11	T9	49.0	12	9.1
S13	T9	45.0	12	8.5

The depth of a strut is the dimension transverse to the plane that the STM was developed in. Based on the AASHTO LRFD Figure 5.6.3.3.2-1(a) which shows the $6d_b$ rule, the depth of all the members was determined to be 18 in. (the full depth of the member). Table A.5-4 summarizes the calculated widths and cross-sectional areas of all the members. The values for ties were included in this table because these values are needed for the node capacity check calculations in Step 7(b). Figure A.5-7 shows the strut widths superimposed on the STM.

Table A.5-4: Member effective widths and areas.

Member	Width (in)	A_{cs} (in^2)
S1	9.0	162
S2	8.5	153
S3	9.0	162
S4	9.0	163
S5	6.7	120
S6	9.0	162
S7	4.2	76
S8	9.0	162
S9	4.6	83
S10	5.2	93
S11	9.1	163
S12	9.0	162
S13	8.5	153
T1	12.0	216
T2	8.0	144
T3	8.0	144
T4	5.2	94
T5	12.0	216
T6	5.2	94
T7	6.0	108
T8	8.0	144
T9	12.0	216
T10	8.0	144

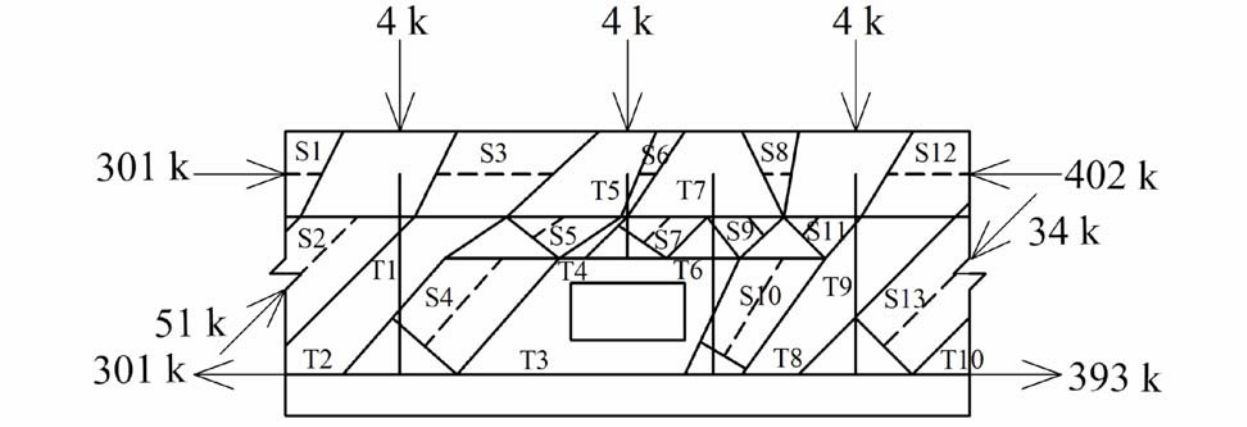

Figure A.5-7: Visualization of strut widths.

As with example A-4, once the areas of the struts were determined, the capacities of the struts were checked according to Section 5.6.3.3.3 of the AASHTO LRFD. For each strut, the strain in the adjoining tie, ε_s, was estimated, in order to determine the principal tensile strain, ε_1, in the strut. The strain in a tie can be estimated to be:

$$\varepsilon_s = \frac{P_{u,Tie}}{A_{st} E_s}$$

After the strain in the tie is determined, the principal tensile strain in the concrete is calculated according to AASHTO LRFD eq. 5.6.3.3.3-2 as:

$$\varepsilon_1 = \varepsilon_s + (\varepsilon_s + 0.002)\cot^2(\alpha_s) \qquad \text{(AASHTO LRFD eq. 5.6.3.3.3-2)}$$

The limiting compressive stress (f_{cu}) in the tie can now be calculated.

$$f_{cu} = \frac{f'_c}{0.8 + 170\varepsilon_1} \le 0.85 f'_c \qquad \text{(AASHTO LRFD eq. 5.6.3.3.3-1)}$$

For members connected to more than one tie, the limiting compressive stress in the strut was calculated based on each of the ties separately, and the smaller of the two compressive stresses was taken as the limiting compressive stress for the strut. Finally, the capacity of the strut can be calculated by multiplying the limiting compressive stress with the smallest calculated area of the strut at either end of the strut.

$$\phi P_n = \phi f_{cu} A_{cs} \qquad \text{(AASHTO LRFD eq. 5.6.3.3.1-1)}$$

For compression in a STM, ϕ is taken as 0.70 (AASHTO LRFD 5.5.4.2.1). Table A.5-5 summarizes the calculations performed for each of the struts. All of the struts were found to have adequate capacity.

Table A.5-5: Summary of strut calculations.

Strut	P_u (k)	Tie Force (k)	A_{st} (in^2)	α_s (degrees)	ε_s	ε_1	f_{cu}	ΦP_n (k)	$\Phi P_n > P_u$?
S1	301	32	0.80	90.0	0.00138	0.00138	4.25	482	yes
S2	51	32	0.80	45.0	0.00138	0.00476	3.11	332	yes
S3	337	32	0.80	90.0	0.00138	0.00138	4.25	482	yes
	337	28	0.88	90.0	0.00110	0.00110	4.25	-	-
S4	43	32	0.80	41.2	0.00138	0.00579	2.80	319	yes
	43	317	10.00	48.8	0.00109	0.00346	3.60	-	-
	43	20	1.00	48.8	0.00069	0.00275	3.94	-	-
S5	58	20	1.00	33.8	0.00069	0.00669	2.58	217	yes
	58	28	0.88	56.2	0.00110	0.00249	4.09	-	-
S6	385	28	0.88	90.0	0.00110	0.00110	4.25	-	-
	385	68	0.88	90.0	0.00266	0.00266	3.99	453	yes
S7	40	34	1.00	44.6	0.00118	0.00444	3.21	-	-
	40	28	0.88	45.4	0.00110	0.00411	3.34	-	-
	40	68	1.76	45.4	0.00133	0.00457	3.17	168	yes
S8	380	68	1.76	90.0	0.00133	0.00133	4.25	482	yes
	380	24	0.80	90.0	0.00103	0.00103	4.25	-	-
S9	52	49	1.00	50.6	0.00169	0.00418	3.31	-	-
	52	68	1.76	39.4	0.00133	0.00627	2.68	157	yes
S10	79	49	1.00	59.3	0.00169	0.00299	3.82	-	-
	79	68	1.76	30.7	0.00133	0.01078	1.90	123	yes
	79	351	10.00	59.3	0.00121	0.00234	4.17	-	-
S11	38	49	1.00	49.0	0.00169	0.00448	3.20	-	-
	38	24	0.80	41.0	0.00103	0.00505	3.01	344	yes
S12	405	24	0.80	90.0	0.00103	0.00103	4.25	482	yes
S13	34	24	0.80	45.0	0.00103	0.00407	3.35	-	-
	34	383	10.00	45.0	0.00132	0.00464	3.15	336	yes

Step 7(b) – Check the capacity of the nodes.

The capacities of the nodes need to be checked for the forces imposed by the anchored ties, at node/strut interfaces where the strut capacity was determined to be larger than the node capacity, and for bearing caused by applied loads or boundary loads. Table A.5-6 summarizes the locations where node/strut interfaces need to be checked (locations where the calculated strut limiting compressive stress is larger than the allowable node limiting compressive stress). The node limiting compressive stress was determined by multiplying the concrete strength by the appropriate reduction factor. According to AASHTO LRFD 5.6.3.5, the limiting compressive stresses are $0.85f'_c$, $0.75f'_c$, and $0.65f'_c$ for CCC, CCT, and CTT nodes, respectively.

Table A.5-6: Summary of determining whether strut capacities exceed node capacities.

Strut	Strut f_{cu} (ksi)	Nodes	Node Type	Node f_{cu} (ksi)	Check Node/Strut Interface?
S1	4.25	Node 1	CCT	3.75	yes
S2	3.11	Node 1	CCT	3.75	no
S3	4.25	Node 1	CCT	3.75	yes
	4.25	Node 4	CCT	3.75	yes

Table A.5-6 (cont.): Summary of determining whether strut capacities exceed node capacities.

Strut	Strut f_{cu} (ksi)	Nodes	Node Type	Node f_{cu} (ksi)	Check Node/Strut Interface?
S4	2.80	Node 2	CTT	3.25	no
	2.80	Node 3	CCT	3.75	no
S5	2.58	Node 3	CCT	3.75	no
	2.58	Node 4	CCT	3.75	no
S6	3.99	Node 4	CCT	3.75	yes
	3.99	Node 6	CCT	3.75	yes
S7	3.21	Node 5	CCT	3.75	no
	3.21	Node 6	CCT	3.75	no
S8	4.25	Node 6	CCT	3.75	yes
	4.25	Node 9	CCT	3.75	yes
S9	3.31	Node 6	CCT	3.75	no
	3.31	Node 7	CCT	3.75	no
S10	1.90	Node 7	CCT	3.75	no
	1.90	Node 8	CTT	3.25	no
S11	3.01	Node 7	CCT	3.75	no
	3.01	Node 9	CCT	3.75	no
S12	4.25	Node 9	CCT	3.75	yes
S13	3.15	Node 10	CTT	3.25	no

Based on Table A.5-6, the capacities of the nodes were checked for strut forces at critical node/strut interfaces as well as for forces imposed by ties and forces imposed by applied loads or boundary loads. Table A.5-7 summarizes the node capacity check calculations. The concrete areas, A_{cs}, used to determine the node capacities at each iterface were determined in Step 7(a). The values are shown in Table A.5-4. All of the nodes interfaces were found to have adequate capacity.

Table A.5-7: Summary of node capacity calculations.

Node	Type	f_{cu} (ksi)	Adjoining Member	A_{cs} (in^2)	P_u (k)	ΦP_n (k)	$\Phi P_n > P_u$?
Node 1	CCT	3.75	S1	162	301	425	yes
	CCT	3.75	S3	162	337	425	yes
	CCT	3.75	Equivalent Load	216	4	567	yes
	CCT	3.75	T1	216	32	567	yes
Node 2	CTT	3.25	T1	216	32	491	yes
	CTT	3.25	T3-T2	144	28	328	yes
Node 3	CTT	3.75	T4	94	20	246	yes
Node 4	CCT	3.75	S3	162	337	425	yes
	CCT	3.75	S6	162	385	425	yes
	CCT	3.75	Equivalent Load	216	4	567	yes
	CCT	3.75	T5	216	28	567	yes
Node 5	CTT	3.25	T5	216	28	491	yes
	CTT	3.25	T6-T4	94	29	213	yes

Table A.5-7 (cont.): Summary of node capacity calculations.

Node	Type	f_{cu} (ksi)	Adjoining Member	A_{cs} (in^2)	P_u (k)	ΦP_n (k)	$\Phi P_n > P_u$?
Node 6	CCT	3.75	S6	162	385	425	yes
	CCT	3.75	S8	162	381	425	yes
	CCT	3.75	T7	108	68	284	yes
Node 7	CCT	3.75	T6	94	49	246	yes
Node 8	CTT	3.25	T7	108	68	246	yes
	CTT	3.25	T8-T3	144	68	328	yes
Node 9	CCT	3.75	S8	162	381	425	yes
	CCT	3.75	S12	162	405	425	yes
	CCT	3.75	Equivalent Load	216	4	567	yes
	CCT	3.75	T9	216	24	567	yes
Node 10	CTT	3.25	T9	216	24	491	yes
	CTT	3.25	T10-T8	144	24	328	yes

Step 8(a) – Check the detailing for the anchorage of the ties.

At Nodes 3 and 7, the #4 bars chosen for ties T4 and T6 must be properly anchored. According to Section 5.11.2.1, the development length, ℓ_{db}, for a #4 bar with no anchorage mechanisms is calculated to be:

$$\ell_{db} = \frac{1.25 \cdot A_b \cdot f_y}{\sqrt{f'_c}} = \frac{1.25 \cdot 0.20in^2 \cdot 60ksi}{\sqrt{5ksi}} = 6.7in \qquad \text{(AASHTO LRFD 5.11.2.1.1)}$$

However, the calculated development length for a straight bar can not be less than 12 in. To conservatively fulfill this requirement, the #4 bars will be extended 20 in. past the edge of the rectangular opening in each direction. With this arrangement, approximately 18 in. of anchorage length has been provided for Node 3, and approximately 14 in. of anchorage length has been provided for Node 7. See Figure A.5-8 for the anchorage length detail of the #4 bars.

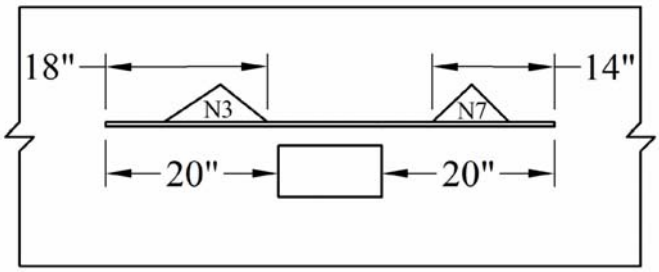

Figure A.5-8: Anchorage details for #4 bars above opening.

Anchorage requirements for the reinforcement for ties 2, 3, 8, and 10 does not need to be detailed because the bars do not terminate in the D-region. The anchorage details for the stirrups designed for Ties 1, 5, 7, and 9 will be assumed to conform to AASTHO LRFD 5.11.2.6.4 and, therefore, be satisfactory.

Step 8(b)- Detail the crack control reinforcement.

The crack control details must conform to the provisions of AASHTO LRFD 5.6.3.6. For Ties 1, 5, and 7 #4 stirrups at 6 in. were designed. If a spacing of 6 in. is assumed for all the vertical crack control, the required area of crack control steel is calculated as follows:

$$A_{st-required} = 0.003 \cdot b \cdot s = 0.003 \cdot 18in \cdot 6in = 0.324in^2$$

Therefore, #4 stirrups spaced at 6 in. will satisfy this requirement (A_{st} = 0.40 in^2).

Similarly, if the maximum spacing of horizontal crack control is also assumed to be 6 in, the required area of steel is calculated to be:

$$A_{st-required} = 0.003 \cdot b \cdot s = 0.003 \cdot 18in \cdot 6in = 0.324in^2$$

Therefore, 2 #4 bars spaced at 6 in. or less will satisfy this requirement (A_{st} = 0.40 in^2).

See Figure A.5-9 for the final details of the disturbed region of the beam caused by the rectangular opening.

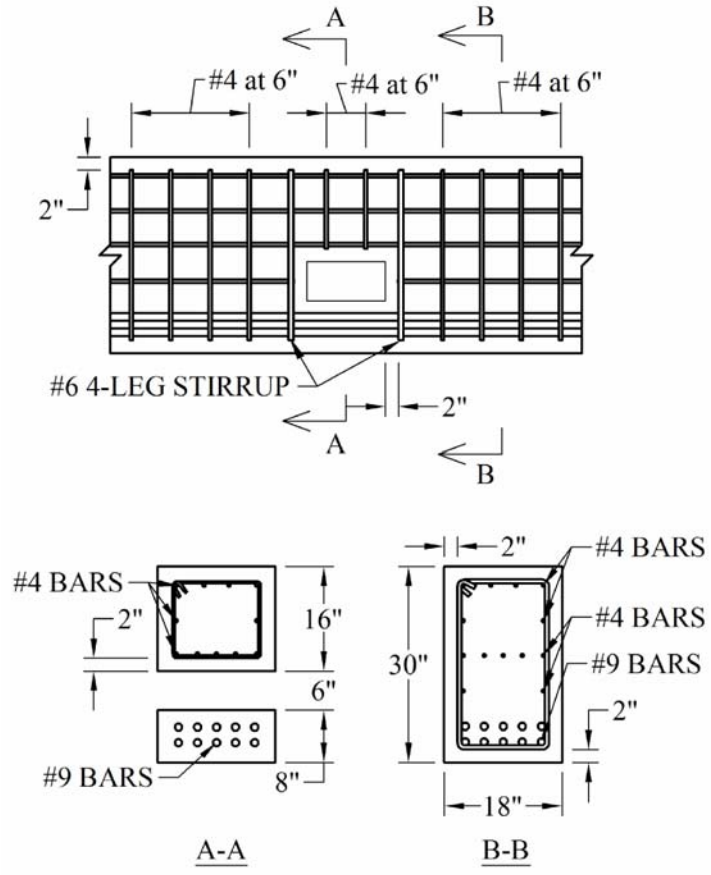

Figure A.5-9: Final detail of the dapped-end of the beam. The maximum spacing between the horizontal #4 bars for crack control should be 6 in. or less.

EXAMPLE A.6 – PIER BASE

Problem Statement:

A river pier is to have the basic configuration shown in Figure A.6-1. The order of construction is to be as follows: drive cofferdam, drive piles, place the tremie seal concrete, pump the cofferdam dry, place footing concrete, place the pier base concrete, then the column bent and the superstructure. The objective is to design the pier base using AASHTO LRFD strut and tie. Steel reinforcing is grade 60 and the concrete in the pier wall has an f_c' of 0.4 ksi.

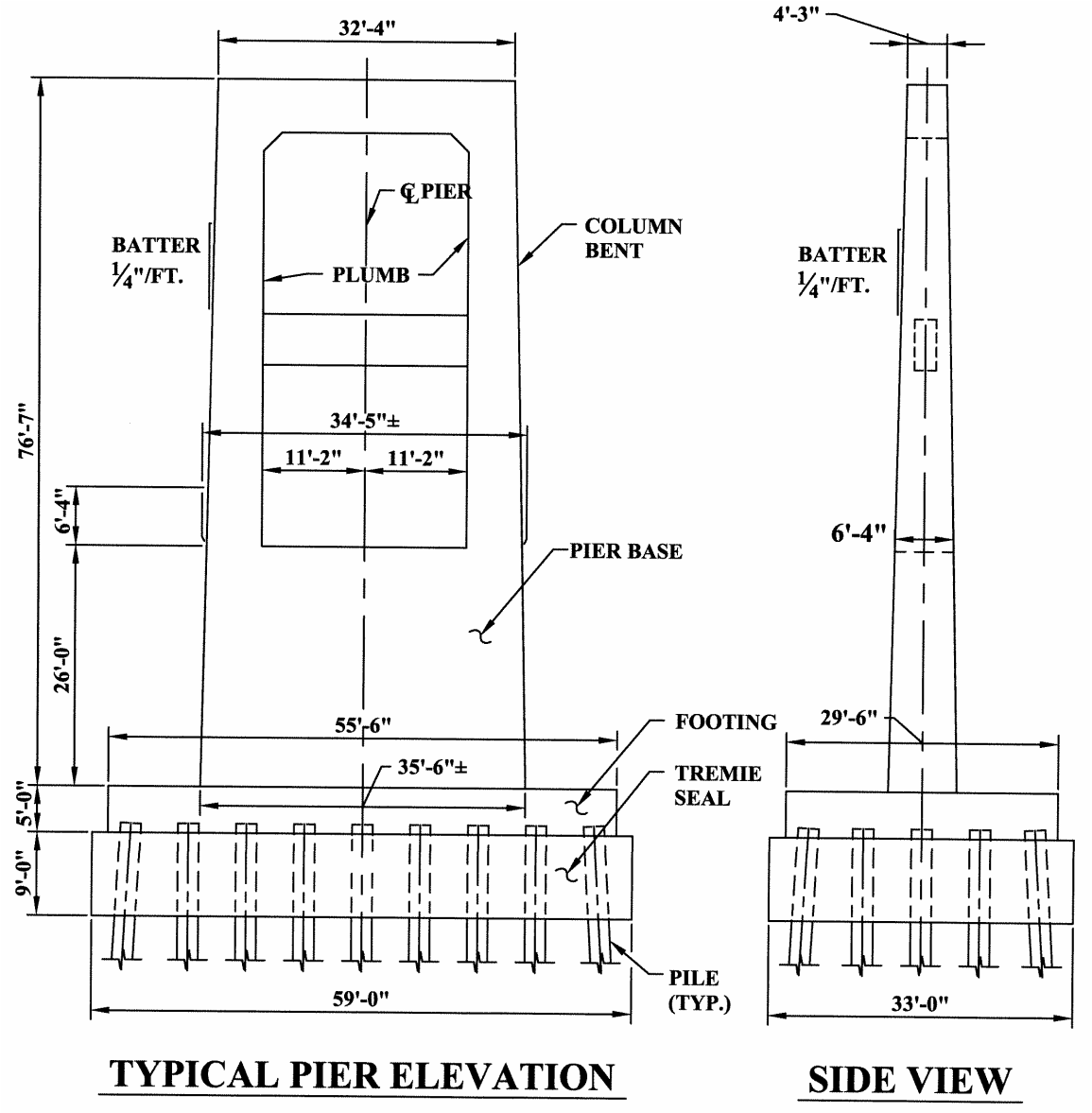

Figure A.6-1: Elevation View of Pier

<u>Step 1</u> – Delineate the D-regions.

The column bents measure 6'-0" by 6'-4" at the top of the pier base. Therefore the idealized D-Regions will be 6'-4" up the column and will include the entire pier base as shown in the Figure below:

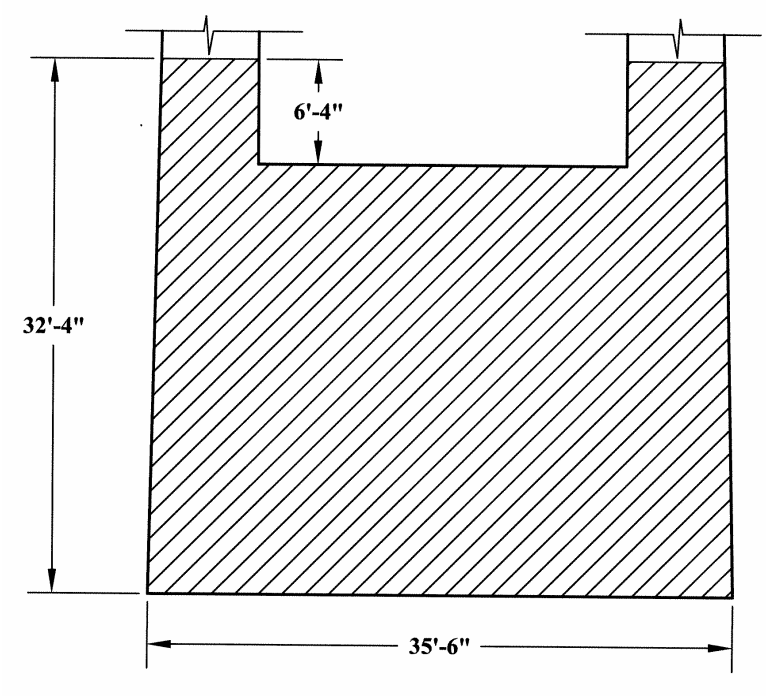

Figure A.6-2: Idealized D-Regions

<u>Step 2</u> – Determine the boundary conditions of the D-region.

Since the focus of this design problem is the Pier Base, it will be necessary to determine the Boundary Conditions at the base of the columns and at the bottom of the Pier Base. Technically, the load conditions 6'-4" up the column should be determined and that portion of the column treated as a D-region. Since the concern of the problem is not the design of the columns, the focus of attention will be the base of the columns.

From a rigid frame analysis of the unfactored dead and live loads it was determined that the reactions at the column bases are:

$D.L. = 1127^{k}$ *Axial*	144^{1-k} *Moment*	26^{k} *Shear*
$LL = 205^{k}$ *Axial*	35^{1-k} *Moment*	6^{k} *Shear*

Total Factored Load at Base of Columns

$$P = 1.25(1127) + 1.75(205) = 1767.5^{k}$$

$$M = 1.25(144) + 1.75(35) = 241.3^{1-k}$$

$$V = 1.25(26) + 1.75(6) = 43^{k}$$

We will conservatively apply the weight of the Pier Base at the column/pier base interface.

Weight of the Pier Base = $\left(\frac{(35.5'+34.42')}{2}\right)(6.875')(26')(0.15kcf) = \frac{937k}{2} = \frac{468k}{column}$

The total axial reaction at the column base =

P + 1.25(weight of pier base) = $1767.5 + 1.25(468k) = 2352.6k$

This results in a total axial reaction at the column base of 2352.6 k.

Resolving the Moment into a Pe we arrive at $241.3\,ft-kip \,/\, 2352.6kips = 0.1ft = 1.25"$

At the base of the columns we get the following:

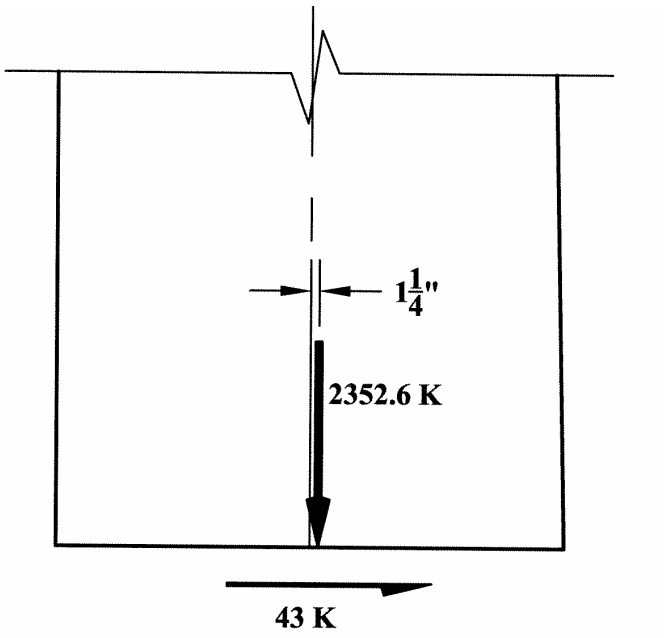

Figure A.6-3: Loads at Base of Column

We will assume a uniform distribution at the bottom of the Pier Base neglecting the moment due to its small magnitude.

$$\frac{2x2352.6kips}{35.5\,ft} = 132.54kips/\,ft$$

Resulting Boundary Conditions

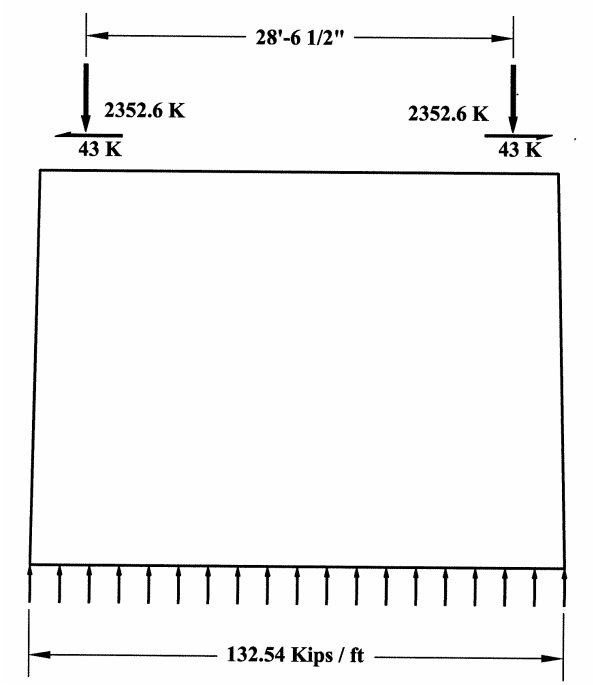

Figure A.6-4: Resulting Boundary Conditions

<u>Steps 3 and 4</u> – Sketch the flow of forces and develop the STM using the visualized flow of forces.

The generalized flow of forces is shown in Figure A.6-5. The idealized strut and tie model is superimposed over the flow of forces. The top tie (member A-B in Figure A.6-6) is located at the assumed centroid of the top reinforcing (12" below the top of concrete). Nodes E and F are placed at the quarter points of the base representing the centroid of the uniform loading at each half of the pier base. The vertical location of nodes C and D is somewhat approximate. There are several approaches such as that shown in AASHTO C5.10.9.4.1-2C and as contained in Schlaich et al. Using Schlaich a value of 0.56 of the horizontal distance between the concentrated loads is arrived at for the vertical distance from nodes A to D and B to C. This results in 0.56(28.54') = 16'.

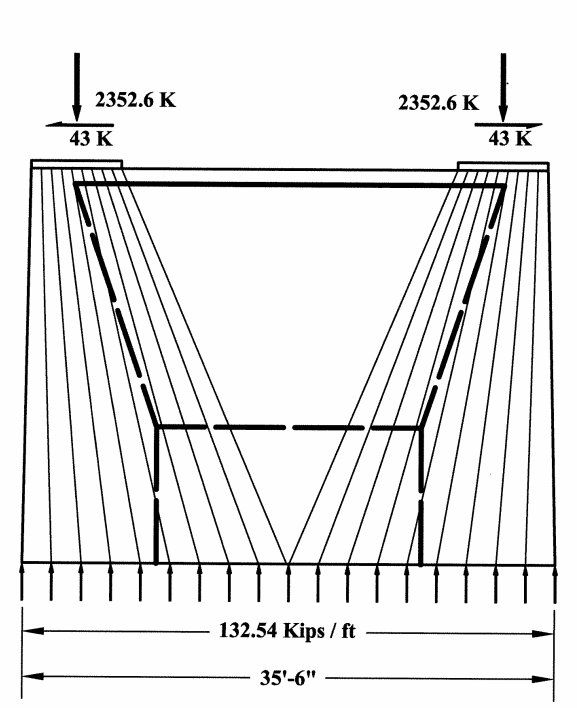

Figure A.6-5 – Flow of Forces

<u>Step 5</u> – Solve for the member forces.

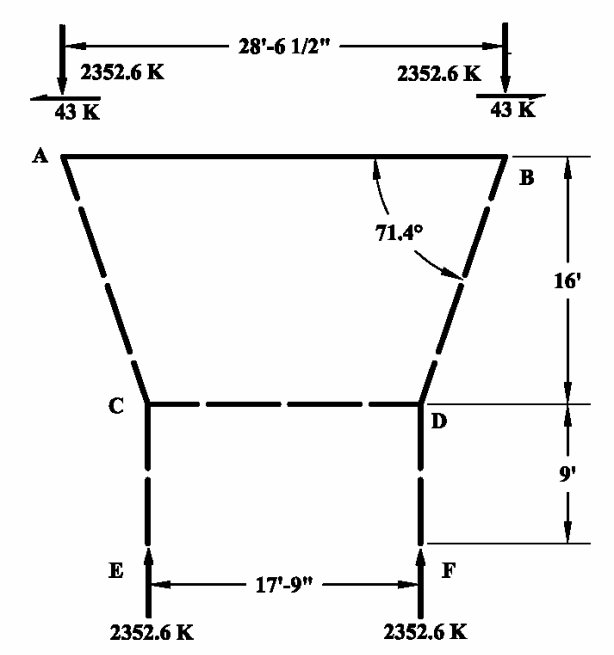

Figure A.6-6: STM Model

Resulting member forces:

AB	834.75^k	Tension
AC	-2482.3^k	Compression
BD	-2482.3^k	Compression
CD	-791.8^k	Compression
CE	-2352.6^k	Compression
DF	-2352.6^k	Compression

<u>Step 6</u> – Select steel area for the tie.

There is only one tie and it has a factored tension force of 834.75^k. Hence the required area of tie reinforcement, A_{st}, is:

$$A_{st} = \frac{P_u}{\phi f_y} = \frac{834.75 kips}{0.9 \times 60 ksi} = 13.2 in^2$$

Since this is not a flexural member, minimum flexural resistance need not be checked.

To meet this requirement the following bars could be used
14 #9's
11 #10's
9 #11's

Use 2 layers of 7-#9's (to facilitate detailing)

$$Total\ Area = 14 in^2$$

<u>Step 7</u> – Check the capacity of the struts and nodes.

<u>Step 7a</u> – Check the nodal zone stress limits.

The nodal zone at the column pier base interface has a stress of

$$f_c = \frac{2532.6 kips}{(72")(76")} = 0.46 ksi$$

This is considerably below the nodal zone stress limit for this CCT node of:

$$0.75\phi f'_c = (0.75)(0.7)(4 ksi) = 2.1 ksi$$

By inspection the node at the bottom of the pier base is acceptable since its area will be considerably larger than the node at the column pier base interface.

Step 7b – Check the capacity of the struts.

Struts AC and BD each carry a compression force of 2482.3^{k}. These struts are anchored at joints A and B that also anchors tension tie AB. Hence this is the most critical strut. From the geometry of the truss, the angle between the strut and the adjoining tension tie is 71.4°. The tension strain in the AB is:

$$\varepsilon_s = \frac{P_u}{A_{st}E_s} = \frac{834.75kips}{(14in^2)(29{,}000ksi)} = 2.06\times10^{-3}$$

At the centerline of the strut this strain is reduced to half this value, per LRFD article C5.6.3.3.3. The principal tensile strain in the strut is calculated using LRFD Equation 5.6.3.3.3-2:

$$\varepsilon_1 = \varepsilon_s + (\varepsilon_s + 0.002)\cot^2\alpha_s = 1.03\times10^{-3} + (1.03\times10^{-3} + 0.002)\cot^2 71.4°$$
$$= 1.03\times10^{-3} + (3.03\times10^{-3}).1133 = 1.37\times10^{-3}$$

and the limiting compressive stress f_{cu}, in the strut using LRFD Equation 5.6.3.3.3-1 is:

$$f_{cu} = \frac{f_c'}{0.8+170\varepsilon_1} \le 0.85f_c' = \frac{4}{0.8+170\times1.37\times10^{-3}} = 3.87 \ge .85\times4 = 3.4ksi$$

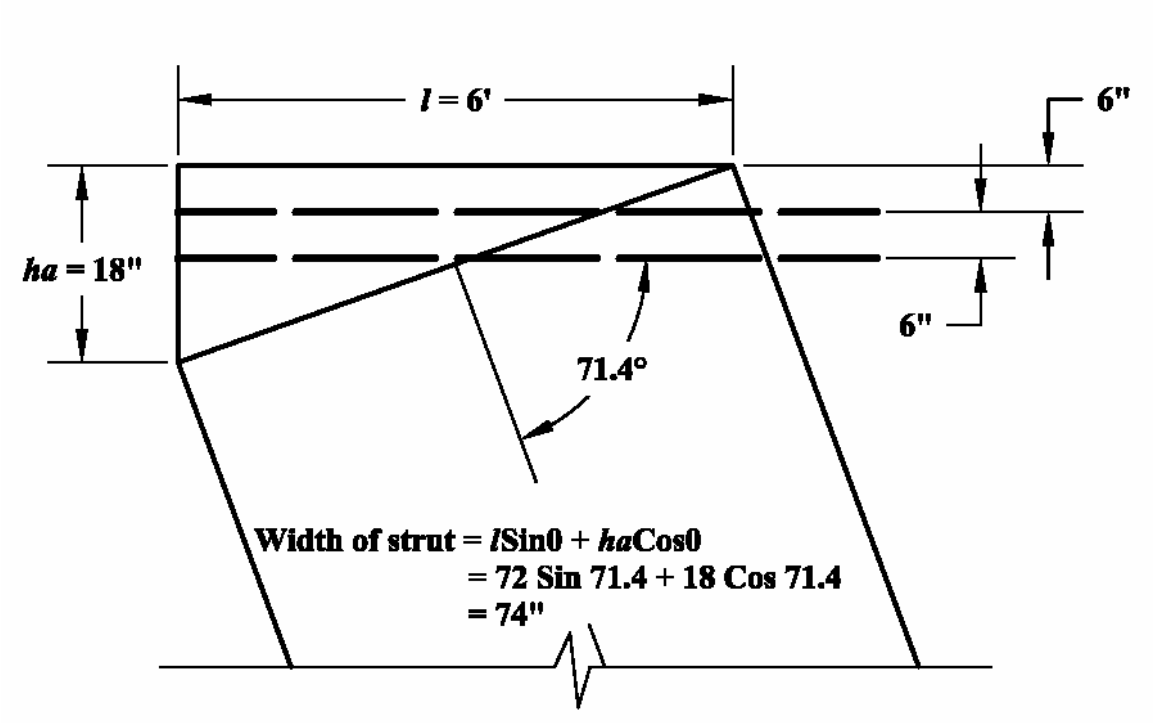

Figure A.6-7: Conditions at Node A

From Figure A.6-7, the cross-sectional dimension of the strut in the plane of the pier base is 74". Since the column bearing surface is spread evenly across the width of the pier base the full thickness of the pier base of 78" will be effective. Hence the nominal resistance of the strut is:

$$P_u = f_{cu} A_{cs} = (3.4ksi)(74in)(78in) = 19{,}624.8kips$$

The factored resistance of the strut is:

$$P_r = \phi P_n = 0.7 \times 19{,}624.8kips = 13{,}737kips$$

This is well in excess of the factored load of $2511.6kips$.

The actual Nodal zone stress is
$2511.6/(74in \times 78in) = 0.435ksi << 0.75\phi f_c^{'} = 0.75(0.7)4ksi = 2.1ksi$ The Nodal zone stress is acceptable.

It is also necessary to check if the tension ties are spread out sufficiently in the effective anchorage area. Nodes A& B are a CCT node which is 18" in depth (see Figure A.6-7). The nodal zone stress to anchor the tension tie force in AB of 834.75^k is $f_c = \dfrac{834.75kips}{(18")(78")} = 0.594ksi$

For this CCT nodal zone, the limiting nodal zone stress is:

$$f_c = .75\phi f_c' = 0.75(0.7)(4ksi) = 2.1ksi$$

The nodal zone stress limit in the anchorage area is acceptable.

<u>Step 8</u> – Detail reinforcement.

<u>Step 8a</u> – Check anchorage of tension tie.

The No. 9 bars are required to develop a force of $834.75kips$ at the inner face of the column. The inner face of the column is at a distance of 72" from the outside face of the pier base. Allowing for a concrete cover of 3" a distance of 69" is available as the embedment length. The stress in the 14 No. 9 bars at the inner face of the column is:

$$f_s = \frac{834.75kips}{14in^2} = 59.63ksi$$

The basic development length, $\ell_{db} = 52"$. As these bars are not required to develop their full yield stress, the development length could be reduced to $\left(\frac{59.63ksi}{60ksi}\right)52" = 51.7" < 69"$ available. Therefore the anchorage is acceptable.

Step 8b – Crack control reinforcement

Check the vertical reinforcement first:

$A_{st} = 0.003bs = 0.003 \times 12 \times \frac{76+89}{2} = 2.97in^2$ Use 4 #8 bars $A_{st} = 3.16\ in^2$

Check the minimum horizontal reinforcement

$A_{st} = 0.003bs = 0.003 \times 12 \times \frac{76+89}{2} = 2.97in^2$ Use 4 #8 bars $A_{st} = 3.16\ in^2$

The recommended detailing of the pier wall is shown in Figure A.6-8. The detailing shown reflects the conditions between the columns and does not reflect the reinforcing extending from the footing or the columns into the wall.

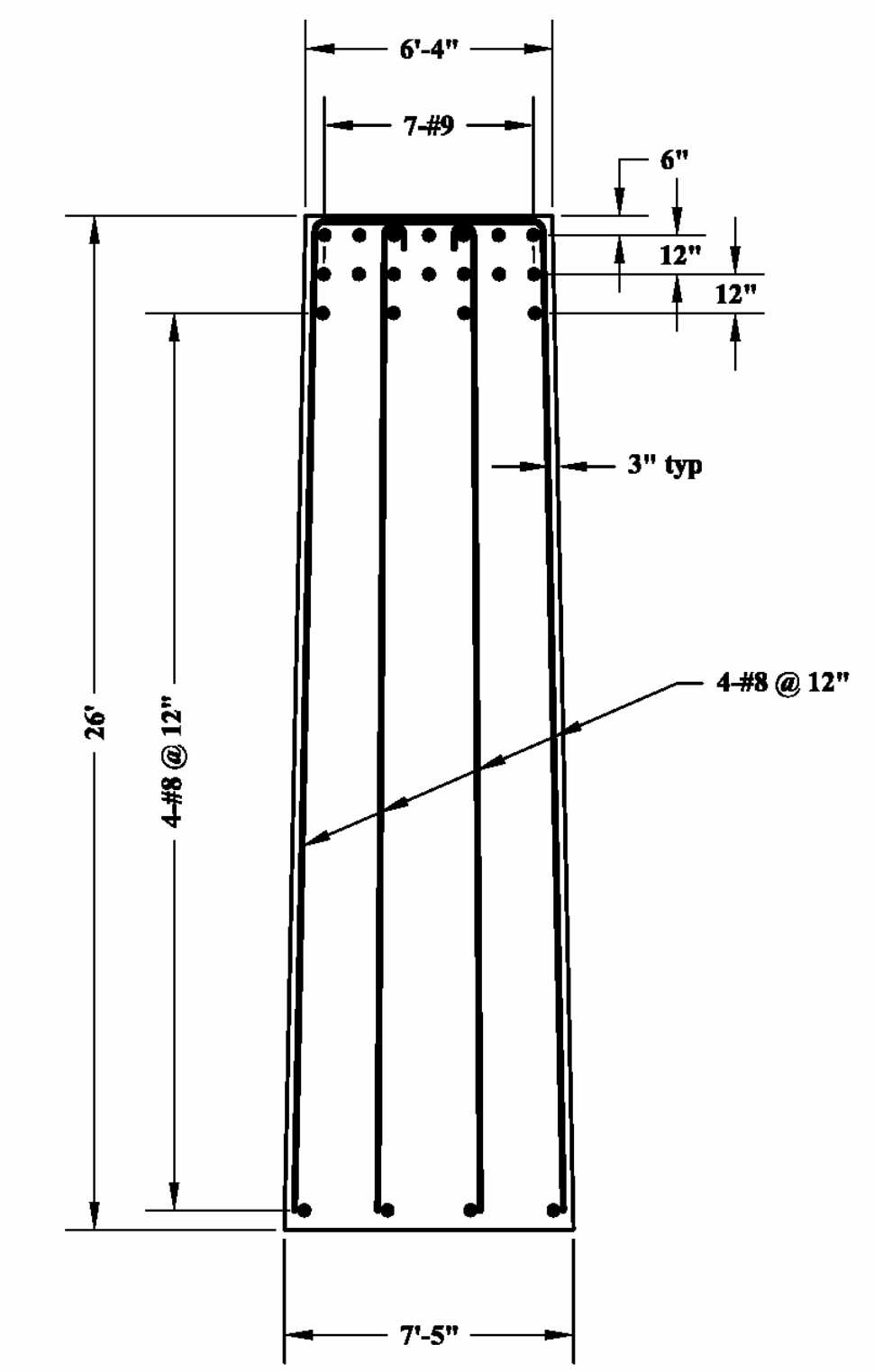

Figure A.6-7: – Detailing of Wall Pier

EXAMPLE A.7 – 78" PRESTRESSED BULB-TEE GIRDER

Problem Statement:

A simple span bridge superstructure with 137'-11" spans consists of 5 – 78" bulb tee girders 138'-11" long spaced at 10'-6". The slab of the bridge is 7" thick.

As shown in figure A.7-1, flexural analysis of the girder has resulted in it being pretensioned with fifty-four 0.6" diameter low relaxation strands (46 with a straight strand profile and 8 draped stands). The specified yield strength of the prestressing strand is 270 ksi. The harping point is located 48'-4" from the end of each beam. The centroid of the undraped strands is 6.13" from the base of the girder and the draped strands is 71.5" from the base of the girder at the end of the girder. The distance from the top of girder to the centroid of top reinforcing steel is 1.75" The specified concrete strength, f'_c, is 10,000 psi for the girder and 3,200 psi for the deck slab, and the specified yield strength of the mild reinforcing steel is 60 ksi.

Using STM, determine the transverse shear reinforcement necessary for the D-region to meet the requirements of LRFD and HL93 loading. Evaluation of bursting stresses for the strand will use the standardized code equations. (Note: This example is included to demonstrate how a STM could be used to model the D-region of a standard prestressed beam. It is highly unlikely that an STM would be used for a typical design case as the one shown.)

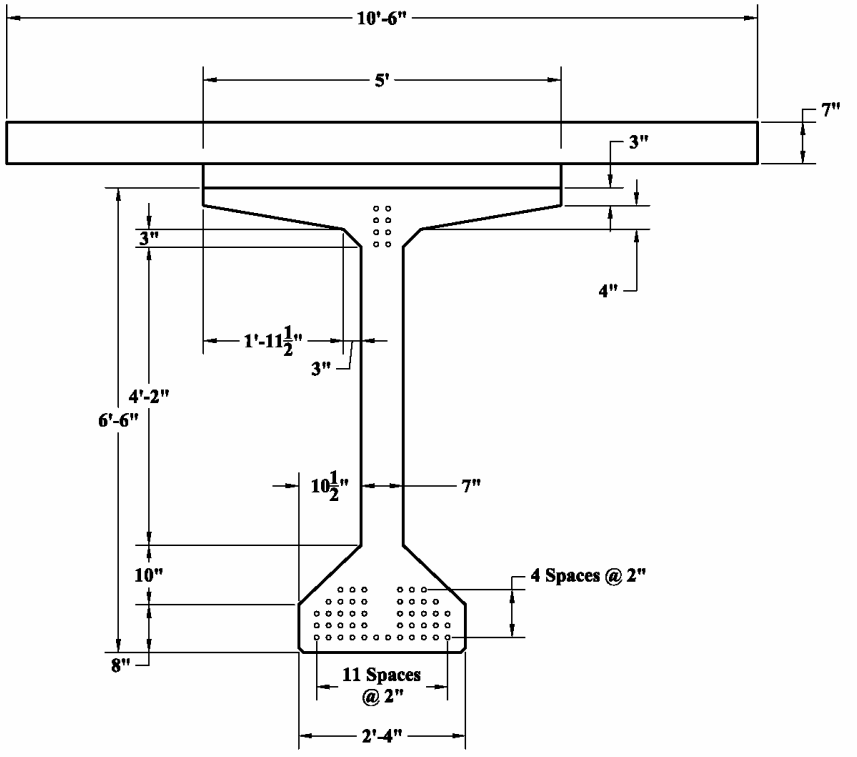

Figure A.7-1 – Cross-Section of Beam and Slab

<u>Step 1</u> – *Delineate the D-regions*.

Using St. Venant's principle that a D-region extends a distance d beyond a geometric change, concentrated load or reaction:

$d = the\ greater\ of\ b_{eff}\ or\ h$

$h = 78"+4"\ haunch + 7"\ slab = 89"$

b_{eff} = 9'-6" based on the requirements of AASHTO 4.6.2.6.

As b_{eff} is greater than h, the D-region will be defined as 9'-6" past C/L Bearing as shown in Figure A.7-2..

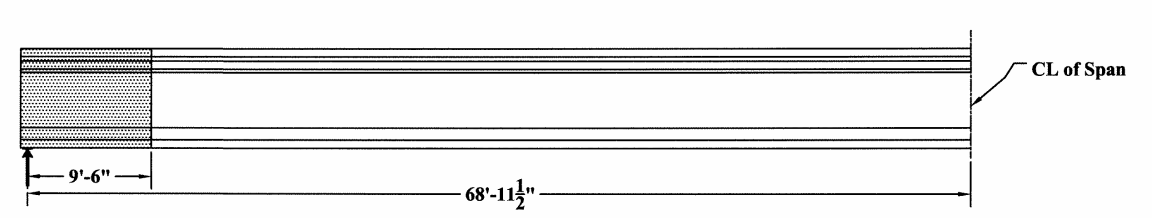

Figure A.7-2 – D-Region of the Beam

<u>Step 2</u> – Determine boundary conditions of D-region.

To make calculating the forces and boundary conditions simpler, the boundary conditions for the initial analysis will be carried to mid-span. AASHTO LRFD Load Case – Strength I will be used.(See figure A.7-3)

Using Impact - $IM = 1.33$ and a Live Load Distribution Factor for shear of $S = 0.36 + \frac{S}{25} = 0.36 + \frac{10.5'}{25} = 0.78$ the boundary conditions can be developed.

$W_{DL} = 2.645 kips / ft$

$$M_{DL_{\max}} = \frac{W_{DL} l^2}{8} = \frac{(2.645 kips / ft)(137.918')^2}{8} = 6{,}289\, ft - kips$$

Based on HL-93 Loading and a truck placement as shown in Step 4, the moment at the center line of the span, $M_{C/L} = 10{,}791.09\, ft - kips$.

Calculating the force couple due to the moment at mid-span.

:

$$T = C = \frac{M}{l_c} = \frac{10{,}791.09'k}{70.12"} = 1846.74^k$$

Where l_c equals the approximate distance between the centroid of the top and bottom flange of the girder.

Calculate the force in the draped prestressing strands.

8 draped 0.6" diameter strands ($A_{strand} = 0.217\ in^2$)

$$f_{ps} = 0.75F_y = 0.75(270\ ksi) = 202.5\ ksi$$

$$F_{D_1} = \#\ of\ strands \times A_{strand} \times f_{ps}$$

$$F_{D_1} = 8 \times 0.217\ in^2 \times 202.5\ ksi = 351.5^k$$

Calculate the prestressing transfer length.

$$\ell_{Transfer} = 50d_b = 50(0.6") = 30"$$

$$\ell_{Draped\ Strand} = \sqrt{(48.33')^2 + (70.12")^2} = 48.68'$$

Since the transfer length is much less than the draped prestressing strand length, we will assume that the full force of the strands is applied at node 1.

Calculate the maximum shear in the D-region:

$$V_{DL_{\max}} = \frac{w\ell}{2} = \frac{2.645^{k/'} \times 138.918'}{2} = 183.7^{\ k}$$

$$V_{LL_{Lane}} = \frac{w\ell}{2} \times S = \frac{0.64^{k/'} \times 138.918'}{2} \times S = 44.45^{\ k} \times 0.78 = 34.67^{\ k}$$ (This is the lane loading component only. The truck component will be added later)

<u>Steps 3 & 4</u> – Visualize the Flow of Forces and Develop a STM

The STM model resulting from this step is illustrated in Figure A.7-2(a). The struts are illustrated by dashed lines and the ties by heavy solid lines. The nodes have been numbered to facilitate referencing. All angles are derived from the physical dimensions of the model.

The external loads acting at these nodes will be calculated using the live load placement shown in Figure A.7-3 and the Dead loads discussed in Step 2.

While the maximum shear value occurs with a 32 kip truck axle positioned over the bearing, the force in strut 0-4 is maximized when the 32 kip truck axle is placed at node 4. See Figure A.7-3 for the loading configuration used.

$$V_{LL_{Truck}} = \left[32^{k} \times \left(\frac{137.918' - 3.708'}{137.918'} \right) + 32^{k} \times \left(\frac{137.918' - 17.708'}{137.918'} \right) + 8^{k} \times \left(\frac{137.918' - 31.708'}{137.918'} \right) \right] \times 0.78 = 50.85^{k}$$

Using AASHTO LRFD Load Case - $Strength\ I - 1.25DL + 1.75(LL + I)$

$$V_{\max} = 1.25\left(183.72^{k}\right) + 1.75\left(1.33 \times 50.85^{k} + 34.67^{k}\right) = 408.65^{k}$$

Node 1: $1.25\left[2.645^{k/'} \times \left(0.5 + \frac{3.708}{2} \right) \right] + 1.75 \times 0.78\left[0.64^{k/'} \times \left(0.5 + \frac{3.708}{2} \right) \right] = 9.84^{k}$

Node 4: $1.25\left[2.645^{k/'} \times \left(\frac{3.708' + 7.0'}{2} \right) \right] + 1.75 \times 0.78\left[0.64^{k/'} \times \left(\frac{3.708' + 7.0'}{2} \right) + 1.33 \times 32^{k} \right] = 80.47^{k}$

Nodes 6 & 10: $1.25 \times \left(2.645^{k/'} \times 7' \right) + 1.75 \times 0.78\left(0.64^{k/'} \times 7' \right) = 29.26^{k}$

Node 8: $1.25 \times \left(2.645^{k/'} \times 7' \right) + 1.75 \times 0.78\left(0.64^{k/'} \times 7' + 1.33 \times 32^{k} \right) = 29.26^{k}$

Node 12: $1.25\left[2.645^{k/'} \times \left(\frac{7.0' + 9.667'}{2} \right) \right] + 1.75 \times 0.78\left[0.64^{k/'} \times \left(\frac{7.0' + 9.667'}{2} \right) + 1.33 \times 8^{k} \right] = 49.36^{k}$

Node 14: $1.25\left[2.645^{k/'} \times \left(\frac{6.896' + 9.667'}{2} \right) \right] + 1.75 \times 0.78\left[0.64^{k/'} \times \left(\frac{6.896' + 9.667'}{2} \right) \right] = 34.61^{k}$

Nodes 16, 18 & 20: $1.25 \times \left(2.645^{k/'} \times 6.896' \right) + 1.75 \times 0.78\left(0.64^{k/'} \times 6.896' \right) = 28.82^{k}$

Node 22: ½ of Node $16 = 14.41^{k}$

Node 21: Resist remaining shear from bearing reaction $= 12.34^{k}$

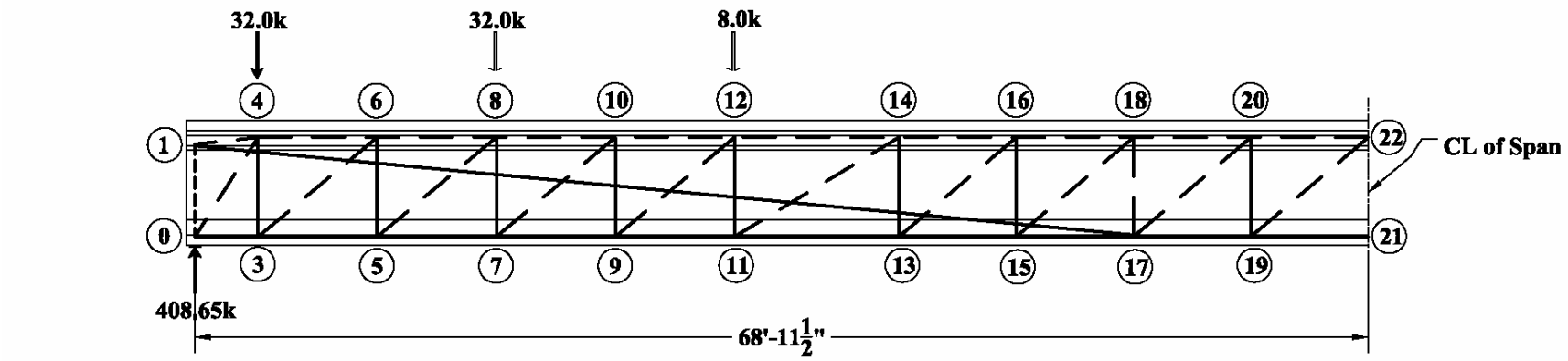

a) STM Indicating Node Designations & Live Load Placement

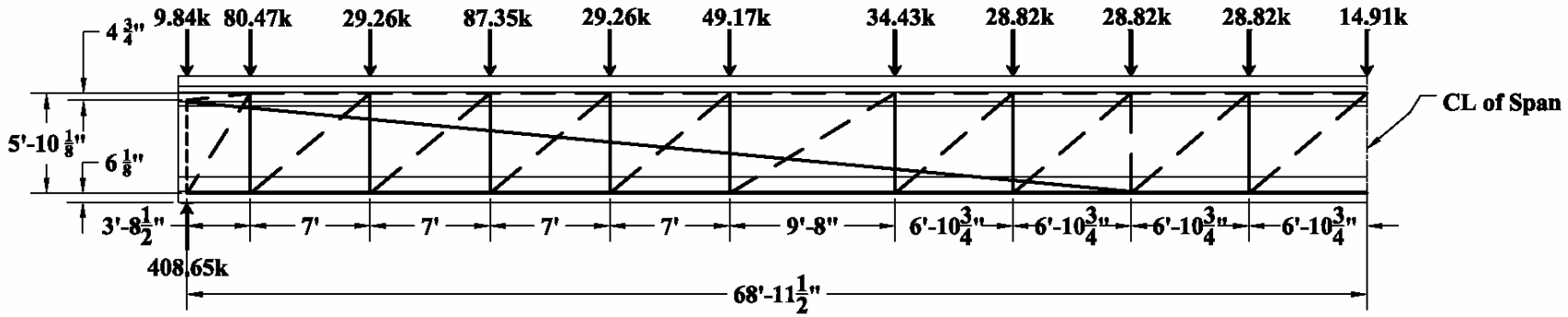

b) STM Indicating External Loading

Figure A.7-3 STM Model and Loading

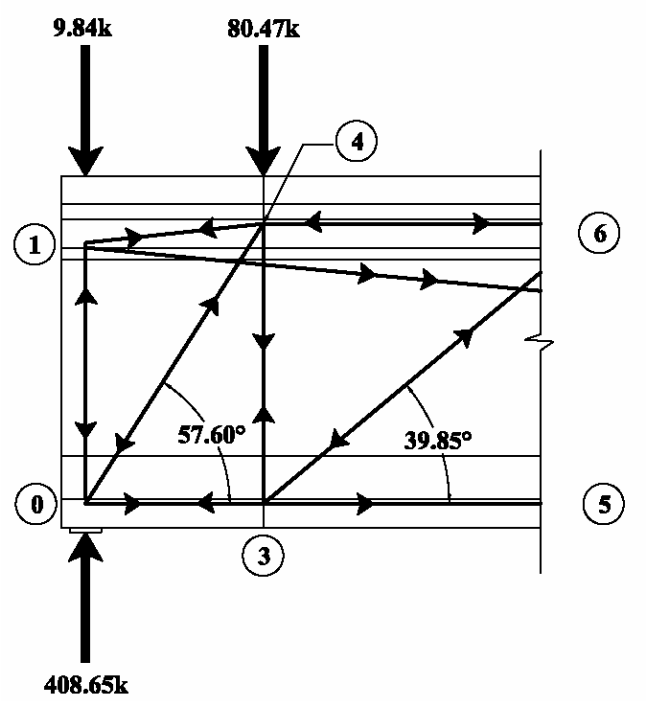

Figure A.7-4 STM Model and Loading of the D-Region

<u>Step 5</u> – Calculate the forces in the struts and ties.

Using the external loading derived in step 4 and the STM shown in Figure A.7-3 the forces in each member of the STM are calculated. Though our primary concern is the D-region all of the STM Member Forces are shown below.

Lower Chords (Ties)			Top Chords (Struts)			Verticals (Ties)		
Member	Force	T or C	Member	Force	T or C	Member	Force	Tor C
0-3	211.5^{k}	T	1-4	351.2^{k}	C	0-1	75.2^{k}	T
3-5	550.9^{k}	T	4-6	561.4^{k}	C	3-4	283.2^{k}	T
5-7	855.2^{k}	T	6-8	900.7^{k}	C	5-6	254.0^{k}	T
7-9	1054.8^{k}	T	8-10	1205.0^{k}	C	7-8	166.6^{k}	T
9-11	1219.3^{k}	T	10-12	1404.5^{k}	C	9-10	137.3^{k}	T
11-13	1365.2^{k}	T	12-14	1569.2^{k}	C	11-12	88.2^{k}	T
13-15	1428.6^{k}	T	14-16	1715.0^{k}	C	13-14	53.7^{k}	T
15-17	1458.0^{k}	T	16-18	1778.4^{k}	C	15-16	24.9^{k}	T
17-19	1844.3^{k}	T	18-20	1807.85^{k}	C	17-18	3.9^{k}	C
19-21	1846.7^{k}	T	20-22	1844.3^{k}	C	19-20	2.07^{k}	T
Diagonals (Struts)								
0-4	394.9^{k}	C	9-12	214.3^{k}	C	17-20	47.8^{k}	C
3-6	442.0^{k}	C	11-14	170.5^{k}	C	19-22	3.20^{k}	C
5-8	396.3^{k}	C	13-16	83.1^{k}	C			
7-10	300.0^{K}	C	15-18	38.6^{k}	C			

<u>Step 6</u> – Select steel area for the ties.

We will first calculate the area of steel required for the horizontal ties, the prestressing strands make up this steel.

Looking first at Node 0, we must determine the load that can be developed in the strands from the face of the node to the end of the beam. Working with Figure A.7-5 we see:

$$W_s = h_t \cos\alpha + l_{bp} \sin\alpha = 12.2(\cos 57.6°) + 9(\sin 57.6°) = 6.54"+7.60" = 14.14"$$

Where 12.2" is the depth over which the prestressing strands are distributed and 9" is the width of the bearing pad.

$$\ell_a = \frac{W_s/2}{\sin\alpha} + 6" = \frac{14.14"/2}{\sin 57.6°} + 6" = 14.37"$$

$$f_{ps} = 0.75F_y = 0.75(270\,ksi) = 202.5\,ksi$$

As determined earlier the transfer length of the strand is 30". Therefore

$$f_{ps_{0-3}} = \frac{14.37"}{30"} \times 202.5\,ksi = 97.0\,ksi$$

Since there are 46 strands in this area of the member:

$$T_{capacity} = (46)(0.217in^2)(97.0ksi) = 968.3^k >> 211.5^k$$

At the remainder of the lower nodes there is sufficient distance behind the strands for them to be fully developed, therefore f_{ps} = 202.5 ksi can be used as the capacity of each strand. Even though we are primarily concerned with the conditions within the D-region, the strand demands outside of the D-region will also be shown in the table below:

$$A_{ps} = \frac{P}{f_{ps}} \qquad \#\ of\ strands\ req'd = \frac{A_{ps}}{A_{strand}}$$

Area of Steel Required for the Straight Strands:

Tie	P	ℓ_a	f_{ps}	A_{ps}	# of strands req'd	# of strands prov'd
0-3	211.5^k	14.4"	97.2ksi	$2.18in^2$	12	13
3-5	550.9^k	-	202.5ksi	$2.72in^2$	14	46
5-7	855.2^k	-	202.5ksi	$4.22in^2$	20	46
7-9	1054.8^k	-	202.5ksi	$5.21in^2$	24	46
9-11	1219.3^k	-	202.5ksi	$6.02in^2$	28	46
11-13	1365.2^k	-	202.5ksi	$6.74in^2$	32	46
13-15	1428.6^k	-	202.5ksi	$7.04in^2$	34	46
15-17	1458.0^k	-	202.5ksi	$7.2in^2$	34	46
17-19	1844.3^k	-	202.5ksi	$9.11in^2$	42	54
19-21	1846.7^k	-	202.5ksi	$9.12in^2$	44	54

Area of Steel Required for the Draped Strands:

Tie	P	ℓ_a	f_{ps}	A_{ps}	# of strands req'd	# of strands prov'd
1-17	351.5^k	-	202.5ksi	$1.74in^2$	8	8

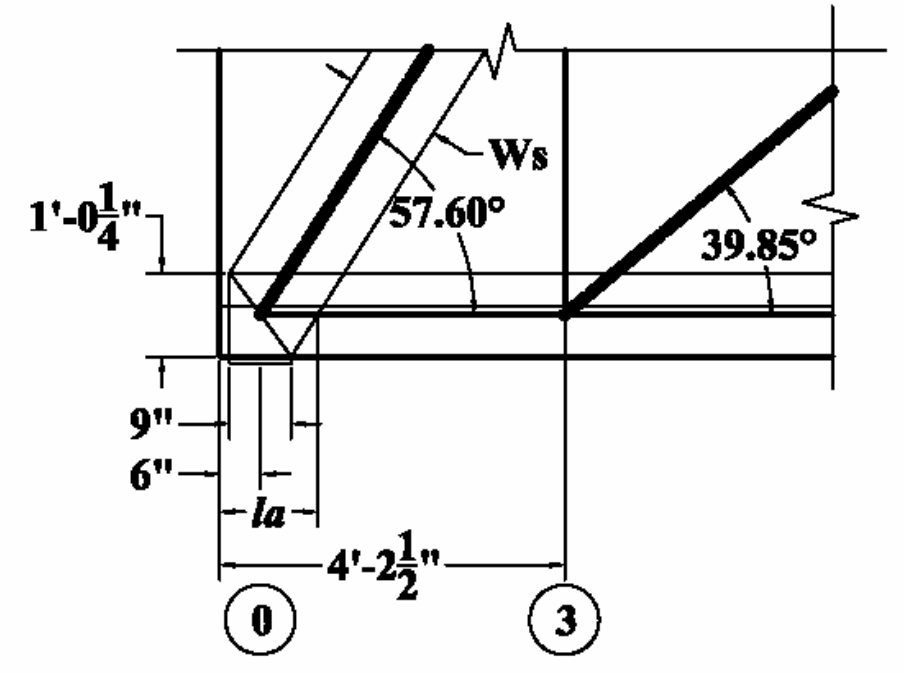

Figure A.7-5: Strut and Tie Configuration at Node 0

Calculated the area of steel required for the vertical ties, this steel will be the shear reinforcing ties.

$$A_{s_{req}} = \frac{P}{\phi F_y}$$

$$\#\ of\ \ stirrups\ req'd = \frac{A_{s_{req}}}{A_{s\ Stirrup}}$$

The width of the stirrup band will be considered to be the tributary length of the beam that the vertical tie represents. For most vertical ties this length is from halfway between the nodes to either side.

In the case of the first panel, we will conservatively use the same stirrup spacing for the full length of the panel between nodes 0-3 that is demanded by the tie at Node 3.:

$$Width\ of\ Stirrup\ Band\ at\ Tie\ 3\text{-}4 = \frac{44.5"}{2} + \frac{84"}{2} = 64.25"$$

$$Width\ of\ Stirrup\ Band\ at\ Tie\ 5\text{-}6 = \frac{84"}{2} + \frac{84"}{2} = 84"$$

$$Spacing\ required = \frac{Band\ Width}{(\#\ of\ \ Stirrups - 1)}$$

Area of Steel Required for Vertical Ties: (Even though we are primarily concerned with the demands within the D-region, for illustrative purposes the demands outside the D-region are also shown below.)

Tie	P	$A_{s_{req}}$	$A_{s\ \#4\ \ Stirrup}$	# of Stirrups	Width of Band	Req'd Spacing	Spacing Provided
3-4	283.2^k	$5.24\ in^2$	$0.4\ in^2$	14	64.25"	5"	5"
5-6	254.0^k	$4.70\ in^2$	$0.4\ in^2$	12	84"	7.6"	7"
7-8	166.6^k	$3.09\ in^2$	$0.4\ in^2$	8	84"	12.0"	Outside of D-Region
9-10	137.3^k	$2.54\ in^2$	$0.4\ in^2$	7	84"	14"	
11-12	88.2^k	$1.63\ in^2$	$0.4\ in^2$	5	100"	25"	
13-14	53.7^k	$1.0\ in^2$	$0.4\ in^2$	3	99⅜"	49.5"	
15-16	24.9^k	$0.46\ in^2$	$0.4\ in^2$	2	82¾"	82.75"	
17-18	3.9^k	$0.07\ in^2$	$0.4\ in^2$	1	82¾"	82.75"	
19-20	2.1^k	$0.04\ in^2$	$0.4\ in^2$	1	82¾"	82.75"	

<u>Step 7</u> – Check the capacity of the struts.

As this STM is intended to model the stresses in the D-region of the prestressed beam, it is unnecessary to check the stress levels in the struts and nodes outside of the prescribed D-region.

The adequacy of the bearing size at Node 0 will first be checked. The limiting stresses under the bearing are dictated by the conditions in the nodal zone. Node 0 is a CCT Type Node with a limiting stress of $0.75\phi f_c'$ where $\phi = 0.7$. The reaction at Node 0 is calculated with the truck rear axle located over Node 4 as shown in Figure A.7-2. The reaction will be some what higher, namely 410.57 kips when the rear axle is directly over the bearing. Therefore this higher load will be used.

$P = 410.57^k$

$$A_{brg_{req'd}} = \frac{410.57^k}{0.75 \times 0.7 \times 10ksi} = 78.20\ in^2$$

$W_{brg} = 28",\ \ell_{brg} = 9"$

$A_{brg} = 28" \times 9" = 252\ in^2 > 78.20\ in^2$ - The bearing Area is okay.

a) Strut 0-4

Strut 0-4 carries a compression force (394.9 kips, see Table in Step 5). This strut is also anchored at Node 0 which also anchors tie 0-3, strut 0-1, and the bearing. The size of strut 0-4 is dictated by the size of the bearing and the depth of tie 0-3. Working with Figure A.7-4 we see:

$$W_s = h_t \cos\alpha + l_{bp} \sin\alpha = 12.2(\cos 57.6°) + 9(\sin 57.6°) = 6.54" + 7.60" = 14.14"$$

The limiting compressive stress in the strut usually is controlled by the tensile strain in the tie which is at the smallest angle to the strut. Again, as shown in Figure A.7-4 this angle measures 57.6 degrees and the force is Tie 0-3 is 211.6 kips.. The strain in tie 0-3 is calculated to be"

$$\varepsilon_{s(Tie0-3)} = \frac{P_u}{A_{st}E_s} = \frac{211.6^k}{(46 \times 0.217in^2)(29{,}000ksi)} = 0.000731$$

At the center of the node the average value of the strain will be one-half of this value, or 0.000366. Therefore, the principal strain, ε_1, can be determined as:

$$\varepsilon_1 = \varepsilon_s + (\varepsilon_s + 0.002)\cot^2\alpha_s = 0.000366 + (.000366 + 0.002)\cot^2 57.6° = 1.319 \times 10^{-3}$$

and the limiting compression stress, f_{cu}, in the strut is:

$$f_{cu} = \frac{f_c^{'}}{0.8 + 170\varepsilon_1} \le 0.85 f_c^{'} = \frac{10}{0.8 + (170)1.319 \times 10^{-3}} = 9.76ksi \ge 0.85(10) = 8.5ksi$$

The thickness of the strut will be taken as the thickness of the web or 7".

$$P_u = f_{cu} A_{cs} = 8.5ksi \times 14.14" \times 7" = 841^k$$

The factored resistance of the strut is:

$$P_r = \phi P_n = 0.7 \times 841^k = 589^k > 394.91^k$$

b) Strut 3-6

Strut 3-6 carries the highest compression force (442.0 kips, see Table in Step 5). This strut is also anchored at Node 3 which also anchors ties 0-3, 3-5 & 3-4. Hence this is the most critical strut. The limiting compressive stress in the strut usually is controlled by the tensile strain in the tie which is at the smallest angle to the strut. Since two of the ties are at the smallest angle are co-linear, we'll use the largest of the strains in each of these ties.

$$\varepsilon_{s(Tie0-3)} = \frac{P_u}{A_{st} E_s} = \frac{211.6^k}{(46 \times 0.217in^2)(29{,}000ksi)} = 0.000731$$

$$\varepsilon_{s(Tie3-5)} = \frac{P_u}{A_{st} E_s} = \frac{550.9^k}{(46 \times 0.217in^2)(29{,}000ksi)} = 0.001903$$

The largest of these two values is 0.001903. Therefore, the principal strain, ε_1, can be determined as:

$$\varepsilon_1 = \varepsilon_s + (\varepsilon_s + 0.002)\cot^2 \alpha_s = 0.001903 + (.001903 + 0.002)\cot^2 39.86° = 7.502 \times 10^{-3}$$

and the limiting compression stress, f_{cu}, in the strut is:

$$f_{cu} = \frac{f_c^{'}}{0.8 + 170\varepsilon_1} \le 0.85 f_c^{'} = \frac{10}{0.8 + (170)7.502 \times 10^{-3}} = 4.82ksi \le 0.85(10) = 8.5ksi$$

We must also examine the strain in Tie 3-4.

$$\varepsilon_{s(Tie3-4)} = \frac{P_u}{A_{st} E_s} = \frac{283.2^k}{(14 \times 0.4in^2)(29{,}000ksi)} = 0.00174$$

Therefore, the principal strain, ε_1, can be determined as:

$$\varepsilon_1 = \varepsilon_s + (\varepsilon_s + 0.002)\cot^2 \alpha_s = 0.00174 + (.00174 + 0.002)\cot^2 50.14° = 4.347 \times 10^{-3}$$

and the limiting compression stress, f_{cu}, in the strut based on the strain in tie 3-4 is:

$$f_{cu} = \frac{f_c^{'}}{0.8 + 170\varepsilon_1} \le 0.85 f_c^{'} = \frac{10}{0.8 + (170)4.347 \times 10^{-3}} = 6.49 ksi \le 0.85(10) = 8.5 ksi$$

Since the above results in a limiting stress of 6.49 *ksi* which is higher than the 4.82 *ksi* resulting from the other ties at this node, the lower limiting stress of those ties will be used.

The nominal resistance of the strut is based on the limiting stress f_{cu} and the strut dimensions. The strut width is a function of the angle and the width of the tie. Since the width of the tie is the band width used to arrive at the reinforcing in tie 3-4(64.25"), the following width of the strut is calculated:

$$W_s = W_t \sin \alpha = 64.25" \times \sin 39.85° = 41.17"$$

The thickness of the strut will be taken as the thickness of the web or 7".

$$P_u = f_{cu} A_{cs} = 4.82 ksi \times 41.17" \times 7" = 1{,}389^k$$

The factored resistance of the strut is:

$$P_r = \phi P_n = 0.7 \times 1{,}389^k = 972^k >> 442.0^k$$

We will next check to see if the tension ties are spread out sufficiently in the anchorage area.

Node 1: (Anchorage of the 8 top strands)

CCT Type Node $\quad f_c = 0.75 \phi f_c^{'}$

$$T = 351.54^k$$

$$A = 7" \times (3 \times 2"_{spcs} + 2" + 2") = 70.0\ in^2$$

$$f_c = \frac{T}{A} = \frac{351.5^k}{70.0\ in^2} = 5.02 ksi$$

$$f_c = 0.75 \phi f_c' = 0.75 \times 0.70 \times 10\ ksi = 5.25\ ksi > 5.02\ ksi \text{ O.K.}$$

Node 3 (Distribution of Tie Steel):

CTT Type Node $\quad f_c = 0.65 \phi f_c^{'}$

$T = 550.9^k$

$A = 7" \times 64.25" = 449.75\ in^2$

$$f_c = \frac{550.9^k}{449.75\ in^2} = 1.22\ ksi$$

$f_c = 0.65\phi f_c' = 0.65 \times 0.7 \times 10\ ksi = 4.55\ ksi > 1.22\ ksi$ O.K.

<u>Step 8</u> – Detail reinforcement.

Use AASHTO LRFD Section 5.8.2.7 to check the maximum spacing of shear reinforcement.

For $v_u < 0.125 f_c'$ $\quad S = 0.8 d_v \le 24"$

For $v_u \ge 0.125 f_c'$ $\quad S = 0.4 d_v \le 12"$

$$V_u = \frac{V_u - \phi V_p}{\phi b_v d_v}$$

$\phi = 0.9,\ b_v = width\ of\ the\ web = 7",\ d_v = moment\ arm\ or\ the\ greater\ of\ 0.72h\ or\ 0.9d_e$

$h = 89" - 0.72h = 64"$

$d_e = 89" - 15.61" = 73.39"$ $\quad 0.9(73.39") = 66.051"$

$d_v = 70.12" \ge 66.051" \ge 64"$

$V_u = P$ $\quad V_p = 0$

$$v_{u_{end}} = \frac{283.2^k}{0.9(7")(70.12")} = 0.641\ ksi$$

$0.125 f_c' = 0.125(10\ ksi) = 1.25\ ksi > 0.641\ ksi$

$v_u < 0.125 f_c'$ $\quad S = 0.8 d_v \le 24"$ $\quad 0.8 d_v = 0.8(70.12") = 56.1"$

Therefore the maximum spacing of shear reinforcement is $S_{Max} = 24"$

Use AASHTO LRFD Section 5.10.10.1 to check the reinforcement required to resist the prestressing anchorages bursting at the end of the beam.

$$P_r = f_s A_s \qquad f_s \le 20\ ksi,\ \ A_s\ is\ within\ \frac{h}{4}\ from\ end\ \frac{h}{4} = \frac{78"}{4} = 19.5"$$

$$P_r = 4\%\ of\ T_{\max} = 0.04 \times 351.5^k = 14.1^k$$

$$14.1^k = 20\ ksi \times A_s$$

$$A_{s_{\min}} = 0.703\ in^2$$

$$\frac{0.703 in^2}{0.4 in^2} = 1.8\ stirrups\ in\ 19.5" \rightarrow 2\ stirrups\ @\ 5"\ spacing$$

Use AASHTO LRFD Section 5.10.10.2 to check the confinement reinforcement for the prestressing steel in the bottom flange.

$$S \le 6"\ for\ 1.5d \qquad d = Total\ Beam\ Depth = 78.0" \qquad 1.5d = 1.5 \times 78" = 117"$$

The maximum spacing is $S \le 6"\ for\ first\ 117"$

Use AASHTO LRFD Section 5.6.3.6 to check the crack control requirements for structures designed using the strut and tie method.

$$A_s = 0.003 A_g\ in\ each\ direction, \quad Use\ 6"\ spacing\ based\ on\ confinement$$

$$A_{cross-section} = 1105\ in^2, \quad h = 78"$$

$$A_s = 0.003 \times 12" \times \frac{A_{cs}}{h} = 0.003 \times 12" \times \frac{1105\ in^2}{78"} = \frac{0.51\ in^2}{12"}$$

$$A_{s_{vertical}} = 2-\#4\ bars\ @ 5"_{spcs.} = \frac{0.4\ in^2}{5"} = \frac{0.96\ in^2}{12"} > \frac{0.51\ in^2}{12"}\ \text{O.K.}$$

In the bottom flange of the beam:

$$A_{s_{horizontal}} = \text{Include the prestressing strand area in for the horizontal crack control}$$

$$A_{s_{horizontal}} = \frac{A_{\#7\,Bar}}{Spacing} + \frac{A_{strands}}{Spacing} = \frac{0.6 in^2}{9"} + \frac{0.217 in^2}{2"} = \frac{2.1\ in^2}{12"} > \frac{0.51\ in^2}{12"}\ \text{O.K.}$$

In the rest of the beam:

Use #7 bars @ 12” spaces in web and top flange

$$A_{s_{horizontal}} = \frac{0.6in^2}{12"} > \frac{0.51in^2}{12"} \text{ O.K.}$$

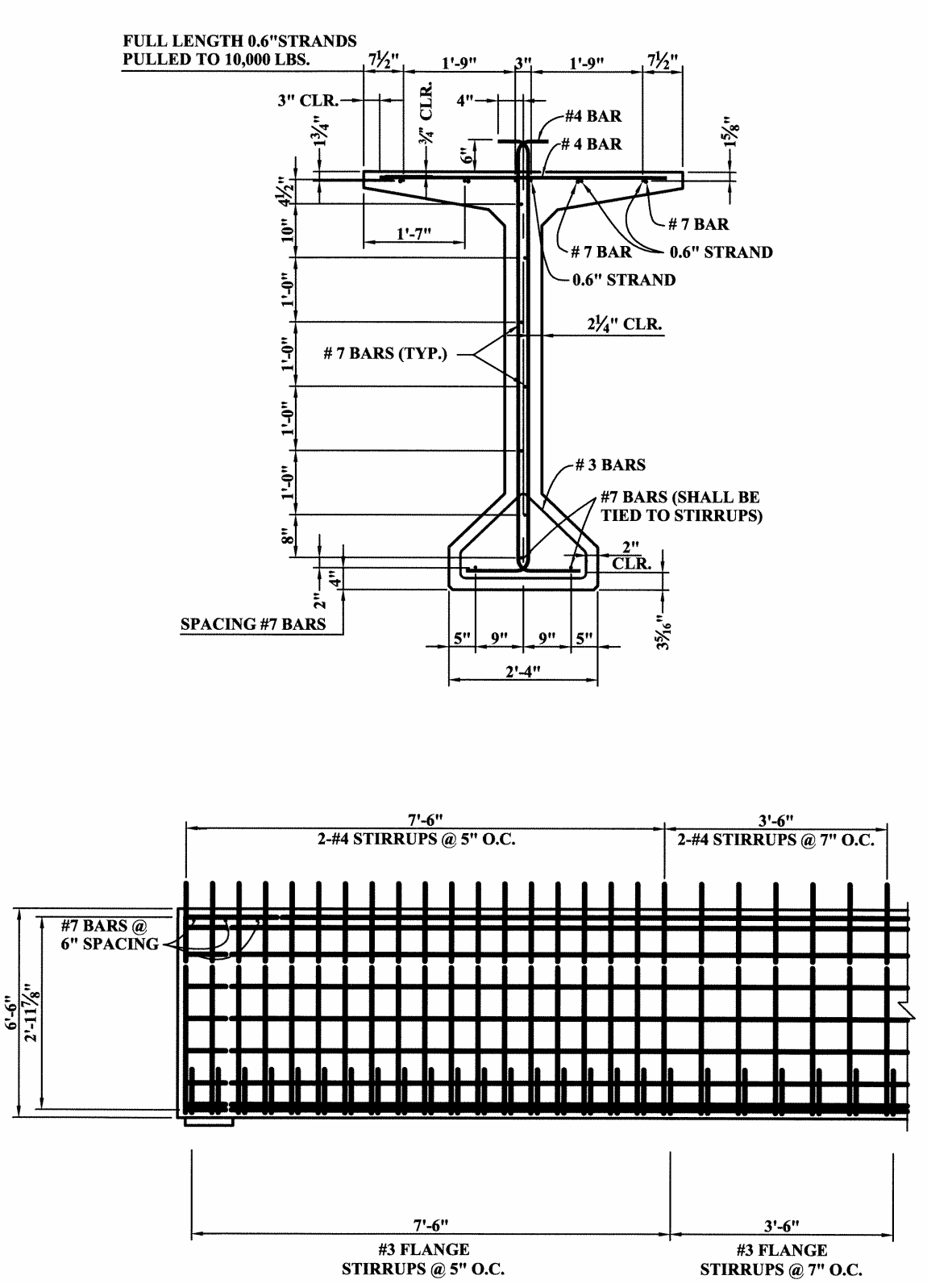

Figure A.7-6: Suggested Reinforcing Detailing

EXAMPLE A.8 – INVERTED TEE BEAM

Problem Statement:

An inverted Tee-Beam Cap of the configuration shown in Figures A.8-1 and A.8-2 supports simple spans of 120' on each side. The super structure consists of 5 precast box beams spaced at 14' center to center of bearings. The maximum live load plus impact reaction is 126.7^k per girder. The dead load reaction is 220^k per girder. This results in the following factored loading at each box location:

$$P = \left[1.25\left(220^k\right) + \left(1.75\right)\left(126.8^k\right)\right] = 497^k$$

Each girder rests on two bearings 14" wide by 24" long. The bearing locations are so close together they will be treated as a single bearing 14" wide by 48" long. The concrete used in the tee beam has an $f_c^{'}$ of 4 ksi and the mild reinforcing is grade 60. Using AASHTO LRFD STM requirements determine the amount of transverse reinforcement that will be required for the tee beam cap. A global evaluation of the cap is not part of this example.

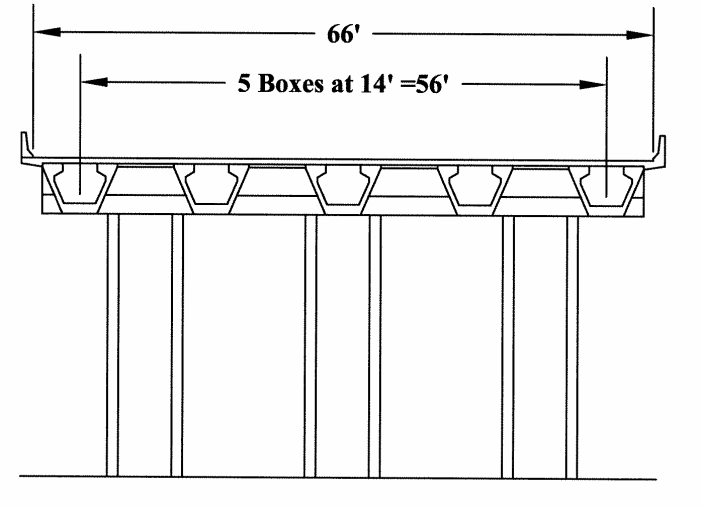

Figure A.8-1: Elevation of Bent Showing Box-Beam Layout

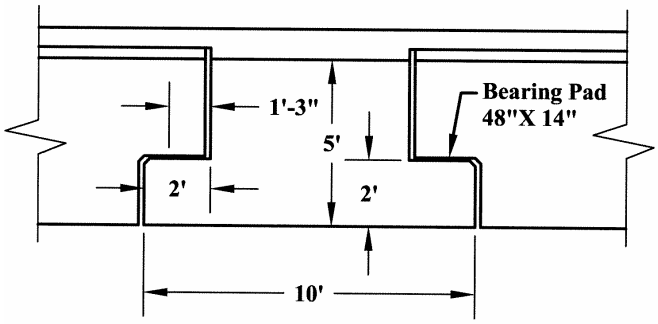

Figure A.8-2: Cross-section of Tee Cap

Step 1* – *Delineate the D-region.

The whole cross-section is a D-region.

Step 2* – *Determine the boundary conditions of the D-region.

There is no D- and B-region interface, the entire cross-section is a D-region..

Step 3* – *Sketch the flow of forces.

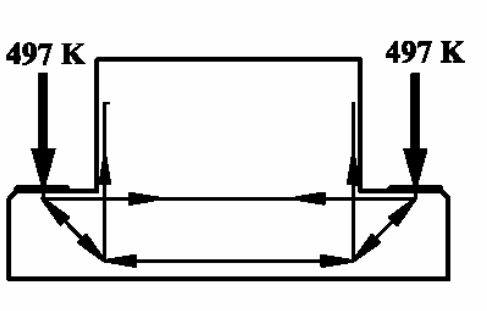

Figure A.8-3: General Flow of Forces

Step 4* – *Draw the STM.

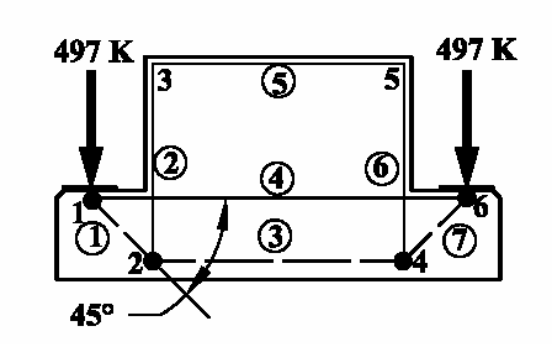

Figure A.8-4: Strut and Tie Model (STM)

The STM is shown in Figure A.8-4. The box girder reactions are transferred to the pier cap hanger elements 2 and 6 by struts 1 and 7. The cap hanger elements 2 and 6 are held in equilibrium by an out of plane strut that runs down the length of the member. Tie 4 carries the horizontal component of the struts 1 and 7 force. Member 5 is a zero force member that represents the leg of an anticipated closed stirrup and will not be included in the analysis. The depth of strut 3 is determined based on the greater of the following:

- The depth of concrete that is required to provide the minimum required strut 3 resistance.

- The development length of the hanger bars, calculated in accordance with LRFD Article 5.11.2.6.2. Assuming number 6 bars are to be used as the hanger bars this results in the following:

$$l_e \geq \frac{(0.44)(d_b)(f\ )}{\sqrt{f_c'}} = \frac{(0.44)(0.75in)(60ksi)}{\sqrt{4}ksi} = 9.9in$$

It is likely that the second requirement will govern and will therefore be used in this design..

<u>Step 5</u> – Solve for the strut and tie forces.

The analysis of the STM under the applied loads results in the member forces shown in Table A.8-1.

Members	Force	C or T
1 and 7	703 kips	C
2 and 6	497 kips	T
3	497kips	C
4	497 kips	T

Table A.8-1: STM Member Forces

<u>Step 6</u> – Select Steel Area for the Ties.

a) Member 4 has a tensile load of 497 kips. The tensile steel required is:

$$A_s = \frac{T}{0.9(f_y)} = \frac{497kips}{0.9(60ksi)} = 9.21in^2$$

Using the requirements of LRFD 5.13.2.5 and the data contained in Figure A.8-5, the length of the cap contributing to the local STM is:

Width of Tie 4 = $W + 4a_f = 48 + 4(17) = 116"$

Where:

W = width of the bearing

a_f = the distance from the center of bearing to the hanger reinforcement

Try 22 #6 bars at 5" on center within the 116" zone.

$$A_s = (22)(0.44) = 9.68in^2 > 9.2in^2 required$$

In order to make the full 116" zone effective and since the proposed spacing of the stirrups is 5" the longitudinal bars resulting from the global analysis will have to have a diameter such that $2(6 \times d_b \geq 5"$ as required by AASHTO 5.6.3.3.2. Therefore the diameter of the longitudinal bars

must be greater than 0.42". Given that this would require only a #4 bar, this should not be a concern.

b) Members 2 and 6 also have a Tensile load of 497 kips

$$A_s = \frac{T}{0.9(f_y)} = \frac{497kips}{0.9(60ksi)} = 9.21in^2$$

Use 22 #6 bars at 5" on center within the 116" zone.

$$A_s = (22)(0.44) = 9.68in^2 > 9.2in^2 required$$

<u>Step 7a</u> – Check strut resistance.

As shown in Table A.8-1, struts 1 and 7 carry a compressive force of 703 kips while strut 3 carries a compressive force of 497 kips. Due to its smaller area and larger force, struts 1 and 7 will control over strut 3 (See Figures A.8-5 & A.8-6). However, for illustration purposes, the evaluation of strut 3 will be presented. Due to the variation in area over the length of strut 1 and the fact that strut resistance is dependent on STM geometry and the forces, its resistance at either end will be different. Both ends will therefore be checked.

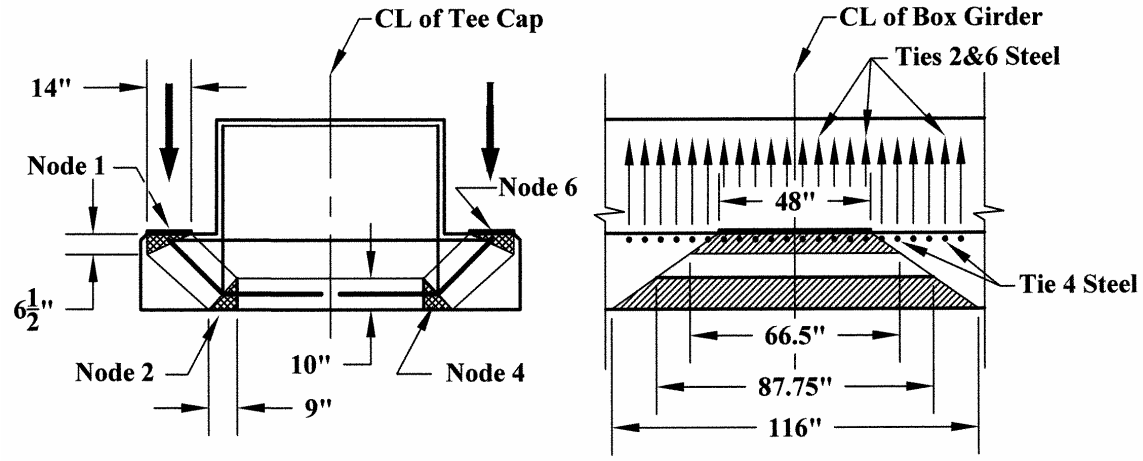

Figure A.8-5: STM Model

At node 1, the area at the node is calculated to be:

The width of strut 1 = $W_s = \left(\sqrt{(6.5)^2 + (14.0in)^2}\right) = 15.43in$

The thickness of the strut = $\left(\frac{(48 + 66.5)}{2}\right) = 57.255in$

The area $A_{strut} = (15.43)(57.25) = 883in^2$

The tensile strain in tie 4 is:

$$\varepsilon_s = \frac{P_u}{A_s E_s} = \frac{497 kips}{(9.68 in^2)29{,}000 ksi} = 0.00177$$

At the centerline of the node, this average strain is used as per LRFD Article C5.6.3.3.3. The angle between strut 1 and tie 4 is $45°$. The principal tensile strain in the strut is calculated using LRFD Equation 5.6.3.3.3-2.

$$\varepsilon_1 = \varepsilon_s + (\varepsilon_s + .002)\cot^2 \alpha_s = 0.000885 + (.000885 + .002)\cot^2 45° = .0038$$

The limiting compressive stress is then calculated using LRFD Equation 5.6.3.3.3-1.

$$f_{cu} = \frac{f_c'}{0.8 + 170\varepsilon_1} \le .85 f_c' \Rightarrow \frac{4 ksi}{0.8 + 170 \times .0038} = 2.75 ksi < .85 f_c'$$

The factored resistance of strut 1 at node 1 is:

$$P_r = \phi P_n = 0.70 \times 2.75 ksi \times 883 in^2 = 1700^k > 703^k$$

The area of strut 1 at node 2 is calculated as follows:

The width of strut 1 = $W_s = \left(\sqrt{(10.0 in)^2 + (9.0 in)^2}\right) = 13.25 in$

The thickness of the strut = $\left(\frac{(116 + 87.75)}{2}\right) = 101.875 in$

The area $A_{strut} = (13.45)(101.875) = 1370 in^2$

The tensile strain in ties 2 and 6 is:

$$\varepsilon_s = \frac{P_u}{A_{st} E_s} = \frac{497^k}{(22)(0.44 in^2)29{,}000 ksi} = .00177$$

At the centerline of the node the strain is reduced by half this value. The angle between strus 1 & 6 and ties 2 & 6 is $45°$. The principal strain in the strut is therefore:

$$\varepsilon_1 = \varepsilon_s + (\varepsilon_s + .002)\cot^2 \alpha_s = .00088 + (.00088 + .002)\cot^2 45° = .0038$$

The limiting compressive stress is:

$$f_{cu} = \frac{f_c'}{0.8 + 170\varepsilon_1} \le .85 f_c' \Rightarrow \frac{4 ksi}{0.8 + 170(.0038)} = 2.75 ksi \le .85 f_c'$$

The factored resistance of strut 1 at node 2 is:

$$P_r = \phi P_n = \phi f_{cu} A_{cs} = 0.70 \times 2.75 si \times 1370 in^2 = 2634^k > 703^k$$

The controlling strut 1 resistance is $1700^k >> 703^k$

Strut 3

Based on Figures A.8-5 and A.8-6 the area of strut 3 can be calculated:

The width of strut 3 = $W_s = 10 in$

The thickness of the strut = $\left(\frac{116 in + 87.75 in}{2} \right) = 101.88 in$

The area $A_{strut} = (10 in)(101.88 in) = 1018.8 in^2$

The tensile strain in tie 2 is:

$$\varepsilon_s = \frac{P_u}{A_s E_s} = \frac{497 kips}{(9.68 in^2)29{,}000 ksi} = 0.00177$$

At the centerline of the node, this average strain is used as per LRFD Article C5.6.3.3.3. The angle between strut 3 and tie 2 is $90°$. The principal tensile strain in the strut is calculated using LRFD Equation 5.6.3.3.3-2.

$$\varepsilon_1 = \varepsilon_s + (\varepsilon_s + .002)\cot^2 \alpha_s = 0.000885 + (.000885 + .002)\cot^2 90° = .000885$$

The limiting compressive stress is then calculated using LRFD Equation 5.6.3.3.3-1.

$$f_{cu} = \frac{f_c'}{0.8 + 170\varepsilon_1} \le .85 f_c' \Rightarrow \frac{4 ksi}{0.8 + 170 \times .000885} = 4.25 ksi >> .85 f_c' = 3.4 kst$$

The factored resistance of strut 3 at node 2 is:

$$P_r = \phi P_n = 0.70 \times 3.4 ksi \times 1018.8^2 = 2425^k > 497^k$$

***Step 7b* – Check nodal zone stress limits.**

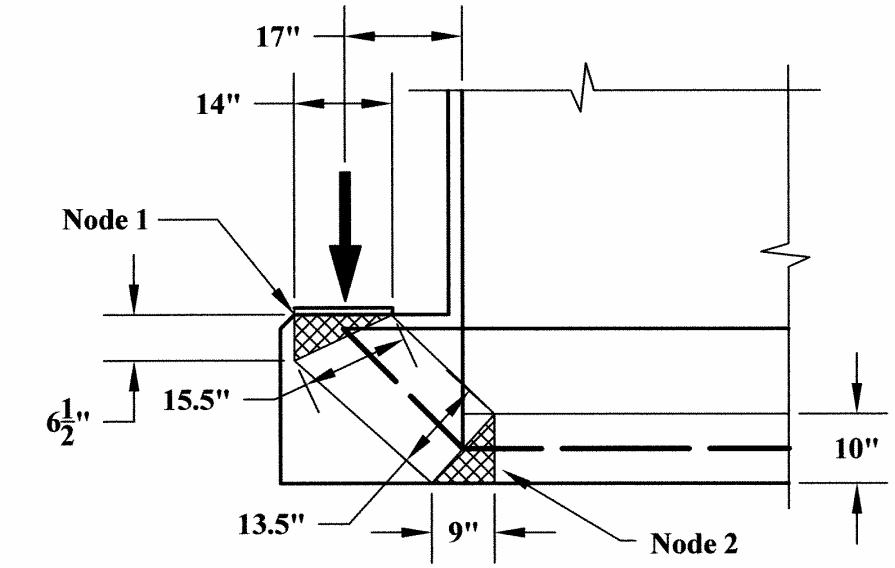

Figure A.8-6: Strut and Node Geometry

Nodal zone 1 has a rectangular top surface matching the bearing pad shape. The top surface of nodal zone 1 has a stress of:

$$f_c = \frac{497^k}{(14in)(48in)} = 0.74ksi$$

This is less than the nodal stress limit for a CCT node of:

$$0.75\phi f_c^{'} = (0.75)(0.70)\times 4ksi = 2.1ksi$$

The surface of nodal zone 1 adjoining strut 1 has an area of 883 in^2 and a stress of:

$$f_c = \frac{734^k}{883in^2} = 0.831ksi < 2.1ksi$$

Nodal zone 2 is okay by inspection as is Strut 3.

Since the structure is symmetrical, nodes 4 and 6 do not require checking.

***Step 8* – Check details of reinforcement**.

Check the development length of tie 4.

Because of the limited available development length, Tie 4 will be hooked and the required development length calculated from LRFD Equation 5.11.2.4.1-1.

$$\ell_{hb} = \frac{38.0 d_b}{\sqrt{F_c'}} = \frac{38 \times .75in}{\sqrt{4ksi}} = 14.25in$$

Check reduced length.

$$\frac{As\ required}{As\ provided} = \frac{9.2in^2}{9.68in^2} = 0.95$$

$\ell_{required} = (.95)(14.25) = 13.54" < 14"$ *available* (Node width of 14" is measured from the edge of the bearing).

Ties 2 and 6 are satisfactory since the depth of the compression strut 3 was determined using the required development length of the tie as a criteria.

Check Crack Control Reinforcing

Minimum reinforcing for the top portion of the tee = $0.003bs = 0.003 \times 72 \times 12 = 2.59in^2 / ft$ (3 legs of #6 stirrups @ 5" = 3.18 in^2/ft., 3-#9 bars at 12 horizontally = 3.0 in^2/ft.)

Minimum reinforcing for the bottom portion of the tee = $0.003bs = 0.003 \times 120 \times 12 = 4.32in^2 / ft$ (5 legs of #6 stirrups @ 5" = 5.30 in^2/ft., 5-#9 bars at 9" horizontally = 6.67 in^2/ft.)

Suggested Detailing

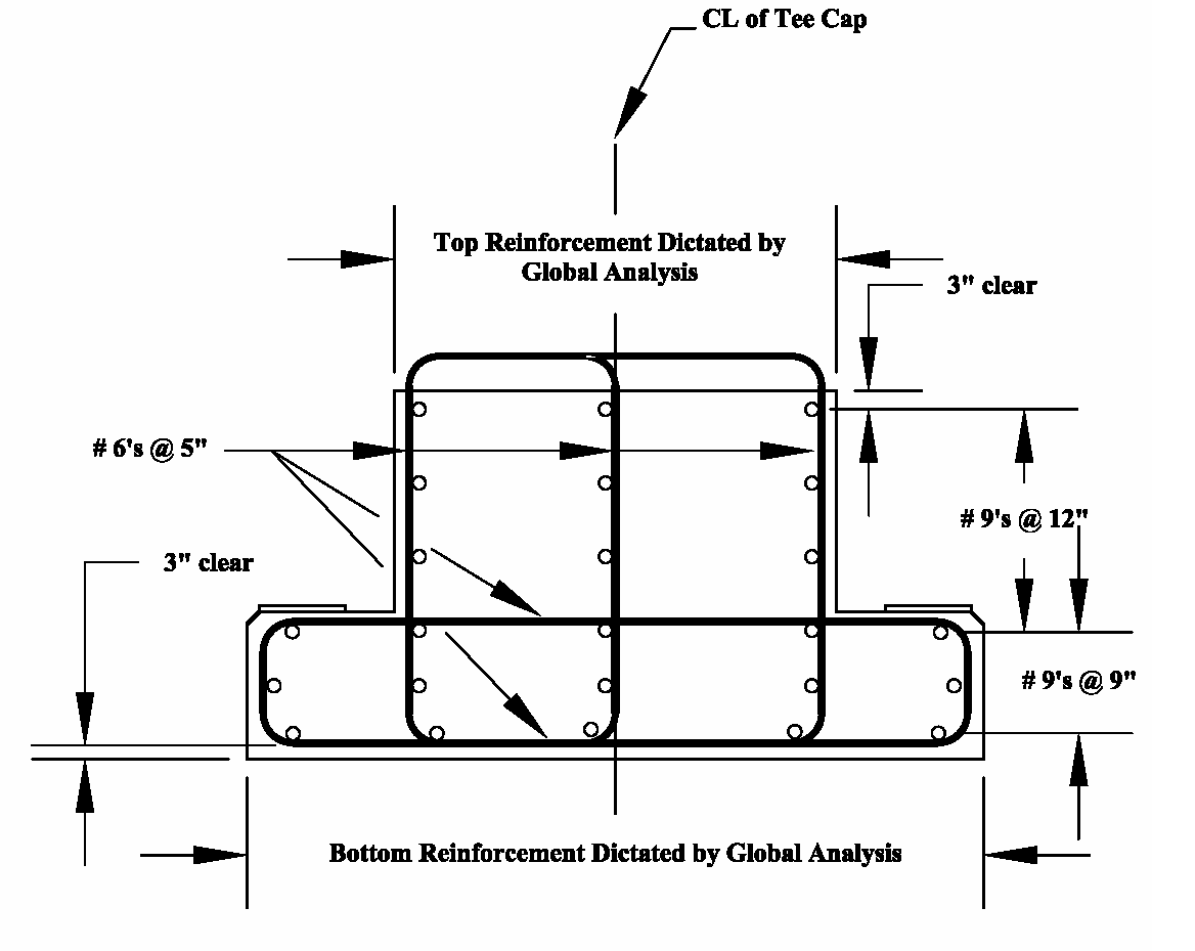

Figure A.8-7: Transverse Reinforcing (Top and Bottom Longitudinal Reinforcement shown is minimum crack control reinforcing. The actual amount will be dictated by a global analysis)

EXAMPLE A.9: MULTI-COLUMN BENT JOINT

Problem Statement:

The columns of the two-column bent shown in Figure A.9-1 have been designed based on the most critical loading cases determined using the provisions of Section 3 of the AASHTO LRFD Bridge Design Specifications. The top of the column is 16 ft above the footing, and the top of the bent is 20 ft above the footing. Four bearing pads are spaced at 7 ft.-4 in. on center on each side of the bent. Each bearing pad is subjected to a 125 kip factored dead load. The concrete compressive strength was assumed to be 5 ksi, and the reinforcement was assumed to be Grade 60. The column reinforcement details can be seen in Figure A.9-2. In addition, the axial load-moment interaction diagram for the columns is given in Figure A.9-3. The axial load-moment diagram includes the effects of confined concrete properties. It should be noted that the design earthquake induces a 915 kip axial load in one column and a 90 kip axial load in the other column.

With the given details about the column design, detail the joint (intersection of the column and beam) for opening and closing moments caused by seismic loading.

The joint must be designed for the column overstrength moment resistance which is 1.3 times the nominal moment capacity.

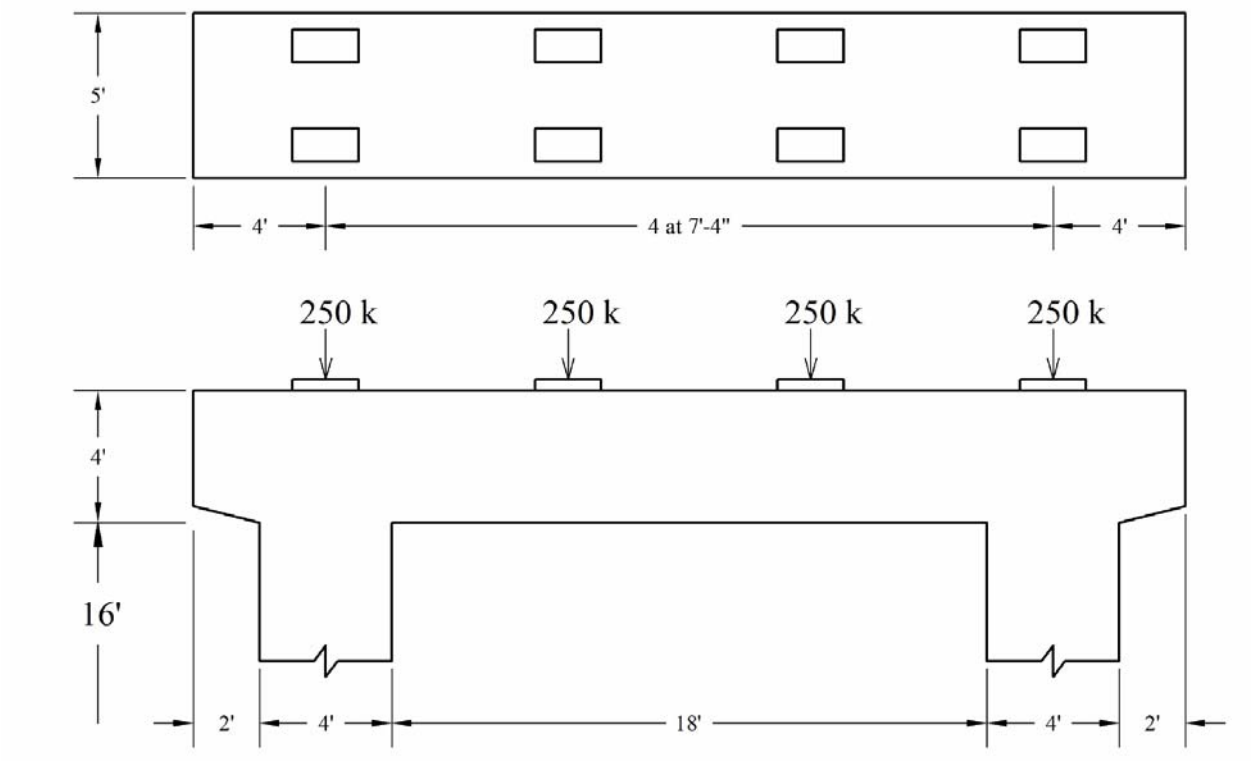

Figure A.9-1: Dimensions of the two-column bent.

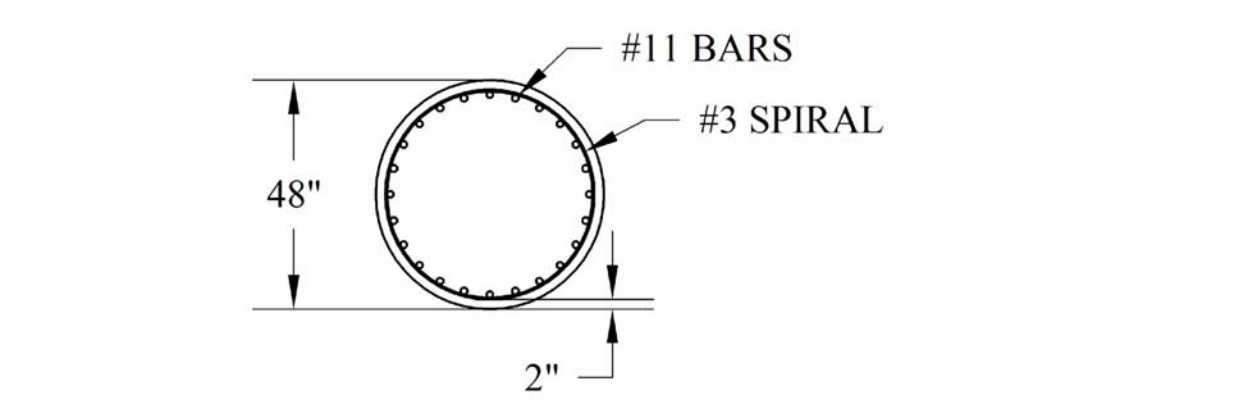

Figure A.9-2: Reinforcement details of columns.

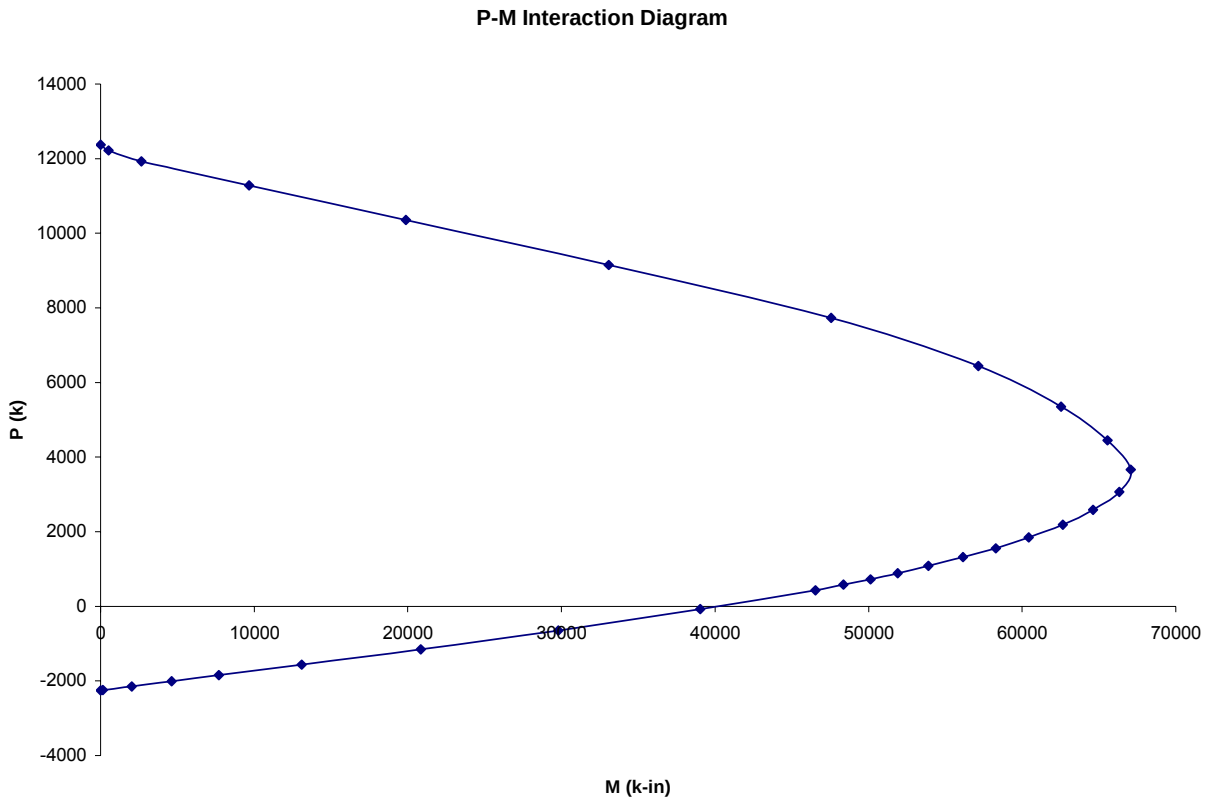

Figure A.9-3: Axial load-moment interaction diagram (includes confined concrete properties).

Step 1 – Delineate the D-regions.

Theoretically, the boundary of the D-regions would be considered to extend as shown in Figure A.9-4.

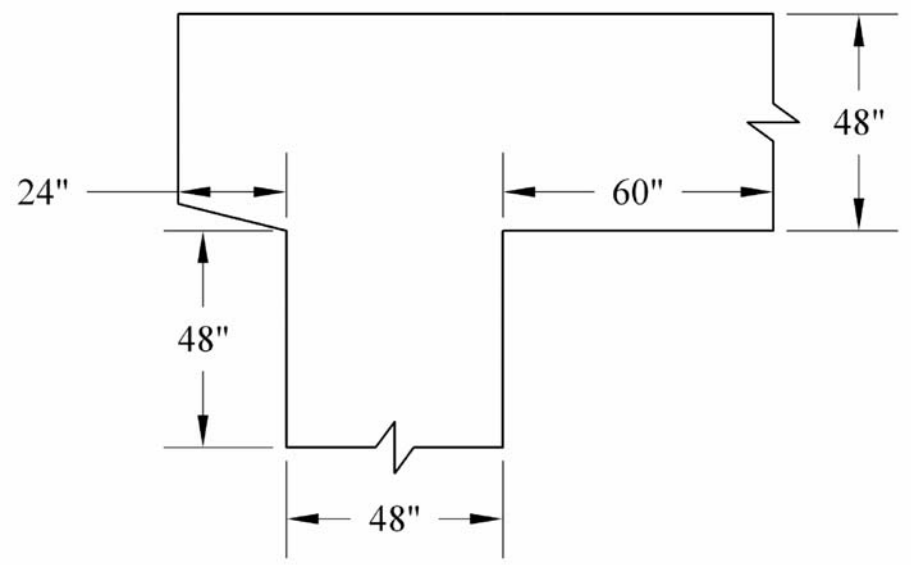

Figure A.9-4: Traditionally accepted extent of D-region.

In Figure A.9-4, the D-region was determined by extending the maximum dimension of each member away from the support. Because the purpose of this example is to design the intersection of the beam and the column for the column overstrength moment resistance during a seismic event, the D-region to be designed was modified to exclude the column (See Figure A.9-5). The D-region was not extended into the column because the plastic hinge region of the column has been designed based on a seismic detailing procedure.

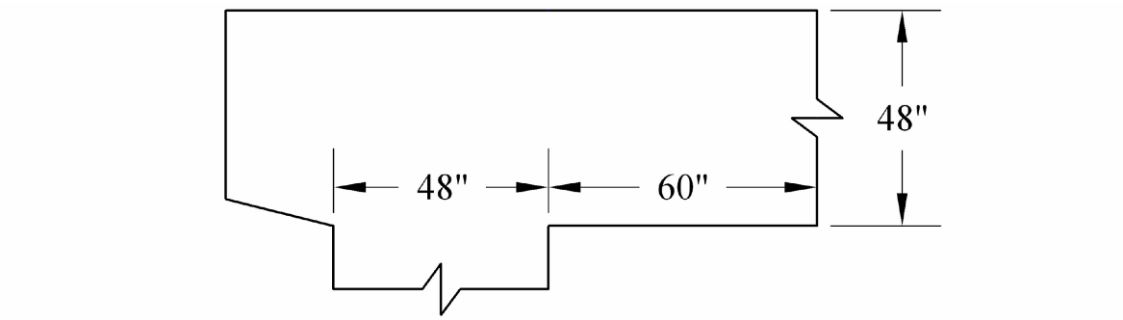

Figure A.9-5: Modified D-region to be designed for the column overstrength moment resistance.

Step 2 – Determine the boundary conditions of the D-region.

In order to determine the boundary conditions of the D-region based on the column overstrength moment resistances, the procedure outlined in Section 3.10.9.4.3c of the AASHTO LRFD Bridge Design Specifications was performed. The overstrength moment resistance determined

for the column with the larger axial load will be used to design the joint for closing moments. The overstrength moment resistance determined for the column with the smaller axial load will be used to design the joint for opening moments.

Step 1, using the given axial loads in each column caused by the design seismic event and the axial load-moment interaction diagram, determine the nominal moment capacity, M_n, for each column. For an axial load of 915 kips, the nominal moment capacity, is approximately 52,165 k-in. For an axial load of 90 kips, the nominal moment capacity is approximately 41,650 k-in. The overstrength moment resistances, M_u, are then calculated to be 1.3 times the nominal moment capacity determined from the axial load-moment interaction diagram.

$$M_{u1} = 1.3 \cdot M_{n1} = 1.3 \cdot 52{,}165k - in = 67{,}815k - in$$

$$M_{u2} = 1.3 \cdot M_{n2} = 1.3 \cdot 41{,}650k - in = 54{,}145k - in$$

Step 2, using the column overstrength moment resistances, determine the corresponding column shear forces. For the purposes of this example, it will be assumed that the columns are in perfect double curvature, so the column shear force can be determined by simply dividing the column overstrength moment by half the column height. The shear forces in each column are now calculated to be:

$$V_1 = \frac{M_{u1}}{h/2} = \frac{67{,}815k - in}{108in} = 628k$$

$$V_2 = \frac{M_{u2}}{h/2} = \frac{54{,}145k - in}{108in} = 502k$$

Step 3, sum the shears of all the columns, apply the sum of the shears at the center of the bent, and calculate the axial forces in the columns. The sum of the shears calculated above is 1,130 k. When this lateral load was applied to the center of the bent, the axial loads in the columns were found to be 965 and 35 kips.

Step 4, using the axial loads calculated from the analysis in Step 3, determine the column overstrength moment resistances and corresponding shears again. If the sum of the calculated shears is within 10 percent of the value previously determined, the calculated column overstrength moment resistances and corresponding shears from this step can be used for the design forces acting on the joint. If the calculated shear is not within 10 percent of the value previously determined, iterate until the calculated shear converges to the desired range. After performing this iterative process with the 965 and 35 kip axial loads, the design axial loads and corresponding overstrength moment resistances were found to be 36 kips and 53,110 k-in when the joint is subjected to opening moments and 965 kips and 68,500 k-in when the joint is subjected to closing moments. These overstrength moment resistances are shown in Figure A.9-6 with the corresponding column shears and boundary conditions of the beam portion of the D-region.

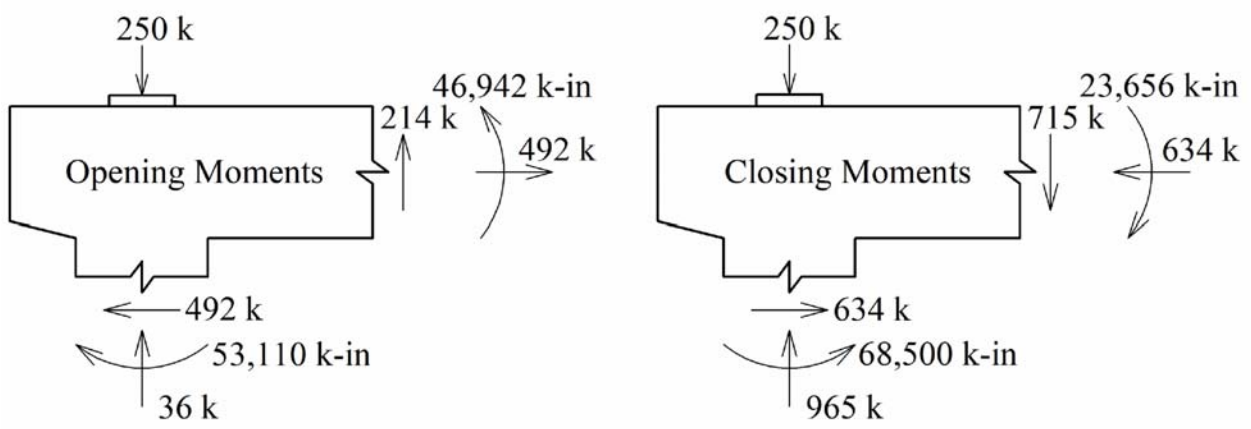

Figure A.9-6: Boundary conditions of D-region.

Steps 3, 4, and 5 – Sketch flow of forces, develop a truss model, and solve for member forces.

As a precursor, it should be noted that Priestley et al. (1996), Sritharan and Ingham (2003), and Sritharan (2005) give thorough information regarding the seismic design of bridge joints using strut-and-tie models. These authors give several examples of sophisticated STMs that can be used for different loading situations taking into account the geometry of the joint. The reader is advised to review these sources to gain more knowledge on the subject of STM design for joints subjected to seismic loading. Although the STMs presented below have some similarities to models developed by Priestley, Sritharan, and Ingham, the trusses developed are slightly simpler and more conservative.

Two local STMs have been developed to model the flow of forces through the joint for both loading cases. The STMs are shown in Figure A.9-7. Node labels are also given in Figure A.9-7. In the figure, the locations of the boundary forces were determined from analysis of the column sections with the appropriate axial loads. The magnitude of the boundary forces will be determined based on their locations and calculated boundary conditions shown in Figure A.9-6.

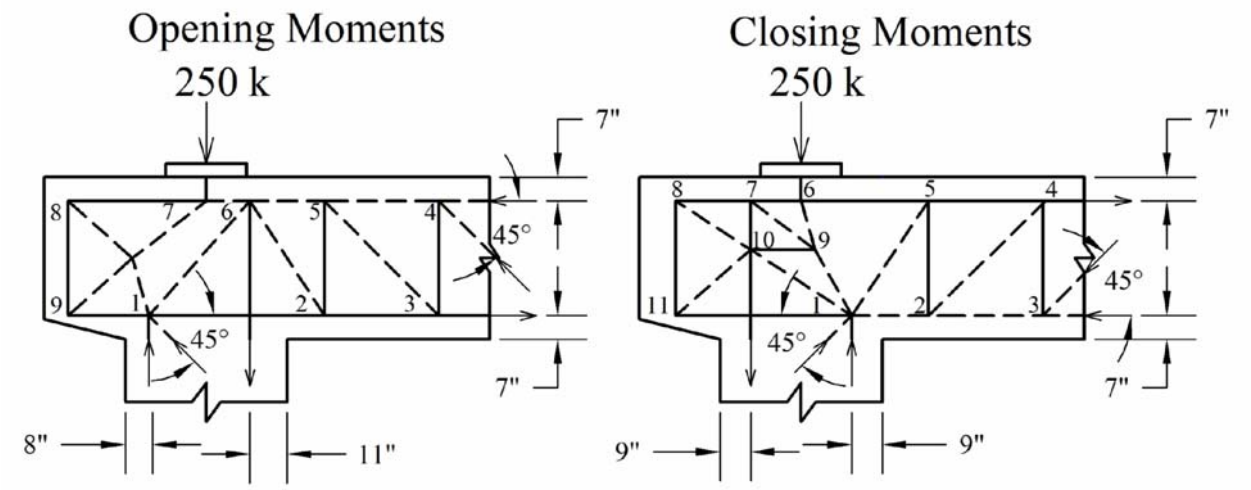

Figure A.9-7: STMs for the opening and closing moments.

In addition to Figure A.9-7, Figure A.9-8 includes member labels and the calculated values for the boundary forces based on the truss configuration. The forces calculated in each of the members are recorded in Table A.9-1. Table A.9-1 also lists the inclination of each member with respect to the horizontal.

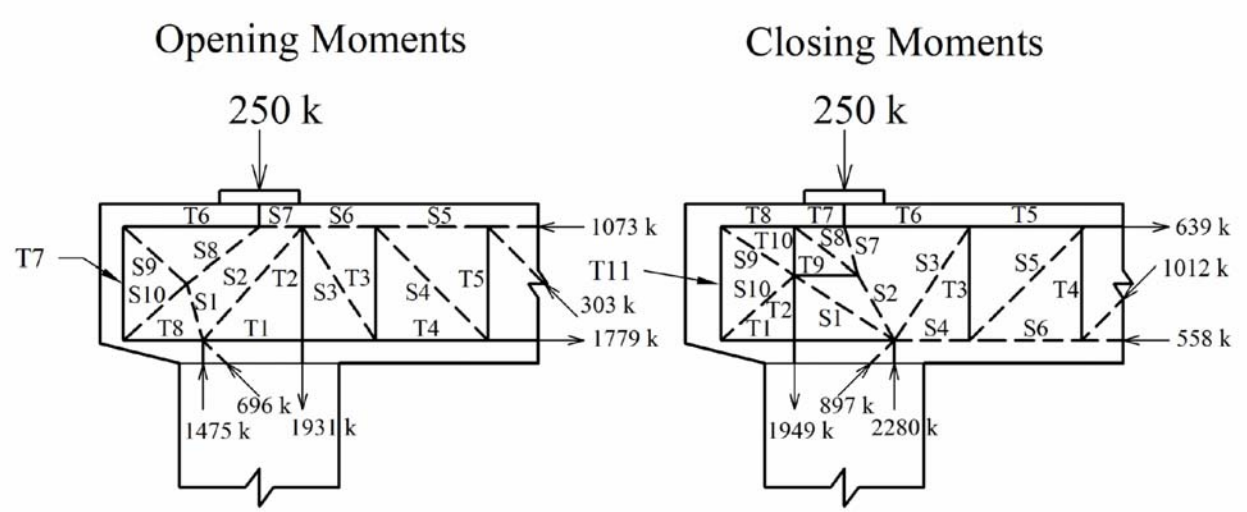

Figure A.9-8: Member labels and calculated boundary forces based on model geometry.

Table A.9-1: List of member forces and inclinations.

Member	Opening Moment Model		Closing Moment Model	
	Angle (degrees)	Force (k)	Angle (degrees)	Force (k)
S1	73.9	261	33.0	1493
S2	48.6	2288	60.9	1586
S3	57.1	255	56.2	860
S4	45.0	303	0.0	1986
S5	48.6	1287	44.3	1011
S6	0.0	1501	0.0	1273
S7	0.0	125	74.0	260
S8	0.0	408	37.1	1881
S9	41.7	264	33.1	311
S10	41.7	264	41.2	258
T1	0.0	2132	0.0	194
T2	90.0	1931	90.0	1949
T3	90.0	214	90.0	715
T4	0.0	1993	90.0	715
T5	90.0	214	0.0	1352
T6	0.0	197	0.0	1829
T7	90.0	176	0.0	1760
T8	0.0	197	0.0	261
T9	N/A	N/A	0.0	798
T10	N/A	N/A	90.0	1136
T11	N/A	N/A	90.0	170

Step 6 – Select steel area for the ties.

The required amount of reinforcement for each tie was determined as follows:

$$A_{st,required} = \frac{P_u}{\phi \cdot f_y} \qquad \text{(AASTHO LRFD 5.6.3.4.1)}$$

For tension in a STM, ϕ is taken as 0.9 (AASHTO LRFD 5.5.4.2.1). Table A.9-2 summarizes the tie calculations and the reinforcement chosen to satisfy the required calculated areas for the opening moment model. Similarly, Table A.9-3 summarizes the tie calculations and the reinforcement chosen to satisfy the required calculated areas for the closing moment model. For ties occurring in each model, the reinforcement was designed for the tie subjected to the largest force. Reinforcement was not designed for Tie 2 in the opening moment model and Ties 2 and 10 in the closing moment model because the ties are comprised of column longitudinal bars which are subjected to the boundary tension force determined from the column overstrength moment resistance.

Table A.9-2: Summary of tie design for opening moment model.

Tie	Tie Force (k)	$A_{st,required}$ (in^2)	Choose	$A_{st,provided}$ (in^2)
T1	2132	39.5	20-#14 bars	45.0
T2	1931	35.8	Column Longitudinal Bars	N/A
T3	214	4.0	5-#6 6-leg stirrups at 6 in.	13.2
T4	1993	36.9	20-#14 bars	45.0
T5	214	4.0	5-#6 6-leg stirrups at 6 in.	13.2
T6	197	3.6	20-#14 bars	45.0
T7	176	3.3	2-#6 4 leg stirrups	3.5
T8	197	3.6	20-#14 bars	45.0

Table A.9-3: Summary of tie design for closing moment model.

Tie	Tie Force (k)	$A_{st,required}$ (in^2)	Choose	$A_{st,provided}$ (in^2)
T1	194	3.6	20-#14 bars	31.2
T2	1949	36.1	Column Longitudinal Bars	N/A
T3	715	13.2	5-#6 6-leg stirrups at 6 in.	13.2
T4	715	13.2	5-#6 6-leg stirrups at 6 in.	13.2
T5	1352	25.0	20-#14 bars	45.0
T6	1829	33.9	20-#14 bars	45.0
T7	1760	32.6	20-#14 bars	45.0
T8	261	4.8	20-#14 bars	45.0
T9	798	14.8	16-#9 bars	16.0
T10	1136	21.0	Column Longitudinal Bars	N/A
T11	170	3.1	2-#6 4-leg stirrups	3.5

Figure A.9-9 shows a proposed reinforcement layout that will satisfy the tie steel requirements for both models. Only the reinforcement designed in this step is shown in Figure A.9-9. Anchorage and crack control considerations will be made in Step 8 of this example.

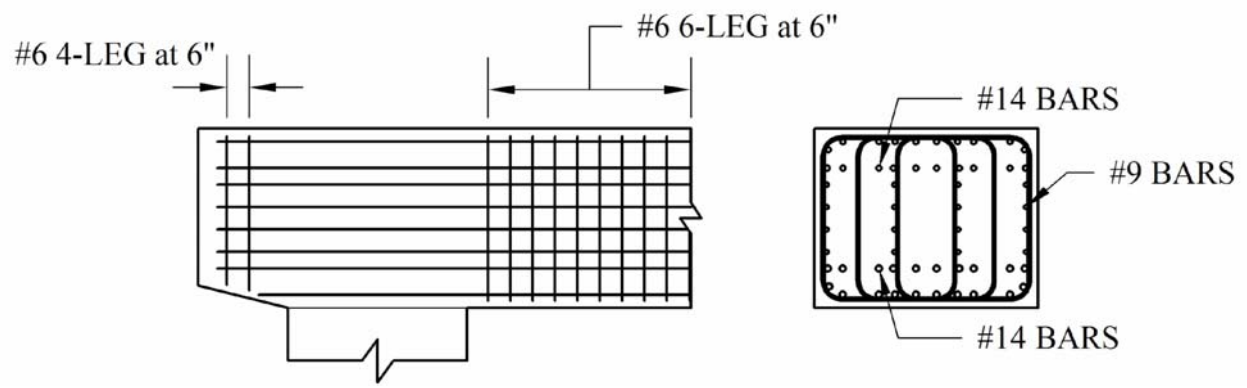

Figure A.9-9: Proposed reinforcement layout to satisfy tie requirements for both models.

Step 7– Check the capacity of the struts and nodes.

Opening Moment Model

The opening moment model will be considered first. Strut 2 is the most critical compression element in the STM for the opening moment model (see Figure A.9-8 and Table A.9-2). Strut 2 is the most critical element because it is anchoring the tie extending from the column, and it is flowing into the compressive boundary forces at the column interface. The force in this strut far exceeds the forces in the other struts in the STM. In order to determine the capacity of this strut, the area of the strut must first be determined. The width of the strut was determined using AASHTO LRFD Figure 5.6.3.3.2-1(a) as follows:

$$w_s = l_a \sin(\theta_s) = (32in) \cdot \sin(48.6^o) = 24in \qquad \text{(AASHTO LRFD 5.6.3.3.2)}$$

In the above equation, l_a was determined at Node 6 by extending the boundaries of the strut 6 bar diameters beyond the column longitudinal bars comprising Tie 2 [$2 \cdot (11in + 6d_b)$].

The depth of the section was also determined using AASHTO LRFD Figure 5.6.3.3.2-1(a). Using the "$6d_b$ rule" applied to Strut 2 based on the reinforcement configuration of Tie 2 (longitudinal bars from the column), the depth of the section was determined to be 60" (the entire depth of the bent). The area of the strut is now calculated to be:

$$A_{cs} = width \cdot depth = 24in \cdot 60in = 1440in^2$$

After the area of the struts was estimated, the principal tensile strain, ε_1, in the strut was calculated knowing that the column longitudinal bars have yielded.

$$\varepsilon_1 = \varepsilon_s + (\varepsilon_s + 0.002)\cot^2(\alpha_s) \qquad \text{(AASHTO LRFD eq. 5.6.3.3.3-2)}$$
$$\varepsilon_1 = 0.00207 + (0.00207 + 0.002)\cot^2(41.4) = 0.0073$$

Knowing principal tensile strain in the strut, the limiting compressive stress, f_{cu}, in the tie can now be calculated.

$$f_{cu} = \frac{f'_c}{0.8 + 170\varepsilon_1} \le 0.85 f'_c \qquad \text{(AASHTO LRFD eq. 5.6.3.3.3-1)}$$

$$f_{cu} = \frac{5ksi}{0.8 + 170(0.0073)} = 2.45ksi \le 0.85 \cdot 5ksi = 4.25ksi$$

Because Strut 2 is connected to a CTT node, the limiting compressive stress in the strut, can not exceed $0.65f'_c$ per AASHTO LRFD 5.6.3.5.

$$f_{cu} = 2.45 \le 0.65 \cdot 5ksi = 3.25ksi$$

The capacity of the strut is now calculated as follows:

$$\phi P_n = \phi \cdot f_{cu} \cdot A_{cs} = 0.7(2.45ksi)(1440in^2) = 2469kips \quad \text{(AASHTO LRFD 5.6.3.3.4)}$$

The capacity of the strut has been found to be larger than the demand given in Table A.9-1.

$$\phi P_n \ge P_u$$
$$2469kips \ge 2288kips$$

Closing Moment Model

For the closing moment model, Struts 1, 2, and 8 are the most critical compression elements. Each of the struts was checked with the same calculations used for Strut 2 of the opening moment model. Table A.9-4 summarizes the determined strut geometry for each member. Table A.9-5 summarizes the strut limiting compressive stress calculation. Table A.9-6 summarizes the strut capacity check calculations. All of the struts were found to have adequate capacity.

Table A.9-4: Strut geometries for closing moment model.

Strut	Width (in)	Depth (in)	A_{cs} (in^2)
S1	17.4	60.0	1047
S2	12.0	60.0	720
S8	20.0	60.0	1200

Table A.9-5: Strut limiting compressive stress calculations.

Strut	Tie	Tie Force (k)	A_{st} (in^2)	α_s (degrees)	ε_s	ε_1	f_{cu}
S1	T1	193	45.0	33.0	0.00015	0.00523	2.96
S2	T9	798	16.0	60.9	0.00172	0.00287	3.88
S8	T9	797	16.0	37.1	0.00172	0.00820	2.28

Table A.9-6: Strut capacity check calculations.

Strut	P_u (k)	A_{cs} (in^2)	f_{cu}				ΦP_n (k)	okay?
			Strut	Node		Limiting		
S1	1492	1047	2.96	10	3.25	2.96	2168.8	yes
S2	1585	720	3.88	9	3.75	3.75	1890.0	yes
S8	1881	1200	2.28	7	3.25	2.28	1913.8	yes

Step 8 (a) – Check the detailing of the anchorage lengths.

Headed anchorages will be provided to the ends of the #14 positive and negative moment longitudinal reinforcement for the beam in order to develop the bars (See Figure A.9-10). The headed anchorages will be assumed to conform to the mechanical anchorage provisions of AASHTO LRFD 5.11.3.

In addition, there is not enough development length for the #11 column longitudinal bars extending into the cap. Mechanical anchorages or hold-down bars need to be used at the top of the column longitudinal bars to provide sufficient anchorage length. Once again, mechanical anchorages must conform to AASHTO LRFD 5.11.3. For hold-down bars (or hangovers), adequate hook length and lap-splice length must be provided. For the purposes of this example, #5 hold-down bars with adequate hook length and lap splice will be assumed.

The horizontal #9 bars used for Tie 9 will have 90-degree hooks in the plane perpendicular to the STM on the left side of the column and remain straight on the right side of the column. The hook development length of the #9 bars is determined as follows:

$$\ell_{hb} = \frac{38.0 \cdot d_b}{\sqrt{f'_c}} = \frac{38.0 \cdot 1.128}{\sqrt{5}} = 19.2in \qquad \text{(AASHTO LRFD 5.11.2.4.1)}$$

This length will be provided before reaching Tie 2 in the closing moment model. The straight bar development length of the #9 bars is determined as follows:

$$\ell_d = \frac{1.25 \cdot A_b \cdot f_y}{\sqrt{f'_c}} = \frac{1.25 \cdot 1 \cdot 60}{\sqrt{5}} = 33.5in \qquad \text{(AASHTO LRFD 5.11.2.1.1)}$$

To be conservative, the #9 bars on the interior of the bent will be extended 34 in. beyond the right side of the column. The exterior #9 bars will continue the length of the D-region to fulfill the crack control requirements (see below).

All stirrups in the D-region will be assumed to conform to AASHTO LRFD 5.11.2.6.4, and, therefore, be adequately anchored.

Step 8 (b) – Check the detailing of the crack control.

Both horizontal and vertical crack control must be designed per Section 5.6.3.6 of the AASHTO LRFD. In the beam, for 6-leg #6 stirrups spaced at 6 in., the ratio of reinforcement area to gross concrete area can be calculated as follows:

$$\frac{6 \cdot A_{st}}{b \cdot s} = \frac{6 \cdot .44in^2}{60in \cdot 6in} = 0.007 \geq 0.003$$

Therefore, the 6-leg #6 stirrups satisfy the crack control requirements.

In the joint, if a spacing of 6 inches is also used, the required area of crack control is calculated to be:

$$A_{st-required} = 0.003 \cdot b \cdot s = 0.003 \cdot 60in \cdot 6in = 1.08in^2$$

To fulfill this requirement closed #6 stirrups will be used in conjunction with the column longitudinal bars. If one longitudinal bar is assumed to contribute to the crack control with each stirrup, the provided area of crack control is 2 in^2.

In the overhang, for the 4-leg #6 stirrups spaced at 6 in., the ratio of reinforcement area to gross concrete area can be calculated as follows:

$$\frac{6 \cdot A_{st}}{b \cdot s} = \frac{4 \cdot .44in^2}{60in \cdot 6in} = 0.0049 \geq 0.003$$

Therefore, the 4-leg #6 stirrups satisfy the crack control requirements.

For the beam, joint and overhang, horizontal #9 bars have been spaced at approximately 6 in. on each face. For these bars the ratio of reinforcement to gross concrete area is calculated to be:

$$\frac{2 \cdot A_{st}}{b \cdot s} = \frac{2 \cdot 1.0in^2}{60in \cdot 6in} = 0.0056 \geq 0.003$$

Therefore, the #9 bars are adequate to fulfill the horizontal crack control.

See Figure A.9-10 for the final bent joint design.

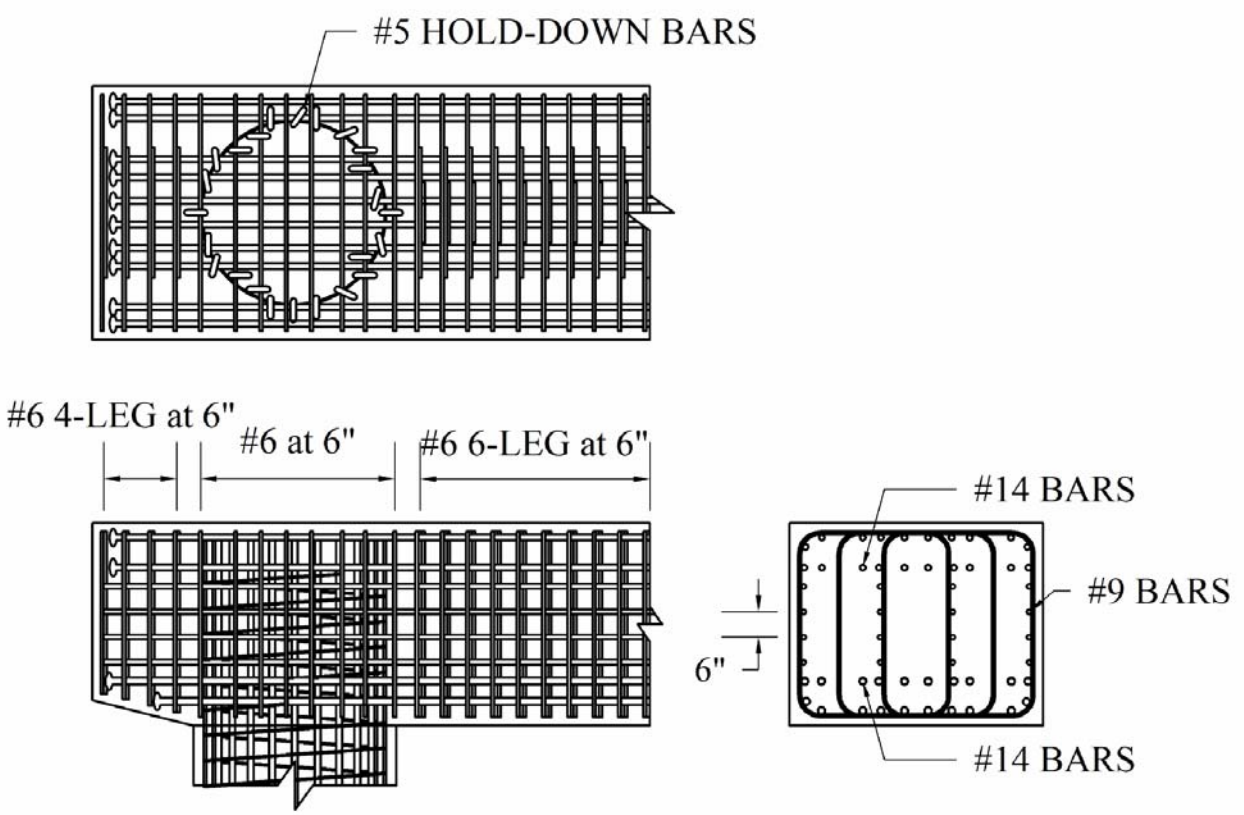

Figure A.9-10: Final details of the joint. The column reinforcement extends to the top of the beam.

EXAMPLE A.10 – INTEGRAL BENT CAP

Problem statement:

A three-span rigid frame structure has the configuration shown in Figure A.10-1. The superstructure consists of a 4-cell cast-in-place box girder carrying a 40' roadway. The box girders are fully supported during casting and are integral with the bent caps. The superstructure geometry is shown in Figure A.10-2 and the geometry of the bent is shown in Figure A.10-3. The bent cap concrete has an f_c' of 4 ksi and the mild reinforcing is grade 60. Detail the reinforcing for the cap using LRFD STM and HL-93 loading.

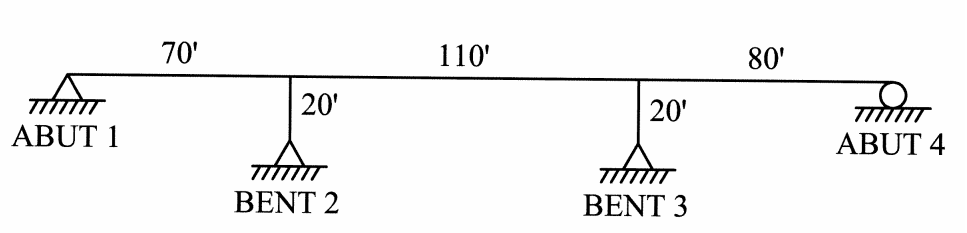

Figure A.10-1: Rigid Frame Geometry

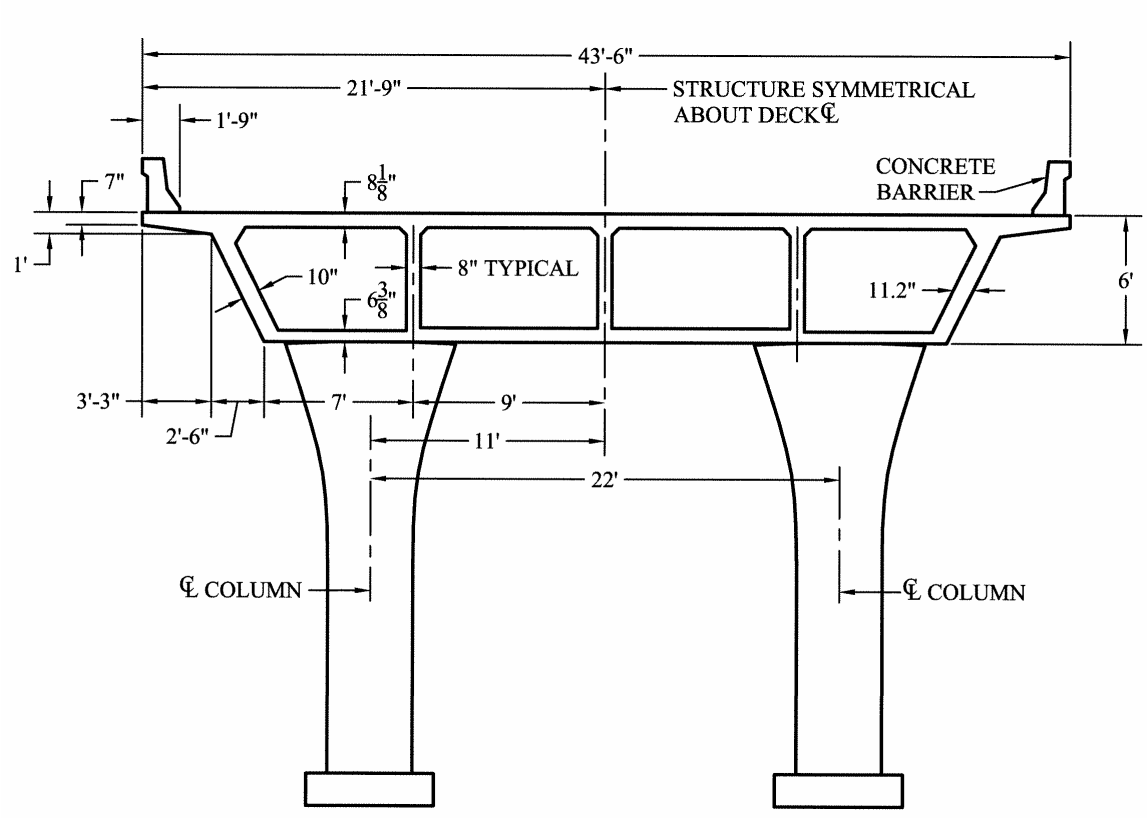

Figure A.10-2: Cross-Section of Structure

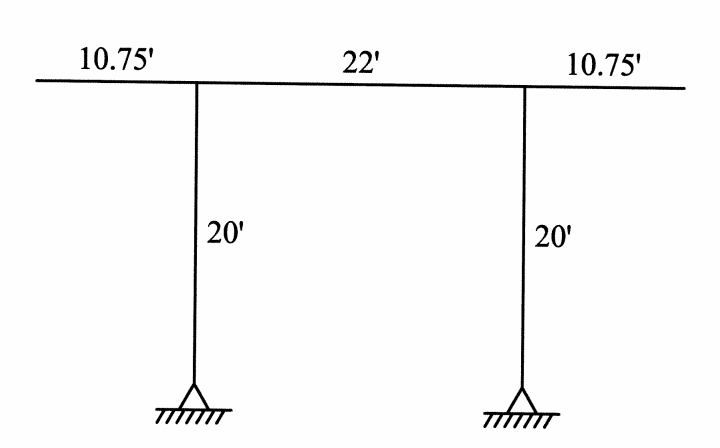

Figure A.10-3: Bent Geometry

Using AASHTO LRFD strut and tie provisions and HL 93 live-loading, design the reinforcing for the integral cap in Bent 3.

<u>Step 1</u> – Delineate the D-region.

The bridge, as shown in Figure A.10-2, has a superstructure depth of 6 ft, a two-column bent substructure, with 4 ft. diameter columns, and a clear distance of 18' between columns. The top of the column is flared for architectural reasons only and the outer 2 feet of the top of the flare is not attached to the integral cap.

Given the depth of the beam and the spacing of the concentrated loads from the box girder webs, the entire cap would be considered as a D-region.

<u>Step 2</u> – Determine the boundary conditions of the D-region.

The first step is to determine the loads acting on the bent cap. Using the weight of the box, barrier rails and future wearing surface a total reaction of 1300^{k} develops on Bent 3. Since there are 5 webs, a 260^{k} loading will be applied at each web location. The integral cap measures 4.5' x 6'; however, 14½" of the depth will be poured in a later stage of construction and has therefore been counted as box load. Therefore a uniform load of $\left(\frac{(54")(72-14.5)}{144}\right)0.150 = 3.23$ kips per foot, will be applied

HL 93 is applied to the spans as shown in Figure A.10-4. Note that the provisions of AASHTO §3.6.1.3.1 govern for the application of the truck loading to maximize the reactions at Bent 3. The resulting live loading on the bent is shown in Figure A.10-6 and A.10-8. The dead load of the superstructure, as well as the live load will be applied equally to the top and bottom of the bent cap. Finite element modeling done by Zayati, Ibrahim and Hida has indicated this is a

reasonable assumption for a structure constructed as this one is. The weight of the bent cap will be applied to the top of the cap.

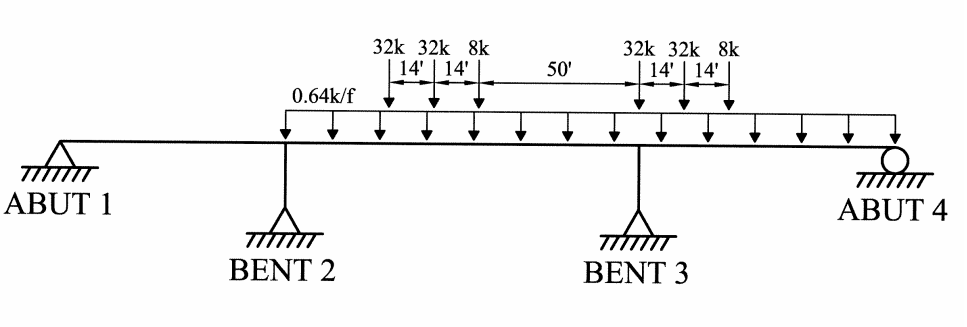

Figure A.10-4: Application of HL-93 Loading to Determine Maximum Reactions

<u>Steps 3 and 4</u> – Visualize the flow of forces and develop the STM.

The flow of forces results in the idealized STM shown in Figure A.10-5. A simple support condition is chosen to represent the column support. Modeling the column supports with two joints or springs could be used to model the column's moment. However, the moments in the columns are relatively low and using the single supports in this case results in conservative values in the truss model. Even though the exterior webs of the boxes are inclined, vertical ties are placed near the centroid of the web element in the model. It is felt this simplification will not result in unconservative results and allow for a more direct solution to the forces in the ties located in this region of the cap. Addition truss elements (ties) have been placed between the webs of the boxes in an attempt to have more efficient struts and to more accurately reflect the change in shear along the length of the cap.

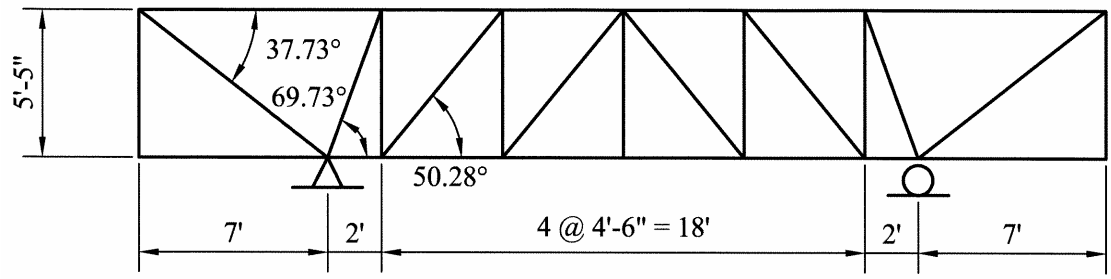

Figure A.10-5: STM Model of Bent Cap

<u>Step 5</u> – Solve for member forces.

There are two live loading cases that must be used. Case I places the live load on the cantilever to maximize the negative moment. This is illustrated in Figure A.10-6 and the resulting forces on the STM are shown in Figure A.10-7. The second case loads the middle of the bent with live load to maximize the positive moment in the cap. This is illustrated in Figure A.10-8 and the

resulting loading on the STM is shown in Figure A.10-9. The resulting forces in the STM for Cases I and II are shown in Table A.10-1. The governing loads will be used in the design of the integral cap.

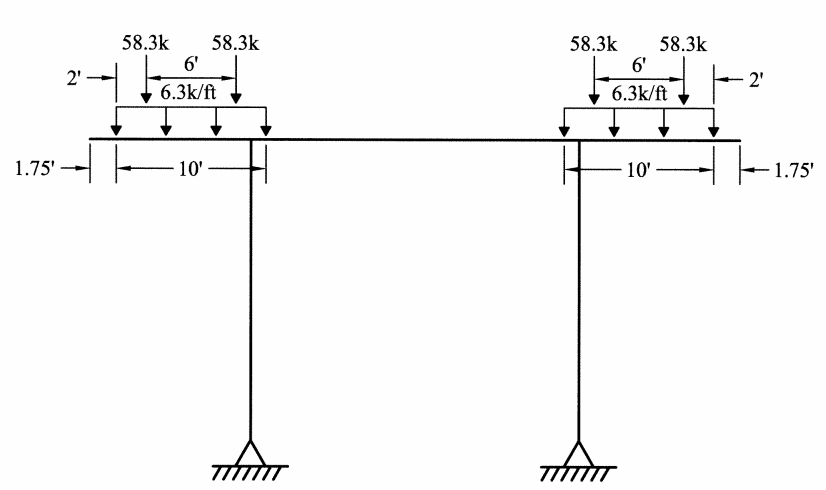

Figure A.10-6 – Live Load Configuration to Maximize Cantilever Moments

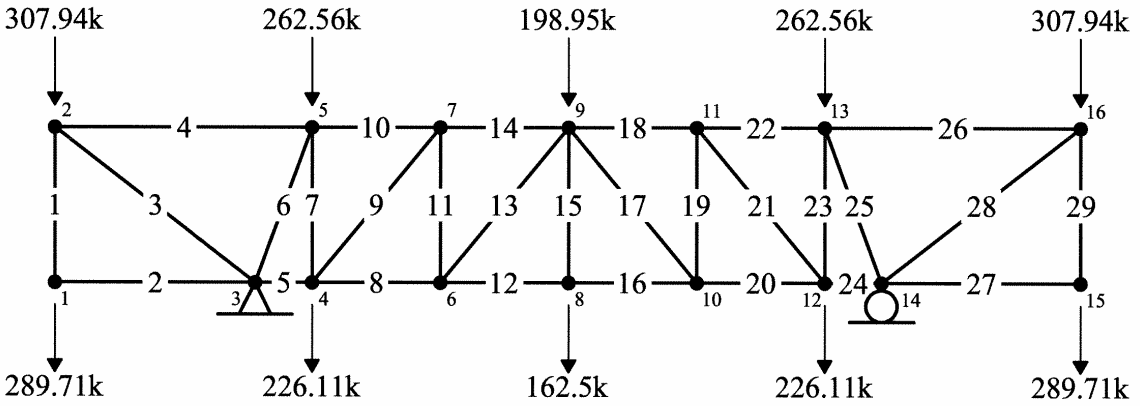

Figure A.10-7 – Factored Loading Resulting from Maximizing of Cantilever Moments

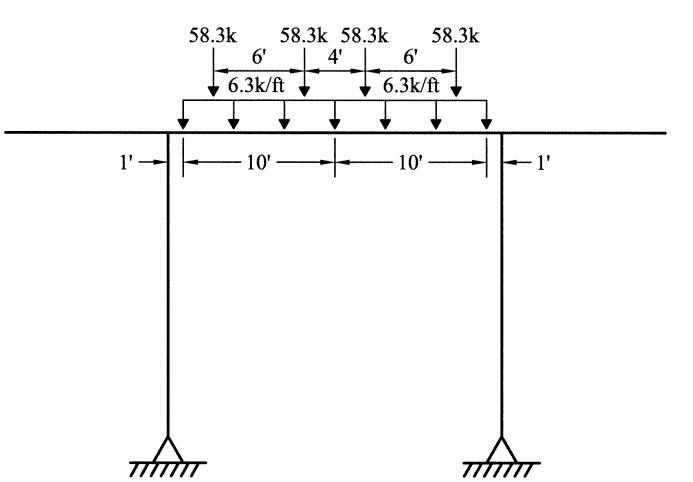

Figure A.10-8 – Factored Live Load Configuration to Maximize Positive Moments

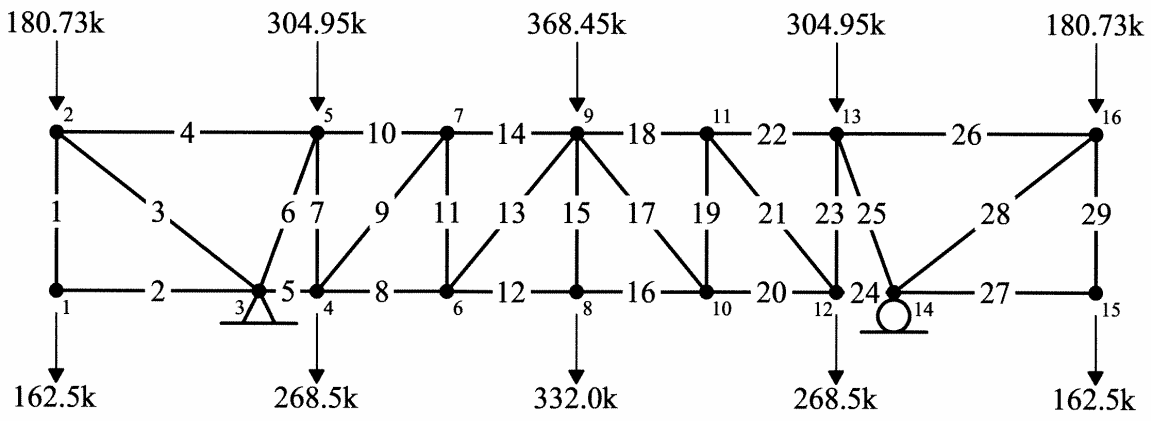

Figure A.10-9 – Loading Resulting from Maximizing of Positive Moments

Table A.10-1

Member	Case I Max Cantilever Loading		Case II Maximum Positive Loading		Member	Case I Max Cantilever Loading		Case II Maximum Positive Loading	
	Force	C or T	Force	C or T		Force	C or T	Force	C or T
1	289.7	T	162.5	T	16	224.9	C	479.4	T
2	0		0		17	235.0	C	455.3	C
3	976.6	C	560.8	C	18	375.0	T	188.4	C
4	772.3		443.6	T	19	180.7	T	350.2	T
5	525.2	C	102.5	C	20	375.0	C	188.4	T
6	713.6	C	984.6	C	21	235.0	C	455.3	C
7	406.8	C	618.7	T	22	525.2	T	102.5	T

8	375.0	T	188.4	T	23	406.8	T	618.7	T
9	235.0	C	455.3	C	24	525.2	C	102.5	C
10	525.2	C	102.5	T	25	713.6	C	984.6	C
11	180.7	T	350.2	T	26	772.3	T	443.6	T
12	224.9	C	479.4	T	27	0		0	
13	235.0	C	455.3	C	28	976.6	C	560.8	C
14	375.0	T	188.4	C	29	289.7	T	162.5	T
15	162.5	T	332.0	T					

<u>Step 6</u> – Select steel area for ties.

a) Ties 4 and 26 have the highest levels of tension (cantilever case). The required area of tension tie reinforcement, A_{st}, is

$$A_{st} = \frac{P_u}{\phi F_y} = \frac{772.3^k}{(0.9)(60)} = 14.3in^2$$

Assume #11 bars

$14.3in^2/1.56in^2/bar = 9.16$ bars Use 9 bars

Use 9 #11 bars @ 6"on-center in the top of the bent.

b) Ties 12 and 16 have the highest tension in the bottom of the integral cap as they are governed by the maximum positive moment.

$$A_{st} = \frac{P_u}{\phi F_y} = \frac{479.4^k}{(0.9)(60)} = 8.88in^2$$

Assume #9 bars

$8.88\ in^2/1in^2/bar = 8.88$ bars Use 9 bars

Use 9 - #9 bars in the bottom of the bent.

The top and bottom bars will be used full length of the cap even though they could be curtailed. The #9 bars will have a 90° bend at each end for development, while the #11 bars will extend into the slab.

c) Sizing the tension ties representing the stirrups.

Will assume No. 5 stirrups with 4 legs (see Figure A.10-12).

1. Stirrup spacing required for Tie 7 (highest load) F=618.7^k:

$$n = \frac{P_u}{\phi A_{st} F_y} = \frac{618.7^k}{(0.9)(4 \times 0.31)(60)} = 9.24 \text{ bars say } 10$$

As stated earlier, the outer 2 feet of the column at the cap-column interface is not connected to the integral bent. On order to anchor the strut at node 5, the stirrups will be continued over the column.

Therefore the stirrups will be placed from the centerline of the column to a point midway of the next panel, a distance of 54". If this structure were to be used in a location of high lateral loading, a local STM of the region above the column would be in order.

$$s \le \frac{54"}{10"} = 5.4" \quad \text{Use a bar spacing of 5"}$$

2. Stirrup spacing required for Tie 11 F = 350.2^k

$$n = \frac{P_u}{\phi A_{st} F_y} = \frac{350.2^k}{(0.9)(4 \times 0.31)(60)} = 5.23$$

The distance to a point halfway between the adjoining nodes = 54". Hence, the required spacing, s, within the region is:

$$s \le \frac{54"}{5.23} = 10.33in$$

3. Stirrup spacing required for Tie 15 F = 332^k

$$n = \frac{P_u}{\phi A_{st} F_y} = \frac{332^k}{(0.9)(4 \times 0.31)(60)} = 4.96$$

The distance to a point halfway between the adjoining nodes = 54". Hence, the required spacing, s, within this region is:

$$s \le \frac{54"}{4.96} = 10.88"$$

4. Stirrup spacing required for Tie 1 F = 289.7^k

$$n = \frac{P_u}{\phi A_{st} F_y} = \frac{289.7^k}{(0.9)(4 \times 0.31)(60)} = 4.32$$

Distance to the face of the column = 60”

$$s \le \frac{60''}{4.32} = 13.89 \text{ use 12” spacing} \qquad A_{st} = 6(4 \times 0.31) = 7.44 in^2$$

It is good at this point to take a look at the minimum reinforcing requirements to insure that an amount of reinforcing greater than that required by load might be required. For crack control in this disturbed region, the ratio of reinforcement area to cross-sectional area shall not be less than 0.003 in both the vertical and horizontal directions. Hence

$$\frac{A_{st}}{b_s} \ge 0.003$$

Therefore:

$$s \le \frac{A_{st}}{0.003b} = \frac{4 \times 0.31}{0.003(54)} = 7.65 in$$

Thus with the exception of the area affected by Tie 1, use No. 5 stirrups with 4 legs spaced at 7” throughout the length of the cap.

<u>Step 7</u> – Check capacity of struts.

a.) The highest compressive force is in Struts 6 and 25 for the maximum positive moment case. The calculated force in these two members = 984.6^k

As this strut is crossed by vertical stirrups, the compressive capacity of this strut may need to be reduced. Since the smallest angle will result in the lowest allowable stress, it is clear by inspection that Tie 7 with a load of 618.7 k and an angle of $20.27°$ will result in the lowest allowable stress in strut 6. The area of Tie 1 = 54”/5 = 10.8 bars, say 11 bars A = 11(4)(.31) = 13.64 in^2

Hence the strain in this stirrup as a result of its 618.7^k tension load is:

$$\varepsilon_s = \frac{P_u}{A_{st} E_s} = \frac{618.7^k}{(13.64 in^2)(29{,}000)} = 1.564 \times 10^{-3}$$

As the smallest angle between the strut and the tension tie is 20.27°, the principal strain, ε_1, can be determined as:

$$\varepsilon_1 = \varepsilon_s + (\varepsilon_s + 0.002)\cot^2 \alpha_s = 1.564 \times 10^{-3} + (1.564 \times 10^{-3} + 0.002)\cot^2 20.27° = .02769$$

And, the limiting compressive stress f_{cu}, in the strut is:

$$f_{cu} = \frac{f_c^{'}}{0.8 + 170\varepsilon_1} \le 0.85 f_c^{'} \Rightarrow \frac{4.0}{0.8 + 170 \times .02769} = 0.73 ksi \le 0.85 f_c^{'}$$

The width of the band, ℓ_a, that this strut crosses is 54" from the centerline of the column. Therefore the width of the strut will be:

$$w = \ell_a \sin = 54" \sin 69.73° = 50.66 in$$

As stated in AASHTO 5.6.3.3.2, the depth of a strut that is anchored by reinforcement is six times the diameter of the bar comprising the longitudinal reinforcement. Since there are 4 stirrup legs, and since the top reinforcement is #11 bars, the thickness of the strut will be:

$$T_{st} = \left[1\tfrac{1}{2}" + 0.625/2 + 6(1.410) + 12(1.410)\right] 2 = 54.38"$$

Use the full width of the cap as the thickness (See Figure A.10-10)

$$P_n = f_{cu} A_{cs} = (.73)(50.66 \times 54) = 1996.8^k$$

The factored resistance of the strut is:

$$P_r = \phi P_n = .7 \times 1996.8 = 1{,}398^k > 984.6^k$$

b.) The highest compressive force is in Struts 3 and 28 from the maximum cantilever loading case is 976.6^k

As this strut is crossed by vertical stirrups, the compressive capacity of this strut may need to be reduced. The area of Tie 1 = 60"/7 = 8.57 bars, say 9 bars A = 9(4)(.31) = 11.16 in^2

Hence the strain in this stirrup as a result of its 289.7^k tension load is:

$$\varepsilon_s = \frac{P_u}{A_{st} E_s} = \frac{289.7^k}{(11.16 in^2)(29{,}000)} = 0.895 \times 10^{-3}$$

As the smallest angle between the strut and the tension tie is 37.73°, the principal strain, ε_1, can be determined as:

$$\varepsilon_1 = \varepsilon_s + (\varepsilon_s + 0.002)\cot^2 \alpha_s = 0.895 \times 10^{-3} + (0.895 \times 10^{-3} + 0.002)\cot^2 37.73° = .00573$$

And, the limiting compressive stress f_{cu}, in the strut is:

$$f_{cu} = \frac{f_c^{'}}{0.8 + 170\varepsilon_1} \le 0.85 f_c^{'} = \frac{4.0}{0.8 + 170 \times 5.73 \times 10^{-3}} = 2.25 ksi \le 0.85 f_c^{'}$$

The width of the band, ℓ_a, that this strut crosses is 60" from the face of the column. Therefore the width of the strut will be:

$$w = \ell_a \sin = 60" \sin 37.73° = 36.72 in$$

As discussed above, in accordance with AASHTO 5.6.3.3.2, the depth of a strut that is anchored by reinforcement is six times the diameter of the bar comprising the longitudinal reinforcement. Since there are 4 stirrup legs, and since the top reinforcement is #11 bars, the thickness of the strut will be:

$$T_{st} = \left[1\tfrac{1}{2}" + 0.625/2 + 6(1.410) + 12(1.410)\right] 2 = 54.38"$$

Use the full width of the cap as the thickness (See Figure A.10-10)

$$P_n = f_{cu} A_{cs} = (2.25)(36.72 \times 54) = 4{,}461^k$$

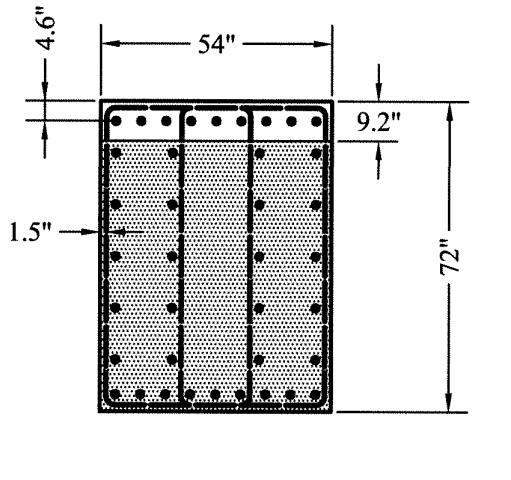

Figure A.10-10 – Strut Width Illustration for Upper Nodes

The factored resistance of the strut is:

$$P_r = \phi P_n = .7 \times 4461 = 3{,}123 > 976.6^k$$

c) From the maximum positive bending case, the maximum load in Struts 9 and 21 F = 455.3^k

Of the 4 diagonal struts crossing the web in the interior portion of the bent, Members 9 and 21 have the highest compression. Member 7 intersects the strut at the smallest angle and the principal strain, ε_1, can be determined.

The strain in Member 7 using the reinforcing in the band from the face of the column to the midpoint of the adjacent panel is 27". Using the minimum reinforcing requirements
n = (27/5) = 5.4 use 6 stirrups

$$A_{st} = (6)(4 \times .31) = 7.44in^2$$

$$\varepsilon_s = \frac{P_u}{A_{st}E_s} = \frac{618.7^k}{(7.44in^2)(29{,}000)} = .00286$$

The principal strain ε_1 can be determined as:

$$\varepsilon_1 = \varepsilon_s + (\varepsilon_s + 0.002)\cot^2 \alpha_s = .00286 + (.00286 + 0.002)\cot^2 39.73° = .0099$$

and the limiting compressive stress, f_{cu}, in the strut is:

$$F_{cu} = \frac{F_c'}{0.8 + 170\varepsilon_1} = \frac{4.0}{0.8 + 170(.0099)} = 1.61ksi$$

The width of the strut will conservatively be taken as sin 57.28(27") = 22.8"

Since the longitudinal bars are #9 bars, the depth of the strut will be calculated as

$$T_{st} = [1\tfrac{1}{2}" + .625 + 6(1) + 12(1)]\,2 = 40.25"$$ (See Figure A.10-11)

$$P_n = F_{cu}A_{cs} = (1.61)(22.8 \times 40.25) = 1{,}478.77^k$$

The factored resistance of the strut is:

$$P_r = \phi P_n = .7(1{,}478.77) = 1035^k > 455.3^k$$

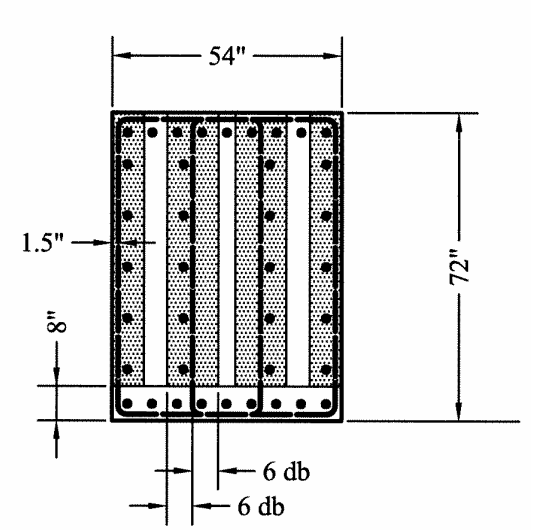

Figure A.10-11 – Strut Width Illustration for Lower Nodes

d) Struts 13 and 17 are okay by inspection.

Check Nodal Zone stresses.

Node 2

Since Node 2 is a CTT node, the stress limit allowed in this case is given as:

$$0.65\phi F_c' = 0.65 \times 0.7 \times 4.0 = 1.82ksi$$

The nodal zone stress to anchor the tension tie force of 772.3^k is:

$$F_c = \frac{772.3}{(4.6)(2)54} = 1.55ksi < 1.82ksi$$

Node 6

Since Node 6 is also a CTT node, the stress limit allowed is 1.82ksi.

The nodal zone stress to anchor the tension tie force of 479.4^k is:

$$F_c = \frac{479.4}{(2)(4)40.25} = 1.48ksi < 1.82ksi$$

Step 8 – Detail reinforcement.

In Step 6, the stirrup spacing was adjusted to satisfy crack control requirements for the vertical ties. Crack control reinforcement also must be provided in the horizontal direction. The vertical spacing between these horizontal bars can not exceed 12 in. Using this maximum spacing, the area of horizontal bars in each layer needs to be:

$$A_{st} = 0.003 b_s = 0.003 \times 54 \times 12 = 1.94 in^2$$

Therefore, use 4 No. 7 horizontal bars at 12" spacing.

The complete reinforcing details can be seen in Figure A.10-12.

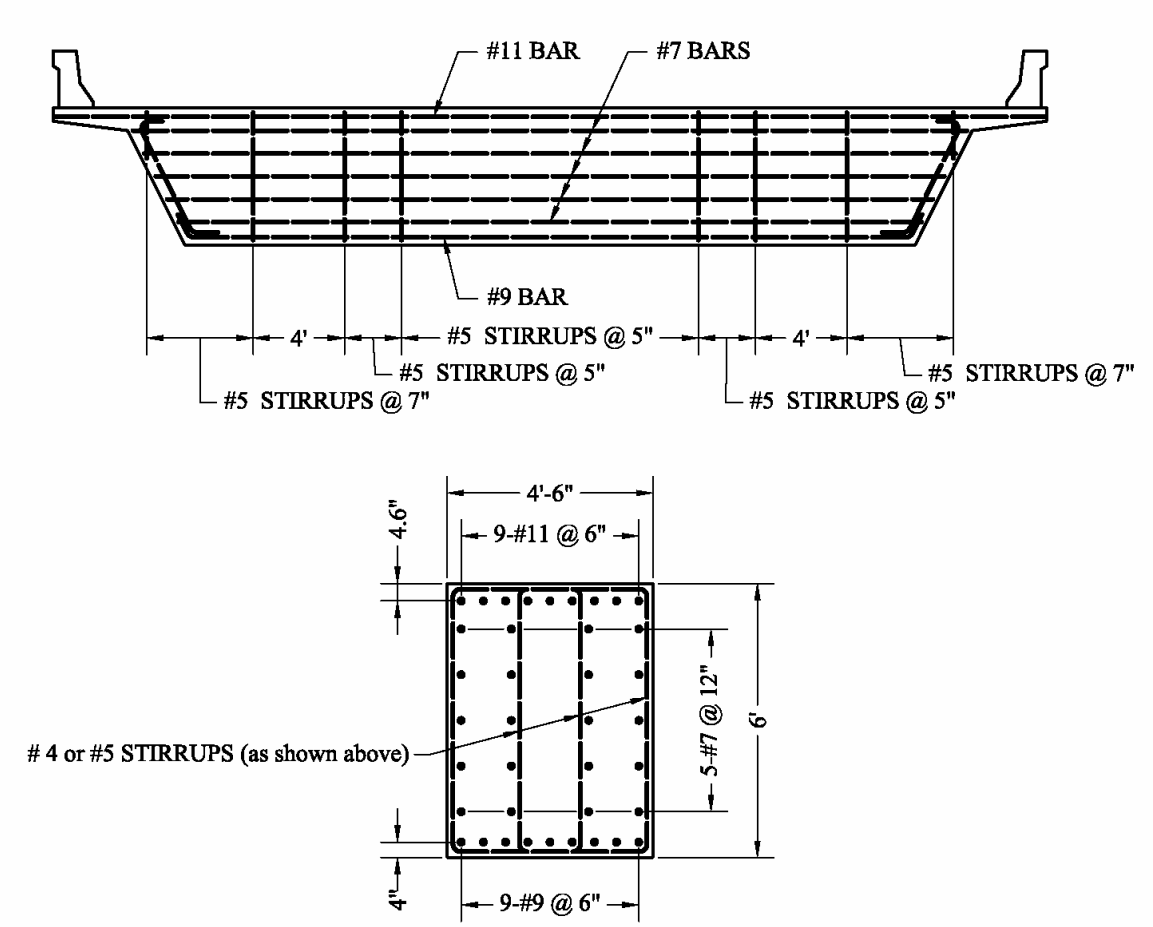

Figure A.10-12 – Reinforcing Details for Cap (Note: To reflect actual conditions, the soffit and deck would have to be shown. The stirrups would have to extend into the deck and the top flexural steel in the cap would have to be adjusted so as not to be in the same plane as the deck steel. The stirrup spacing would have to be adjusted as necessary in the areas where the girders frame into the cap and in the column areas. These items are not shown for reasons of clarity)

APPENDIX B

LITERATURE SEARCH MATERIAL

LIST OF CATEGORIES

B.1 GENERAL STRUT-AND-TIE MODEL INFORMATION/RESEARCH

Brown, M. D., Sankovich, C. L., Bayrak, O., Jirsa, J. O., Breen, J. E., and Wood, S. L.
Examination of the AASHTO LRFD Strut and Tie Specifications
University of Texas at Austin. Center for Transportation Research, CTR-0-4371-2; May 93; 316p
ABSTRACT: The design of reinforced concrete members for shear was studied. Both strut-and-tie models (STM) and sectional methods were examined. Initially, the response of isolated struts was observed. Various layout of reinforcement were used within the isolated struts. Three series of deep beam tests were also conducted. The first series was used to examine the effects of load distribution (uniform or concentrated) and distribution of shear reinforcement (horizontal and vertical) on shear strength of deep beams. The effects of beam width and shear span-to-depth ratio on shear strength were studied using the second series of beam tests. In the final series, the effects of load distribution on specimens without shear reinforcement were observed. A database of approximately 1,200 experimental results was compiled. The database, along with the experimental program, was used to evaluate the levels of conservatism of North American STM code provisions as well as sectional design provisions. A new design procedure was developed to improve the safety of STM design procedures. Along with the new procedures, an expression was created to determine the necessary amount of reinforcement within bottle-shaped strut. Finally, recommendations to improve the conservatism of sectional design provisions were developed.
KEYWORDS: structural concrete; shear; strut-and-tie modeling; uniform load; concentrated loads

Bergmeister, K. , Breen, J.E. , Jirsa, J.O. , and Kreger, M.E.
Detailing for Structural Concrete
Final Report, University of Texas at Austin. Center for Transportation Research, CTR-0-1127-3F; FHWA/TX-93/1127-3F; NTIS No: PB95-206314/HDM; May 93; 316p
ABSTRACT: The report is the final report in a series which investigates the applications of strut-and-tie modeling for typical details in structural concrete bridges. It summarizes the state of the art of strut-and-tie modeling and presents specific recommendations for choosing the critical dimensions and carrying out detailed computations using such strut-and-tie models. Separate sections treat the overall modeling and detailing process, checking compression struts, detailing tension ties, evaluating TTT, CCC, CCT and CTT nodes, and incorporating prestressing forces. The report includes a series of examples showing application of strut-and-tie models in detailing deep beams, corbels, anchorage zones, dapped ends, openings, and pretensioned beams. In addition, a number of detailing aids are included in an appendix.
KEYWORDS: highway bridges; concrete structures; struts; compressive strength; concrete beams; shear strength; mathematical models

Collins, M.P. and Mitchell, D.
Rational Approach to Shear Design--The 1984 Canadian Code Provisions
ACI Journal, *Proceedings* V. 83, No. 6, Nov-Dec 1986, p 925-933
ABSTRACT: The 1984 Canadian Concrete Code contains new shear design provisions that are believed to be more rational and more general than the shear regulations of the 1983 ACI Building Code. New shear design procedures are summarized and their use is illustrated by means of design examples.
KEYWORDS: beams (supports); building codes; deep beams; detailing; reinforced concrete; shear properties; shear strength; structural design.

Cook, W.D and Mitchell, D.
Studies of Disturbed Regions near Discontinuities in Reinforced Concrete Members
ACI Structural Journal, V. 85, No. 2, Mar-Apr 1988, p 206-216
ABSTRACT: Discontinuities caused by abrupt changes in cross-sectional dimensions or by concentrated loads result in what is termed “disturbed regions” due to the disturbance in the flow of the stresses around the discontinuities. The use of simple strut and tie models to analyze and design disturbed regions such as corbels, dapped end beams, beams with openings, and deep beams is explained. Strength predictions of a corbel and a dapped end beam using strut and tie models are compared with test results. Complete response predictions using a non-linear finite element computer program are used to verify the strut and tie models and to provide further insight into the response of disturbed regions.
KEYWORDS: beams (supports); brackets; corbels; deep beams; detailing; finite element method; openings; reinforced concrete; shear properties; structural analysis; structural design.

Lampert, P. and Thurlimann, B.
Ultimate Strength and Design of Reinforced Concrete Beams in Torsion and Bending
IABSE, *Publications*, Vol. 31-I, 1971, pp. 107-131.
ABSTRACT: It is shown that, with respect to ultimate strength, prestressed members can be treated as nonprestressed members with an equivalent amount of normal reinforcement. The theory for reinforced beams can be extended to reinforced and prestressed beams. The experimental behavior of reinforced concrete beams under torsion confirmed the validity of a space truss model. The design equations are based on a space truss with 45//0 diagonals. Design rules and detailing requirements for beams subjected to torsion- bending- shear are given.

Marti, P.
Basic Tools of Reinforced Concrete Beam Design
ACI Journal, *Proceedings,* V. 82, No. 1, Jan-Feb 1985, p 46-56
ABSTRACT: The application of consistent equilibrium and ultimate strength considerations to the design and detailing of reinforced concrete beams are described. Basic tools include struts and ties, nodes, fans, and arches. Comparisons with experiments on a shear wall coupling beam and on a deep beam, and three design examples illustrate the practical application of these tools.
KEYWORDS: beams (supports); deep beams; detailing; girders; shear strength; limit design method; plastic analysis; reinforced concrete; shear walls; strength; structural design.

Marti, P.
Dimensioning and Detailing
Structural Concrete, IABSE Colloquium, Stuttgart 1991. International Association for Bridge and Structural Engineering, Zurich, 1991, p. 411-443.
ABSTRACT: Truss model approaches and related theories are presented in an attempt to provide a synthesis of recently-developed methods, permitting a consistent dimensioning and detailing of structural concrete members.

Marti, P.
Discussion of Truss Models in Detailing
Concrete International: Design and Construction, Vol. 8, No. 10, 1986, pp. 66-68.

Marti, P.
Truss Models In Detailing
Concrete International; Vol. 7; No. 12; December 1985; pp 66-73.
ABSTRACT: Truss models have been developed and applied to the ultimate strength design and detailing of reinforced concrete members. three design examples illustrate the practical application of truss models: an indirectly supported continuous beam under variable distributed loads, an eccentrically loaded spandrel beam, and a continuous box-girder subjected to concentrated movable load.
KEYWORDS: beams (supports); beep beams; detailing; girders; limit design method; reinforced concrete; shear properties; design; torsion.

Mitchell, D., Collins, M. P., Bhide, S. B., and Rabbat B. G.
AASHTO LRFD Strut-and-Tie Model Design Examples. Ed. 1.
Portland Cement Association, Skokie, IL, 2004, 60 pp.

Mörsch, E.
Concrete-Steel Construction (English Translation by E. P. Goodrich)
McGraw Hill, New York, 1909, 368 pp.

Reineck, K.-H. (Editor)
SP-208: Examples for the Design of Structural Concrete with Strut-and-Tie Models
American Concrete Institute, Farmington Hills, MI, 2002, 242 pp.

Ritter, W.
Die Bauweise Hennebique
Schweizerische Bauzeitung, Vol. 33, No. 5, pp. 41-43; No. 6, pp. 49-52; No. 7, p 59-61; Zurich, 1899.

Schlaich, J., Schaefer, K., and Jennewein, M.
Toward a Consistent Design of Structural Concrete.
PCI Journal, Vol. 32, No. 3, May-Jun 1987, p 74-150
ABSTRACT: A unified design concept, which is consistent for all types of structures and all their parts, is required. To be satisfactory, this concept must be based on realistic physical models. Strut-and-tie models, a generalization of the well known truss analogy method for beams, are proposed as the appropriate approach for designing structural concrete, which includes both reinforced and prestressed concrete structures. This report shows how suitable models are developed and proposed criteria according to which the model's elements can be dimensioned uniformly for all possible cases. The concept is explained using numerous design examples, many of which treat the effect of prestress.
KEYWORDS: concrete construction--structural design; struts; concrete reinforcements; mathematical models identifiers; structural concrete

Schlaich, J. and Schaefer, K.
Design and Detailing of Structural Concrete Using Strut-and-Tie Models.
Structural Engineer, Vol. 69, No. 6, Mar 19 1991, 13p
ABSTRACT: So-called 'details' are as important for a structure's behaviour and safety as the standard problems of design which are covered in the Codes. A unified design concept which covers also the details consistently for all types of concrete structure is described in this paper. It is based on strut-and-tie models including the truss model for beams as a special case. After the principles of the method and the modeling process are explained, simplified rules are proposed for dimensioning all the individual members of the model and their nodes. Some examples show the application of the method and demonstrate, also its use for the improvement of the conceptual design of details.
KEYWORDS: concrete construction--structural design; struts; concrete reinforcements; mathematical models identifiers: structural concrete

Yun, Y.M. and Ramirez, J.A.
Strength of Struts and Nodes in Strut-Tie Model
Journal of Structural Engineering, Vol. 122, No. 1, Jan 1996, p 20-29
ABSTRACT: General approaches for determining the effective stress levels of concrete struts and for verifying the bearing capacity of nodal zones in strut-tie models are proposed. The effective stress levels of concrete struts are determined by implementing the principal stress ratios of the finite elements (used in the finite-element nonlinear analysis of a two-dimensional plain concrete) corresponding to the strut regions of the strut-tie model. Based on the obtained geometry of the struts, nodal zones are developed and their bearing capacity is verified using a finite-element nonlinear analysis with a failure criteria that incorporates the different state of stresses. To illustrate the proposed approaches, an analysis of a reinforced concrete beam tested to failure is conducted using the strut-tie model approach with the aid of interactive computer graphics program NLSTAT.
KEYWORDS: struts; strength of materials; stresses; bearing capacity; finite element method; failure (mechanical); concrete beams and girders; interactive computer graphics; computer software

B.2 DEEP BEAMS

Aguilar, G., Matamoros, A.B., Parra-Montesinos, G.J., Ramirez, J.A., and Wight, J.K.
Experimental Evaluation of Design Procedures for Shear Strength of Deep Reinforced Concrete Beams
ACI Structural Journal, Vol. 99, No. 4, Jul-Aug 2002, p 539-548
ABSTRACT: In this paper, results from the monotonie testing of four reinforced concrete deep beams are presented. The behavior of the deep beams is described in terms of cracking pattern, load-versus-deflection response, failure mode, and strains in steel reinforcement and concrete. Despite different failure modes, the failure loads and corresponding ultimate deflections were similar in all four specimens. Yielding of both longitudinal and transverse reinforcement occurred prior to failure. Based on the test results, the shear design procedures contained in the ACI 318-99 Code and Appendix A of the ACI 318-02 Code were evaluated. Both design procedures yielded conservative predictions of the shear strength of the single-span deep beams.
KEYWORDS: beam; reinforced concrete; shear strength; strut; test

Al-Nahlawi, K.A. and Wight, J.K.
Beam Analysis Using Concrete Tensile Strength in Truss Models
ACI Structural Journal, V.89, No. 3, May-June 1992, p 284-290

ABSTRACT: Presents truss modeling as a tool for analysis and design of concrete beams subjected to bending and shear behavior.
KEYWORDS: beams (supports); high-strength concrete; models; trusses; reinforced concrete; shear strength; tensile strength.

Alshegeir, A. and Ramirez, J.A.
Analysis of Disturbed Regions with Strut-and-Tie Models
Structural Engineering Research Report No. CE-STR-90-1, Purdue University, West Lafayette, Indiana, 1990, Part I, 303 pp, Part II, 303 p
DISSERTATION

Alshegeir, A. and Ramirez, J. A.
Strut-tie Approach in Pretensioned Deep Beams
ACI Structural Journal, Vol. 89, No. 3, May-Jun 1992, p 296-304
ABSTRACT: This paper presents an evaluation of the strength and behavior of prestressed concrete deep beams using the strut-tie method. Strut-tie systems reflecting actual support and loading conditions are developed for three pretensioned deep beams tested to failure. The strut-tie approach is used to illustrate the effects of prestressing, concrete compressive strength, and reinforcement detailing on the behavior and strength of these members.
PART OF ABOVE DISSERTATION

Collins, M.P. and Mitchell, D.
Shear and Torsion Design of Prestressed and Non-Prestressed concrete Beams
PCI Journal, Vol. 25, No. 5, Sep-Oct 1980, p 32-100
ABSTRACT: Shear and torsion design recommendations which are believed to be more rational and more general than current code provisions are presented. The use of the design recommendations is illustrated by means of several design examples. Comparisons with the result of other design methods are made.

Dei Poli, S., Di Prisco, M., and Gambarova, P.G.
Stress Field in Web of RC Thin-Webbed Beams Failing in Shear
Journal of Structural Engineering, Vol. 116, No. 9, Sep 1990, p 2496-2515
ABSTRACT: The resistant mechanisms of the reinforced and prestressed thin-webbed beams failing in shear are effective on the condition that the web reinforcement and thickness are suitably designed. With regard to this, a rational model is developed for the limit analysis of a thin web at the onset of shear collapse because of stirrup yielding, also considering the aggregate interlock (along the shear cracks), the bending stiffness of the inclined concrete struts, the bond properties of the stirrups, and the ultimate capacity (in shear and compression) of the struts. The proposed model is an improved version of the well-known Morsch's truss, which is well suited to the modeling of a regularly cracked web subjected to prevailing shear. By solving a nonlinear system of equations regarding the equilibrium, compatibility, constitutive laws of the web, and the various contributions to the web state of stress are investigated. The assumption introduced by other scholars, and adopted here also, that the web be subjected to a diagonal compression field, proves to be based on clear physical phenomena.
KEYWORDS: web beams; concrete; reinforced; models; shear failure; limit analysis

Hawkins, N.M., Kuchma, D.A., Mast, R.F., and Reineck, K-H
Simplified Shear Design of Structural Concrete Members
Transportation Research Board, *NCHRP Report 549*, 2005, 402 pp.

Ramirez, J.A. and Breen, J.E.
Evaluation of a Modified Truss-Model Approach for Beams in Shear.
ACI Structural Journal, Vol. 88, No. 5, Sep-Oct 1991, p 562-571
ABSTRACT: A modified truss model design approach with variable angle of inclination diagonals and a concrete contribution for beams with web reinforcement is proposed as a viable and economic design tool. Computed values were compared with a wide range of test results of reinforced and prestressed concrete beams failing in shear. The modified truss model approach was shown to be conservative and in good agreement with test results. A diminishing concrete contribution is proposed to supplement the strength of the variable angle truss model for reinforced concrete beams. For prestressed concrete beams the proposed modified truss model utilizes a constant concrete contribution. A maximum allowable compressive stress of 30 root f'_c together with lower angle limits of

30 deg for reinforced concrete beams and 25 deg for prestressed beams, was shown to provide adequate safety against web crushing failures prior to yielding of the stirrup reinforcement.
KEYWORDS: trusses—mathematical models; beams and girders; stresses—shear; concrete construction—prestressing; concrete

Rogowsky, D.M., MacGregor, J.G., Ong, Y.S.
Tests of Reinforced Concrete Deep Beams
ACI Journal, Vol. 83, Issue 4, July-August 1986, p 614-623
ABSTRACT: Tests of 7 simply supported and 17 two-span deep beams are reported. The behavior ranged from brittle for beams without vertical web reinforcement to ductile for beams with large amounts of vertical web reinforcement. Horizontal web reinforcement had no effect on the capacity. The ACI Building Code overestimated the strength of continuous deep beams and those having horizontal shear reinforcement.

Rogowsky, D.M. and MacGregor, J.G.
Design of Reinforced Concrete Deep Beams.
Concrete International: Design and Construction, Vol. 8, No. 8, Aug 1986, p 49-58
ABSTRACT: Three procedures are currently used for design of load transfer members such as deep beams: -Empirical design methods, -Two or three dimensional analysis, either linear or nonlinear, and by means of trusses dimensional a composed of concrete struts and steel tension ties. Most of this article will deal with the strut and tie model for deep beam design. Before doing so, the other two options will be examined briefly.
KEYWORDS: concrete construction--reinforced concrete; beams and girders--concrete; structural design--loads; trusses--composite identifiers: deep beams; plasticity; shear strength

Zayati, F., Ibrahim, A.M.M., and Hida, S.
LRFD Design of Integral Bent Caps
Transportation Research Board Annual Meeting 2007, 22 pp
ABSTRACT: Cast-in-place concrete box girder highway bridges with integral bent cap substructures are the preferred bridge type in California. In the AASHTO Load and Resistance Factor Bridge Design Specifications (LRFD), two methods are available for the design of integral bent caps: Sectional Method for flexural members, and Strut and Tie Method (STM) for flexural and deep members. Although many existing bent caps are considered deep beams according to LRFD provisions, many practicing engineers elect to use the Sectional Method exclusively for design due to its familiarity and lack of guidance using STM. Design examples using STM were recently published but none dealt with integral bent caps. When applying STM to integral bent caps, several issues, unique to this geometry, need to be addressed. These issues are discussed in this paper, and solutions are provided. Three different integral bent cap design examples are also illustrated.
KEYWORDS: Bent Cap, LRFD, Design, Concrete, Strut and Tie

B.3 PILE CAPS AND FOOTINGS

Adebar, P., Kuchma, D., and Collins, M.P.
Strut-and-Tie Models for the Design of Pile Caps: an Experimental Study.
ACI Structural Journal, Vol. 87, No. 1, Jan-Feb 1990, p 81-92
ABSTRACT: Describes the test results from six large pile caps that failed in two-way shear. ACI Building Code procedures for the shear design of pile caps are unable to predict the experimental results because the procedures neglect certain important parameters, such as the amount of longitudinal reinforcement, and overemphasize other parameters, such as the effective depth. Strut-and-tie models were found to describe more accurately the behavior of deep pile caps.
KEYWORDS: foundations--piles; columns--concrete; concrete products--slabs; struts; stresses--shear; structural design identifiers: pile caps; ACI Building Code; strut-and-tie models; shear strength; footings; reinforced concrete

Adebar, P. and Zhou, Z.
Design of Deep Pile Caps Using Strut-and-Tie Models
University of British Columbia, Vancouver, BC, Can Conference
Restructuring: America and Beyond Structures Congress; Proceedings of the 13th Structures Congress. Part 2 (of 2); Boston, MA, USA; ASCE, New York, NY, USA. p 1623-1626.

ABSTRACT: A simple design procedure is proposed in which the maximum bearing stress is considered the best indicator of the shear strength of deep pile caps, and a strut-and-tie model is used to determine the amount and arrangement of longitudinal reinforcement. The proposed method was found to better predict the results of 48 pile cap tests than the ACI Building Code and CRSI Handbook procedures.
KEYWORDS: structural design; piles; model structures; stresses; shear strength; reinforcement; building codes; loads (forces) identifiers: pile caps; strut-and-tie models; bearing stress; shear forces.

Siao, W.B.
Strut-and-Tie Model for Shear Behavior in Deep Beams and Pile Caps Failing in Diagonal Splitting
ACI Structural Journal, Vol. 90, No. 4, Jul-Aug 1993, p 356-363
ABSTRACT: A strut-and-tie model is used to predict the shear strength of deep beams and pile caps failing. The accuracy of this approach can be verified by comparison against results of actual strength obtained from experimental testing and published by others.
KEYWORDS: piles; shear stress; beams and girders; mooring cables identifiers: strut-and-tie model; mooring production vessels; pile caps diagonal splitting; deep beam shear behavior

B.4 CORBELS

Fattuhi, N.I.
Strength of FRC Corbels in Flexure
Journal of Structural Engineering, Vol. 120, Issue 2, Feb. 1994, p 360-377
ABSTRACT: Tests were carried out on 38,150 × 150 × 200 mm reinforced concrete corbels subjected to vertical loading. Steel fibers were used as shear reinforcement in 28 corbels. Parameters varied included volumes of main bars and fibrous reinforcements, effective depth or cover to main bars, and shear span. The tests confirmed earlier findings in that considerable improvement in ductility and strength of corbels resulted when the volume of fibers was increased. It was possible to change the mode of failure from being diagonal splitting or shear to flexure, when corbels were reinforced with relatively low volume of main bars. To estimate the flexural strength of reinforced concrete corbels subjected to vertical load, two methods, using a flexural model and a truss model, are presented. Comparison between the experimental and calculated strengths of corbels show that the two values obtained in each case are in satisfactory agreement.

Foster, S.J., Powell, R.E., and Selim, H.S.
Performance of High-Strength Concrete Corbels
ACI Structural Journal, Vol. 93, No. 5, September-October 1996, pp. 555-563.
ABSTRACT: In this study, 30 high-strength concrete corbels were tested to destruction. Variables considered in the investigation are shear span-to-depth ratio, concrete strength (45 to 105 MPa [6500 to 15,200 psi), and the provision of secondary reinforcement. The investigation examines corbel behavior in the context of the previous parameters and compares the experimental results with the ACI 318-879 design method and the plastic truss model of Rogowsky and MacGregor. Particular attention is given to determining the concrete efficiency factor of members failing in compression, and the results are compared with the efficiency model proposed by Warwick and Foster. The results of the investigation show that good load predictions can be obtained using the plastic truss model when combined with the Warwick and Foster efficiency factor. It is concluded that he design method given in ACI 318-89 is not appropriate for corbels fabricated using high-strength concrete.
KEYWORDS: brackets; corbels, high-strength concretes; shear properties; structural design; trusses

Huang, F.C., Lee, I.S., and Mo, Y.L.
Designing Pier Caps with Strut-and-Tie Models
Concrete International, Vol. 20, Issue 1, January 1998, p 43-47.
ABSTRACT: A pier cap is a structural component which transfers external loads in both vertical and horizontal directions to the column. The strut-and-tie design modeling of a pier cap in a high speed rail project subjected to both vertical and horizontal forces was discussed. The modeling used in the pier cap can be utilized in identifying other candidate structures and in developing the strut-and tie model for their design
KEYWORDS: pier caps; strut-and-tie models

Sabnis, G.M. and Solanki, H.
Reinforced Concrete Corbels--Simplified
ACI Structural Journal, V. 84, No. 5, Sept.-Oct. 1987, pp. 428-432
ABSTRACT: Various methods are used in designing reinforced concrete brackets. The paper demonstrates the simplification of truss analogy. A summary of previous work is reviewed. The proposed method was developed using a simplified approach with truss analogy. Test series of 16 investigations are analyzed and calculated according to the proposed method. Two examples demonstrate the recommended design procedure. Some recommendations for the detailing are also discussed.
KEYWORDS: brackets; corbels; detailing; reinforced concrete; structural design; theories**.**

Yong, Y-K. and Balaguru, P.
Behavior of Reinforced High-Strength-Concrete Corbels
Journal of Structural Engineering, Vol. 120, No. 4, Apr 1994, p 1182-1200
ABSTRACT: Results of an experimental investigation on the behavior of corbels made with high-strength concrete in excess of 40 MPa are presented. A total of 16 life-size corbels were tested, two of which were unreinforced. The primary variables of the investigation were presence of horizontal force, reinforcement ratio, and shear-span-to-depth (a/d) ratio. Silica-fume and high-range water-reducing ad-mixtures were used to obtain the high-strength concrete. All 14 reinforced concrete corbels failed in a stable manner. The primary steel yielded before failure in all cases but one. The behavior of the corbels during testing and the analysis of results indicate that high-strength concrete may be rationally incorporated into designs of corbels. The truss analogy model provided relatively accurate strength predictions compared with the American Concrete Institute's procedure. The code limit of 5.5 MPa (800 psi) for maximum average shear stress limits the full use of the available shear strength of high-strength corbels.
KEYWORDS: structural members; reinforced concrete; failure (mechanical); structural analysis; mechanical testing; codes (standards); mechanical properties; shear strength; structural loads; strength of materials identifiers: high strength concrete corbel; horizontal force; reinforcement ratio; shear span to depth ratio

B.5 DAPPED-END BEAMS

Barton, D.L., et. al.
Investigation of Strut-and-Tie Models for Dapped Beam Details; Research rept. (Interim)
Final Report, University of Texas at Austin. Center for Transportation Research, CTR-3-5-87/9-1127-1; RR-1127-1; FHWA/TX-92+1127-1; NTIS No: PB92-227735/HDM ; May 91; 205p
ABSTRACT: The objective of the test program undertaken in the study was to develop experimental data for defining various elements of strut-and-tie models. The data was used extensively in establishing design guidelines for details of structural reinforced concrete. The experimental program was divided into three phases. The first phase consisted of tests of four dapped beam details. A dapped beam was selected as a typical detail, commonly used in highway structures, and one for which several different design approaches have been proposed. Phases two and three consisted of tests of isolated portions (nodes) of the structure as modeled using the strut-and-tie approach. Nine CTT (compression-tension-tension) and ten CCT (compression-compression-tension) nodes were tested. At these nodes three forces converge at a point in the strut-and-tie model. Variables included reinforcement arrangement and layout, concrete strength, bearing area of the effective strut, and anchorage details. The results indicated that the dapped beam detail can be efficiently and effectively designed using a strut-and-tie model. The isolated node tests provide useful information on the performance of the concrete in the compression strut and on the anchorage of reinforcement in the node. The node tests provide an inexpensive way to determine critical data for developing design guidelines.
KEYWORDS: model tests; reinforcement (Structures); struts; beams(Supports); reinforced concrete; stress analysis; experimental data; structural members; concrete structures; structural analysis; trusses; design criteria; tension tests; crack propagation; highway bridges; loads (forces); deflection; structural design.

Taher, A.E.-D.M.F.
Strengthening of Critically Designed Girders with Dapped Ends
Proceedings of the Institute of Civil Engineers: Structures and Buildings, Vol. 158, No. 2, April 2005, p 141-152
ABSTRACT: Reinforced concrete (RC) beams with dapped ends are frequently found in bridge girders and precast concrete construction. A reduction in depth near the supports tends to produce a stress concentration and hence requires special analysis and detailing of any reinforcement used. Improper dimensioning and distribution of reinforcing steel can lead to undesirable cracking and failure mechanisms that need to be predicted in order that a

proper strengthening system be applied. The experimental programme described in this paper incorporated 52 specimens with dapped ends; three main defects were intentionally introduced at the recess zone and 12 different strengthening techniques were applied. The defects included an inadequate development length of bottom longitudinal reinforcement at the dapped ends, and elimination of either horizontal or vertical shear reinforcement at the ends. External bonding of the steel angle at the reentrant corner, unbonded bolt anchoring, external steel plate jacketing, exterior carbon fibre wrapping and/or stripping were applied in order to determine the best strengthening technique. A strut-and-tie model was used in the analysis of such discontinuity regions and a strength enhancement index procedure was introduced. A comparative study was undertaken in order to evaluate the various strengthening techniques applied.
KEYWORD: beams; girders/failures/rehabilitation; reclamation; renovation

Lin, I.J., Hwang, S.J., Lu, W.Y., and Tsai, J.T.
Shear Strength of Reinforced Concrete Dapped-End Beams
Structural Engineering and Mechanics, Vol. 16, No. 3, 2003, p 275-294
ABSTRACT: In this study, 24 high-strength concrete dapped-end beams were tested to study the effects of the amount of main dapped-end reinforcement, the nominal shear span-to-depth ratio, and the concrete strength on the shear strength of dapped-end beams. Test results indicate that the shear strength of dapped ends increases with the increase in the amount of main dapped-end reinforcement and the concrete strength. The shear strength of dapped-end beam increases with the decrease of nominal shear span-to-depth ratio. A simplified method for determining the shear strength of reinforced concrete dapped ends is also proposed in this paper. The shear strengths predicted by the proposed method and the approach of PCI Design Handbook are compared with test results. The comparison shows that the proposed method can more accurately predict the shear strength of reinforced concrete dapped-end beams than the approach of PCI Design Handbook.
KEYWORDS: reinforced concrete dapped-end beams; high strength concrete; softened strut-and-tie model

Lu, W.Y., Lin, I.J., Hwang, S.J., and Lin, Y.H.
Shear Strength of High-Strength Concrete Dapped-End Beams
Journal of the Chinese Institute of Engineers, Vol. 26, No. 5, 2003, p 671-680
ABSTRACT: In this study, 12 high-strength concrete dapped-end beams were tested to study the effects on shear strength of dapped-end beams of the concrete strength, the amount of main dapped-end reinforcement, and the nominal shear span-to-depth ratio. The test results indicate that the shear strength of dapped-end beams increases with the increase of the concrete strength, the amount of main dapped-end reinforcement, and the decrease of nominal shear span-to-depth ratio. An analytical model for determining the shear strength of reinforced concrete dapped-end beams is also proposed. Both the shear strengths predicted by the proposed model and the approach of the PCI Design Handbook are compared with test results of this study and those of Mattock and Chan (1979). The comparison shows that the proposed model can predict the shear strength of reinforced concrete dapped-end beams more accurately than the approach of the PCI Design Handbook.
KEYWORDS: concrete softening, dapped-end beam, reinforced concrete, shear strength, strut-and-tie

Wang, Q. and Guo, Z.
Experimental Investigation of the Shear Capacity of RC Dapped End Beams and Design Recommendations
Structural Engineering and Mechanics, Vol. 21, No. 2, 2005, p 221-235
ABSTRACT: In this paper, the shear resistance behavior of reinforced concrete (RC) dapped end beams is investigated by 24 tests until failure load. The main parameters considered are the dapped end height, the type and effective range to provided stirrups, and the bent form of the longitudinal reinforcement. The failure behavior of dapped end beams is presented and some conclusions are given. Inclined stirrups and longitudinal bent reinforcement have more influence on the shear capacity than vertical stirrups. Additionally, the shear mechanism of dapped end beams is analyzed. Relatively, simple semi-empirical equations for shear strength have been derived based on the results of 22 dapped end beams. The predicted results are in close agreement with the experimental ones. Finally, some design suggestions for the ultimate shear strength of dapped end beams are presented.
KEYWORDS: reinforced concrete (RC); dapped end beams; shear capacity; shear failure; ultimate shear strength; shear resistance mechanisms

B.6 OPENINGS

Ashour, A.L. and Rishi, G.
Tests of Reinforced Concrete Continuous Deep Beams with Web Openings
ACI Structural Journal, Vol. 97, No. 3, May-June 2000, p 418-426
ABSTRACT: Test results of 16 reinforced concrete two-span continuous deep beams with web openings are reported. All test specimens had the same geometry and main longitudinal top and bottom reinforcement. The main parameters considered were the size and position of the web openings, and web reinforcement arrangement. Two modes of failure were observed, depending on the position of the web openings. For beams having web openings within interior shear spans, the failure is developed by diagonal cracks between the web opening corners and the edges of the load and central support plates. For beams having web openings within exterior shear spans, the mode of failure is characterized by major diagonal cracks within interior and exterior shear spans. The diagonal cracks that occurred in the interior shear span extended to join the edges of the load and central support plates, and at the same time, the diagonal cracks that formed at the web opening corners propagated both ways towards the edges of the had and end support plates. Web openings within interior shear spans caused more reduction on the beam capacity than those within exterior shear spans. The vertical web reinforcement had more influence on the beam capacity than the horizontal web reinforcement. An upper-bound analysis of the two failure mechanisms that occurred in the experiments is introduced, and design equations are developed.
KEYWORDS: Codes; Continuous beams; Cracks; Deep beams; Deflection; Failure mechanisms; Plasticity; Reinforced Concrete; Shear strength; Web openings; Web reinforcement

Maxwell, B.S. and Breen, J.E.
Experimental Evaluation of Strut-and-Tie Model Applied to Deep Beam with Opening
ACI Structural Journal, Vol. 97, No. 1, January-February 2000, p 142-148
ABSTRACT: Where geometric discontinuities exist in structural concrete members, current code documents provide little direction for design. The design of these unusual members can be better understood by using the strut-and-tie model. Combinations of two distinctly different strut-and-tie models were used to design four deep beams each with a geometric discontinuity in the form of a large opening. This paper describes the performance of four physical models that were constructed based on these varied designs. The deep beams were simply supported and tested using a point load. Each of the four beams resisted considerably more than the factored design load. This successful test series reveals the power, versatility, reliability, and predictability of the strut-and-tie modeling technique.
KEYWORDS: deep beams; openings; structural concretes

Taylor, C.P., Cote, P.A., and Wallace, J.W.
Design of Slender Reinforced Concrete Walls with Openings
ACI Structural Journal, Vol. 95, No. 4, July-August 1998, p 420-433
ABSTRACT: This paper summarizes the results of an experimental and analytical study of slender reinforced concrete structural walls with an opening at the base. The primary objectives of this research were the evaluation of a displacement-based approach for the selection of transverse boundary reinforcement, and the evaluation of a strut and tie model for the selection of the horizontal shear reinforcement. Two approximately quarter-scale wall specimens were constructed and tested under constant axial stress and reverse cyclic lateral loading. Experimental results show that, when designed using a combined displacement-based and strut and tie approach, slender structural walls with openings at the base exhibit stable hysteretic behavior and significant ductility. The displacement-based design technique allowed transverse boundary reinforcement to be provided as needed rather than selected based on a nominal value. The strut and tie model was found to be an effective tool for the design of discontinuous regions, where simplified code equations are not appropriate.
KEYWORDS: Capacity design; Displacement-based design; Earthquake loads; Flexural response; Inelastic design; Moment-curvature response; Openings; Plane-sections; Reversed cyclic loads; Shear deformations; Shear walls; Structural walls; Strut and tie modeling

Chen, B.S., Hagenberger, M.J., and Breen, J.E.
Evaluation of Strut-and-Tie Modeling Applied to Dapped Beam with Opening
ACI Structural Journal, Vol. 99, No. 4, July-August 2002, p 445-450
ABSTRACT: Strut-and-tie modeling is a valuable tool for designing irregular concrete members. The ACI 318-02 Building Code contains pro-visions pertaining to design using strut-and-tie models. This paper presents the experimental results of tests conducted on small-scale, simply-supported dapped beams with openings. The design of each test specimen was developed by independent student teams using the ACI provisions for strut-and-tie

models. Each of the four specimens resisted loads greater than the factored design load and exhibited little distress at service load levels. The successful test series illustrates the applicability and conservative nature of strut-and-tie modeling for design.
KEYWORDS: Beam; Plasticity; Structural concrete; Strut

B.7 ANCHORAGE ZONES

Burdet, O.
Analysis and Design of Post-Tensioned Anchorage Zones of Concrete Bridges
Ph.D. Dissertation, University of Texas at Austin, May 1990.

Sanders, D.
Design and Behavior of Anchorage Zones in Post-Tensioned Concrete Members
Ph.D. Dissertation, University of Texas at Austin, August 1990, 574 pp.

Wollmann, G.P.
Design of Anchorage Zones in Post-Tensioned Concrete Structures
Ph.D. Dissertation, University of Texas at Austin, May 1992.

B.8 CRACK CONTROL/SERVICEABILITY/SHEAR AND WEB REINFORCEMENT

Adebar, P. and van Leeuwen, J.
Side-Face Reinforcement for Flexural and Diagonal Cracking in Large Concrete Beams
ACI Structural Journal, Vol. 96, No. 5, September-October 1999, p 693-704
ABSTRACT: The current ACI Building Code and AASHTO Bridge Code requirements for side-face reinforcement are meant to control flexural cracking in the webs of large concrete beams and may not provide adequate diagonal crack control for certain exposure conditions. Twenty-one large concrete beam elements with 1200-mm-(47-in.)-deep webs were tested in a specially constructed apparatus to study the influence of amount and arrangement of side-face reinforcement in controlling both flexural and diagonal cracking in large concrete beams. The amount of side-face reinforcement was varied from 50 to 300 percent of what is required by the current ACI Building Code and AASHTO Bridge Code. Deformed reinforcing bars, welded wire fabric, and hooked steel fiber were included in the study. Over 11,000 crack widths were measured with a microscope on the 21 specimens, and an analysis of the crack data reveals the relationship between crack width and average strain, and the ratio of maximum to average crack widths. A procedure is presented for estimating diagonal crack widths in the webs of large beams due to service level shear stresses, and a general design procedure is presented for the amount of side-face reinforcement needed to control both flexural and diagonal cracking in the webs of large concrete beams. The required spacing of side-face longitudinal reinforcing bars depends on the maximum, acceptable crack width, strain of the longitudinal reinforcement on the flexural tension side, magnitude of the applied shear stress, amount of transverse reinforcement, and the diameter of and cover to the side-face reinforcing bars. A design example illustrates the proposal.
KEYWORDS: beams (supports); cracking (fracturing); flexural strength; girders; reinforced concrete; shear properties

Brown, M.D. and Bayrak, O.
Minimum Transverse Reinforcement for Bottle-Shaped Struts
ACI Structural Journal, Vol. 103, No. 6, November-December 2006, p 813-821
ABSTRACT: Strut-and-Tie modeling involves the use of struts to model the flow of compression within a concrete member. Bottle-shaped struts are wider at their midpoint than at either end. As the struts widen near the midpoint, tensile stresses transverse to the direction of compression are developed. Reinforcement must be placed within the strut to carry the transverse tension. This paper presents an equilibrium-based approach to determining the necessary amount of transverse reinforcement for a bottle-shaped strut. A database of 476 test specimens was then used to evaluate the equilibrium-based equations along with a series of three tests of deep beams. The strut efficiency factors presented I Appendix A of ACI 318-05 were used in this evaluation. Current ACI 318-05 provisions allow the design of a deep beam without any shear reinforcement; this issue is highlighted and its shortcomings discussed.
KEYWORDS: reinforcement; shear; structural concrete; strut-and-tie modeling.

Frosch, R.J.
Modeling and Control of Side Face Beam Cracking
ACI Structural Journal, Vol. 99, No. 3, May-June 2002, p 376-385
ABSTRACT: As the use of thicker concrete covers has been increasing due to durability concerns, the question arises whether current design provisions for the control of side face cracking remain applicable. This study investigates the background for the existing provisions and develops a physical model and procedure for the calculation of side face crack widths. The calculation procedure is supported by an evaluation of existing test data. Based on this procedure, analyses are conducted that investigate side face crack width profiles as well as parameters necessary to control side face cracking for varying concrete covers. Design recommendations are presented that provide a unified approach to the control of side-face cracking as well as bottom-face cracking.
KEYWORDS: beam; crack-control reinforcement; cracking

Ghoneim, M.
Shear Strength of High Strength Concrete Deep Beams
Journal of Engineering and Applied Science, Vol. 48, No. 4, August 2001, p 675-693
ABSTRACT: This paper presents an experimental study of the behavior of high-strength concrete (HSC) deep beams. Ten simply supported specimens were tested under two-point top loading. Effects of the concrete compressive strength, the shear span-to-depth ratio, the vertical web reinforcement ratio and the horizontal web reinforcement ratio were investigated. The test results reveal that the influence of concrete strength on the ultimate capacity of deep beams is more noticeable at lower a/d ratios. It is also shown that the use of orthogonal web reinforcement comprising both vertical and horizontal reinforcements is essential for crack control and to preserve the integrity of the inclined compression struts. The results further indicated that the beneficial effect of the vertical web reinforcement is more significant at a/d ratio of 0.95 and confirmed the established knowledge that the effect of horizontal web reinforcement diminishes with the increase of a/d ratio. The comparisons reported in this paper showed that the deep-beam provisions in both the ACI 318-95 and the Egyptian Code ECP-95 will insure safe designs for HSC deep beams. The design equations in the CIRIA Guide (1984) may overestimate the capacity of HSC deep beams. The study also investigates the applicability of the softened plastic strut-and-tie models outlined in the Canadian Code CAN3-A23.3-M94 and the CEB-FIP Model Code (1990) to HSC deep beams.
KEYWORDS: deep beams; high-strength concrete; shear strength; web reinforcement

Kong, F.K., Robins, P.J, and Cole, D.F.
Web Reinforcement Effects on Deep Beams
ACI Journal, Vol. 67, No. 12, December 1970, p 1010-1017
ABSTRACT: Reports on tests of 35 simply supported deep beams with the span/depth ratios L/D ranging from 1 to 3 and clear shear span/depth ratios x/D from 0. 23 to 0. 7. The effects of seven different types of web reinforcement on deflections, crack widths, crack patterns, failure modes, and ultimate loads in shear were studied. It was found that the effectiveness of the various types of web reinforcement depended on the L/D and x/D ratios. For low L/D and x/D ratios, only horizontal web reinforcement at close spacing near the bottom of the beam was effective.

Tan, K.H., Tang, C.Y., and Tong, K.
A direct Method for Deep Beams with Web Reinforcement
Magazine of Concrete Research, Vol. 55, No. 1, February 2003, p 53-63
Shear Strength of High Strength Concrete Deep Beams
Journal of Engineering and Applied Science, Vol. 48, No. 4, August 2001, p 675-693
ABSTRACT: This paper take account of the effect of web reinforcement, be it in vertical, horizontal, inclined or orthogonal configurations. This is because test results have indicated that the contribution of web reinforcement to shear strength is indeed significant and should not be ignored. An original and rational strut-and-tie model for tensile contribution of both reinforcement and concrete is proposed, which takes account of their influence on the principal tensile stress. The proposed model is verified against three case studies of a total of 116 beams. Generally, the predictions are not only accurate and consistent in each case study, but also conservative.

Yoon, Y.S., Cook, W.D., and Mitchell, D.
Minimum Shear Reinforcement in Normal, Medium, and High-Strength Concrete Beams
ACI Structural Journal, Vol. 93, No. 5, September-October 1996, p 576-584
ABSTRACT: This paper presents the evaluation of minimum shear reinforcement requirements in normal, medium, and high-strength reinforced concrete beams. Twelve shear tests were conducted on full-scale beam specimens

having concrete compressive strengths of 36, 67, and 87 MPa. Different amounts of minimum shear reinforcement were investigated, including the traditional amounts required by older codes and the amounts required by the 1989 ACI Code (revised 1992) and the 1994 CSA Standard. The performance of the different amounts of shear reinforcement are discussed in terms of shear capacity, ductility, and crack control at service load levels. An assessment of the 1989 ACI and 1994 CSA provisions for minimum shear reinforcement is also presented.
KEYWORDS: beams (supports); crack control; ductility; high-strength concrete; minimum shear reinforcement; shear strength; splitting cracks; stirrups

Zhu, R.R.H., Wanichakorn, W., Hsu, T.T.C., and Vogel, J.
Crack Width Prediction Using Compatibility-Aided Strut-and-Tie Model
ACI Structural Journal, Vol. 100, No.4, July August 2003, p 413-421
ABSTRACT: Unacceptable diagonal cracks frequently occur at service load in the vicinity of the re-entrant corners in structures such as the dapped ends of bridge girders and the ledges of inverted T bent caps. Such diagonal cracks are not only visually intimidating but also impose a potential danger of corrosion of reinforcing bars. Controlling such cracking is difficult due to the lack of a rational theory for crack prediction. In this paper, a compatibility-aided strut-and-tie model (CASTM) is proposed for predicting the diagonal crack widths at re-entrant corners. The validity of this model is supported by tests of seven full-scale specimens.
KEYWORDS: bent caps; cracking; reinforced concrete

B.9 COMPUTER AIDED DESIGN FOR STRUT-AND-TIE MODELING

Alshegeir, A. and Ramirez, J.A.
Computer Graphics in Detailing Strut-Tie Models
Journal of Computing in Engineering, Vol. 6, No. 2, Jul. 1992, p 220-232
ABSTRACT: An interactive computer-graphics program implementing the strut-tie model approach for analysis and design of reinforced and prestressed concrete members is presented. The program consists of three parts. The first and second parts can be considered as a pre- and postprocessor for a finite element code to analyze plane stress and plane strain problems as well as plane truss problems. The results of the first part (direction of compressive principal stresses) provide guidance in the development of strut-tie models. In the second part of the program, the chosen strut-tie model is analyzed to determine the forces in the individual components of the model. The third part is a design routine for dimensioning and detailing the components of the proposed strut-tie model (struts, nodes, ties). The features and the interaction between the parts of the program are demonstrated with the design of a reinforced concrete, dapped-end beam. Computer graphics is shown to be an efficient way to develop and detail strut-tie models for the design of reinforced concrete structures.

Benabdallah, S., Ramirez, J.A., and Lee, R.H.
Computer Graphics in Truss-Model Design Approach
Journal of Computing in Engineering, Vol. 3, No. 3, Jul. 1989, p 285-301
ABSTRACT: The main objective of this paper is to extend and simplify the use of truss models in the design of reinforced concrete members for flexure and shear by means of user-friendly, interactive computer graphics. An interactive computer-graphics program, which replaces the traditional drawing board and calculator in the development of truss models for reinforced concrete members, is presented. The interactive program allows the designer to input the selected truss model graphically, then analyze it, display the results and revise the truss model if necessary. The interaction between the graphics and analysis tools was found to be the most efficient method to transfer the truss parameters to the analysis routines. The features of the truss-model program are demonstrated with the design example of an inverted-T bent cap in a bridge structure.

CAST V. 0.9.11 (Computer Aided Strut-and-Tie - program)
University of Illinois at Urbana-Champaign, Urbana, IL
DESCRIPTION: CAST utilizes a single interface for creation or modification of strut-and-tie models, truss analysis, selection of reinforcing steel, and capacity checks of struts and nodes.

Fachwerk V. 0.3.0 (STM program developed in Gernmany)
Vontobel, A., Germany
DESCRIPTION: Fachwerk addresses to structural engineers who are involved with analyzing and designing reinforced concrete structures. Fachwerk intends to simplify the application of discontinuous stress fields and strut-

and-tie models. The program calculates strut-and-tie models. It only uses the equilibrium conditions. Thus, unlike common programs, it is not assuming elastic behavior.

RC-Pier V. 7.0.0 (Design program for reinforced concrete substructures and foundations)
Leap Software Inc, Tampa, FL
DESCRIPTION: RC-PIER allows users to design cap beams, biaxial columns, and footings through LFD, LRFD or working stress methods. Users can apply advanced design methodologies such as Strut-and-Tie (STM) modeling to obtain optimized structures.

Salem, H.M.
Computer-Aided Analysis of Reinforced Concrete using a Refined Nonlinear Strut and Tie Model Approach
Journal of Advanced Concrete Technology, Vol. 4, No. 2, 2006, p 325-336
ABSTRACT: This paper presents a computer program for implementing a refined nonlinear strut and tie model approach for the practical design and analysis of disturbed regions in structural concrete. Nonlinear techniques in the selection, analysis and verification processes of a strut and tie model are incorporated in this program to eliminate the limitations of the conventional strut and tie model relating to the behavior and strength prediction of reinforced concrete. For the verification of the proposed model, the model results are compared to the experimental results of one-quarter-scale simply supported bottom-loaded deep beams. Analytical results showed a lower bound solution that agreed well with the experimental results. It was concluded that the nonlinear strut and tie model allows more economical design than the conventional strut and tie model. It was also concluded that for higher strength concrete, the strength of struts and nodal zones given by the ACI-318 02 code is unconservative and needs refinement to account for the brittleness of high-strength concrete.

Tjhin, T.N. and Kuchma, D.A.
Computer-Aided Analysis of Reinforced Concrete using a Refined Nonlinear Strut and Tie Model Approach
ACI Structural Journal, Vol. 99, No. 5, Sept.-Oct. 2002, p 586-594
ABSTRACT: The strut-and-tie method (STM) is gaining recognition as a code-worthy and consistent methodology for the design of D- (discontinuity) regions in structural concrete. Unfortunately, the development of code provisions for the STM has been hampered by uncertainties in defining the strength and dimensions of the idealized load-resisting truss (or strut-and-tie model). In addition, the has been encumbered by an iterative and time-consuming design procedure in which many geometric details need to be considered. To overcome this problem, researchers are developing computer-based design tools, including the authors' computer-aided strut-and-tie (CAST) design tool. CAST provides a graphical working environment for all aspects of the design process, including definition of the D-region, selection of the strut-and-tie model, truss analysis, member definitions, and creation of a design summary. This study reports on the STM, the barriers to its advancement, the capabilities of computer-based design tools, and the CAST program. It also makes suggestions for future STM research.

Yun, Y.M.
Computer Graphics for Nonlinear Strut-Tie Model Approach
Journal of Computing in Engineering, Vol. 14, No. 2, Apr. 2000, p 127-133
ABSTRACT: This paper presents an interactive computer graphics program for implementing the nonlinear strut-tie model approach for the practical design and analysis of disturbed regions in structural concrete. The graphics program consists of three parts. The first and second parts are considered as the pro- and post-processors for a nonlinear finite-element analysis of 2D plain concrete and plane truss structures. The results of the first part provide guidance in the development of strut-tie models and in the evaluation of effective strength levels for concrete struts. The third part is a design routine for dimensioning and detailing the components of the developed strut-tie model. This graphics program implementing the nonlinear strut-tie model approach has been shown to be efficient in the development, analysis, and detailing of strut-tie models for the analysis and design of structural concrete including disturbed regions.

APPENDIX C – CATALOG OF DESIGN SPECIFICATIONS

ACI Committee 318. *Building Code Requirements for Structural Concrete and Commentary* (ACI 318-05/318R-05). American Concrete Institute, Farmington Hills, MI, 2005, 430 pp.

Building and Civil Engineering Standards Committee. *Plain, Reinforced and Prestressed Concrete Structures, Part 1: Design and Construction* (DIN 1045-1). Deutsches Institut für Normung (DIN-Normen), Berlin, Germany, July 2001, 122 pp.

CEB-FIP Model Code 1990. Comité Euro-International du Béton, Thomas Telford Services, Ltd., London, 1993, 437 pp.

Concrete Design Committee P 3101 for the Standards Council. *Concrete Structures Standard: Part 1-The Design of Concrete Structures* (NZS 3101-1). Standards New Zealand, Wellington, 2006, 685 pp.

CSA Technical Committee on Canadian Highway Bridge Design Code. CAN/CSA-*S6-06 Canadian Highway Bridge Design Code*. Canadian Standards Association, Mississauga, Ontario, November 2006, 788 pp.

CSA Technical Committee on Reinforced Concrete Design. *A23.3-04 Design of Concrete Structures*. Canadian Standards Association, Rexdale, Ontario, December 2005, 250 pp.

FIP Commission 3 on Practical Design Working Group. *Recommendations for Practical Design of Structural Concrete*. Fédération Internationale de la Précontrainte, London, September 1999, 113 pp.

Highway Subcommittee on Bridges and Structures. *AASHTO LRFD Bridge Design Specifications, Third Edition*. American Association of State Highway and Transportation Officials (AASHTO), Washington, DC, 2004.

APPENDIX D – CATALOG OF DEEP BEAM DATABASE SOURCES

Aguilar, G., Matamoros , A. B., Parra-Montesinos, G. J., Ramirez, J. A, and Wight, J. K. "Experimental Evaluation of Design Procedures for Shear Strength of Deep Reinforced Concrete Beams." *ACI Structural Journal*. V. 99, No. 4, July-August, 2002, pp 539-548.

Clark, A. P., "Diagonal Tension in Reinforced Concrete Beams." *ACI Journal*, V. 48, No. 2, October, 1951, pp. 145-156.

de Paiva, H. A. R. and Siess, C. P., "Strength and Behavior of Deep Beams." *ASCE Structural Journal*, V. 91, No. ST5, October, 1965, pp. 19-41.

Foster, S. J. and Gilbert, R. I., "Experimental Studies on High Strength Concrete Deep Beams." *ACI Structural Journal*, V. 95, No. 4, July-August , 1998, pp. 382-390.

Ghoneim, M., "Shear Strength for High Strength Concrete Deep Beams." *Journal of Engineering and Applied Science.* V. 48, No. 4, August, 2004, pp. 675-693.

Kong, F.-K. and Robins, P. J., "Web Reinforcement Effects on Deep Beams." *ACI Journal*, V. 67, No. 12, December, 1970, pp. 1010-1017.

Kong, P. Y. L. and Rangan, B. V., "Shear Strength of High-Performance Concrete Beams." *ACI Structural Journal*, V. 95, No. 6, November-December, 1998, pp. 677-688.

Moody, K. G., Viest, I. M., Elstner, R. C., and Hognestad, E., "Shear Strength of Reinforced Concrete Beams: Part 1-Tests of Simple Beams." *ACI Journal*, V. 26, No. 4, December, 1954, pp. 317-333.

Oh, J.-K. and Shin, S.-W., "Shear Strength of Reinforced High-Strength Concrete Deep Beams." *ACI Structural Journal*, V. 98, No. 2, March-April, 2001, pp. 164-173.

Quinteros-Febres, C. G., Parra-Montesinos, G., and Wight, J. K., "Strength of Struts in Deep Beam Concrete Members Designed Using Strut-and-Tie Method." *ACI Structural Journal*, V. 103, No. 4, July-August, 2006, pp. 577-586.

Ramakrishnan, V. and Ananthanarayana, Y., "Ultimate Strength of Deep Beams in Shear." *ACI Journal*, V. 65, No. 2, February, 1968, pp. 87-98.

Rogowski, D. M., Macgregor, J. G., and Ong, S. Y., "Tests of Reinforced Concrete Deep Beams." *ACI Journal*, V. 83, No. 4, July-August, 1986, pp.614-623.

Shin, S.-W., Lee, K.-S., Moon, J.-I., and Ghosh, S. K., "Shear Strength of Reinforced High-Strength Concrete Beams with Shear Span-to-Depth Ratios between 1.5 and 2.5." *ACI Structural Journal*, V. 96, No. 4, July-August, 1999, pp. 549-556.

Smith, K. N. and Vantsiotis, A. S., "Shear Strength of Deep Beams." *ACI Journal*, V. 79, No. 3, May-June, 1982, pp. 201-213.

Subedi, N. K., Vardy, A. E., and Kubota, N., "Reinforced Concrete Deep Beams-Some Test Results." *Magazine of Concrete Research*, V. 38, No. 137, December, 1986, pp. 206-219.

Tan, K. H., Kong, F.-K., Teng, S., and Guan, L., "High-Strength Concrete Deep Beams with Effective Span and Shear Span Variations." *ACI Structural Journal*, V. 92, No. 4, July-August, 1995, pp. 395-405.

Tan, K. H., Kong, F.-K., Teng, S., and Guan, L., "Effect of Web Reinforcement on High-Strength Concrete Deep Beams." *ACI Structural Journal*, V. 94, No. 5, September-October, 1997, pp. 572-582.

Tan, K. H. and Lu, H. Y., "Shear Behavior of Large Reinforced Concrete Deep Beams and Code Comparisons." *ACI Structural Journal*, V. 96, No. 5, September-October, 1999, pp. 836-845.

Xie, Y., Ahmad, S. H., Yu, T., Hino, S., and Chung, W., "Shear Ductility of Reinforced Concrete Beams of Normal and High-Strength Concrete." *ACI Structural Journal*, V. 91, No. 2, March-April, 1994, pp. 140-149.

BIBLIOGRAPHY

ACI Committee 318. *Building Code Requirements for Structural Concrete and Commentary* (ACI 318-05/318R-05). American Concrete Institute, Farmington Hills, MI, 2005, 430 pp.

Adebar, P., "The Behaviour of Pile Caps: An Experimental Investigation," MASc thesis, Department of Civil Engineering, University of Toronto, January 1987, 135 pp.

Adebar, P., Kuchma, D., and Collins, M. P. "Strut-and-Tie Models for the Design of Pile Caps: An Experimental Study." *ACI Structural Journal*. V. 87, No. 1, January-February, 1990, pp 81-92.

Aguilar, G., Matamoros , A. B., Parra-Montesinos, G. J., Ramirez, J. A, and Wight, J. K. "Experimental Evaluation of Design Procedures for Shear Strength of Deep Reinforced Concrete Beams." *ACI Structural Journal*. V. 99, No. 4, July-August, 2002, pp 539-548.

Alshegeir, A., J.A. *Analysis of Disturbed Regions with Strut-and-Tie Models*. Dissertation, Department of Civil Engineering, Purdue University, December 1992, 274 pp.

Bergmeister, K. , Breen, J.E. , Jirsa, J.O. , and Kreger, M.E. *Detailing for Structural Concrete.* Center for Transportation Research Report 0-1127-3F, University of Texas, Austin, May 1993, 300 pp.

Brown, M. D., Bayrak, O. "Minimum Transverse Reinforcement for Bottle-Shaped Struts." *ACI Structural Journal*. V. 103, No. 6, November-December, 2006, pp 813-821.

Brown, M. D., Sankovich, C. L., Bayrak, O., Jirsa, J. O., Breen, J. E., and Wood, S. L. *Examination of the AASHTO LRFD Strut and Tie Specifications*. Center for Transportation Research Report 0-4371-2, University of Texas, Austin, April 2006, 330 pp.

Building and Civil Engineering Standards Committee. *Plain, Reinforced and Prestressed Concrete Structures, Part 1: Design and Construction* (DIN 1045-1). Deutsches Institut für Normung (DIN-Normen), Berlin, Germany, July 2001, 122 pp.

CEB-FIP Model Code 1990. Comité Euro-International du Béton, Thomas Telford Services, Ltd., London, 1993, 437 pp.

Clark, A. P., "Diagonal Tension in Reinforced Concrete Beams." *ACI Journal*, V. 48, No. 2, October, 1951, pp. 145-156.

Collins M. P. and Mitchell, D. "Rational Approach to Shear Design—The 1984 Canadian Code Provisions." *ACI Journal*. V. 83, No. 6, November-December 1986, pp 925-933.

Collins, M. P., and Mitchell, D. *Prestressed Concrete Structures*. Prentice Hall Inc., Englewood Cliffs, NJ, 1991, 776 pp.

Concrete Design Committee P 3101 for the Standards Council. *Concrete Structures Standard: Part 1-The Design of Concrete Structures* (NZS 3101-1). Standards New Zealand, Wellington, 2006, 685 pp.

CSA Technical Committee on Canadian Highway Bridge Design Code. CAN/CSA-*S6-06 Canadian Highway Bridge Design Code*. Canadian Standards Association, Mississauga, Ontario, November 2006, 788 pp.

CSA Technical Committee on Reinforced Concrete Design. *A23.3-04 Design of Concrete Structures*. Canadian Standards Association, Rexdale, Ontario, December 2005, 250 pp.

de Paiva, H. A. R. and Siess, C. P., "Strength and Behavior of Deep Beams." *ASCE Structural Journal*, V. 91, No. ST5, October, 1965, pp. 19-41.

FIP Commission 3 on Practical Design Working Group. *Recommendations for Practical Design of Structural Concrete*. Fédération Internationale de la Précontrainte, London, September 1999, 113 pp.

Foster, S. J. and Gilbert, R. I., "Experimental Studies on High Strength Concrete Deep Beams." *ACI Structural Journal*, V. 95, No. 4, July-August , 1998, pp. 382-390.

Ghoneim, M., "Shear Strength for High Strength Concrete Deep Beams." *Journal of Engineering and Applied Science.* V. 48, No. 4, August, 2004, pp. 675-693.

Highway Subcommittee on Bridges and Structures. *AASHTO LRFD Bridge Design Specifications, Third Edition*. American Association of State Highway and Transportation Officials (AASHTO), Washington, DC, 2004.

Kong, F.-K. and Robins, P. J., "Web Reinforcement Effects on Deep Beams." *ACI Journal*, V. 67, No. 12, December, 1970, pp. 1010-1017.

Kong, P. Y. L. and Rangan, B. V., "Shear Strength of High-Performance Concrete Beams." *ACI Structural Journal*, V. 95, No. 6, November-December, 1998, pp. 677-688.

Lampert, P. and Thurlimann, B., "Ultimate Strength and Design of Reinforced Concrete Beams in Torsion and Bending." IABSE, *Publications*. V. 31-I, 1971, pp. 107-131.

Macgregor, J. G., *Reinforced Concrete Mechanics and Design*. Ed. 3. Prentice Hall Inc., Upper Saddle River, NJ, 1997, 939 pp.

Marti, P. "Basic Tools of Reinforced Concrete Beam Design." *ACI Journal*. V.82, No. 1, January-February, 1985, pp 45-56.

Maxwell, B. S. "An Experimental Study of a Structural Concrete Deep Beam with a Large Opening Using the Strut-and-Tie Model." *Departmental Report*, University of Texas, Austin, Texas, December 1996.

Maxwell, B. S. and Breen, J. E., "Experimental Evaluation of Strut-and-Tie Model Applied to Deep Beam with Opening." *ACI Structural Journal.* V. 97, No. 1, January-February, 2000, pp 142-148.

Mitchell, D., Collins, M. P., Bhide, S. B., and Rabbat B. G., *AASHTO LRFD Strut-and-Tie Model Design Examples*. Ed. 1. Portland Cement Association, Skokie, IL, 2004, 60 pp.

Moody, K. G., Viest, I. M., Elstner, R. C., and Hognestad, E., "Shear Strength of Reinforced Concrete Beams: Part 1-Tests of Simple Beams." *ACI Journal*, V. 26, No. 4, December, 1954, pp. 317-333.

Mörsch, E. *Concrete-Steel Construction* (English Translation by E. P. Goodrich). McGraw Hill, New York, 1909, 368 pp.

Oh, J.-K. and Shin, S.-W., "Shear Strength of Reinforced High-Strength Concrete Deep Beams." *ACI Structural Journal*, V. 98, No. 2, March-April, 2001, pp. 164-173.

Priestley, M. J. N., Seible, F., and Calvi, M., *Seismic Design and Retrofit of Bridges*. John Wiley and Sons, New York, NY, 1996, 686 pp.

Quinteros-Febres, C. G., Parra-Montesinos, G., and Wight, J. K., "Strength of Struts in Deep Beam Concrete Members Designed Using Strut-and-Tie Method." *ACI Structural Journal*, V. 103, No. 4, July-August, 2006, pp. 577-586.

Ramakrishnan, V. and Ananthanarayana, Y., "Ultimate Strength of Deep Beams in Shear." *ACI Journal*, V. 65, No. 2, February, 1968, pp. 87-98.

Reineck, K. H., Kuchma, D. A., Kim, K. S., and Marx, S., "Shear Database for Reinforced Concrete Members without Shear Reinforcement." *ACI Structural Journal*. V. 100, No. 2, March-April, 2003, pp. 240-249.

Ritter, W. "Die Bauweise Hennebique." *Schweizerische Bauzeitung*. V. 33, No. 7, 1899, pp 49-52.

Rogowski, D. M., Macgregor, J. G., and Ong, S. Y., "Tests of Reinforced Concrete Deep Beams." *ACI Journal*, V. 83, No. 4, July-August, 1986, pp.614-623.

Schlaich, J., Schaefer, K., and Jennewein, M. "Towards a Consistent Design of Structural Concrete." *PCI Journal*. V. 32, No. 3, May-June, 1987, pp 74-150.

Schlaich, J. and Schäfer, K. "Design and Detailing of Structural Concrete Using Strut-and-Tie Models." *The Structural Engineer*. V. 69, No. 6, May-June, 1991, pp 113-125.

Shin, S.-W., Lee, K.-S., Moon, J.-I., and Ghosh, S. K., "Shear Strength of Reinforced High-Strength Concrete Beams with Shear Span-to-Depth Ratios between 1.5 and 2.5." *ACI Structural Journal*, V. 96, No. 4, July-August, 1999, pp. 549-556.

Smith, K. N. and Vantsiotis, A. S., "Shear Strength of Deep Beams." *ACI Journal*, V. 79, No. 3, May-June, 1982, pp. 201-213.

Sritharan, S., "Strut-and-Tie of Bridge Tee Joints Subjected to Seismic Actions." *Journal of Structural Engineering*, V. 131, No. 9, September, 2005, pp. 1321-1333.

Sritharan, S. "Improved Seismic Design Procedure for Concrete Bridge Joints." *Journal of Structrural Engineering*, V. 131, No. 9, September, 2005, pp. 1334-1344.

Sritharan, S. and Ingham, J. M. "Application of Strut-and-Tie Concepts to Concrete Bridge Joints in Seismic Regions." *PCI Journal*, V. 48, No. 4, July-August, 2004, pp. 66-90.

Subedi, N. K., Vardy, A. E., and Kubota, N., "Reinforced Concrete Deep Beams-Some Test Results." *Magazine of Concrete Research*, V. 38, No. 137, December, 1986, pp. 206-219.

Tan, K. H., Kong, F.-K., Teng, S., and Guan, L., "High-Strength Concrete Deep Beams with Effective Span and Shear Span Variations." *ACI Structural Journal*, V. 92, No. 4, July-August, 1995, pp. 395-405.

Tan, K. H., Kong, F.-K., Teng, S., and Guan, L., "Effect of Web Reinforcement on High-Strength Concrete Deep Beams." *ACI Structural Journal*, V. 94, No. 5, September-October, 1997, pp. 572-582.

Tan, K. H. and Lu, H. Y., "Shear Behavior of Large Reinforced Concrete Deep Beams and Code Comparisons." *ACI Structural Journal*, V. 96, No. 5, September-October, 1999, pp. 836-845.

Xie, Y., Ahmad, S. H., Yu, T., Hino, S., and Chung, W., "Shear Ductility of Reinforced Concrete Beams of Normal and High-Strength Concrete." *ACI Structural Journal*, V. 91, No. 2, March-April, 1994, pp. 140-149.

Yun, Y. M., and Ramirez, J. A. "Strength of Struts and Nodes in Strut-and-Tie Model." *Journal of Structural Engineering*. V. 122, No. 1, January, 1996, pp 20-29.

Zhu, R.R.H., Wanichakorn, W., Hsu, T.T.C., and Vogel, J. "Crack Width Prediction Using Compatibility-Aided Strut-and-Tie Model." *ACI Structural Journal*, V. 100, No. 4, July-August 2003, pp 413-421.